

Biogeochemical Controls of the Transport and Cycling of Persistent Organic Pollutants in the Polar Oceans

Cristóbal Galbán Malagón

**Department of Environmental Chemistry
Institute of Environmental Assessment and Water
Research (IDAEA-CSIC)
Barcelona**

**This thesis was supervised by Dr. Jordi Dachs from the
Institute of Environmental Assessment and Water
Research (IDAEA-CSIC) of Barcelona.**

**Programa de Doctorado:
Ciencias de el Mar**

**Memoria presentada para optar al grado de Doctor por la
Universidad Politécnica de Cataluña**

Director:

Ponente:

**Dr. Jordi Dachs
IDAEA-CSIC**

**Dr. Agustín Sánchez-Arcilla
UPC**

“La mayoría de las ideas fundamentales de la ciencia son esencialmente sencillas y, por regla general pueden ser expresadas en un lenguaje comprensible para todos”

Albert Einstein

***Dedicada a mi mujer a mis
padres y hermanos pero muy
especialmente a mi hijo
Santiago por que llegó para
alegrarnos todas las
mañanas y especialmente las
noches. Sin tu ayuda esta tesis
se habría escrito antes.
¡Gracias por todo!***

Abstract

Humanity is currently using more than 200000 synthetic organic compounds in many industrial, agricultural and domestic applications. Many of these chemicals reach the environment and have a harmful effect on ecosystems and humans. Among them, the group of persistent organic pollutants (POPs) comprises several families of compounds that have physical and chemical properties that give them the ability to be distributed and impact globally (semivolatility, high persistence and bioaccumulation capacity due to their hydrophobicity).

In the present thesis, the coupling of atmospheric transport and biogeochemical cycles in the Arctic and Southern Ocean has been studied for Hexachlorocyclohexanes (HCHs), Hexachlorobenzene (HCB) and Polychlorinated Biphenyls (PCBs). Three oceanographic cruises were conducted, one in the North Atlantic and the Arctic Ocean (2007) and two in the Southern Ocean surrounding the Antarctic Peninsula (2008 and 2009). During these campaigns, air (gas and particulate), water (dissolved and particulate) and biota (phytoplankton) were sampled simultaneously allowing to report a complete picture of POPs cycling in polar areas. In the case of the Southern Ocean, the largest data set available for PCBs, HCH and HCB has been generated.

The atmospheric and seawater concentrations were low, among the lowest reported for the Polar Oceans, and in the case of the Southern Ocean there is a clear historical trend of decreasing concentrations, consistent with reduced emissions in source regions. Long range atmospheric transport was identified as the main POPs input to polar ecosystems agreeing with previous works. However, it has been found that secondary local sources from soil and snow influences strongly the atmospheric concentrations overland in the Antarctic region, and over the adjacent Southern ocean in the case of HCHs. Atmospheric residence times calculated from the measurements were in agreement with the prediction from environmental fate models. The atmospheric residence times were longer for the less hydrophobic PCBs and shorter for the more hydrophobic, consistent with the role of the biological pump sequestering atmospheric PCBs. Once POPs reach the Polar regions the main route of entry of these compounds to surface waters is by

atmospheric deposition, mainly by diffusive exchange between the gas and dissolved phase with minor contributions from dry deposition of aerosol bound POPs. Estimated bioconcentration factors revealed that concentration of POPs in phytoplankton were correlated with the chemical hydrophobicity, but some discrepancies with model predictions were observed. The biological and degradative pumps are identified as the two main processes that control the fate and occurrence of POPs in the surface water column, and also are able to modulate the atmospheric transport of POPs to remote areas. POPs such HCHs are prone to be efficiently degraded by bacterial communities in surface waters, depleting the seawater concentrations and increasing the diffusive air-water exchange to the Arctic and Southern Ocean. Conversely, the biological pump decreases the dissolved phase concentrations of the more hydrophobic PCB congeners increasing the air to water fugacity gradients and enhancing the diffusive air-water exchange fluxes. This is the first time that the influence of the biological pump on POP cycling is demonstrated for Oceanic waters. Finally, HCB was close to air-water equilibrium showing that neither the biological and degradative pumps are efficient sequestration processes for the highly persistent and mid-hydrophobic compounds. Overall, the results show clearly that biogeochemical processes occurring in the water column affect the atmospheric deposition and long range transport of POPs to remote regions. The magnitude of these processes may show a clear seasonality and are suitable to be perturbed under the current scenario of climate change.

Resumen

En la actualidad se usan en aplicaciones domésticas más de 200.000 compuestos orgánicos sintéticos. Muchos de estos compuestos químicos que se liberan al medio ambiente son nocivos para el medio ambiente y los humanos. Entre estos compuestos se encuentran los contaminantes orgánicos persistentes (COPs) que comprenden una serie de familias de compuestos que comparten una serie de características físico-químicas que les permiten estar distribuidos globalmente (semivolatilidad, elevada persistencia y capacidad de bioacumulación por sus características hidrofóbicas).

En la presente tesis doctoral se ha estudiado en profundidad el acoplamiento entre el transporte atmosférico y los ciclos biogeoquímicos Hexaclorociclohexanos (HCHs), Hexaclorobenceno (HCB) y Bifenilos Policlorados (PCBs) en los Océanos Polar Ártico y Polar Antártico. Durante esta tesis se han realizado tres campañas oceanográficas, una al Atlántico Norte y al Océano Polar Ártico (2007), y dos en el Océano Polar Antártico y en aguas circundantes a la Península Antártica (2008 y 2009). Durante estas tres campañas oceanográficas se han tomado muestras de aire (gas y particulado), agua (disuelto y particulado) y biota (fitoplankton) de forma simultánea lo que permitió tener un amplio conocimiento de el ciclo de los COPs en zonas polares. En el caso de el Océano Polar Antártico y en aguas circundantes a la Península Antártica se ha generado la mayor cantidad de datos en un mismo trabajo, incluso se han generado datos que hasta ahora no se habían publicado como las concentraciones de fitoplankton.

Las concentraciones medidas en el la atmósfera y aguas superficiales fueron bajas, siendo en algunos casos las concentraciones más bajas jamás encontradas en el océano polares, en el caso de el Océano Polar Antártico se ha encontrado una significativa tendencia histórica de concentraciones decrecientes lo cual es consistente con la reducción de emisiones de COPs en origen. El transporte atmosférico a larga distancia ha sido identificado como la vía de entrada principal de entrada de los COPs a sistemas polares. Sin embargo, se ha encontrado que hay fuentes secundarias provenientes de el suelo y la nieve con una clara influencia sobre las concentraciones atmosféricas en zonas de el

continente Antártico y aguas costeras adyacentes en el caso de los HCHs. Los tiempos de residencia atmosférica calculados están en los mismos rangos con los modelos predictivos. Los tiempos de residencia atmosférica fueron más largos para los compuestos menos hidrofóbicos y más cortos para los más hidrofóbicos lo cual es consistente con la bomba biológica. Una vez estos compuestos alcanzan las regiones polares la principal ruta de entrada de estos compuestos al agua superficial es por deposición atmosférica, principalmente por intercambio difusivo entre la fase gas y la fase disuelta, se ha comprobado que la contribución de la deposición seca es significativamente menor. Los factores de bioconcentración revelaron que la concentración de COPs en el fitoplankton se correlacionaba con la hidrofobicidad química, pero se encontraron discrepancias con los modelos predictivos. Las bombas biológica y degradativa han sido identificadas como los dos procesos principales que controlan el destino y ocurrencia de COPs en la columna de agua superficial e incluso son capaces de modular el transporte atmosférico de COPs a áreas remotas. COPs como los HCHs son eficientemente degradados por las comunidades bacterianas de aguas superficiales disminuyendo su concentración aumentando los flujos difusivos de deposición entre la fase gas y la superficie disuelta en el Océano Polar Antártico y en aguas circundantes a la Península Antártica. Por otro lado, la bomba biológica disminuye las concentraciones de el disuelto de los COPs más hidrofóbicos aumentando el gradiente de fugacidades y favoreciendo la deposición por intercambio difusivo aire-agua. La presente tesis es la primera que ha demostrado la influencia de la bomba biológica influye de forma significativa el ciclo de los COPs. El HCB se ha encontrado en equilibrio en ambas zonas de estudio y no se ha demostrado que hubiera influencia de la bomba biológica o de procesos degradativos en aguas superficiales. Como conclusión final se ha demostrado a través de los resultados que los procesos biogeoquímicos en la columna de agua afectan a la deposición atmosférica y el transporte a larga distancia de COPs a regiones remotas. La magnitud de estos procesos muestra una clara estacionalidad que puede ser perturbada en un actual escenario de cambio climático.

Agradecimientos.

Se piensa que escribir los agradecimientos de una tesis puede ser una tarea fácil comparado con la redacción de una tesis doctoral o un artículo científico, definitivamente no lo es. Es difícil pensar en todas las personas que han compartido conmigo los muchos momentos que he vivido desde que llegué a Barcelona hace ya casi seis años. Hasta ahora una de las mejores épocas que he vivido en toda mi vida. En los agradecimientos uno reflexiona sobre todos los momentos que uno ha vivido en estos años y trata de recordar a todas las personas que en cierto modo me han acompañado.

El mayor agradecimiento es para la persona que ha confiado en mí para poder llevar a cabo este proyecto con total libertad para hacer las cosas bajo mi criterio sabiendo dirigirme y orientarme, demostrando infinita paciencia en algunos momentos, hasta cuando le preguntaba dudas de secundaria. ¡Gracias Jordi!

También quiero agradecer a mis padres todo el apoyo que me han dado en todo este tiempo, por haberme dado la posibilidad de formarme y darme siempre su consejo cuando he tenido momentos complicados a lo largo de mi carrera una parte de esta tesis también es vuestra.

A mis hermanos Carlos y Cristina de ellos he aprendido que el tesón y la constancia dan sus frutos aunque las situaciones sean complicadas. Carlos ánimo con todo que las cosas siempre van a mejor sé que todo te va a salir bien y no te rindas. A Cristina la pitufa de la casa cuando me marché de casa ella acababa de empezar el bachillerato y ahora casi una médica ánimo que ya no te queda nada.

Al resto de mi familia y especialmente a los que ya no están que se que me miran de alguna forma desde algún sitio. Un abrazo abuelo

A mis amigas Sasi y Fátima...Sabela parece mentira nos conocemos desde los diez años y hemos vivido muchos momentos importantes, Fátima tu llegaste más tarde pero como si hubieras estado siempre. Siempre hemos estado juntos en

momentos importantes para nuestras vidas espero que este día sea otro más si no sé que os acordaréis de mi cuando esté delante de el tribunal.

A todos los compañeros que forman o han formado parte de el grupo de investigación. A Sabino por dejarme su habitación para vivir cuando llegué a Barcelona. A Naiara por enseñarme a trabajar en el barco cuando apenas llevaba 48 horas de tesis doctoral y enseñarme con rigurosidad como se deben hacer las cosas sobre todo con la presión que se tiene en una campaña oceanográfica, ánimo con la tesis que ya está ahí. A Ana por demostrarme que el trabajo incansable da sus frutos y que la constancia es una de las mayores virtudes. A María José por ayudarme en el laboratorio con todo el trabajo sin su ayuda una parte importante de esta tesis no se habría podido realizar, por enseñarme como se deben hacer las cosas en el laboratorio y como no debo hacerlas, por tener siempre buenas palabras cuando eran necesarias, por tener malas palabras cuando eran más necesarias ;-) y por decirme las cosas como se tenían que decir y cuando se tenían que decir. Han sido muchas horas y que yo sepa nadie a muerto ni ha sufrido heridas graves . A Gema por las conversaciones sobre el animalismo y el respeto a los animales suerte con la licenciatura. A Javi Zúñiga por su tremenda frialdad en el laboratorio y capacidad para mantener la calma y analizar las cosas objetivamente...ánimo con la tesis. A Mari Carmen todo carácter por esas risas se oían a través de la pared, por compartir tu buen humor siempre que puedes, suerte con la tesis y con ese primer artículo. A Belén la última en llegar y la que tiene más datos para analizar te vas a volver loca con tanto excel suerte con la tesis. A Javi Castro la persona más calmada y analítico rivalizando con el otro Javi...cuando se ponen a hablar de química uno se siente un ignorante. A Elena por enseñarme todo lo que hay a mayores de la ciencia pura y siempre tener una buena conversación a la hora de comer...mucho suerte en Colombia sé que todo os irá genial. Linda de ti no me olvido quizás seas la persona que más me ha influenciado y que más empeño a puesto en apoyarme en todas las cosas (*as you said -I want you to be brilliant...maybe now is time*), siempre dispuesta a tomar un té calmadamente y enseñarme casi como si también fuera tu alumno de doctorado, muchas gracias por tu apoyo durante tu estancia en el IDAEA fue una pena que fuera tan corta, muchas gracias por los “*evening brainstorming*“. A Maria y a

Mariana las últimas incorporaciones al grupo ánimo con esta etapa que acabáis de empezar.

No me quiero olvidar de mi cuadrilla de risas a bordo de el Hespérides ojalá pudierais estar en este momento conmigo pero bueno estamos todos desperdigados por el mundo adelante. Un fuerte abrazo para Sergio, Pedro, Sebas e Íñigo (este llegó el último pero pisando fuerte...vaya risas con el momento Coca-Cola dopada durante la ley seca)

Los compañeros de las pachangas de fútbol Raúl, Jon, Iñaki, CR9, Jaume (la cucaracha, la cucaracha...), Quique, Pablo (más solo que una cobra), Anuar, Alex, Alberto, Javi, Giorgio (relax man), Nicola...tenemos alguna pendiente todavía que las barrigas empiezan a pesar y vamos tarde para la operación trikini.

A Sergi por siempre contarme las maravillas de el código abierto y tratar de buscar siempre una solución para los problemas de informática. A Raul por tener esa gran selección de música bizarra (temazo tras temazo).

Ahora voy a poner una larga lista de nombres y espero no olvidarme de nadie que no va a ser fácil. A Ester Vizcaíno (Lola Solo Una), A Marta Fort (siempre me ha escuchado), a Eric Jover, Victor Matamoros, Alain Hildenbrant, Sandra Pérez, Joan Antón, Jordi López (siempre atento a resolver dudas), Josep Sanchís (Gracias por esa colaboración a medias), a Gene, a Laura Morales, a Esteban Abad, Vicky, a Maria (siempre con una sonrisa), a Roser, Dori, Ester Marco (gracias por los cigarros, jejeje), Silvia, Joana, a Barend (siempre dispuesto a responder mis dudas).

Por último a quien más tengo que agradecer por todo lo que me ha tenido que soportar este último año con mis cambios de humor, mis agobios, mis miedos es a mi mujer. Mane muchas gracias por estar siempre a mi lado apoyándome cuando más cansado estaba y ayudar a levantarme cuando me había caído. Gracias por formar parte de mi vida, crear una familia conmigo y por haberme dado a Santiago lo más preciado que tengo y sin el cual ya no me puedo imaginar mi vida. Esta tesis tiene mucho de vosotros dos.

Table of Contents

- Chapter 1. Introduction...1

- 1. Anthropogenic global change and organic pollutants...1
- 2. Persistent Organic Pollutants (POPs)...3
- 3. Physical Chemical Properties and environmental Partitioning of POPs...9
 - 3.1 *Relevant Physical-chemical properties for non-ionic POPs*...9
 - 3.2 *Octanol-water partition coefficients (K_{OW}) and estimation of partitioning between water and organic matter*...10
 - 3.3 *Henry's Law Constant (HLC) and Air-water partition coefficient (K_{AW})*...13
 - 3.4 *Octanol-air partition coefficients (K_{OA}) and Gas-particle partition coefficients (K_P)*...14
 - 3.5 *Fugacity as a criterion for equilibrium between environmental media*...16
- 4. Global transport and dynamics of POPs: Role of the atmosphere and oceans...18
 - 4.1 *Sources of POPs to the Environment*...19
 - 4.2 *Global transport of POPs*...21
 - 4.3 *Carbon cycle and biogeochemical controls on POPs*...24
- 5. POPs cycling in the Polar Oceans...26
 - 5.2 *Atmospheric-surface exchange and ice melting*...28
 - 5.2.1 *Diffusive exchange between the atmosphere and oceans*...28
 - 5.2.2 *Dry deposition*...29
 - 5.2.3 *Wet deposition*...30
 - 5.3 *Water column processes*...31
 - 5.3.1 *Degradation*...31
 - 5.3.2 *Water column exportation processes to deep ocean*...32
 - 5.3.2.1 *The biological pump*...32
 - 5.3.2.2 *Turbulent flux and water mass subduction*...33
- 6. Selected POPs for study...34
 - 6.1 *Hexachlorobenzene (HCB)*...35
 - 6.2 *Hexachlorocyclohexanes (HCHs)*...36
 - 6.3 *Polychlorinated byphenyls (PCBs)*...37
- 7. Polar Oceans and the regions of study...39
 - 7.1 *The Arctic*...39
 - 7.2 *Antarctica and Southern Ocean*...40
 - 7.3 *Regions of study in the Arctic and Southern Ocean*...41
- References...47

- Chapter 2. Objectives...63

- **Chapter 3. The Oceanic Biological Pump Modulates the Atmospheric Transport of Persistent Organic Pollutants to the Arctic...65**

Abstract...67

1. Introduction...69

2. Results...71

2.1 Occurrence of PCBs in the GC and AO...71

2.2 Decreasing PCB concentrations during atmospheric transport...72

3. Discussion...74

4. Methods...84

References...86

- **Chapter 4. The “degradative” and “biological” pumps controls on the atmospheric deposition and sequestration of Hexachlorocyclohexanes and Hexachlorobenzene in the North Atlantic and Arctic Oceans...91**

Abstract...93

1. Introduction...95

2. Material and methods...98

2.1 Sampling cruise...98

2.2 Sampling procedures...98

2.3 Chemical analysis...99

2.4 Quality assurance and quality control...101

3. Results and Discussion...101

3.1 Occurrence of HCHs and HCB in seawater and phytoplankton...101

3.2 Atmospheric occurrence of HCHs and HCB...102

3.3 Field derived atmospheric residence times...103

3.4 Atmospheric deposition of HCHs and HCB...104

3.5 Removal fluxes from the water column...107

3.6 Importance of the degradative and biological pumps...110

References...112

- **Chapter 5. Polychlorinated Biphenyls, Hexachlorocyclohexanes and Hexachlorobenzene in seawater and phytoplankton from the Southern Ocean (Weddell, South Scotia, and Bellingshausen Seas)...121**

Abstract...123

1. Introduction...125

2. Materials and Methods...126

2.1 Sampling...126

2.2 Chemical Analysis...128

2.3 Quality control and assurance...129

2.4 Characteristic decreasing or e-folding times...129

2.5 <i>Bioconcentration factors</i> ...	130
3. Results and Discussion ...	130
3.1 <i>Occurrence of organochlorine pesticides (OCPs) in Seawater and phytoplankton</i> ...	130
3.2 <i>Occurrence of PCBs in seawater and phytoplankton</i> ...	133
3.3 <i>Decrease of PCB and OCP in the Southern Ocean seawater</i> ...	136
3.4 <i>Factors driving PCBs, HCHs and HCB concentrations in phytoplankton</i> ...	138
References...	142
• Chapter 6. Atmospheric Occurrence and Deposition of Hexachlorobenzene and Hexachlorocyclohexanes in the Southern Ocean and Antarctic Peninsula ...	151

Abstract...153

1. Introduction...155

2. Material and Methods...156

 2.1 *Sampling and site description*...156

 2.2 *Analytical Methods*...158

 2.2.1 *Atmospheric and aerosol extraction and fractionation of OCPs*...158

 2.2.2 *OCPs Identification and Quantification*...159

 2.3 *Quality Control and Quality Assurance*...159

 2.4 *Statistical Analysis*...160

3. Results and Discussion...160

 3.1 *Atmospheric occurrence of HCHs and HCB*...160

 3.1.1 *Gas phase concentrations of α -HCH and γ -HCH*...160

 3.1.2 *Gas phase concentrations of HCB*...163

 3.1.3 *Aerosol phase concentration of α -HCH, γ -HCH and HCB*...164

 3.2 *Influence of the air-mass backtrajectories on atmospheric concentrations of HCHs and HCB*...165

 3.3 *Antarctica as a secondary source of HCHs and HCBs*...166

 3.4 *Air-Sea diffusive exchange and dry deposition processes*...168

4. Conclusions...173

References...175

- **Chapter 7. Factors affecting the atmospheric occurrence and deposition of Polychlorinated Biphenyls in the Southern Ocean**...181

Abstract...183

1. Introduction...185

2. Materials and Methods...187

 2.1 *Sampling*...187

 2.2 *Chemical Analysis*...188

 2.3 *Quality Control and Quality Assurance*...189

	<i>2.4 Atmospheric back trajectories</i> ...	190
3. Results and Discussion ...		
	<i>3.1 Occurrence of PCBs in the Southern Ocean Atmosphere</i> ...	190
	<i>3.2 Gas-particle partitioning of PCBs</i> ...	195
	<i>3.3 Air-water diffusive exchange and dry deposition of PCBs</i> ...	197
	<i>3.4 Temperature dependence of gas phase concentrations</i> ...	202
	<i>3.5 Factors affecting the atmospheric occurrence of PCBs in the Southern Ocean</i> ...	204
4. Conclusions ...		206
References ...		207
•	Chapter 8. Conclusions ...	215
•	Appendix A ...	219
•	Appendix B ...	249
•	Appendix C ...	269
•	Appendix D ...	293
•	Appendix E ...	313
•	Appendix F. List of Acronyms ...	343

Chapter 1

Introduction

1. Anthropogenic global change and organic pollutants

Since the first steps of humanity, notably since the Neolithic revolution, (5000-8000 years ago), the composition of the biosphere has been modified, first slightly (Ruddiman, 2003), but these changes that have increased exponentially during the last 200 years (Steffen et al. 2007). In fact, as human population grows the anthropogenic impact increases markedly. First societies were formed by small groups of hunters, nomads and scavengers and their environmental impacts were negligible compared to modern and industrial ages. During the beginning of humanity, the time needed to increase the population by 10 million was a hundred thousands years, nowadays it only takes 6 weeks (McMichael, 1993). With this growth rates in population, it is projected that human population will reach 11 billion people in the next 50 years (Lutz et al., 2001).

The population has increased markedly since the industrial revolution around 1750 and even at a higher rate during the last 50 years (Figure 1). There is also an increase of use of water, fertilizers, fossil fuels, and chemicals (Dachs and Mejanelle 2010). Indeed, there is a direct relationship between the industrialization and greenhouse gasses atmospheric concentration (IPCC 4th assesment), and also on the use and emission of synthetic organic chemicals to the environment. Crutzen defined the last 250 years as Anthropocene (Crutzen and Stoermer, 2000; Crutzen, 2002; Kirch, 2005). Actually, anthropocene could be divided in two different recognized stages. The early stage goes from 1800 to 1945 (2nd World War) comprising the early industry development. The later stage goes from 1945 to present comprising an unprecedented development of heavy industry, human development and resources demand.

Introduction

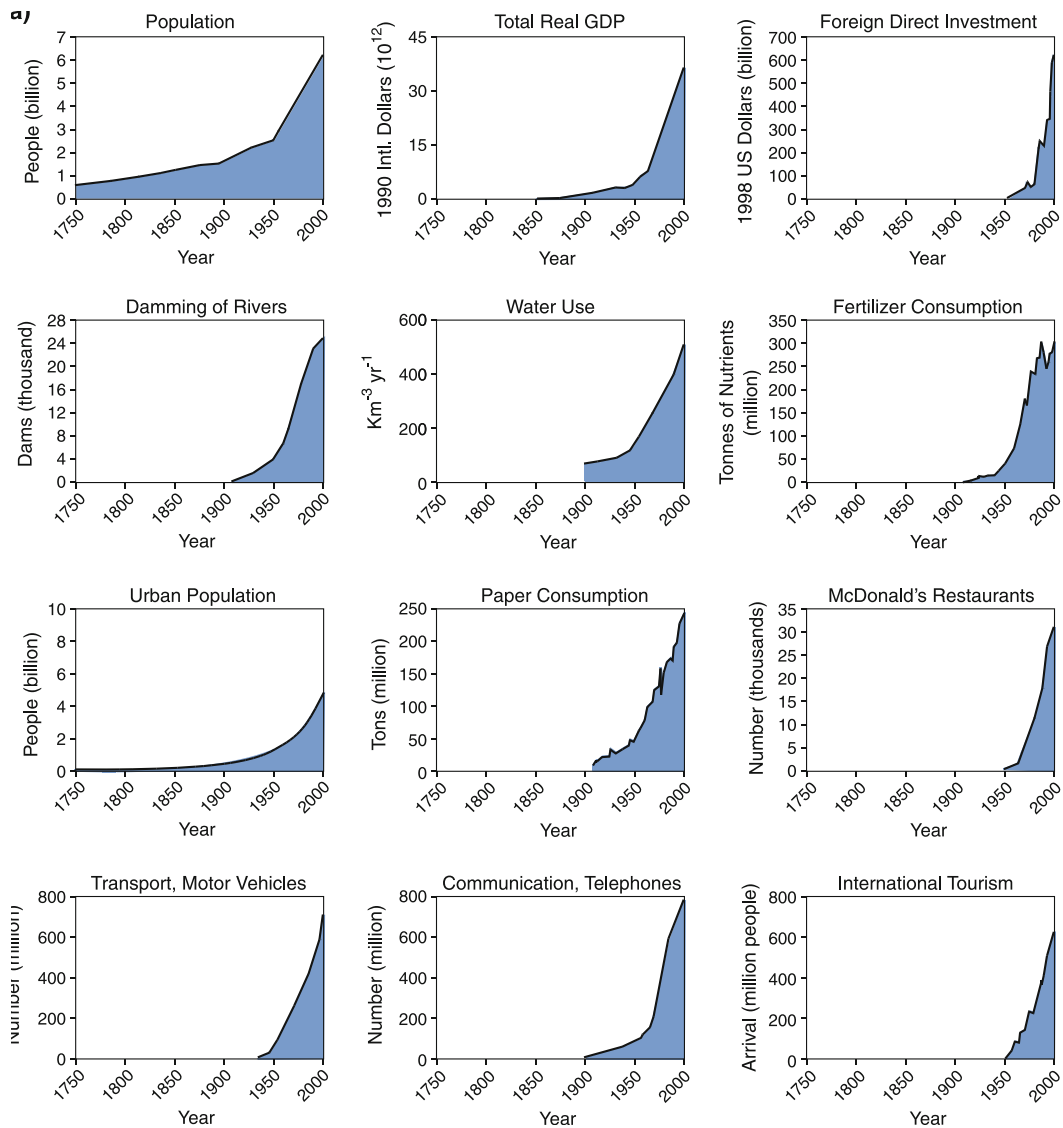


Figure 1. Increasing of the world population in billions of persons during the anthropocene and for other indicators (Steffen et al. 2007)

During the Anthropocene, there are direct human impacts on ecosystems by means of mining, land-use change, ecosystem fragmentation, ecosystem destruction, population migration events; or indirect by means of greenhouse gasses and pollutants emissions. As an example it has been noted that human activities induce changes in the biogeochemical cycling of the principal elements in the earth (C, N, S, O and P) and the increase of pollution levels and number of pollutants. In the case of the pollution emissions is important to mention the case of greenhouse gasses (CO_2 , CH_4 ...), atmospheric acidifiers (SO_4^{2-} , NO_3^- , NO_x), ozone depletion catalyzers (CFCs, BrO_3), heavy metals (Cd, Pb, Hg, Co...), and legacy and emerging persistent organic pollutants (PCBs, HCHs, PAHs, DDTs,

Dioxin...). Even though organic pollutants are at trace levels in the environment, there are thousand of them already identified, and a larger number still to be studied. All these perturbations of the composition of the atmosphere induce an adverse effect on ecosystem and human health. Therefore, chemical pollution is just another vector of global change, that goes beyond the climate and temperature rise, and which effect has not been quantified in terms of the Earth system (Rockstrom et al. 2009).

Remote Polar Regions, such as the Arctic and Antarctica, are considered sentinels of global change (IPCC 2007, Summary for Policymakers, in *Climate Change 2007: Synthesis Report*, p. 11). While there is an important body of literature on organic pollutants in the Arctic, the Antarctica has received much less attention. In addition, there are few studies on the cycling of organic pollutants in the Polar Oceans.

2. Persistent Organic Pollutants (POPs).

The increase in production and use of organic chemicals is correlated to the increase of human population and its industrial development. The use of synthetic organic chemicals is coupled to the development of chemical and agrochemical industry, and includes chemicals used in industry, agriculture, domestic and health products, and the use of fossil fuels. So far, there are 71 million of compounds that have been registered (www.cas.org), but about 297,000 are in use by the contemporaneous human society (<0.01%). Recently, it has been reported that at least 100,000 of these compounds are in commerce and used in a myriad of “domestic” and industrial applications with an increasing demand (Muir and Howard, 2006). Even though, many of these chemicals have beneficial applications for human health and security (fragrances pharmaceuticals, flame-retardants), once in the environment they can pose a risk for the environment (Morley et al., 2006). Among the synthetic organic chemicals used during the last century, some have raised a notorious concern for their effects to wildlife and humans once released to the environment, leading to national and international legislations controlling or banning their use. Especially relevant are those known as persistent organic pollutants (POPs), which are characterized by its persistence, potential for bioaccumulation, and capacity for long range transport which allow

Introduction

them to be distributed globally. They are hazardous to the environment due to its toxic effects at both organism and at ecosystem level. Many POPs are semi-volatile, so they have the capacity to be atmospherically transported and redistributed across different environmental media to proximate and distant ecosystems. In fact, POPs are distributed globally in biotic and abiotic compartments (Klanova et al., 2011; Dachs and Mejanelle 2010; Gioia et al., 2006; 2008; Jaward et al., 2004), reaching remote areas like the Arctic and Antarctic ecosystems (Wania and Mackay, 1996). Within POPs, there are industrial chemicals and by-products, such as polychlorinated biphenyls (PCBs) and hexachlorobenzene (HCB), a number of organochlorine pesticides (aldrin, chlordane, dieldrin, dichlorodiphenyltrichloroethane (DDT), endrin, heptachlor, mirex, toxaphene and hexachlorocyclohexane). In addition, there are by-products of combustion processes such as polychlorinated dibenzo dioxins and furans (PCDD/Fs). The POPs that are currently banned are called “legacy POPs”. Emissions of legacy POPs are linked to past use of them in many applications (for example PCBs in transformers), or to a remobilization of historical reservoirs in soils, vegetation, seawater and sediments.

The first public awareness of the consequences of POPs usage came from Rachel Carson book “Silent Spring” (Carson, 1962). In this book, she reflected the fact that some compounds such as DDTs not only affected mosquito populations, but also it was associated with a high mortality of birds. However, this book contains the writer’s reflection with a lack scientific perspective, which led to an important criticism to her conclusions (Figure 2). Unfortunately, her hypotheses were not far away from reality, and nowadays contaminations by POPs is recognized as a primary concern of the environmental health (Tanabe, 2002), and there are thousands of reports on their widespread in the environment and harmful effects (Iwata et al., 1993; Meijer et al., 2003, Wania and Mackay, 1993; 1995).

The United Nations Environmental Program (UNEP) and the World Health organization (WHO), through resolution 18/32 initiated a consultative process to evaluate an initial POPs list in 1997 (Table 1), in collaboration with the Intergovernmental Forum on Chemical Safety (IFSC). IFSC recommendations gave a first step to negotiate an international treaty on POPs.



Figure 2. Using a children's nursery rhyme to suggest an ecological food chain. J. W. Taylor, 'This is the dog that bit the cat that killed the rat that ate the malt that came from the grain that Jack sprayed.', Punch Magazine, March 6, 1963

In subsequent years, followed a series of international negotiation meetings in different countries (i.e Montreal 1998, Bangkok 1998, Nairobi 1999, Vienna 1999, Geneva 1999, Bonn 2000, Johannesburg 2000). Finally, the Stockholm convention on POPs was signed in 2001. Taking the final step toward regulating the production and use of some POPs with the objective of:

"...protect human health and the environment from persistent organic pollutants..."

Extract from the article 1 of Stockholm Convention on Persistent Organic Pollutants

By signing and ratifying the Stockholm protocol, parties are committed to reduce / eliminate the production, use or release of 12 families of POPs (Table 1). In 2011 this list was actualized and now includes 25 families of compounds. However, there are previous/contemporaneous efforts of UNEP for international legislation on pollutants. The United Nations Economic Commission for Europe (UNECE) in 1979 met in Geneva for the Convention on Long-range Transboundary air pollution (CLRAT). While at first this convention was focused on the emission of sulphurs and its effects on the acidification of the medium, there were additional protocols regulating several air pollutants (nitrogen oxides, volatile organic compounds and POPs). The protocol on POPs came from the

Introduction

Aarhus convention in 1989 and was adopted in 2003. The protocol objective was to eliminate production, usage, discharges, emissions and release of POPs to the environment. Despite of having an intention similar to the Stockholm Convention, the Aarhus protocol includes a list of 16 POPs and additional 7 compounds have been added recently (Table 1). Moreover, the European Commission (EC) developed the European Community regulation on chemicals and their safe use (EC 1907/2006). It deals with the registration, evaluation, authorisation and restriction of chemical substances (REACH), this law entered into force in 2007. The adoption of REACH normative implies a quality step forward in international chemicals regulation because it sets the usage approval prior to commercial exploitation. Manufacturers and importers are required to gather information on the properties of their chemical substances allowing safe handling and registering the information in a database centre run by the European Chemicals Agency (ECHA) in Helsinki. The contribution of all these international legislation provided an international dimension to the environmental problematics on POPs, even though the regulated POPs are a very small fraction of all potential organic pollutants.

Both the Stockholm Convention and REACH use the current knowledge of the long-range transport, bioaccumulation processes, and persistence to prioritize chemicals to be considered as pollutants (and POPs), and as a screening criteria before they are introduced in the market, respectively. Therefore, the scientific knowledge developed during the last three decades is used in the current legislation of organic pollutants. In addition, the Stockholm convention aims at controlling and monitoring the global occurrence and temporal trends of POPs in the environment. Therefore, the study of the environmental fate and cycling of POPs, it is not only important of its implicit scientific interest, but also because current legislation is based on scientific knowledge, even though science is often 20 year ahead of legislation. The environmental fate and impact of organic pollutants can be predicted from their physical chemical properties, such as vapour pressure, the solubility in water and the octanol-water partition coefficients. Thus, criteria used to prioritize POP is based on these chemical properties and current knowledge of POP cycling in the environment (table 2).

Introduction

Nowadays, it is impossible to assess the environmental fate and cycling of POPs without a consideration of their properties and partitioning behaviour.

Table 1. List of persistent organic pollutants included in the Stockholm convention and the Convention on Long-Range Transboundary air-pollution (CLRTAP)

Stockholm Convention		
Insecticide	Industrial Chemical	Unintentional Production
Aldrin	PBDEs ^a	HCB
Dieldrin	Hexachlorobenzene	PCDDs
Endrin	Pentachlorobenzene ^a	PCDFs
Chlordane	PCBs	Pentachlorobenzene ^a
Chlordecone ^a	Perfluorooctane sulfonic acid ^a	PCBs
Heptachlor	Perfluooctanated sulfonyl fluoride ^a	
Hexachlorobenzene		
Hexachlorocyclohexane(a and b) ^a		
Lindane ^a		
Mirex		
Pentachlorobenzene ^a		
Endosulfan ^a		
Toxaphene ^a		
Pentachlorobenzene ^a		
Convention on Long-Range Transboundary Air Pollution		
Insecticide	Industrial Chemical	Unintentional Production
Aldrin	PBDEs ^b	HCB
Dieldrin	Hexachlorobenzene	PCDDs
Endrin	Pentachlorobenzene ^b	PCDFs
Chlordane	PCBs	Pentachlorobenzene ^b
Chlordecone	Perfluorooctane sulfonic acid ^b	PCBs
Heptachlor	Perfluooctanated sulfonyl fluoride ^b	
Hexachlorobenzene	Brominated dioxins and Bromo-Chloro dioxins ^b	
Hexachlorocyclohexane(a and b)	Octachlorostyrene ^b	
Lindane	Organometals ^b	
Mirex	Polychlorinated Naphtalenes ^b	
Pentachlorobenzene	PAHs	
Endosulfan	Short Chain Paraffins ^b	
Toxaphene		
Pentachlorobenzene ^b		

^aIncluded in 2011 amendments

^bIncluded in 2009 amendments

Introduction

Table 2. POPs definition under the UNECE criteria as proposed in the Aarhus protocol

Property	Criteria for definition as POPs
Potential for LRAT	$P_v^a < 1000\text{Pa}$ or
	Half-Life in air > 2 d and
	Presence in remote regions
Persistence	Half-Life in water > 2 months or
	Half-Life in soils > 6 months or
	Half-Life in sediments > 6 months
Bioaccumulation	$\text{Log}K_{ow}^b > 6$ or
	$\text{BCF}^c > 5000$ or
	evidence of high toxicity

^a Vapor Pressure

^b Octanol-water partition coefficients

^c Bioconcentration Factors

3. Physical Chemical Properties and environmental Partitioning of POPs.

3.1 Relevant Physical-chemical properties for non-ionic POPs

The physical chemical properties of POPs play a key role on the environmental partitioning of POPs, on the potential for long-range transport through the atmosphere and oceans, on their persistence, and on bioaccumulation processes. The relevant physico-chemical properties that need to be considered when studying the environmental partitioning and cycling of POPs are the vapour pressure (P_V), solubility in water (S_W), Polarity (S_O), hydrophobicity, air-water partition coefficients ($\text{Log}K_{AW}$), octanol-air partition coefficients ($\text{Log}K_{OA}$) and octanol-water partition coefficients ($\text{Log}K_{OW}$).

Vapor pressure (P_V): The vapour pressure is the atmospheric pressure exerted by a vapour in a closed system that is in thermodynamic equilibrium with its condensed pure phases (solid or liquid) at a given temperature. It informs about the tendency of the chemical to escape from the liquid (or a solid) phase and its units are Pascals (Pa). The organic compounds with higher P_V will have higher tendencies to partition to the atmosphere and undergo atmospheric transport. P_V for most legacy POPs range from 0.0001 to 0.01 Pa. P_V depends on temperature, so at higher temperatures, P_V is higher.

Solubility in water (S_W): The solubility in water is the maximum concentration of a chemical in water when it is in contact with the pure compound (solid, liquid, or gas). Non-ionic organic compounds tend to have low solubilities in water, and its value depend on the polarity of the solute and temperature. Its units in the international system are mol m^{-3} . For example compounds with higher solubility will tend to be in the surface waters from the continent or oceans, while lower solubility compounds tend to be in sediments, bound to particles or in the air depending on the vapour pressure. Legacy POPs have very low S_W values because they are either non-polar or have low polarities.

Solubility in organic matter and octanol (S_{Oct}): The solubility in organic matter is the saturated concentrations of the solute as dissolved in the organic matter (absorption) when it is in contact with the pure compound. Since most

Introduction

legacy POPs are highly hydrophobic (low S_W), they have high tendency to partition in organic matter and lipids of particles and organisms. However, the composition of organic matter pools in the environment can vary, and by tradition, octanol has been taken as a surrogate of organic matter. Therefore, physical chemical properties for organic compounds are tabulated for the partition to octanol, and the environmental partitioning of chemicals is referred to the octanol-water and octanol-air partition coefficients.

3.2 Octanol-water partition coefficients (K_{OW}) and estimation of partitioning between water and organic matter.

Octanol-water partition coefficient (K_{OW}): K_{OW} is the ratio between S_{Oct} and S_W :

$$K_{OW} = \frac{S_{Oct}}{S_W} \quad [1.1]$$

Therefore, K_{OW} is dimensionless. K_{OW} has been tabulated for thousands of organic compounds and can also be predicted from chemical structure. K_{OW} depends on temperature, with lower values at higher temperatures. K_{OW} are usually tabulated at 298K and it can be temperature-corrected to environmental conditions by (Harner and Bidleman, 1996),:

$$\frac{K_{OW_{T_0}}}{K_{OW_{T_{298.15}}}} = e^{\left[\frac{-\Delta U_{OW}}{R} \left(\frac{1}{T_0} - \frac{1}{298.15} \right) \right]} \quad [1.2]$$

Where $K_{OW_{T_0}}$ and $K_{OW_{T_{298.15}}}$ are the octanol water partition coefficients at T_0 and at 298.15 K, $-\Delta U_{OW}$ is the enthalpy of phase change from octanol to water (kJ mol^{-1}), and R is the ideal gas constant ($\text{kJ mol}^{-1} \text{K}^{-1}$). Typical values of $-\Delta U_{OW}$ for hydrophobic organic pollutants are of 35 kJ mol^{-1} .

Characteristic values of K_{OW} for most legacy POPs, such as PCBs and HCH, range from $10^{3.5}$ to 10^8 at 298 K. These values are more than one order of magnitude higher in the polar oceans.

Introduction

Dissolved organic carbon–water partition coefficient (K_{DOC}): Since the dissolved organic carbon (DOC , KgC m^{-3}) is the major pool of carbon in oceanic waters, it is important to assess how K_{DOC} is predicted. K_{DOC} is given by:

$$K_{DOC} = \frac{C_{W_{DOC}}}{C_W DOC} \quad [1.3]$$

Where $C_{W_{DOC}}$ and C_W are the concentrations of the selected compound associated to dissolved organic carbon (ng KgC^{-1}) and the concentration of the selected compound found in the truly dissolved phase (ng m^{-3}). DOC is a heterogenous mixture of organic compounds, and has a lower sorption capacity than octanol, particulate organic carbon, or lipids. Experimental measurements have reached experimental values for K_{DOC} , but with an important variability, but an average correlation between K_{DOC} and K_{OW} is usually used (Totten et al., 2001):

$$K_{DOC} = 0.1K_{OW} \quad [1.4]$$

Phytoplankton-water partitioning or bioconcentrations factors (BCFs): Phytoplankton and bacteria do not have known active mechanisms for the uptake of POPs from water. Therefore, the bioconcentration of POPs in phytoplankton is due to passive uptake due to molecular diffusion. Conversely, Bioaccumulation refers to the accumulation of chemicals in organisms due to ingestion, which is not relevant for phytoplankton. $BCFs$ (L kg^{-1}) are given by,

$$BCF = \frac{C_{Phyto}}{C_W} \quad [1.5]$$

Where C_{Phyto} is the concentration of the chemical in the phytoplankton (ng kg^{-1}) and C_W is the concentration in the dissolved seawater (ng L^{-1}) when the chemical is at equilibrium. Theoretically, only the chemicals in the truly dissolved phase are bioavailable for bioconcentration, thus, very often $BCFs$ are estimated using $C_{W_{DOC}}$ to derive the truly dissolved C_W . An analogous approach can be used to estimate the partitioning between particulate organic matter (POM) and water. POP can be estimated from the particulate organic carbon (POC , Hedges et al., 2002).

Introduction

K_{OW} has been found to be an important predictor of the BCF (Mackay and Fraser, 2000; Voutsas et al., 2002). Generally, BCF are related to K_{OW} by,

$$BCF = f_{OC}K_{OW} \quad [1.6]$$

Where f_{OC} is the fraction of organic carbon in phytoplankton. Therefore, the more hydrophobic is a chemical, the higher is its BCF value. However, in the case of the more hydrophobic POPs ($\log K_{OW} > 7$), the predictions are weak and there is lack of correspondence between predicted results and field derived BCF values, Some explanations have been suggested for this phenomenon, such as deviations from equilibrium due to the uptake kinetics (lack of equilibrium), or the low permeability of the membranes to big molecules (Skoglund et al., 1996, Del Vento & Dachs 2002). The uptake of chemicals in phytoplankton can also be estimated by:

$$\frac{dC_{Phyto}}{dt} = k_U C_W - (k_D + k_G) C_{Phyto} \quad [1.7]$$

Where k_U , k_D and k_G are the first order rate of uptake, depuration and growth rates for the studied organisms. Under steady state conditions

$$\frac{dC_{Phyto}}{dt} = 0 \quad [1.8]$$

Thus

$$BCF = \frac{C_{Phyto}}{C_W} = \frac{k_U}{k_D + k_G} \quad [1.9]$$

Therefore, during a phytoplankton bloom (high k_G), the BCF will be lower. Under field conditions, it is quite unusual to find steady state conditions, and there are deviations of a direct relationship between BCF and K_{OW} due to lack of equilibrium or grow dilution (Skoglund et al., 1996; Axelman et al., 1997; Jeremiason et al., 1999; Baker, 2002). In addition, in phytoplankton, bioconcentration of POPs can occur at the surface and inside the cell (Del Vento and Dachs, 2002). It was revealed that in the case of phytoplankton the absorption into the cell is the most important process (Skoglund et al., 1996) and in the case

Introduction

of bacteria the opposite dominates due to the high surface to volume ratio for bacteria (Axelman et al., 1997; Sobek et al., 2006). However, further research is needed in order to study the uptake, depuration and growth kinetics for bacteria and phytoplankton and their influence on POPs cycling.

3.3 Henry's Law Constant (HLC) and Air-water partition coefficient (K_{AW}).

The partition coefficient between air and water (given by the Henry's Law Constant, HLC) is the ratio defined by:

$$HLC = \frac{P_V}{S_W} \quad [1.10]$$

HLC has units of Pa m³ mol⁻¹. Usually HLC constant is used as dimensionless (H')

$$H' = \frac{HLC}{RT} \quad [1.11]$$

Where H' is the dimensional Henry's law constant, R is the gas constant (8.31 Pa m³ mol⁻¹ K⁻¹) and T is the sea surface temperature (K). This equation is analogous to the dimensionless calculated air water partition coefficients K_{AW} following:

$$H' = K_{AW} = \frac{C_G}{C_W} \quad [1.12]$$

Where C_G and C_W are the concentrations in the air and water (ng m⁻³) at equilibrium. HLC and H' depend on the environmental conditions and they should be corrected for temperature [4] and salinity [5] following:

$$\frac{HLC_{T_0}}{HLC_{T_{298.15}}} = e^{\left[\frac{-\Delta U_{AW}}{R} \left(\frac{1}{T_0} - \frac{1}{298.15} \right) \right]} \quad [1.13]$$

$$HLC_S = 1.3HLC_{T_0} \quad [1.14]$$

Where HLC_{T_0} , $HLC_{T_{298.15}}$ and HLC_S are the HLC corrected by temperature, the HLC at 298.15 K, and the HLC corrected by temperature and salinity,

Introduction

respectively. $-\Delta U_{AW}$ is the enthalpy of phase change (kJ mol^{-1}), T_0 is the sea surface temperature (K), and 1.3 is the correction factor for accounting the effect of salinity on POP solubility in seawater. Briefly, HLC increase at higher salinities and for higher temperatures (Rice et al., 1997).

3.4 Octanol-air partition coefficients (K_{OA}) and Gas-particle partition coefficients (K_p)

The octanol air partition coefficient (K_{OA}) is defined by:

$$K_{OA} = \frac{C_{Oct}}{C_G} \quad [1.15]$$

Where C_{Oct} and C_G are the concentration of the chemical in the octanol phase and in the gas phase (ng m^{-3}) at equilibrium. Since there are very few measurements of K_{OA} , it is usually derived from HLC and K_{OW} following (Kömp and McLachlan, 1997; Harner and Bidleman, 1998; Shoeib and Harner, 2002):

$$K_{OA} = \frac{K_{OW}(RT)}{HLC} \quad [1.16]$$

However, there is a non-negligible uncertainty in the measurements and estimations of K_{OW} , HLC , K_{OA} , the influence of temperature on their values, and also differences in the activity of dry and wet octanol used for the estimation of K_{OW} (Meylan and Howard, 2005).

K_{OA} is appropriate for predicting the gas-particle partitioning of organic compounds, which in turn it is also important to predict the magnitude and relevance of the different atmospheric deposition processes. The gas-particle partition coefficient (K_p), (Pankow, 1994) is defined by:

$$K_p = \frac{C_{Aero}}{C_G TSP} \quad [1.17]$$

Introduction

Where C_G , (ng m^{-3}) and C_{Aero} , (ng m^{-3}) are the gas and aerosol phase concentration, and TSP is the total suspended particulate matter in the atmosphere (mg m^{-3}). The fraction of aerosol bound POPs is calculated following:

$$\theta = \frac{C_{Aero}}{C_{Aero} + C_G} \quad [1.18]$$

Combining equation 12 and 13 results:

$$\theta = \frac{K_P(TSP)}{1 + K_P(TSP)} \quad [1.19]$$

K_P has been reported to correlate with K_{OA} (Pankow, 1994; Finizio et al., 1997). Further, it has been described that aerosol soot carbon influences K_P (Dachs and Eisenreich, 2000; Buchelli and Gustafsson, 2003). So, K_P is also driven by the adsorption to soot phase, using the soot air partition coefficient (K_{SA} , $\text{m}^{-3} \text{kg}^{-1}$) and elemental carbon resulting. However, the influence of soot carbon is only relevant for planar compounds, such as dioxins and polycyclic aromatic hydrocarbons (PAHs), but not for other legacy POPs such as PCBs. Thus,

$$K_P = f_{OM} \frac{\zeta_{OCT}}{\zeta_{OM}} \frac{MW_{OCT}}{MW_{OM} \rho_{OCT}} K_{OA} + f_{EC} \frac{a_{EC}}{a_{OC}} K_{SA} \quad [20]$$

Where f_{OM} and f_{EC} are the mass fraction of organic matter and elemental carbon in the atmospheric particles, MW_{OCT} and MW_{OM} are the molecular mass of the octanol and organic matter respectively, ρ_{OCT} is the octanol density, a_{EC} and a_{OC} are the surface area of elemental carbon (field and reference values). This equation is usually simplified assuming that:

$$\frac{MW_{OCT}}{MW_{OM} \rho_{OCT}} = 1 \quad [1.21]$$

and

$$\frac{\zeta_{OCT}}{\zeta_{OM}} = 1 \quad [1.22]$$

Introduction

K_P is important in order to estimate the contribution of the particulate and the gaseous phase to depositional inputs to the ocean (Jurado et al. 2004, 2005), and it is temperature dependent, becoming higher in cold environments.

3.5 Fugacity as a criterion for equilibrium between environmental media

Fugacity (f) is a concept widely used to investigate the environmental partitioning of non-ionic organic chemicals, including the air-water equilibrium or dis-equilibrium (Mackay et al. 1979). The word fugacity comes from the Latin word *fugere* that means *fly* or *run away* from a determined place. Fugacity is commonly defined as the escaping tendency of the studied compound from a phase (water, air, soil, biota, sediments,...). In environmental modelling, fugacity gives us information about the tendency for diffusion of a selected chemical compound from one phase to another phase (for example, air and water). At equilibrium, the fugacity of the chemical is equal in the different compartments. There is a net diffusion of chemicals from high to low fugacity phases until equilibrium is reached. Fugacity in the case of gases is equal to the partial pressure (Pa) and in consequence it is directly related with the concentration of the selected compound, in the gas phase. The fugacity of a chemical in a given environmental compartment or phase (f_x) is estimated by

$$f_x = \frac{C_x}{MWZ_x} \quad [1.23]$$

Where C_x is the concentration of a selected compound in the studied phase (g m^{-3}), MW is the molecular weight of a selected compound (g mol^{-1}) and Z_x is the fugacity capacity ($\text{mol m}^{-1} \text{Pa}^{-1}$), which describes the capacity of the phase or environmental compartment to retain the selected compound. In the case of the air and water, Z_A and Z_W are:

$$Z_A = \frac{1}{RT} \quad [1.24]$$

$$Z_w = \frac{HLC}{RT} = HLC' \quad [1.11]$$

Introduction

The advantage of working with fugacities instead of concentrations is because the direct comparison of fugacities in the different compartments provide information on the direction of the net exchange or the occurrence of equilibrium conditions. The fugacity ratio between the air and water ($f_w f_A^{-1}$) is widely used in the literature on POPs cycling in the environment, and it is given by,

$$\frac{f_w}{f_A} = \frac{C_w H'}{C_G} \quad [1.25]$$

When $f_w f_A^{-1}$ is close 1, it means that the compounds are close to equilibrium between air and water. $f_w f_A^{-1} < 1$ indicates that there is a net deposition from air to water, while for $f_w f_A^{-1} > 1$ there is a net volatilization from water to air. It is noteworthy that the ratio of fugacity has some critics (Hoff, 1994; Bruhn et al., 2003) because of the uncertainties associated to the fugacity estimations. It is assumed that uncertainties associated to values of R , T and MW are negligible compared to those associated to C_G , C_w and HLC (Bruhn et al., 2003). The uncertainty associated to C_G and C_w measurements for a single laboratory is of ≈ 0.15 . HLC uncertainty has been considered larger ≈ 1 (Bruhn et al., 2003), however Li and collaborators (2003) recently estimated a more appropriate value of ≈ 0.3 for the uncertainty of HLC . In light of the above uncertainty on the fugacity estimations, it was proposed a more appropriate range of fugacity ratios for assessment of the direction of exchange in which $f_w f_A^{-1} < 0.3$, $0.3 < f_w f_A^{-1} < 3.1$, and $f_w f_A^{-1} > 3.1$ points that there is net deposition, close to equilibrium conditions, and net volatilization between the air and water, respectively.

In figure 3 are summarized all the physicochemical properties (vapour pressure, solubility in water and octanols) and partition coefficients among air, water, octanol, organic and inorganic phases.

Introduction

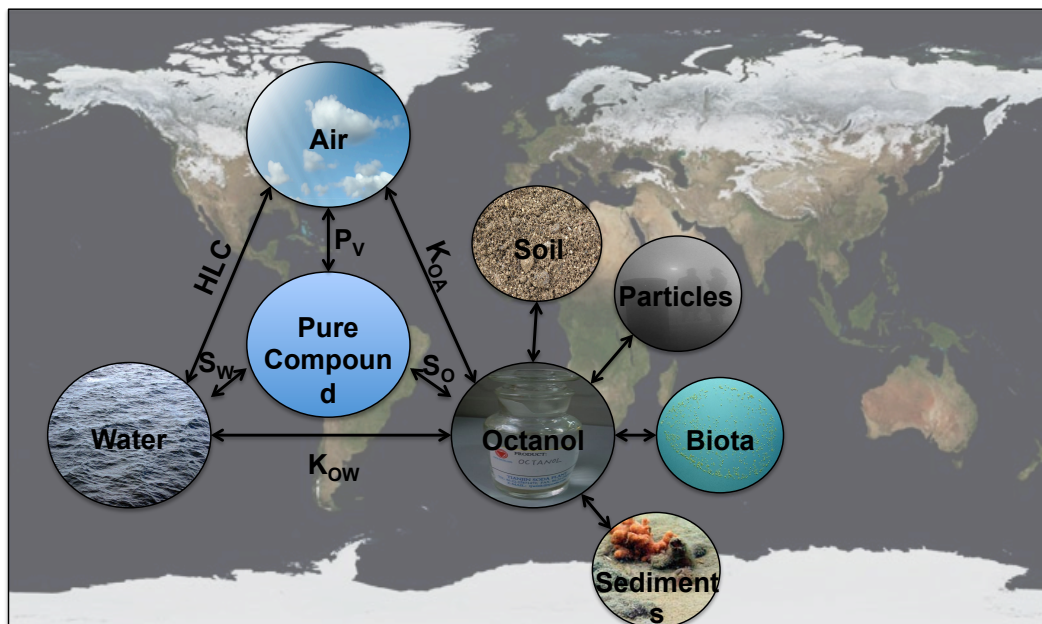


Figure 3. Summary of the partition coefficients among air, water, octanol, organic and inorganic phases

4. Global transport and dynamics of POPs: Role of the atmosphere and oceans

4.1 Sources of POPs to the Environment

In the last fifty years, the amount of studies investigating the sources and emissions of POPs has been increasing considerably at both regional and global scales (Nizzetto et al. 2010). Despite all this research effort, considerably discrepancy and uncertainty exist for the emissions and source type for POPs, even for those that have been studied for 50 years, such as PCBs. There are two main types of sources of POPs:

Primary sources. Primary sources for POPs include all the sources that involved intentional or unintentional release of POPs to the environment by humans or anthropogenic activities. Among them, we can mention industrial and agrochemical use for PCBs and Pesticides as a source to the environment due to intentional use. Conversely, during combustion processes at high temperature it is possible that there is the release of PCDD/Fs, which is unintentional. Other unintentional primary sources are, hazardous waste incineration (Thacker et al., 2013), waste landfills (Gioia et al., 2011; Breivik et al., 2011), by products of

Introduction

certain industrial processes or products (Lundin et al., 2013). The study of primary sources from a quantitative point of view has been very difficult due to the lack of information on production, types of use, waste procedures, etc, for the different organic chemicals used by humans. Even the estimated emissions of legacy POPs such as those for PCB (Breivik et al. 2002a, 2002b and 2004), the uncertainty is high, and current though is that the real emissions were higher than the higher end estimates given in that assessment.

Secondary sources: Secondary sources of POPs are those that involve remobilization of POPs from environmental compartments where they were accumulated or trapped after environmental release from primary sources. These reservoirs can be soils, sediments, vegetation, ice, surface waters... It is well known that due to international legislations the primary sources have clearly been reduced (Li et al., 2005; Breivik et al., 2007; Schenker et al., 2008; Hassanin et al., 2005) and the remobilization from the environmental compartments (secondary sources) become more important. In addition, changing environmental conditions due to human activities, or climatic change in particular, are also increasing the secondary sources of POPs to the environment. (Dalla Valle et al., 2007; Nizzetto et al., 2010, Ma et al. 2011). The secondary sources of POPs are more relevant in remote regions where primary emissions have always being of limited magnitude

4.2 Global transport of POPs

The atmospheric compartment is critical in the global distribution of POPs, even more for the remotest environments. Emissions from primary and secondary sources to the atmosphere and the subsequent transport by atmospheric circulation (Barrie, 1992), provide a very efficient mechanism to distribute POPs globally, followed by deposition. Atmospheric deposition is the major process of POPs input to oceans especially in open sea and the remote oceans (Bidleman, 1988; Iwata et al., 1993; Macdonald et al., 2000, Jurado et al. 2004, 2005). Even though oceanic currents play a role on the long range transport of non-volatile organic pollutants such as perfluorinated acids (Prevedouros et al., 2006), they role as a transport vector of semivolatile organic compounds is thought to be of minor magnitude when compared with the atmosphere. However, oceans also play a key

Introduction

role in the cycling of POPs globally. First, oceans are an important reservoir of POPs (Jurado et al. 2004), second in importance after soils if we consider the surface oceans (Dalla Valle et al. 2005), but it could be the main reservoir if the deep ocean was considered. In addition, the ocean is thought to be one of the main sinks for most POPs (Dachs et al., 2002, Lohmann et al. 2013). The other main global sink is degradation, and the main “chemical reactor” of planet Earth is the atmosphere.

Once POPs are atmospherically deposited to the ocean, they enter the biogeochemical cycles occurring in the surface ocean. Since POPs are hydrophobic, these cycles are closely linked with the cycle of organic carbon. Thus, once in the water column, POPs may bioconcentrate and bioaccumulate in planktonic organisms, and thus enter the food chain. In order to understand the sources of semivolatile POPs to the ocean, it is key to quantify the atmospheric deposition of POPs. In the atmosphere, POPs can be found in the gas and the aerosol phases, and POPs can be removed from the atmosphere following three main mechanisms that affect differently those POPs found in the gas and aerosol phase. The three main mechanisms are; diffusive air-water exchange, dry deposition or aerosol-bound POPs, and wet deposition by scavenging of gas and aerosol phase POPs. The diffusive exchange is a bidirectional process while the dry and wet depositions are unidirectional. Once POPs enter the water compartment, POPs can be found either in the dissolved phase (C_w), sorbed to particles (C_p), or in other major pools of marine organic carbon such as phytoplankton (C_{phyto}). Since the direction of POPs diffusive exchange is bidirectional POPs can revolatilize back to atmosphere, remain in seawater, or they could be exported through the water column to sediments. As a final sink sediments are an important reservoir of POPs, and even though there are virtually no measurements, it is thought that meso-pelagic and deep waters could also be important reservoirs of POPs. The proximity of coastal or ice-covered areas may account for additional sources of POPs to oceans. For example, freshwater discharge from rivers and seasonal ice melting is an important input of POPs to the Arctic ocean (Carrizo and Gustafsson., 2011). Also, ice could act as an important secondary source to the atmospheric compartment in polar areas during the summer periods (Gioia et al. 2008, Cabrerizo et al. 2013).

Introduction

At local, regional and global scale, the partitioning processes driven by diffusion, such as air-water diffusive exchange, tend to drive the concentrations in the different compartment to equilibrium. However, other processes not driven by diffusion such as advection, degradation or sedimentation drive the system away from equilibrium. Thus the distribution of POPs in the environment is a dynamic process influenced by climatic conditions, biogeochemical processes, air and water mass movement and geographical range.

One of the first environmental variables being studied was temperature, and it was found that gas phase concentrations tend to increase during warm periods. This phenomena and the ubiquitous occurrence of POPs in polar areas, led Wania and Mackay to suggest the global distillation theory in a seminal paper (Wania and Mackay 1996). In this theory, the earth system was treated as a distiller, and it was suggested that semivolatile chemicals would show a net volatilization from warm regions (sources) and a net deposition to cold areas (sinks). Another major driver of the POP reservoirs and cycling is organic matter. Regions where there is higher organic matter content in soils or the surface ocean will tend to act as main reservoirs of POPs, thus trapping POPs during their atmospheric transport. The more volatile POPs, which are also the less hydrophobic may have a higher capacity for long range transport, which is consistent with their higher abundance in the Arctic (Macdonald et al. 2000). This was called the global fractionation, first though to be due to cold trapping leading to a latitudinal fractionation, also observed in other regions with gradients in temperature and organic matter (Wania and Mackay, 1996, Beyer et al., 2000; Bignert et al., 1998; Ockenden et al., 1998; Agrell et al., 1999; Grimalt et al., 2001; Wengman et al., 2006). Latitudinal fractionation over oceans and soils has been observed only in the case of latitudes higher than 60° N (Sobek and Gustafsson, 2004; Meijer et al., 2003). The study of the influence of organic matter on the global distribution of POPs have gained importance during the last decade, and it was first observed in soils (Meijer et al., 2003).

Introduction

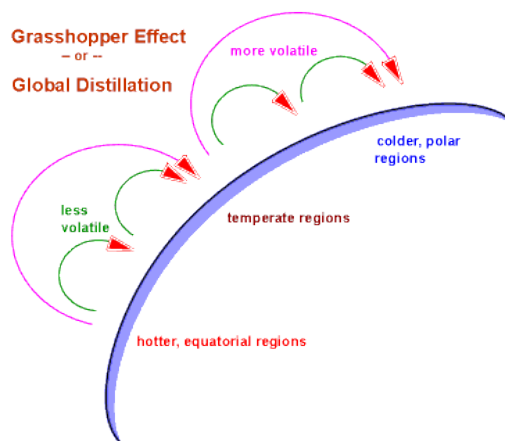


Figure 4. Schematics of the global Distillation and fractionation of POPs (Wania and Mackay, 1996). Adapted from *Environmental Canada*

In the ocean, phytoplankton is an important pool of organic matter, and in addition plays a key role in the biological pump. Several field studies have described the occurrence of POPs in sinking organic matter particles (Dachs et al. 1999, Dachs et al., 2000 Lipiatou et al. 2003). This sinking flux of POPs bound to organic matter may decrease the POP concentrations in the surface ocean, thus modifying the magnitude of the diffusive air-water exchange. Dachs et al. (2002) suggested that this process was an additional control on the global distribution of POPs, but this work was based on environmental models. The same models can be used to assess the atmospheric residence time and grasshopping potential of POPs (Jurado and Dachs, 2008), which have showed that the atmospheric residence time of hydrophobic POPs are lower in the high productive regions in the North Atlantic/Arctic Ocean, and the souther Ocean (Figure 5). Also it was suggested that exportation of POPs bound to particles trough the food chain are an important loss system over productive areas (Scheringer et al., 2004). All the mentioned processes have in common one concept, the organic matter plays a key role in the distribution of POPs in oceans, but unfortunately this process was studied more in depth for terrestrial ecosystems (Eisenberg et al., 1998; Wania and McLachlan, 2001; Cabrerizo et al., 2011) or lakes (Nizzetto et al., 2012) rather than oceans. Only recently, field studies have been pointed out that organic matter is an important driver of POPs fate in the environment (Nizzetto et al., 2010; 2012, Berrojalbiz et al. 2011).

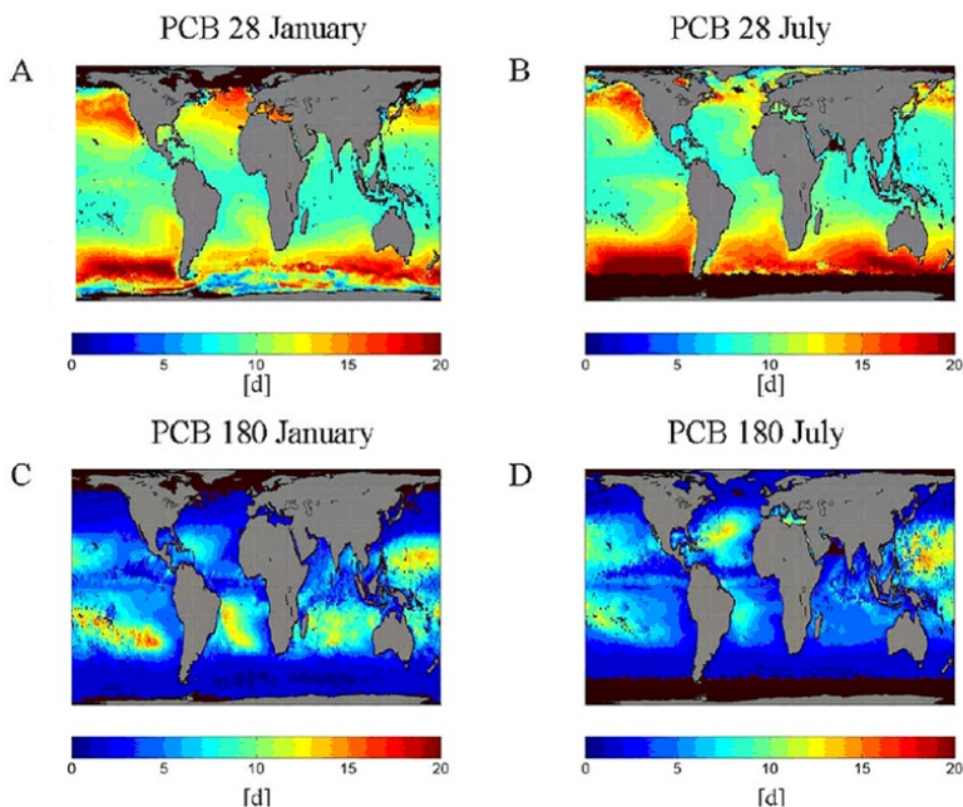


Figure 5. Atmospheric residence times for PCBs 28 and 180 over the global Oceans. The short atmospheric residence times over the Polar Oceans were due to the influence of the biological pump (Jurado & Dachs 2008).

4.3 Carbon cycle and biogeochemical controls on POPs

According to the foregoing, it is clear that the organic carbon is a significant driver of POPs biogeochemical cycling. Most of the aquatic partitioning coefficients for POPs correlate with K_{OW} . Organic carbon in the sea has been considered to be in two operational fractions (Figure 6) i) the dissolved organic carbon (*DOC*) and ii) the particulate organic carbon (*POC*). The difference between these two phases is purely operational and due to the methods used for their isolation; *DOC* has been defined as the carbon that flows through a 0.4-0.7 μm pore size diameter filter and the fraction retained in the filters is the *POC* (Lalli and Parsons, 1997; Valiela, 1995). Also *DOC* could be separated in two fractions, the truly dissolved and the colloidal phase (Gustafsson et al., 2001) being the truly dissolved the most abundant ranging from 50% to 80% of total *DOC* (Wells and Goldberg, 1992; Kepkay, 1994; Kepkay et al., 2000)

Introduction

The *DOC* phase covers a vast number of nano-particles and aggregates of different sizes ranging from humic acids to proteins, lipids or even viruses and small bacteria. Important progresses had been made recently about the potential role of *DOC* on POPs cycling in freshwater and seawater systems and also its influence on the accumulation of POPs (Gustafsson et al., 2001, García-Flor et al., 2005; Katsoyiannis and Samara, 2007; Nizzetto et al., 2010; 2012). However, due to methodological limitations, there is still a gap in our knowledge of the role of the colloidal fraction on POPs cycling.

The *POC* fraction includes larger particles from biogenic origin like big bacteria, phytoplankton and zooplankton, fecal pellets, detritus... All of these particles could be dead or alive. Meanwhile, while *DOC* lacks of migration capability, a fraction of *POC* is able to move through water column (i.e migration movements or by gravitational settling). In effect, the influence of *POC* on POPs cycling has received more attention than *DOC*.

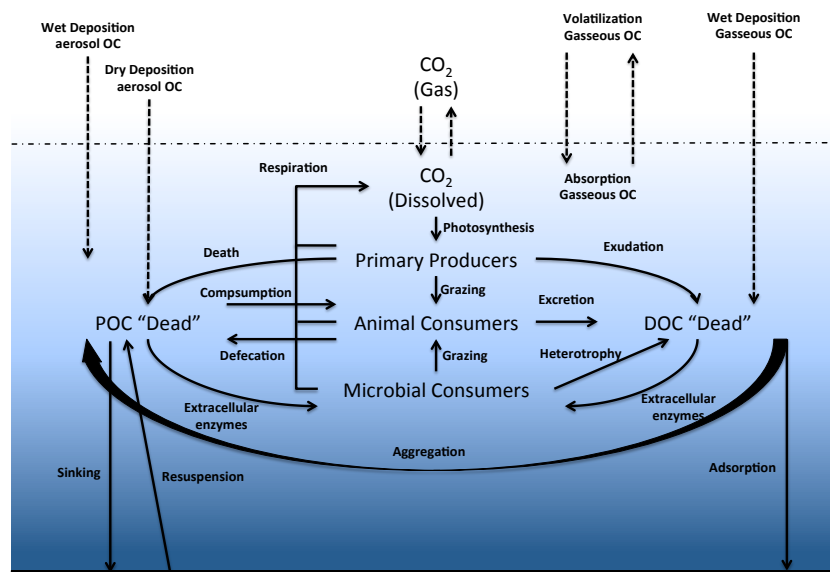


Figure 6. Carbon Cycle in marine systems, adapted from Valiela (1995)

Over-simplifying the carbon cycle, there are two principal processes of the organic carbon cycling in the oceans, the fixation of dissolved CO₂ and the grazing over phytoplankton by the zooplankton or the grazing of the microbial community over phytoplankton and zooplankton (Figure 6). The interaction of these three compartments generates *DOC* and *POC*. So far, the incorporation of POPs in the marine organic matter as coupled to these processes has not been

Introduction

assessed deeply, and only until recent years these processes have received some attention. Thus there is an important uncertainty regarding the processes involved in the biogeochemistry of POPs (Arnot and Gobas, 2006). However, published results in the last decade highlighted the potential role of the different OC pools on POPs cycling. For example, Berrojalbiz et al. (2011) has shown that POP concentrations in phytoplankton from the Mediterranean Sea are lower when the biomass is higher, a result consistent with the role of the biological pump. Recently, Nizzetto et al., in 2011 assessed the coupling between the phytoplankton biomass dynamics and the distribution and fate of persistent organic pollutants (POPs) in a lake pelagic ecosystem, concluding that during high productivity periods (algal blooms) the food web transfer of POPs is less efficient than the exportation of POPs to deep waters by means of the biological pump and *POC* sedimentation. Also it has been found that copepods are able to sequester considerable amounts of POPs through the water column due to its vertical migration (Pucko et al., 2013; Bidleman et al., 2013) and through faecal pellets production and sedimentation (Borga et al., 2002a; 2002b; Hoekstra et al., 2002; Fowler and Knauer, 1986; Dachs et al., 1996), thus exporting POPs to deep water and sediments, and also transferring POPs through the food chain (Sobek et al., 2006b; Berrojalbiz et al., 2009). Little is known about the role of microbial communities' effect on POPs cycling, regardless that on the other hand it has been demonstrated that their role is one of the most important in organic matter cycling over *DOC* and also over *POC* (Wallberg and Andersson, 2000). Most of the work on the microbial influence on oceanic POPs has focused on HCHs. It has been reported that microbes could degrade HCHs in the water column (Harner et al., 1999; 2000) and contribute as a significant sink of HCHs (Pućko et al., 2011). Besides of this pioneering studies, there are gaps in our knowledge, such as a quantitative assessment of the role of OC remineralization on POP cycling.

Global change is an important modulator of the carbon cycling, and it is logical to think that the POPs cycling will be affected in a similar way by remobilizing POPs from reservoirs or altering the food chain transfer, and so forth. Because of that is important to investigate the linkages between these two cycles. This is especially relevant in the Polar Oceans, where global change is clearly apparent

Introduction

5. POPs cycling in the Polar Oceans

Figures 7 and 8 summarize the major contaminant pathways between the atmosphere and the polar surface environments including sea surface, snow/ice and lakes. The study of POPs cycling in the environment is complex due to constant changing of the environmental conditions (ice melting, ice break-up...). Here we examine the main pathways for POPs in polar environments including degradation in the atmosphere and surface waters, and exchange processes between the atmosphere and seawater, and the transport of POPs from surface waters to the deep ocean. Even though these processes have been assessed individually for the Polar oceans, mainly the Arctic, there are very few previous studies that consider the different atmospheric deposition processes and their coupling with the water column biogeochemical processes affecting POPs.

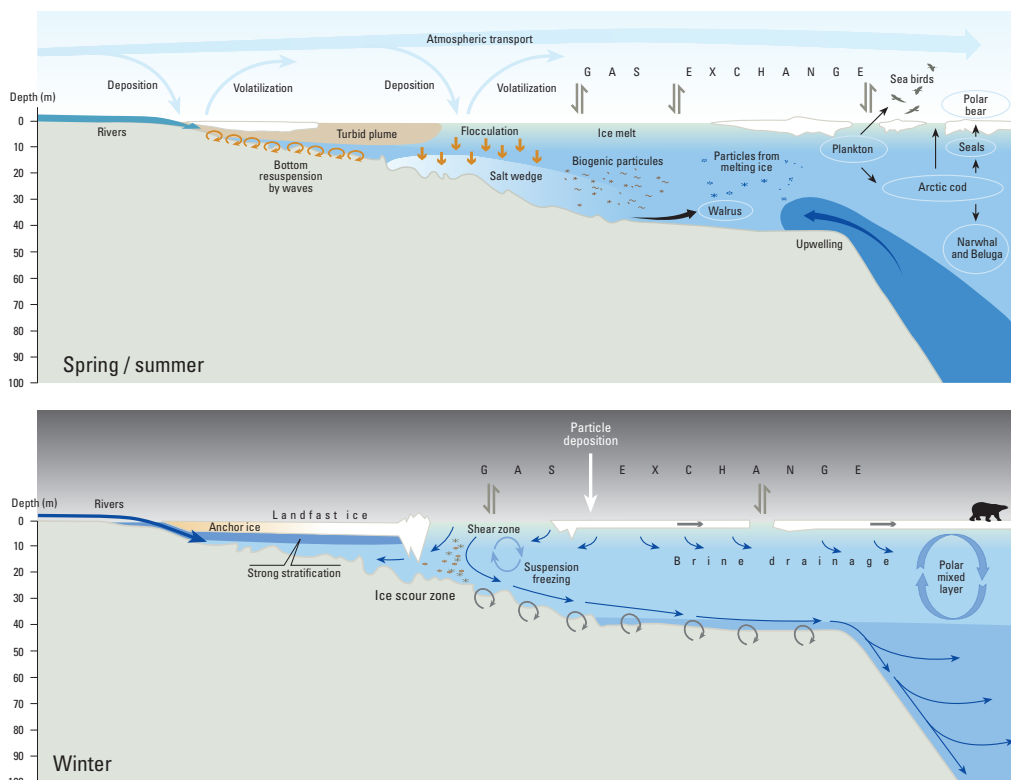


Figure 7. Representation of the POPs distribution and cycling during Spring/Summer and Winter in the Arctic environment. This example is also applicable for the Antarctic region. Reproduced from AMAP Assessment Report (AMAP, 1998).

5.1 Atmospheric degradation of POPs

The main degradation process of POPs in the atmosphere is by reaction of gas-phase compounds with hydroxyl radicals (OH). It has been hypothesized that

Introduction

reaction with OH is a dominant loss flux over water masses (Anderson and Hites, 1996). In addition, it has been shown that PCBs are depleted significantly due to the oxidative attack of hydroxyl radicals in temperate regions (Mandalakis et al., 2003). Later studies reported that hydroxyl radical oxidation was overestimated (Axelman and Gustafsson, 2002). Further, Jaward and colleagues (2004) reported that diurnal variations on POPs concentrations in the oceanic atmosphere were not related to OH radicals influence, only, revealing that there are another underlying process which influence strongly the atmospheric concentrations, probably related to atmosphere-ocean exchange driven by the organic carbon cycling.

The atmospheric degradation due to OH radicals process is parameterised ($\text{ng m}^{-2} \text{d}^{-1}$) by:

$$F_{Deg_{OH}} = hk_{OH}C_{OH}C_G \quad [1.26]$$

Where h is the averaged atmospheric boundary layer (m), k_{OH} is the degradation rate constant in the air ($\text{m}^3 \text{molec}^{-1} \text{d}^{-1}$), C_{OH} is the OH radical concentration (molec m^{-3}) and C_G is the POPs concentration in the gas phase (ng m^{-3}). OH radical concentrations are strongly influenced by the sunlight being higher during the day and negligible during the night. It has been reported that concentrations in the North Atlantic are 25 times lower than at mid-latitudes. The concentrations of atmospheric OH hydroxyl radicals in the air can be estimated from the temperature following (Beyer et al., 2003):

$$C_{OH} = (0.5 + 4(T - 273.15)) \cdot 10^5 \quad [1.27]$$

However, the atmospheric degradation by other atmospheric free radicals has not been assessed although there are reported considerable concentrations of BrO, ClO, IO (Barrie and Platt, 1997).

Introduction

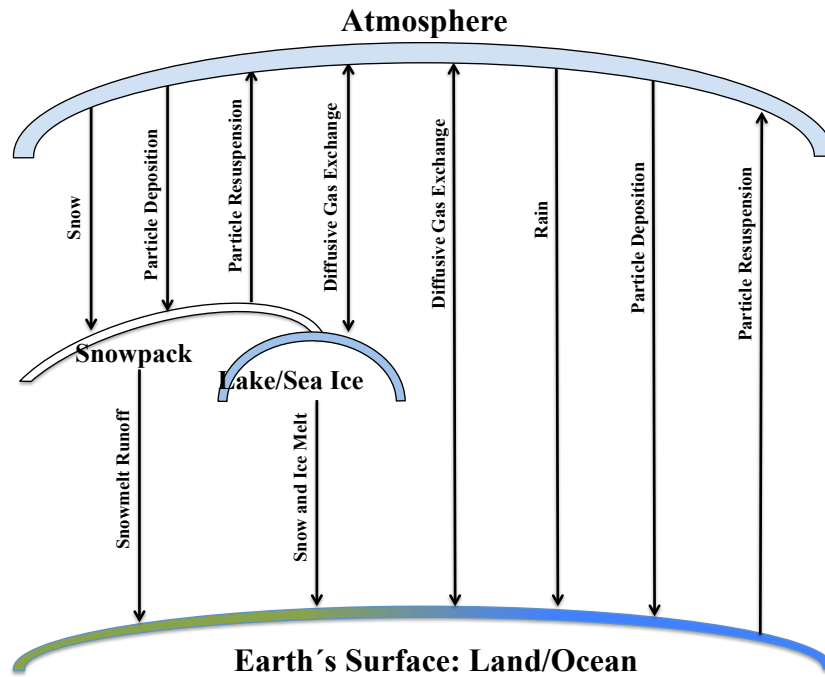


Figure 8. Schematics of the processes of atmosphere-surface exchange (Barrie et al., 1997)

5.2 Atmospheric-surface exchange and ice melting.

Figure 7 summarizes the POPs pathways between the atmospheric compartment and the surface including terrestrial and oceanic compartments. The cycling of POPs in Polar areas is more complex than in other oceans due to the presence of intermediate compartments (i.e. snow and ice).

5.2.1 Diffusive exchange between the atmosphere and oceans.

Diffusive exchange between the atmosphere and water is a two-direction process. The diffusive exchange between water and air is traditionally described by the two-film model (Liss and Slater, 1974). The rate of transfer is assumed to be limited by molecular diffusion across the thin air and water films at the interface. It can be estimated by:

$$F_{AW} = F_{ABS} - F_{VOL} = k_{AW} \left(\frac{C_G}{HLC'} C_W \right) \quad [1.28]$$

Where C_G and C_W are the concentrations of dissolved and gaseous POPs in water and air (mol m^{-3}), k_{AW} is the mass transfer coefficient (m d^{-1}) between the air

and water, H' is the dimensionless Henry's law constant. These relationships have been applied extensively to study the exchange of POPs in the Arctic, such as those of HCHs (Bidleman and McConnell 1995; Cotham and Bidleman, 1991; Jantunen and Bidleman 1995) or PCBs (Gioia et al., 2008). It is important to note that gas exchange takes place even under equilibrium conditions, when absorption and volatilization are balanced and the net air-water diffusive flux is zero. Thus the mass of material transported by gas exchange is much larger than is apparent from the net flux. For this reason Murphy (1995) suggested that gas exchange must be calculated as two separated terms one for volatilization and one for absorption. The Arctic Ocean represents the largest reservoir of contaminants in the Arctic with a total burden thousands of times greater than air, thus the air-water exchange represents the most important potential source of POPs for the Arctic atmosphere (Jantunen and Bidleman, 1995).

5.2.2 Dry deposition

The dry deposition flux is the deposition of aerosol bound contaminants in the absence of precipitation. Also, dry deposition can account for a large portion of the removal of trace chemicals from the troposphere (Wesely and Hicks, 2000). The atmospheric transport and subsequent sedimentation brings airborne particles to the surface layer (snow, ice, land, ocean) coming from the atmosphere. Then, due to processes of convection, diffusion and impactation, aerosols are trapped on the surface (Voldner et al., 1986). Particle transport rate depends on the type of surface, POPs properties and atmospheric state. Dry deposition can be calculated following (Baker and Hites, 1999):

$$F_{DD} = v_D C_{Aero} [29]$$

Where F_{DD} is the dry deposition flux ($\text{ng m}^{-2} \text{d}^{-1}$), v_D is the dry deposition velocity (m d^{-1}) and C_{Aero} is the concentration of POPs in the aerosol phase (ng m^{-3}). v_D depends on particle size, wind speed, atmospheric stability, and particle composition and properties (Williams, 1982, Jurado et al. 2004). The only field measurements of dry deposition of aerosol bound organic pollutants over the ocean suggest that v_D has a value around 0.1 cm s^{-1} (Del Vento & Dachs 2007). In the case of the Arctic, most of the aerosols that reach the region are smaller than

Introduction

1 μ m and for this size the v_D reported from different studies ranged from 0.05 to 0.1 cm s⁻¹ (Ibrahim et al., 1983; Davidson 1989), consistent with the measurements done over the subtropical ocean (Del Vento et al. 2007). This v_D values have been used to estimate the dry deposition of POPs in the Arctic and Subarctic areas (McVeety and Hites, 1988; Jantunen and Bidleman, 1995).

5.2.3 Wet deposition

Wet deposition is a process that includes the deposition of contaminants incorporated to the rain or falling snow (Barrie et al., 1992). Rain and snow scavenges both POPs from the gas and aerosol phase. It is a very efficient process, but with an intermittent intensity. Wet deposition (F_{WD}) can be estimated following (Bidleman, 1988):

$$F_{WD} = p_0 C_{R/S} = p_0 W_P (C_P + C_G) \quad [30]$$

Where p_0 is the precipitation rate (m s⁻¹) and $C_{R/S}$ is the concentration of contaminants in the rain or snow defined by:

$$C_{R/S} = W_P (C_{Aero} + C_G) \quad [1.31]$$

Where W_P is the scavenging ratio for POPs defined as the ratio of POPs concentration in the rain/snow and the total atmospheric concentrations ($C_{Aero} + C_G$). W_P could be considered as a partition coefficient defined based on the particle and gaseous washout (W_{PW} and W_{GW}) (Ligocki et al., 1985a;1985b, Bidleman, 1988), and it can be estimated by:

$$W_P = W_{GW} (1 - \theta) + W_{PW} (\theta) \quad [1.32]$$

Where θ is the fraction of POPs bound to aerosols. W_{GW} is the ratio of the rain/snowflake dissolved phase to gas phase POP concentrations, rapid equilibrium is assumed between the gas phase and the dissolved phase in the rain drops or snow flake. Therefore, W_{GW} equals the inverse of the *HLC*. Conversely, reported W_{GW} from field measurements have been found to be higher than estimated using the *HLC* (Dickhut and Gustafsson, 1995), maybe due to the adsorption of POPs to the rain-drop surface (Jurado et al. 2005). On the other

hand, there is a considerable variability in W_{PW} estimates (Jurado et al. 2005), but a value of 2×10^5 is commonly used for rain (Mackay et al., 1986). Snow has a higher surface area than rain-drops, and thus snow scavenging is even a more efficient deposition process than rain.

5.2.4 Snow and ice melting

Runoffs from snowpack melt, and sea-ice melt delivers water and particulate matter to Polar Oceans. Thus, it is expected that dissolved and particle bound POPs would be delivered too from their winter reservoirs to freshwater and later to oceans or directly to oceans. But recently it has been described that during high wind speed events and/or summer periods, HCHs and PCBs could revolatilize from ice and snow to the atmosphere (Cabrerizo et al., 2013; Kang et al., 2012; Halsall, 2004, Gioia et al. 2008).

5.3 Water column processes.

5.3.1 Degradation.

POP degradation can follow two paths, the biotic (biodegradation by means of microbial activity) and abiotic (hydrolysis and photodegradation). Degradation fluxes ($\text{ng m}^{-2} \text{d}^{-1}$) are given by:

$$F_{DegTot} = F_{DegH} + F_{DegM} + F_{DegP} \quad [1.33]$$

Where F_{DegH} , F_{DegM} and F_{DegP} are the hydrolysis, microbial and photochemical degradation fluxes ($\text{ng m}^{-2} \text{d}^{-1}$) defined as follows:

$$F_{DegH} = hk_{DegH} C_{WDOC} \quad [1.34]$$

$$F_{DegM} = hk_{DegM} C_{WDOC} \quad [1.35]$$

$$F_{DegP} = hk_{DegP} C_{WDOC} \quad [1.36]$$

Where h is the surface water column depth (m), k_{DegH} , k_{DegM} and k_{DegP} are the hydrolysis, microbial and photochemical degradation rates (d^{-1}), and C_{WDOC} is the POPs truly dissolved concentrations (ng m^{-3}). The hydrolysis rate under

Introduction

environmental conditions is extremely low and usually is neglected (Sinkkonen and Paasivirta, 2000). Degradation rates have shown to have a correlation with temperature (Ngabe et al., 1993) being rates much lower in cold surface waters than in temperate or warm waters. The biodegradation by means of microbial communities is presumably highly dependent on the kind of community, even though it has not been studied. Photodegradation in water includes reaction with OH radicals, ozone, nitrogen oxides and other radicals photochemically produced. Photolysis on surface waters occurs mainly in the upper mixed layer and is especially important on coastal waters (Sinkkonen and Paasivirta, 2000). However, C_{OH} is too low to be an important degradation driver in natural waters (Haag and Yao, 1992). It has also been investigated the photodegradation rates for PCBs showing that the half lives of POPs in surface waters ranges from 0.25 to 27 years (Sinkkonen and Paasivirta, 2000). Biodegradation by microbial communities is more important in anaerobic matrices like sediments. But on the other hand, it has been reported that microbial degradation in surface waters is the responsible for the depleting of HCHs in Arctic surface waters and in the water column (Harner et al., 1999; 2001; Púcko et al., 2011), showing that microbial biodegradation is more effective than photolysis in oceanic surface waters (Ngabe et al., 1993) and also responsible of the enantiomeric ratio reported for surface waters (Harner et al., 2000 and Pucko et al., 2011).

5.3.2 Water column exportation processes to deep ocean

5.3.2.1 The biological pump

In the open ocean, the particulate pool is dominated by biogenic matter in the water column. This suspended matter includes two types of particles present in variable proportions and having different spectral properties: living pigmented algal cells, and weakly pigmented or non pigmented particles mainly derived from phytoplankton as well as other living heterotrophs such as bacteria (Brickaud and Stramski, 1990). POPs bound to these two kind of particles. A fraction of the particulate pool sinks to deep water, and because the composition of these particles is rich in organic matter, they scavenge the surface water column of POPs, thus leading to lower concentrations in the dissolved phase. This process enhances the air-water diffusive exchange, a process known as biological pump

Introduction

(Dachs et al., 2002, Jurado & Dachs 2008, Nizzetto et al. 2012). Predicting the flux of organic matter in the ocean is not a simple task, and even though it has received considerable attention by the organic carbon scientific community, there is not an accepted parameterization. Therefore, when available, it is always useful to predict the settling fluxes of POPs from the measured or reported fluxes of organic or biogenic matter (F_{OM} or $F_{Biogenic}$, $\text{Kg m}^{-2} \text{d}^{-1}$), and the concentration of POPs in particles or phytoplankton (C_{POM} , C_{Phyto} , ng Kg^{-1}) by:

$$F_{Sink} = F_{Biogenic} \cdot C_{Phyto} \quad [1.37]$$

$$F_{Sink} = C_{POM} F_{OM} \quad [1.38]$$

Sinking fluxes of POPs through the water column has been pointed as the most important removal process depleting POPs from surface waters (Gustafsson et al., 1997; Dachs et al 2002; Scheringer et al., 2004). The sequestration of POPs by the biological pump, not only controls the concentrations of POPs in phytoplankton, and enhances the fluxes from air to water, but also controls the atmospheric residence time of POPs during their global transport and dispersion processes (Fowler and Knauer., 1986; Gustafsson et al., 1997; Dachs et al., 1999; Dachs and Eisenreich, 2000; Berglund et al., 2001a; 2001b; Dachs et al., 2002; Scheringer et al., 2004; Jurado & Dachs 2008, Berrojalbiz et al., 2011).

5.3.2.2 Turbulent flux and water mass subduction.

Turbulent eddy diffusion fluxes are responsible of the concentration gradients through the water column in stratified waters (Lohmann et al. 2013). This flux causes a homogeneous distribution of pollutants influenced by the effect of eddy diffusion in the water body. This flux is dependent on the turbulent diffusivity of the water mass, and the direction of the flux depends on the concentration gradient from the most concentrated to the less concentrated. However, even though this process is responsible for the vertical transport of non hydrophobic compounds, it is negligible when compared to sinking fluxes for hydrophobic POPs (E. Jurado, personal communication).

Subduction of surface waters associated to the thermohaline circulation, is perhaps the most important physical process in the transport of legacy POPs from

Introduction

the surface to deeper waters (Lohmann et al., 2006). During subduction, the profile of the organic pollutants does not change, since this the magnitude of this process is the same for all compounds regardless of their hydrophobicity (Lohmann et al., 2006). So this process is relatively more important for water-soluble PCBs such as lower chlorinated PCBs (mono, di, tri or tetra-chlorinated) which are not very effectively transported by the biological pump. However, the subduction is a local/regional process associated to deep water formation areas in the Arctic and Antarctic (Lohman et al., 2006). While this work focused the study of subduction transport trough the water column in the Norwegian, Labrador, Weddell and Ross Seas, there are other deep water formation areas both in the Arctic and Antarctica (Hay, 1993). The subduction process has been pointed to be an important sink pathway regionally for PCBs HCHs and HCB (Lohmann et al., 2006). The subduction of water masses (F_{Subd} , $\text{kg m}^{-2} \text{ yr}^{-1}$) could be estimated following Lohmann et al., 2006:

$$F_{Subd} = \frac{C_W r_{Subd}}{a} 3.15 \cdot 10^{-5} \quad [1.39]$$

Where C_W is the dissolved seawater concentration of POPs (pg L^{-1}), r_{Subd} is the rate of deep-water formation in the chosen area (S_V), a is the studied area (m^2) and 3.15×10^{-5} is a conversion factor ($\text{yr L s}^{-1} \text{m}^{-3}$).

Recently, Stemmler and Lammel (2013) pointed that POPs transport associated to deep-water formation is not a final sink but rather an horizontal and vertical global distribution process. Highlighting that finally POPs will be transported to surface in other oceanic regions, or may eventually enter the food chain and reach human population due to development of deep-fisheries (Payne, 2013; Bailey et al., 2009; Domingo et al., 2007).

6. Selected POPs for study

The compounds selected for this study were hexachlorocyclohexanes (HCHs), hexachlorobenzene (HCB) and polychlorinated biphenyls (PCBs). All of them are legacy POPs, thus currently not in use, and cover a wide range of physico-chemical properties. The interest for they study is due to the concern raised by their toxic impacts to organisms and humans, their persistence,

Introduction

bioaccumulation potential and capacity to undergo long range atmospheric transport. They are considered “classic POPs” and even though they were banned or have had a restricted use for decades, they are still globally distributed in the environment.

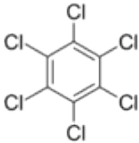
Even though there are thousands of articles reporting the abundance and cycling of these compounds in the environment, the number of them covering the oceanic environment is much reduced, and of only dozens for the Polar Oceans.

6.1 Hexachlorobenzene (HCB)

Hexachlorobenzene’s molecular formula is C_6Cl_6 (see Table 3). It is a fungicide formerly used in wood and seed for crop production. The industrial production of HCB started in 1945 in the USA and it is believed that the production peak of 10000 tonnes per year was in the 70s and 80s (Barber et al., 2005). The highest production during the 70s was in Europe (Rippen and Frank, 1986). It was also a by-product and impurity in many industrial chemical processes (Jacoff et al., 1986). In addition, it has been released to the environment from old dumps and incomplete combustion. However, production and emission data reported in the bibliography are scarce and it is difficult to know the total amount of HCB produced and used in the last 60 years. Its environmental behaviour is determined by its physic-chemical properties. HCB has higher volatility and moderate values of K_{OA} and K_{OW} compared to other legacy POPs. These properties determine that HCB can be considered a “multi hopper” and can be distributed globally in a series of multiple deposition-volatilization steps (Wania and Mackay, 1996, Lohmann et al., 2007). In addition, HCB is highly persistent in the environment, and there is not known degradative process that is relevant for its environmental fate in aerobic conditions.

Introduction

Table 3. Molecular structure and physico-chemical properties of Hexachlorobenzene (HCB). P_V : Vapor pressure, HLC : Henry's Law Constant, $\text{Log}K_{OW}$: octanol-water partition coefficient, $\text{Log}K_{OA}$: octanol-air partition coefficient.

Compound	Chemical Structure	P_V (Pa)	HLC (Pa m ⁻³ mol ⁻¹)	$\text{Log} K_{OW}$ Dimensionless	$\text{Log} K_{OA}$ Dimensionless
HCB		0.303 ^a	5.07 ^b	5.64 ^c	6.78 ^d

^aHincley et al., 1990

^bMackay and Shiu, 1981

^cShen & Wania, 2005

^dHarner & Mackay, 1995

6.2 Hexachlorocyclohexanes (HCHs)

Hexachlorocyclohexanes molecular formula is $C_6H_6Cl_6$ (see Table 4 and Figure 9). Its main use and introduction vector to the environment has been as a pesticide, but in the World War II was used as smog bomb. HCHs are harmful and toxic. It has been reported that chronic exposure is linked to neurological and immunological deficiencies in humans and it has been linked to cancer in rats too (Schulte-Hermann et al., 1981). HCH is usually presented as two commercial formulations, Lindane and technical hexachlorocyclohexane (HCH). Lindane consists almost entirely of γ -HCH and technical HCH contains a total of eight HCH isomers, among which only the α , β , γ , δ and ϵ , isomers are stable and commonly identified. Technical HCH contains a quite constant isomer proportion α , 60–70%; β , 5–12%; γ , 10–12%; δ , 6–10%; and ϵ , 3–4% (Kutz et al., 1991 and Iwata et al., 1993). Around 10,000,000 tons of technical HCH has been released in the last 60 years (Li, 1999a), and 84% was emitted by Northern Hemisphere countries (Li, 1999a). Although technical HCH is no longer generally used, applications of Lindane still continue in many countries and its emissions have been estimated to be 720,000 tons for the last 40 years (Voldner, 1995). In the case of HCHs, there has been a clear trend in the reduction of primary emissions and this trend was clearly correlated with gas phase concentrations measured in the arctic atmosphere for α -HCH (Li and Bidleman, 2003), and for α -HCH and β -HCH concentrations in the air measured at Alert Arctic Station (Li and Macdonald, 2005).

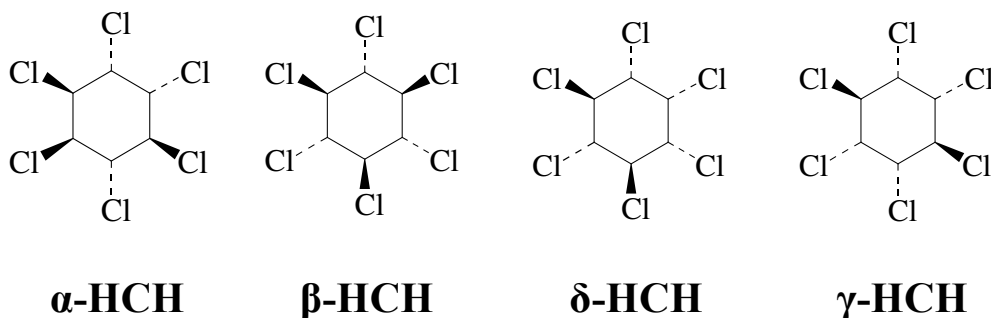


Figure 9. Chemical structure of four isomers of HCHs

HCHs are more soluble in water than HCB, but both have a similar volatility, thus HCH have a lower HLC values. HCH also have the potential to be atmospherically transported by successive steps of deposition and revolatilization. α and γ isomers are the most abundant in the environment and their principal distribution vector in the environment is the Long Range Atmospheric transport, but in the case of β it has been reported that the most important transport way to the arctic was the transport by water masses. This compounds are less persistent than HCB and several processes have been identified that could degrade HCHs in the environment (microbial degradation, atmospheric OH degradation). In addition, it has been noted that isomerization as a result of solar radiation is an important process in the cycling of HCHs.

Table 4. Molecular structure and physico-chemical properties of Hexachlorocyclohexanes (HCB). P_V : Vapour pressure, HLC : Henry's Law Constant, $\text{Log}K_{OW}$: octanol-water partition coefficient, $\text{Log}K_{OA}$: octanol-air partition coefficient.

Compound	P_V (Pa)	HLC (Pa mol ⁻¹ m ⁻³)	$\text{Log} K_{OW}$	$\text{Log} K_{OA}$
α -HCH	0.1 ^a	0.36 ^d	3.94 ^b	7.464 ^b
β -HCH	0.053 ^b	0.023 ^d	3.92 ^b	8.74 ^b
δ -HCH	0.3 ^a	0.165 ^d	4.14 ^f	8.848 ^e
γ -HCH	0.073 ^c	0.0825 ^e	3.83 ^b	7.74 ^b

^aMackay et al., 1992

^bXiao and Wania, 2004

^cWillwet et al., 1998

^dSashuvar et al., 2003

^dSashuvar et al., 2003

^eMajewsky and Capel, 1995

^fHansch et al., 1995

^eShoeb & Harner, 2002

6.3 Polychlorinated biphenyls (PCBs)

Polychlorinated biphenyls are a family of isomers with the molecular formula of $C_{12}H_{10-x}Cl_x$ ($x = 1-10$). The PCBs family includes 209 isomers, even though not all of them are found in the environment. PCBs are formed by electrophilic chlorination of biphenyl with chlorine gas. It was synthesized for the

Introduction

first time in 1865, and later it was produced in low quantities in 1881. The production at large scale was initiated in the 1920s and ended in the 1980s (Breivik et al. 2002a and 2002b). PCBs were produced as complex mixtures with different isomers and different grades of chlorination. PCBs were used in a myriad of applications as coolants and insulating fluids (transformer oil) for transformers and capacitors, as plasticizers, coatings of electrical wiring and electronic components, pesticide extenders, cutting oils, reactive flame-retardants, lubricating oils, hydraulic fluids, sealants, among others.

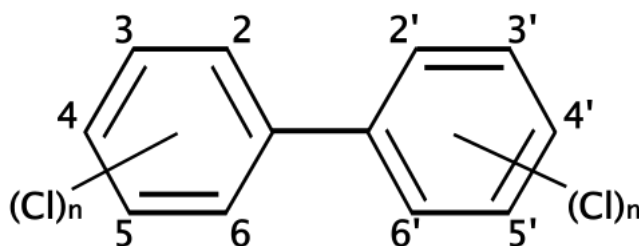


Figure 10. Chemical structure of a generic PCB

From the physical properties point of view, they have high dielectric constants, very high thermal conductivity, high flash points (from 170 to 380 °C)[8]. In addition, they are chemically fairly inert, being extremely resistant to oxidation, reduction, addition, elimination, and electrophilic substitution. Even though the toxicity of PCBs was not recognized initially, later on, many studies reported a direct link between PCBs and Non-Hodgkin Lymphoma (Hardell et al., 1996a; 1996b; 1997; Rothman et al., 1997, Kramer et al., 2012). During 1968, there was an episode of 1800 people sick in Japan caused by the consumption of rice oil contaminated with industrial coolant containing PCBs. Poisoned people suffered of chloracne, intestinal problems and nervous disorders and effects continued during five years after the poisoning event. It was called the Yusho disease (Tsukimura et al., 2012) and similar incident occurred in Taiwan in 1979 (Li et al., 2013). It has been reported that PCBs are also present in human milk, blood and cord blood samples (Carrizo et al., 2006; Vizcaíno et al., 2010), with significant effects on child development.

From the point of view of chemical properties (Table 5), the lower chlorinated PCBs have higher volatility and lower K_{OA} and K_{OW} than the more

chlorinated PCBs. Therefore, the environmental fate and transport will depend on these different properties. Most PCBs are “multihoppers”, but the most hydrophobic congeners are considered as “single hoppers” (Lohmann et al. 2006). The congeners with higher K_{OW} also tend to bioaccumulate and biomagnify more in biota.

Table 5. Molecular structure and physico-chemical properties of Hexchlorobenzene (HCB). P_V : Vapour pressure, HLC : Henry's Law Constant, $\text{Log}K_{OW}$: octanol-water partition coefficient, $\text{Log}K_{OA}$: octanol-air partition coefficient.

Compound	P_V (Pa)	HLC (Pa mol⁻¹ m⁻³)	$\text{Log} K_{OW}$ Dimensionless	$\text{Log} K_{OA}$ Dimensionless
PCB28	0.0234 ^a	30.2 ^a	5.66 ^a	7.85 ^a
PCB52	0.0107 ^a	25.12 ^a	5.91 ^a	8.22 ^a
PCB99	0.00029 ^b	51.8 ^d	6.97 ^b	9.06 ^f
PCB151	0.00019 ^c	73.5 ^d	6.85 ^e	9.68 ^g
PCB180	0.000013 ^a	37.3 ^d	8.51 ^a	10.52 ^f

^aLi et al., 2003

^bHardy, 2002

^cFischer et al., 1992

^dBamford et al., 2002

^eHansch et al., 1995

^fHarner and Bidleman, 1996

^gChen et al., 2002

7. Polar Oceans and the regions of study

7.1 The Arctic

The Arctic region extends across North America, North Europe and North Asia, including the Arctic oceans in between, covering an area of $13.4 \times 10^6 \text{ km}^2$. Formerly it was accepted that the Arctic was delimited by the Arctic Circle from 66° N to 90° N . But also there are other definitions based on temperature, vegetation, ecosystems types, ... Attending to temperature, Arctic is usually defined as the region where the average temperature during the warmest month is below 10° C (Stonehouse, 1986), and the northernmost tree line roughly follows the isotherm boundary of this region (Linell and Tedrow, 1981). The Arctic is known as one of the most fragile ecosystems in the world (Laxon et al., 2003). The raising awareness of the threats to the Arctic has led to the development of several international actions to protect it. The first action was taken in 1996 with the formation of the Arctic Council promoting the Arctic Environmental Protection Strategies (AEPSs) by means of five international programs. These programs by themselves are not independent and also they overlap in an effective network of collaborations. However each has a different purpose.

Introduction

Arctic Monitoring and Assessment Program (AMAP). This program focuses on monitoring and assessment of levels and effects of anthropogenic pollution in the Arctic.

Conservation of Arctic Flora and Fauna (CAFF). This program is responsible of coordination in research on species and habitats of Arctic flora and fauna.

Emergency Prevention, Preparedness and Response (EPPR). This program has the objective to provide a framework for future cooperation in responding to future threats to Arctic environment.

Protection of the Arctic Marine Environment (PAME). This program has the objective to protect and prevent the arctic marine environment from pollution independently of the origin (i.e Oil Spills, diffuse pollution..).

Sustainable Development and Utilization (SDU). This program focuses on the proposition of a sustainable development of the Arctic including the use of renewable resources by Arctic indigenous population.

7.2 Antarctica and Southern Ocean

Antarctica is the Earth's southernmost continent in the South Pole and it is surrounded by the Southern Ocean covering an approximate area of $14 \times 10^6 \text{ km}^2$. The Antarctic region ranges from 60°S to 90°S. The most important difference between the Arctic and Antarctica is that Antarctica is a continent by itself while the Arctic not. The Southern Ocean around Antarctica has a larger sea ice cover, but this is seasonal and thinner than Arctic's ice. However, variations in the formation and destruction of sea ice are less abrupt than in the Arctic (Laxon et al., 2003). The Antarctica, from a climatic point of view is the coldest, driest, and windiest continent on earth. Antarctica is considered a desert, with one of the lowest precipitation of only $200 \text{ mm m}^2 \text{ y}^{-1}$ along the coast and far less inland. Conversely, the maritime Antarctica is a highly productive region, especially around the Antarctic Peninsula. The yearly average temperature of Antarctica is $-57 \text{ }^\circ\text{C}$ but during austral summer is quite higher and similar to Arctic temperature, with averaged values of -12.9°C . However, in the maritime Antarctica the climate

Introduction

is much warmer. The Antarctica, as well as Arctic, has been considered a fragile ecosystem. While the international concern about the fragility of Arctic ecosystems, started in the early 90, the Antarctic treaty was proposed in 1957 and signed in 1961. This treaty regulates the international relations with respect to Antarctic Continent. Antarctic Treaty sets aside Antarctica as a scientific reserve establishing freedom of scientific investigation and banning military activity on that continent (Moore, 2008). During the International Geophysical year (1957), it was proposed that there was a need for further international organization of scientific activities in Antarctica and a regulating committee. In 1957, it was also created the Scientific Committee on Antarctic Research (SCAR). Nowadays, SCAR develops many programs and actions promoting and funding Antarctic and Southern Ocean research. SCAR by means of the Antarctic secretariat acts as a consultive expert council during negotiations and policy making related to Antarctic continent and Southern Ocean waters.

7.3 Regions of study in the Arctic and Southern Ocean

The Southern ocean and the Atlantic sector of the Arctic Ocean are ideal regions to study the coupling between atmospheric deposition and biogeochemical cycling of POPs. These regions have a high primary productivity (Figure 11), and the extent of the biological pump is especially relevant. Therefore, the study of the POP cycling in these regions allow to assess for the first time in the marine environment, the biogeochemical controls that the biological pump exert on the atmospheric transport of POPs, and on the occurrence of POPs in the atmosphere and seawater.

Introduction

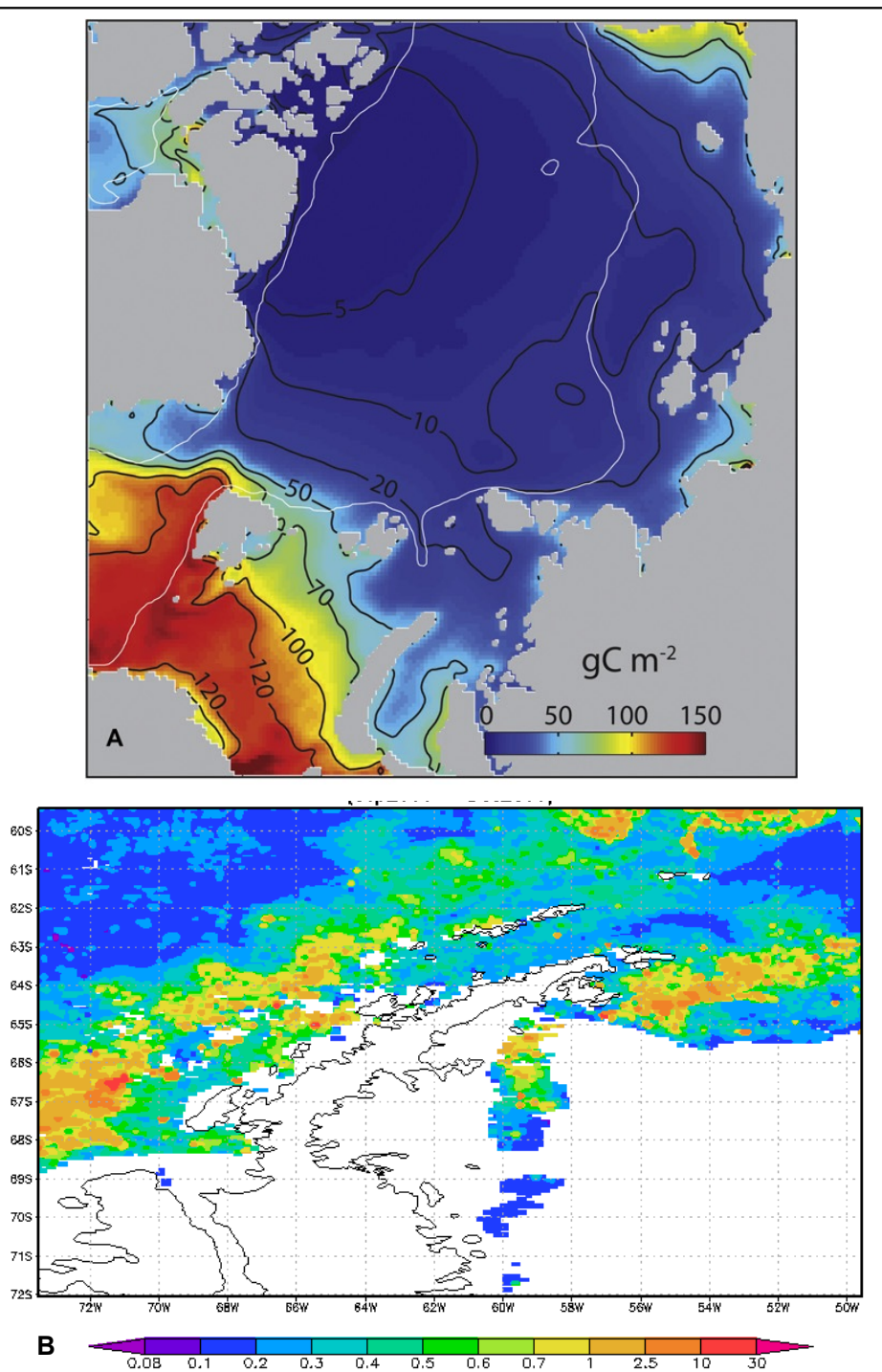


Figure 11. Primary productivity in the Arctic Ocean (g C m^{-2} upper panel) and in the Southern ocean around the Antarctic Peninsula in 2009 (mg Chl a m^{-3} lower panel).

This PhD thesis reports the results from one sampling cruise in the Arctic (ATOS I), and three sampling cruises in Antarctica (ICEPOS, ESSASSI, ATOS II). Figures 12 and 13 depict the ship trajectory during the fourth cruises. The PhD candidate participated in the cruises ATOS I, ESSASSI, and ATOS II, and generated the oceanic and atmospheric POP results for these cruises. The Arctic

Introduction

cruise allowed to study POPs in the North Atlantic and the ice margin region of the Arctic Ocean. The three Southern Ocean cruises, allowed to study the POP transport and cycling in the Bransfield Strait, and the South Scotia, Bellingshausen and Weddell Seas.

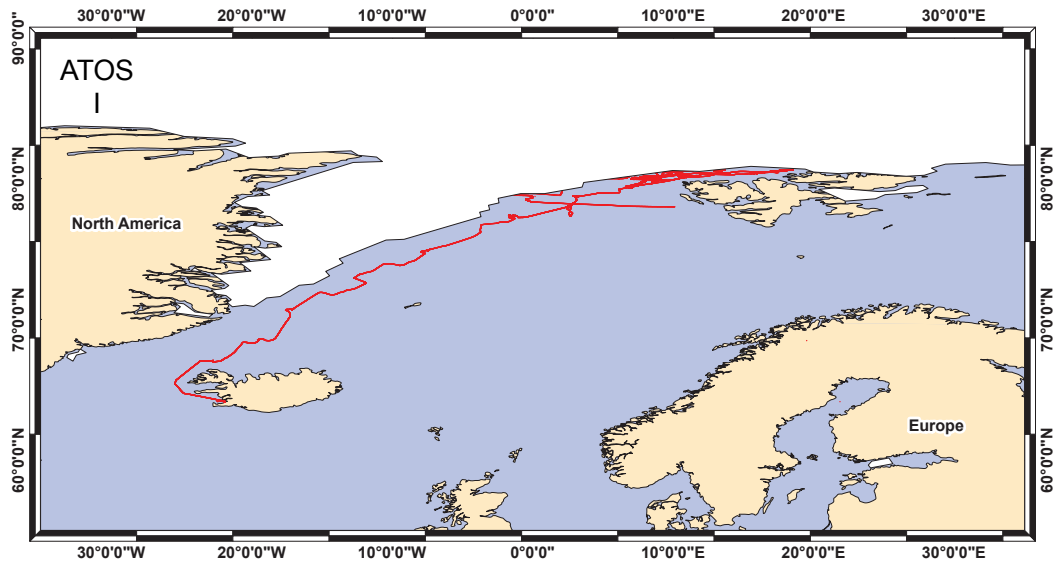


Figure 12. Trajectory of the ship during the ATOS I campaign in the Arctic

Introduction

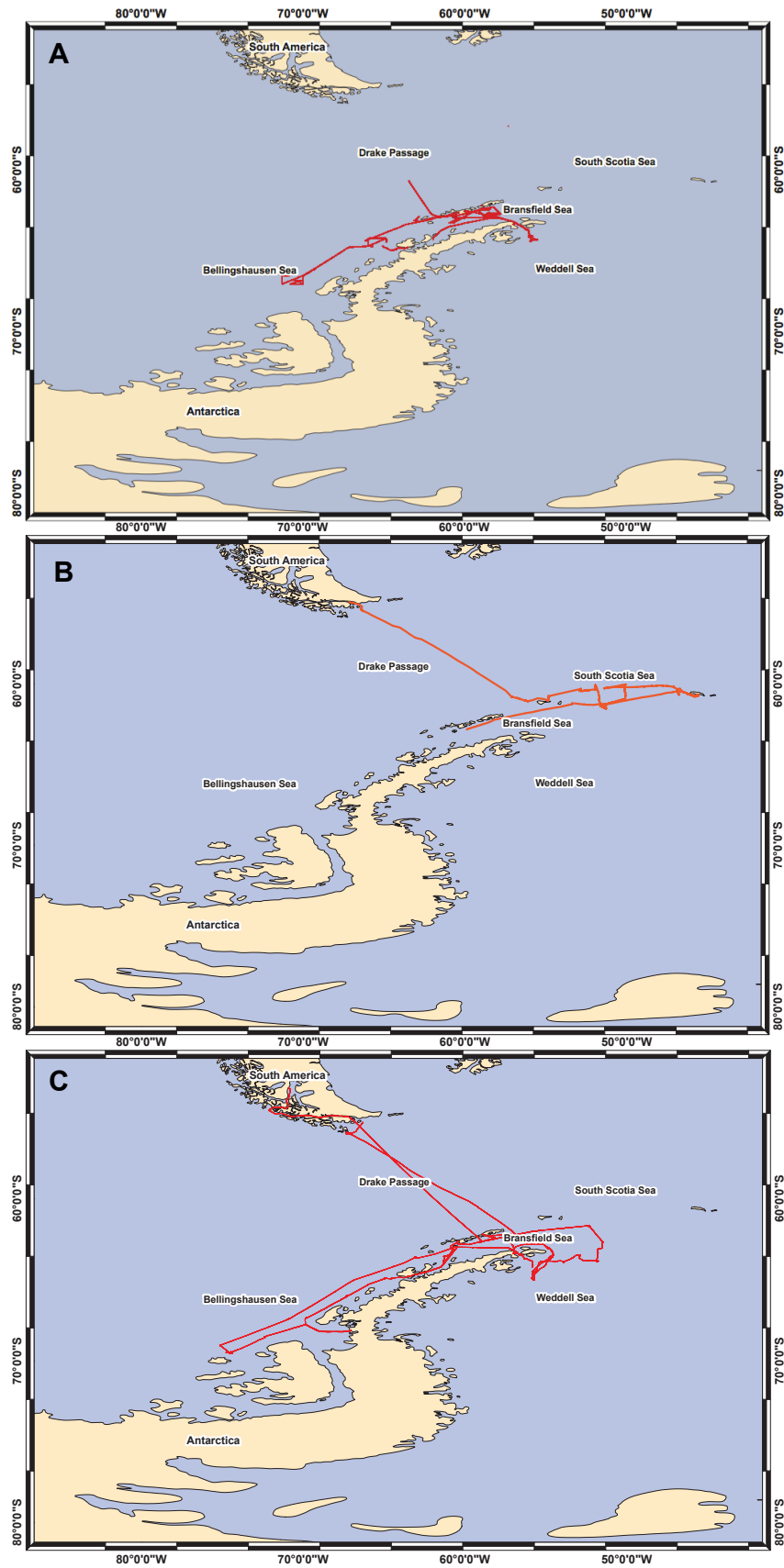


Figure 13. Trajectory of the ship during the ICEPOS (A), ESSASSI (B) and ATOS II (C) campaigns in the Southern Ocean.

References

Agrell, C., Okla, L., Larsson, P., Backe, C. and Wania, F. (1999). Evidence of latitudinal fractionation of polychlorinated biphenyl congeners along the Baltic sea region. *Environmental Science and Technology* 33 (8), 1149-1155.

Anderson, P. N. and Hites, R. A. (1996). OH radical reactions: the major removal pathway for polychlorinated biphenyls from the atmosphere. *Environmental Science and Technology* 30 (5), 1757-1763.

Arnot, J. A., and Gobas, F. A. P. C. (2006). A review of bioconcentration factor (BCF) and bioaccumulation factor (BAF) assessments for organic chemicals in aquatic organisms. *Environmental Reviews*, 14(4), 257-297.

Axelmann, J. and Gustafsson, O. (2002). Global sinks of PCBs: A critical assessment of the vapour- phase hydroxy radical sink emphasizing field diagnostic and model assumptions. *Global Biogeochemical Cycles* 16 (4), 58-1/58-13.

Axelmann, J., Broman, D. and Näf, C. (1997). Field measurements of PCB partitioning between water and planktonic organisms: influence of growth, particle size and solute-solvent interactions. *Environmental Science and Technology* 31 (3), 665-669.

Bailey, D. M., Collins, M. A., Gordon, J. D. M., Zuur, A. F., and Priede, I. G. (2009). Long-term changes in deep-water fish populations in the northeast atlantic: A deeper reaching effect of fisheries? *Proceedings of the Royal Society B: Biological Sciences*, 276(1664), 1965-1969.

Baines, S. B., Pace, M. L. and M., K. D. (1994). Why does the relationship between sinking flux and planktonic primary production differ between lakes and oceans? *Limnology Oceanography* 39 (2), 213-226.

Baker, J. E. (2002). Critical pathways of Bioaccumulation in aquatic food webs. "State of the art workshop: Bioaccumulation of organic compounds and mercury in aquatic food webs". Ispra, Italia., JRC.

Baker, J. I. and Hites, R. A. (1999). Polychlorinated Dibenzo-p-dioxins and Dibenzofurans in the Remote North Atlantic Marine Atmosphere. *Environmental Science and Technology* 33 (1), 14-20.

Bamford, H. A., Poster, D. L., Huie, R. E., and Baker, J. E. (2002). Using extrathermodynamic relationships to model the temperature dependence of henry's law constants of 209 PCB congeners. *Environmental Science and Technology*, 36(20), 4395-4402.

Barber, J. L., Sweetman, A. J., Van Wijk, D., and Jones, K. C. (2005). Hexachlorobenzene in the global environment: Emissions, levels, distribution, trends and processes. *Science of the Total Environment*, 349(1-3), 1-44.

Barkan, J., and Alpert, P. (2010). Synoptic analysis of a rare event of saharan dust reaching the arctic region. *Weather*, 65(8), 208-210.

Barrie, L. A., Gregor, D., Hargrave, B., Lake, R., Muir, D., Shearer, R., . . . Bidleman, T. (1992). Arctic contaminants: Sources, occurrence and pathways. *Science of the Total Environment*, 122(1-2), 1-74.

Barrie, L., and Platt, U. (1997). Arctic tropospheric chemistry: An overview. *Tellus, Series B: Chemical and Physical Meteorology*, 49(5), 450-454.

Berglund, O., Larsson, P., Ewald, G., and Okla, L. (2001a). Influence of trophic status on PCB distribution in lake sediments and biota. *Environmental Pollution*, 113(2), 199-210.

Berglund, O., Larsson, P., Ewald, G., and Okla, L. (2001b). The effect of lake trophy on lipid content and pcb concentrations in planktonic food webs. *Ecology*, 82(4), 1078-1088.

Berrojalbiz, N., Lacorte, S., Calbet, A., Saiz, E., Barata, C., and Dachs, J. (2009). Accumulation and cycling of polycyclic aromatic hydrocarbons in zooplankton. *Environmental Science and Technology*, 43(7), 2295-2301.

Berrojalbiz, N., Dachs, J., Del Vento, S., Ojeda, M. J., Valle, M. C., Castro-Jiménez, J., . . . Hanke, G. (2011). Persistent organic pollutants in mediterranean seawater and processes affecting their accumulation in plankton. *Environmental Science and Technology*, 45(10), 4315-4322.

Beyer, A., Mackay, D., Matthies, M., Wania, F. and Webster, E. (2000). Assessing long-range transport potential of persistent organic pollutants. *Environmental Science and Technology* 34 (4), 699-703.

Beyer, A., Wania, F., Gouin, T., Mackay, D. and Matthies, M. (2003). Temperature dependence of the characteristic travel distance. *Environmental Science and Technology* 37 (4), 766-771.

Bidleman, T. (1988). Atmospheric processes. *Environmental Science and Technology* 22 (4), 361- 367.

Bidleman, T. F., and McConnell, L. L. (1995). A review of field experiments to determine air-water gas exchange of persistent organic pollutants. *Science of the Total Environment*, 159(2-3), 101-117.

Bidleman, T.F., Stern, G.A., Tomy, G.T., Hargrave, B.T., Jantunen, L.M., Macdonald, R.W., (2013). Scavenging Amphipods: Sentinels for Penetration of Mercury and Persistent Organic Chemicals into Food Webs of the Deep Arctic Ocean. *Environmental Science and Technology*. 47 (11), 5553-5561

Bignert, A., Olsson, M., Persson, W., Jensen, S., Zakrisson, S., Litzen, K., . . . , Alsberg, T. (1998). Temporal trends of organochlorines in Northern Europe, 1967-1995. Relation to global fractionation, leakage from sediments and international measures. *Environmental Pollution* 99 (2), 177-198.

Borgå, K., Gulliksen, B., Gabrielsen, G. W., and Skaare, J. U. (2002a). Size-related bioaccumulation and between-year variation of organochlorines in ice-associated amphipods from the arctic ocean. *Chemosphere*, 46(9-10), 1383-1392.

Introduction

Borgå, K., Poltermann, M., Polder, A., Pavlova, O., Gulliksen, B., Gabrielsen, G. W., and Skaare, J. U. (2002b). Influence of diet and sea ice drift on organochlorine bioaccumulation in arctic ice-associated amphipods. *Environmental Pollution*, 117(1), 47-60.

Breivik K, Sweetman A, Pacyna JM, Jones KC, 2002a. Towards a global historical emission inventory for selected PCB congeners – a mass balance approach. 1. Global production and consumption. *Science of the Total Environment*. Vol. 290 (1-3): 181-198.

Breivik K, Sweetman A, Pacyna JM, Jones KC, 2002b. Towards a global historical emission inventory for selected PCB congeners – a mass balance approach. 2. Emissions. *Science of the Total Environment*. 290 (1-3) 199-224.

Breivik, K., Alcock, R., Li, Y.F., Bailey, R.E., Fiedler, H., and Pacyna, J.M. (2004). Primary sources of selected POPs: regional and global scale emission inventories. *Environmental Pollution*, 128, 3-16.

Breivik, K., Sweetman, A., Pacyna, J. M., and Jones, K. C. (2007). Towards a global historical emission inventory for selected PCB congeners - A mass balance approach. 3. an update. *Science of the Total Environment*, 377(2-3), 296-307.

Breivik, K., Gioia, R., Chakraborty, P., Zhang, G., and Jones, K. C. (2011). Are reductions in industrial organic contaminants emissions in rich countries achieved partly by export of toxic wastes? *Environmental Science and Technology*, 45(21), 9154-9160.

Bricaud, A., Stramski, D. (1990). Spectral absorption coefficients of 'living phytoplankton and nonalgal biogenous matter: A comparison between the Peru upwelling area and Sargasso Sea. *Limnology and Oceanography*. 35(1), 562-582.

Brown, D. P. (1987). Mortality of workers exposed to polychlorinated biphenyls - an update. *Archives of Environmental Health*, 42(6), 333-339.

Bruhn, R., Lakaschus, S., and McLachlan, M. S. (2003). Air/sea gas exchange of PCBs in the southern baltic sea. *Atmospheric Environment*, 37(24), 3445-3454.

Bucheli, T. D. and Gustafsson, O. (2003). Soot sorption of non-ortho and ortho substituted PCBs. *Chemosphere* 53, 515-522.

Cabrerizo, A., Dachs, J., Moeckel, C., Ojeda, M. J., Caballero, G., Barceló, D., and Jones, K. C. (2011). Factors influencing the soil-air partitioning and the strength of soils as a secondary source of polychlorinated biphenyls to the atmosphere. *Environmental Science and Technology*, 45(11), 4785-4792.

Cabrerizo, A., Dachs, J., Barceló, D., and Jones, K. C. (2013). Climatic and biogeochemical controls on the remobilization and reservoirs of persistent organic pollutants in antarctica. *Environmental Science and Technology*, 47(9), 4299-4306.

Carrizo, D., Grimalt, J. O., Ribas-Fito, N., Sunyer, J., and Torrent, M. (2006). Physical-chemical and maternal determinants of the accumulation of organochlorine compounds in four-year-old children. *Environmental Science and Technology*, 40(5), 1420-1426.

Carrizo, D., and Gustafsson, O. (2011). Distribution and inventories of polychlorinated biphenyls in the polar mixed layer of seven pan-arctic shelf seas and the interior basins. *Environmental Science and Technology*, 45(4), 1420-1427.

- Carson, R.L. (1962). *Silent Spring*. Houghton Mifflin Company, NY, USA.
- Chen, J., Xue, X., Schramm, K. -, Quan, X., Yang, F., and Kettrup, A. (2002). Quantitative structure-property relationships for octanol-air partition coefficients of polychlorinated biphenyls. *Chemosphere*, 48(5), 535-544.
- Choi, S., and Wania, F. (2011). On the reversibility of environmental contamination with persistent organic pollutants. *Environmental Science and Technology*, 45(20), 8834-8841.
- Cotham Jr., W. E., and Bidleman, T. F. (1991). Estimating the atmospheric deposition of organochlorine contaminants to the arctic. *Chemosphere*, 22(1-2), 165-188.
- Crutzen, P.J.; Stoermer, E.F. (2000). The Anthropocene. *Global Change Newsletter* 41: 17-18.
- Crutzen, P. J. (2002). The "anthropocene". Paper presented at the Journal De Physique. IV : JP, , 12(10) Pr10/1-Pr10/5.
- Dachs, J., Bayona, J.M., Fowler, S.W., Miquel, J.C. and Albaigés, J. (1996) Vertical fluxes of polycyclic aromatic hydrocarbons and organochlorine compounds in the western Alboran Sea (southwestern Mediterranean). *Marine Chemistry*, 52 (1), 75-86.
- Dachs, J., Eisenreich, S. J., Baker, J. E., Ko, F.-C. and Jeremiason, J. D. (1999). Coupling of phytoplankton uptake and air-water exchange of persistent organic pollutants. *Environmental Science and Technology* 33 (20), 3653-3660.
- Dachs, J., and Eisenreich, S. J. (2000). Adsorption onto aerosol soot carbon dominates gas-particle partitioning of polycyclic aromatic hydrocarbons. *Environmental Science and Technology*, 34(17), 3690-3697
- Dachs, J., Eisenreich, S. J. and Hoff, R. M. (2000). Influence of eutrophication on air-water exchange, vertical fluxes, and phytoplankton concentrations of persistent organic pollutants. *Environmental Science and Technology* 34 (6), 1095-1102.
- Dachs, J., Glenn IV, T. R., Gigliotti, C. L., Brunciak, P., Totten, L. A., Nelson, E. D., ..., Eisenreich, S. J. (2002a). Processes driving the short-term variability of polycyclic aromatic hydrocarbons in the Baltimore and northern Chesapeake Bay atmosphere, USA. *Atmospheric Environment* 36 (14), 2281-2295.
- Dachs, J., Lohmann, R., Ockenden, W. A., Méjanelle, L., Eisenreich, S. J. and Jones, K. C. (2002b). Oceanic biogeochemical controls on global dynamics of Persistent Organic Pollutants. *Environmental Science and Technology* 36 (20), 4229-4237.
- Dachs, J., and Méjanelle, L. (2010). Organic pollutants in coastal waters, sediments, and biota: A relevant driver for ecosystems during the anthropocene? *Estuaries and Coasts*, 33(1), 1-14.
- Dalla Valle, M., Codato, E. and Marcomini, A. (2007) Climate change influence on POPs distribution and fate: A case study. *Chemosphere*, 67(7), 1287-1295.
- Davidson, C. I., Harrington, J. R., Stephenson, M. J., Small, M. J., Boscoe, F. P., and Gandley, R. E. (1989). Seasonal variations in sulfate, nitrate and chloride in the greenland ice sheet: Relation to atmospheric concentrations. *Atmospheric Environment*, 23(11), 2483-2493.

Introduction

Del Vento, S. and Dachs, J. (2002). Prediction of uptake dynamics of persistent organic pollutants by bacteria and phytoplankton. *Environmental Toxicology and Chemistry* 21 (10), 2099-2017.

Dickhut, R. M. and Gustafsson, K. E. (1995). Atmospheric Washout of Polycyclic Aromatic Hydrocarbons in the Southern Cheseapeake Bay Region. *Environmental Science and Technology* 29, 1518-1525.

Domingo, J. L., Bocio, A., Falcó, G., and Llobet, J. M. (2007). Benefits and risks of fish consumption. part I. A quantitative analysis of the intake of omega-3 fatty acids and chemical contaminants. *Toxicology*, 230(2-3), 219-226.

Eisenberg, J. N. S., Bennett, D. H. and Mckone, T. E. (1998). Chemical dynamics of Persistent Organic Pollutants: a sensitivity analysis relating soil concentration levels to atmospheric emissions. *Environmental Science and Technology* 32 (1), 115-123.

Fasham, M. J. R. (2003). *Ocean Biogeochemistry: a synthesis of the Joint Global Ocean Flux Study (JGOFS)*.

Finizio, A., Mackay, D., Bidleman, T. and Harner, T. (1997). Octanol-air partition coefficient as a predictor of partitioning of semi-volatile organic chemicals to aerosols. *Atmospheric Environment* 31 (15), 2289-2296.

Fischer, R. C., Wittlinger, R., and Ballschmiter, K. (1992). Retention-index based vapor pressure estimation for polychlorobiphenyl (PCB) by gas chromatography. *Fresenius' Journal of Analytical Chemistry*, 342(4-5), 421-425.

Fowler, S. W., and Knauer, G. A. (1986). Role of large particles in the transport of elements and organic compounds through the oceanic water column. *Progress in Oceanography*, 16(3), 147-194.

García-Flor, N., Guitart, C., Abalos, M., Dachs, J., Bayona, J. M. and Albaigés, J. (2005). Enrichment of organochlorine contaminants in the sea surface microlayer: An organic carbon-driven process. *Marine Chemistry* 96, 331-345.

Gioia, R., Steinnes, E., Thomas, G. O., Meijer, S. N., and Jones, K. C. (2006). Persistent organic pollutants in european background air: Derivation of temporal and latitudinal trends. *Journal of Environmental Monitoring*, 8(7), 700-710.

Gioia, R., Nizzetto, L., Lohmann, R., Dachs, J., Temme, C., and Jones, K. C. (2008). Polychlorinated biphenyls (PCBs) in air and seawater of the atlantic ocean: Sources, trends and processes. *Environmental Science and Technology*, 42(5), 1416-1422.

Gioia, R., Dachs, J., Nizzetto, L., Berrojalbiz, N., Galbán, C., Del Vento, S., Méjanelle, L., Jones K.C. 2011. Sources, transport and fate of organic pollutants in the oceanic environment. In Quante M.; Ebinghaus R., Flöser, G. *Persistent Pollution: Past, Present and Future*. Springer Verlag, Geersthacht, Germany, 111-141

Gioia, R., Lohmann, R., Dachs, J., Temme, C., Lakaschus, S., Schulz-Bull, D., ..., Jones, K. C. (2008). Polychlorinated biphenyls in air and water of the north atlantic and arctic ocean. *Journal of Geophysical Research D: Atmospheres*, 113(19)

Gioia, R., Eckhardt, S., Breivik, K., Jaward, F. M., Prieto, A., Nizzetto, L., and Jones, K. C. (2011). Evidence for major emissions of PCBs in the west african region. *Environmental Science and Technology*, 45(4), 1349-1355.

Grimalt, J. O., Fernández, P., Berdié, L. and R., V. (2001). Selective trapping of organochlorine compounds in mountain lakes of temperate areas. *Environmental Science and Technology* 35 (13), 2690-2697.

Gustafsson, Ö., Gschwend, P. M. and Buesseler, K. O. (1997a). Settling removal rates of PCBs into the northwestern Atlantic derived from ²³⁸U-²³⁴Th disequilibria *Environmental Science and Technology* 31 (12), 3544-3550.

Gustafsson, Ö., Nilsson, N. and Bucheli, T. D. (2001). Dynamic colloid-water partitioning of pyrene through a coastal baltic spring bloom. *Environmental Science and Technology* 35 (20), 4001-4006.

Haag, W. R., and David Yao, C. C. (1992). Rate constants for reaction of hydroxyl radicals with several drinking water contaminants. *Environmental Science and Technology*, 26(5), 1005-1013.

Halsall, C. J. (2004). Investigating the occurrence of persistent organic pollutants (POPs) in the arctic: Their atmospheric behaviour and interaction with the seasonal snow pack. *Environmental Pollution*, 128(1-2), 163-175.

Hansch, C., Leo, A.J., Hoekman, D. (1995) *Exploring QSAR, Hydrophobic, Electronic, and Steric Constants*. ACS Professional Reference Book, American Chemical Society, Washington, DC.

Hardell, L., Liljegren, G., Lindström, G., Van Bavel, B., Broman, K., Fredrikson, M., . . . Johansson, B. (1996a). Increased concentrations of chlordane in adipose tissue from non-hodgkin's lymphoma patients compared with controls without a malignant disease. *International Journal of Oncology*, 9(6), 1139-1142.

Hardell, L., Van Bavel, B., Lindström, G., Fredrikson, M., Hagberg, H., Liljegren, G., . . . Johansson, B. (1996b). Higher concentrations of specific polychlorinated biphenyl congeners in adipose tissue from non-hodgkin's lymphoma patients compared with controls without a malignant disease. *International Journal of Oncology*, 9(4), 603-608.

Hardell, L., Liljegren, G., Lindström, G., van Bavel, B., Fredrikson, M., and Hagberg, H. (1997). Polychlorinated biphenyls, chlordanes, and the etiology of non-hodgkin's lymphoma. *Epidemiology (Cambridge, Mass.)*, 8(6), 689.

Hardy, M. L. (2002). A comparison of the properties of the major commercial PBDPO/PBDE product to those of major PBB and PCB products. *Chemosphere*, 46(5), 717-728.

Harner, T., and Mackay, D. (1995). Measurement of octanol - air partition coefficients for chlorobenzenes, PCBs, and DDT. *Environmental Science and Technology*, 29(6), 1599-1606.

Harner, T., and Bidleman, T. F. (1996). Measurements of octanol-air partition coefficients for polychlorinated biphenyls. *Journal of Chemical and Engineering Data*, 41(4), 895-899.

Introduction

Harner, T., and Bidleman, T. F. (1998). Measurement of octanol-air partition coefficients for polycyclic aromatic hydrocarbons and polychlorinated naphthalenes. *Journal of Chemical and Engineering Data*, 43(1), 40-46.

Harner, T., Kylin, H., Bidleman, T. F., and Strachan, W. M. J. (1999). Removal of and α -hexachlorocyclohexane and enantiomers of γ -hexachlorocyclohexane in the eastern arctic ocean. *Environmental Science and Technology*, 33(8), 1157-1164.

Harner, T., Jantunen, L. M. M., Bidleman, T. F., Barrie, L. A., Kylin, H., Strachan, W. M. J., and Macdonald, R. W. (2000). Microbial degradation is a key elimination pathway of hexachlorocyclohexanes from the arctic ocean. *Geophysical Research Letters*, 27(8), 1155-1158.

Hassanin, A., Johnston, A. E., Thomas, G. O., and Jones, K. C. (2005). Time trends of atmospheric PBDEs inferred from archived U.K. herbage. *Environmental Science and Technology*, 39(8), 2436-2441.

Hay, W. W. (1993). The role of polar deep water formation in global climate change. *Annual Review of Earth and Planetary Sciences*, 21, 227-254.

Hedges, J. I., Baldock, J. A., Gélinas, Y., Lee, C., Peterson, M. L., and Wakeham, S. G. (2002). The biochemical and elemental compositions of marine plankton: A NMR perspective. *Marine Chemistry*, 78(1), 47-63.

Henry Wöhrschimmel, H., Matthew MacLeod, M., and Hungerbühler, K. 2013. Emissions, Fate and Transport of Persistent Organic Pollutants to the Arctic in a Changing Global Climate. *Environmental Science and Technology*. 47 (5), 2323-2330

Hinckley, D. A., Bidleman, T. F., Foreman, W. T., and Tuschall, J. R. (1990). Determination of vapor pressures for nonpolar and semipolar organic compounds from gas chromatographic retention data. *Journal of Chemical and Engineering Data*, 35(3), 232-237.

Hoekstra, P. F., O'Hara, T. M., Teixeira, C., Backus, S., Fisk, A. T., and Muir, D. C. G. (2002). Spatial trends and bioaccumulation of organochlorine pollutants in marine zooplankton from the alaskan and canadian arctic. *Environmental Toxicology and Chemistry*, 21(3), 575-583.

Hoff, R. M. (1994). An error budget for the determination of the atmospheric mass loading of toxic chemicals in the great lakes. *Journal of Great Lakes Research*, 20(1), 229-239.

Holsen, T. M., and Noll, K. E. (1992). Dry deposition of atmospheric particles: Application of current models to ambient data. *Environmental Science and Technology*, 26(9), 1798-1807.

Hung, H., Blanchard, P., Halsall, C. J., Bidleman, T. F., Stern, G. A., Fellin, P., . . . Konoplev, A. (2005). Temporal and spatial variabilities of atmospheric polychlorinated biphenyls (PCBs), organochlorine (OC) pesticides and polycyclic aromatic hydrocarbons (PAHs) in the canadian arctic: Results from a decade of monitoring. *Science of the Total Environment*, 342(1-3), 119-144.

Hung, H., Sum, C. L., Wania, F., Blanchard, P., and Brice, K. (2005). Measuring and simulating atmospheric concentration trends of polychlorinated biphenyls in the northern hemisphere. *Atmospheric Environment*, 39(35), 6502-6512.

Ibrahim, M., Barrie, L. A., and Fanaki, F. (1983). An experimental and theoretical investigation of the dry deposition of particles to snow, pine trees and artificial collectors. *Atmospheric Environment - Part A General Topics*, 17(4), 781-788.

IPCC. (2007), Summary for Policymakers, in *Climate Change 2007: Synthesis Report*, p. 11

Iwata, I., Tanabe, S., Sakai, N. and Tatsukawa, R. (1993). Distribution of persistent organochlorines in the oceanic air and surface seawater and the role of ocean on their global transport and fate. *Environmental Science and Technology* 27, 1080-1098.

Jacoff, F. S., Scarberry, R., and Rosa, D. (1986). Source assessment of hexachlorobenzene from the organic chemical manufacturing industry. *IARC Scientific Publications*, (77), 31-37.

Jantunen, L. M., and Bidleman, T. F. (1995). Reversal of the air - water gas exchange direction of hexachlorocyclohexanes in the bering and chukchi seas: 1993 versus 1988. *Environmental Science and Technology*, 29(4), 1081-1089.

Jaward, F. M., Barber, J. L., Booij, K., Dachs, J., Lohmann, R. and Jones, K. C. (2004). Evidence for dynamic air-water coupling and cycling of persistent organic pollutants over the open Atlantic Ocean. *Environmental Science and Technology* 38 (9), 2617-2625.

Jeremiason, J. D., Eisenreich, S. J., Paterson, M. J., Beaty, K. G., Hecky, R., and Elser, J. J. (1999). Biogeochemical cycling of PCBs in lakes of variable trophic status: A paired-lake experiment. *Limnology and Oceanography*, 44(3 II), 889-902.

Jurado, E., Lohmann, R., Meijer, S., Jones, K.C., and Dachs, J. (2004). Latitudinal and seasonal capacity of the surface oceans as a reservoir of polychlorinated biphenyls. *Environmental Pollution*, 128, 149-162.

Jurado, E., and Dachs, J. (2008). Seasonality in the "grasshopping" and atmospheric residence times of persistent organic pollutants over the oceans. *Geophysical Research Letters*, 35(17).

Kang, J. -, Son, M. -, Hur, S. D., Hong, S., Motoyama, H., Fukui, K., and Chang, Y. -. (2012). Deposition of organochlorine pesticides into the surface snow of east antarctica. *Science of the Total Environment*, 433, 290-295.

Katsoyiannis, A., and Samara, C. (2007). The fate of dissolved organic carbon (DOC) in the wastewater treatment process and its importance in the removal of wastewater contaminants. *Environmental Science and Pollution Research*, 14(5), 284-292.

Kepkay, P. E. (1994). Particle aggregation and the biological reactivity of colloids. *Marine Ecology Progress Series*, 109(2-3), 293-304.

Kepkay, P. E., Bugden, J. B. C., Lee, K., and Stoffyn-Egli, P. (2000). Application of ultraviolet fluorescence (UVF) spectroscopy to monitor oil-mineral aggregate (OMA) formation. Paper presented at the Environment Canada Arctic and Marine Oil Spill Program Technical Seminar (AMOP) Proceedings, , 23(2) 1051-1064.

Kirch, P. V. (2005). *Archaeology and global change: The holocene record*

Introduction

Klánová, J., Diamond, M., Jones, K., Lammel, G., Lohmann, R., Pirrone, N., . . . Weiss, P. (2011). Identifying the research and infrastructure needs for the global assessment of hazardous chemicals ten years after establishing the stockholm convention. *Environmental Science and Technology*, 45(18), 7617-7619.

Kömp, P., and McLachlan, M. S. (1997). Octanol/air partitioning of polychlorinated biphenyls. *Environmental Toxicology and Chemistry*, 16(12), 2433-2437.

Kramer, S., Hikel, S. M., Adams, K., Hinds, D., and Moon, K. (2012). Current status of the epidemiologic evidence linking polychlorinated biphenyls and non-hodgkin lymphoma, and the role of immune dysregulation. *Environmental Health Perspectives*, 120(8), 1067-1075.

Lalli, C. M., and Parsons, T. R. (1997). *Biological oceanography: An introduction*. second edition

Lam, P. J., Doney, S. C., and Bishop, J. K. B. (2011). The dynamic ocean biological pump: Insights from a global compilation of particulate organic carbon, CaCO₃, and opal concentration profiles from the mesopelagic. *Global Biogeochemical Cycles*, 25(3)

Laxon, S., Peacock, H., and Smith, D. (2003). High interannual variability of sea ice thickness in the arctic region. *Nature*, 425(6961), 947-950.

Li, M. -, Tsai, P. -, Chen, P. -, Hsieh, C. -, Leon Guo, Y. -, and Rogan, W. J. (2013). Mortality after exposure to polychlorinated biphenyls and dibenzofurans: 30 years after the "yucheng accident". *Environmental Research*, 120, 71-75.

Li, N., Wania, F., Lei, Y. D., and Daly, G. L. (2003). A comprehensive and critical compilation, evaluation, and selection of physical-chemical property data for selected polychlorinated biphenyls. *Journal of Physical and Chemical Reference Data*, 32(4), 1545-1590.

Li, Y. F. (1999). Global technical hexachlorocyclohexane usage and its contamination consequences in the environment: From 1948 to 1997. *Science of the Total Environment*, 232(3), 121-158.

Li, Y. F., and Macdonald, R. W. (2005). Sources and pathways of selected organochlorine pesticides to the arctic and the effect of pathway divergence on HCH trends in biota: A review. *Science of the Total Environment*, 342(1-3), 87-106.

Li, Y. F., Venkatesh, S., and Li, D. (2005). Modeling global emissions and residues of pesticides. *Environmental Modeling and Assessment*, 9(4), 237-243.

Ligocki, M. P., Leuenberger, C. and Pankow, J. F. (1985a). Trace of organic compounds in rain-II. Gas Scavenging of neutral organic compounds. *Atmospheric Environment* 19 (10), 1609-1617.

Ligocki, M. P., Leuenberger, C. and Pankow, J. F. (1985b). Trace of organic compounds in rain-III. Particle Scavenging of neutral organic compounds. *Atmospheric Environment* 19 (10), 1619-1626.

Linell, K. A., and Tedrow, J. C. F. (1981). Soil and permafrost surveys in the arctic. *Soil and Permafrost Surveys in the Arctic.*

Liss, P. S., and Slater, P. G. (1974). Flux of gases across the air-sea interface. *Nature*, 247(5438), 181-184.

Lohmann, R., Jurado, E., Dijkstra, H. A., and Dachs, J. (2013). Vertical eddy diffusion as a key mechanism for removing perfluorooctanoic acid (PFOA) from the global surface oceans. *Environmental Pollution*, 179, 88-94.

Lohmann, R., Jurado, E., Pilson, M. E. Q., and Dachs, J. (2006). Oceanic deep water formation as a sink of persistent organic pollutants. *Geophysical Research Letters*, 33(12)

Lundin, L., Gomez-Rico, M. F., Forsberg, C., Nordenskjöld, C., and Jansson, S. (2013). Reduction of PCDD, PCDF and PCB during co-combustion of biomass with waste products from pulp and paper industry. *Chemosphere*, 91(6), 797-801.

Lutz, W., Sanderson, W., and Scherbov, S. (2001). The end of world population growth. *Nature*, 412(6846), 543-545.

M.L. Wesely, B.B. Hicks, (2000). A review of the current status of knowledge on dry deposition, *Atmospheric Environment*, Volume 34, Issues 12–14, 2261-2282.

Ma, J., Daggupaty, S., Harner, T., and Li, Y. (2003). Impacts of lindane usage in the canadian prairies on the great lakes ecosystem. I. coupled atmospheric transport model and modeled concentrations in air and soil. *Environmental Science and Technology*, 37(17), 3774-3781.

MacDonald, R. W., Barrie, L. A., Bidleman, T. F., Diamond, M. L., Gregor, D. J., Semkin, R. G., ..., Yunker, M. B. (2000). Contaminants in the Canadian Arctic: 5 years of progress in understanding sources, occurrence and pathways. *Science of The Total Environment* 254, 93-234.

Mackay, D., (1979). Finding fugacity feasible. *Environmental Science and Technology*, 13 (10), 1218–1223

Mackay, D., and Paterson, S. (1981). Calculating fugacity. *Environmental Science and Technology*, 15(9), 1006-1014.

Mackay, D., Shiu, W.Y. (1981). A critical review of Henry's law constants for chemicals of environmental interest. *J Phys Chem Ref Data* 10:1175–1199.

Mackay, D., Paterson, S. and Schroeder, W. H. (1986). Model describing the rates of transfer processes of organic chemicals between atmosphere and water. *Environmental Science and Technology* 20 (8).

Mackay, D. and Fraser, A. (2000). Bioaccumulation of persistent organic chemicals: mechanisms and models. *Environmental Pollution* 110, 375-391.

Mandalakis, M. and Stephanou, E. G. (2004). Wet deposition of Polychlorinated Biphenyls in the eastern Mediterranean. *Environmental Science and Technology* 38 (11), 3011-3018.

Mandalakis, M., Berresheim, H. and Stephanou, E. G. (2003). Direct evidence for destruction of Polychlorobiphenyls by OH radicals in the Subtropical Troposphere. *Environmental Science and Technology* 37 (3), 542-547.

McMichael, A. J. (1993). Planetary overload: Global environmental change and the health

Introduction

of the human species. Planetary Overload: Global Environmental Change and the Health of the Human Species,

McVeety, B. D., and Hites, R. A. (1988). Atmospheric deposition of polycyclic aromatic hydrocarbons to water surfaces: A mass balance approach. *Atmospheric Environment*, 22(3), 511-536.

Meijer, S. N., Ockenden, W. A., Sweetman, A. J., Breivik, K., Grimalt, J. O. and Jones, K. C. (2003). Global distribution and budget of PCBs and HCB in background surface soils: implications for sources and environmental processes. *Environmental Science and Technology* 37 (7), 1300-1305.

Meylan, W. M., and Howard, P. H. (2005). Estimating octanol-air partition coefficients with octanol-water partition coefficients and henry's law constants. *Chemosphere*, 61(5), 640-644.

Moore, J. K. (2008). Particular generalisation: The antarctic treaty of 1959 in relation to the anti-nuclear movement. *Polar Record*, 44(2), 115-125.

Morley, M. C., Snow, D. D., Ceccle, C., Denning, P., and Miller, L. (2006). Emerging chemicals and analytical methods. *Water Environment Research*, 78(10), 1017-1053.

Muir, D. C. G., and Howard, P. H. (2006). Are there other persistent organic pollutants? A challenge for environmental chemists. *Environmental Science and Technology*, 40(23), 7157-7166.

Murphy, T. J., Hornbuckle, K. C., and Eisenreich, S. J. (1995). Comment on 'seasonal variations in air-water exchange of polychlorinated biphenyls in lake superior' [1]. *Environmental Science and Technology*, 29(3), 846-848.

Ngabe, B., Bidleman, T. F., and Falconer, R. L. (1993). Base hydrolysis of α - and γ -hexachlorocyclohexanes. *Environmental Science and Technology*, 27(9), 1930-1933.

Nizzetto, L., Gioia, R., Li, J., Borgå, K., Pomati, F., Bettinetti, R., . . . Jones, K. C. (2012). Biological pump control of the fate and distribution of hydrophobic organic pollutants in water and plankton. *Environmental Science and Technology*, 46(6), 3204-3211.

Nizzetto, L., MacLeod, M., Borgå, K., Cabrerizo, A., Dachs, J., Guardo, A. D., ..., Jones, K. C. (2010). Past, present, and future controls on levels of persistent organic pollutants in the global environment. *Environmental Science and Technology*, 44(17), 6526-6531.

Ockenden, W. A., Sweetman, A. J., Prest, H. F., Steinnes, E., and Jones, K. C. (1998). Toward an understanding of the global atmospheric distribution of Persistent Organic Pollutants: the use of semipermeable membrane devices as time-integrated passive samplers. *Environmental Science and Technology* 32 (18), 2795-2803.

Pankow, J. F. (1994). An absorption model of gas/particle partitioning of organic compounds in the atmosphere. *Atmospheric Environment* 28 (2), 185-188.

Payne, M. R. (2013). Fisheries: Climate change at the dinner table. *Nature*, 497(7449), 320-321.

Pomeroy, J. and H.G. Jones, (1996). Windblown snow: sublimation, transport and changes to polar snow. In: E. Wolff and R.C. Bales (eds.). Chemical exchange between the

atmosphere and polar snow. *Global Environmental Change*. NATO ASI Series I, Volume 43, pp. 453-490. Springer-Verlag, Heidelberg, Germany.

Prevedouros, K., Cousins, I.T., Buck R.C., and Korzeniowski, S.H. (2006). Sources, Fate and Transport of Perfluorocarboxylates. *Environmental Science and Technology*, 40(1), 32-44.

Pučko, M., Stern, G. A., Macdonald, R. W., Barber, D. G., Rosenberg, B., and Walkusz, W. (2011). When will α -HCH disappear from the western arctic ocean? *Journal of Marine Systems*.

Pučko, M., Walkusz, W., MacDonald, R. W., Barber, D. G., Fuchs, C., and Stern, G. A. (2013). Importance of arctic zooplankton seasonal migrations for α -hexachlorocyclohexane bioaccumulation dynamics. *Environmental Science and Technology*, 47(9), 4155-4163.

Rippen, G., and Frank, R. (1986). Estimation of hexachlorobenzene pathways from the technosphere into the environment. *IARC Scientific Publications*, (77), 45-52.

Rothman, N., Cantor, K. P., Blair, A., Bush, D., Brock, J. W., Helzlsouer, K., . . . Strickland, P. T. (1997). A nested case-control study of non-hodgkin lymphoma and serum organochlorine residues. *Lancet*, 350(9073), 240-244.

Ruddiman, W. F. (2003). The anthropogenic greenhouse era began thousands of years ago. *Climate Change*. 61, 261-293.

Schenker, U., Scheringer, M., and Hungerbühler, K. (2008). Investigating the global fate of DDT: Model evaluation and estimation of future trends. *Environmental Science and Technology*, 42(4), 1178-1184.

Scheringer, M. (2009). Long-range transport of organic chemicals in the environment. *Environmental Toxicology and Chemistry*, 28(4), 677-690.

Scheringer, M., Salzmann, M., Stroebe, M., Wegmann, F., Fenner, K., and Hungerbühler, K. (2004). Long-range transport and global fractionation of POPs: Insights from multimedia modeling studies. *Environmental Pollution*, 128(1-2), 177-188.

Schulte-Hermann, R., Ohde, G., Schuppler, J. and Timmermann-Trosiener, I. (1981). Enhanced proliferation of putative preneoplastic cells in rat liver following treatment with the tumor promoters phenobarbital, hexachlorocyclohexane, steroid compounds, and nafenopin. *Cancer Research*, 41(6), 2556-2562.

Shen, L., and Wania, F. (2005). Compilation, evaluation, and selection of physical-chemical property data for organochlorine pesticides. *Journal of Chemical and Engineering Data*, 50(3), 742-768.

Shoeib, M., and Harner, T. (2002). Using measured octanol-air partition coefficients to explain environmental partitioning of organochlorine pesticides. *Environmental Toxicology and Chemistry*, 21(5), 984-990.

Sinkkonen, S., and Paasivirta, J. (2000). Degradation half-life times of PCDDs, PCDFs and PCBs for environmental fate modeling. *Chemosphere*, 40(9-11), 943-949.

Skoglund, R. S., Stange, K. and Swackhamer, D. (1996). A kinetics model for predicting the accumulation of PCBs in phytoplankton. *Environmental Science and Technology* 30 (7), 2113-2120.

Introduction

Sobek, A., and Gustafsson, Ö. (2004). Latitudinal fractionation of polychlorinated biphenyls in surface seawater along a 62° N-89° N transect from the southern norwegian sea to the north pole area. *Environmental Science and Technology*, 38(10), 2746-2751.

Sobek, A., Olli, K., and Gustafsson, Ö. (2006). On the relative significance of bacteria for the distribution of polychlorinated biphenyls in arctic ocean surface waters. *Environmental Science and Technology*, 40(8), 2586-2593.

Sobek, A., Reigstad, M., and Gustafsson, Ö. (2006). Partitioning of polychlorinated biphenyls between arctic seawater and size-fractionated zooplankton. *Environmental Toxicology and Chemistry*, 25(7), 1720-1728.

Stemmler, I., and Lammel, G. (2013). Evidence of the return of past pollution in the ocean: A model study. *Geophysical Research Letters*, 40(7), 1373-1378.

Stonehouse, B. (1986). Arctic air pollution. *Arctic Air Pollution*.

Tanabe, S. (2002). Higher contamination in the future population of developed nations. *Marine Pollution Bulletin*, 44(12), 1315-1316.

Thacker, N., Sheikh, J., Tamane, S. M., Bhanarkar, A., Majumdar, D., Singh, K., . . . Trivedi, J. (2013). Emissions of polychlorinated dibenzo-p-dioxins (PCDDs), dibenzofurans (PCDFs), and dioxin-like polychlorinated biphenyls (PCBs) to air from waste incinerators and high thermal processes in india. *Environmental Monitoring and Assessment*, 185(1), 425-429.

Totten, L. A., Brunciak, P. A., Gigliotti, C. L., Dachs, J., Glenn, T. R., Nelson, E. D. and Eisenreich, S. J. (2001). Dynamic Air-Water Exchange of Polychlorinated Biphenyls in the New York-New Jersey Harbor Estuary. *Environmental Science and Technology* 35 (19), 3834-3840.

Tsukimori, K., Uchi,H., Mitoma, C., Yasukawa, F., Chiba, T., Todaka, T., . . . , Furue, M. (2012). Maternal exposure to high levels of dioxins in relation to birth weight in women affected by Yusho disease. *Environment International*. 38(1), 79-86.

UNEP. (2001) Final act of the plenipotentiaries on the Stockholm Convention on persistent organic pollutants; United Nations Environment Program Chemicals. www.pop.int.

Valiela, I. (1995). *Marine Ecological Processes*. Springer, New York.

Vizcaino, E., Grimalt, J. O., Lopez-Espinosa, M. -, Llop, S., Rebagliato, M., and Ballester, F. (2010). Maternal origin and other determinants of cord serum organochlorine compound concentrations in infants from the general population. *Environmental Science and Technology*, 44(16), 6488-6495.

Voldner, E. C. (1995). Global usage of selected persistent organochlorines. *Science of the Total Environment*, 160-161, 201-210.

Voldner, E. C., Barrie, L. A., and Sirois, A. (1986). A literature review of dry deposition of oxides of sulphur and nitrogen with emphasis on long-range transport modelling in north america. *Atmospheric Environment - Part A General Topics*, 20(11), 2101-2123.

Voutsas, E., Magoulas, K., and Tassios, D. (2002). Prediction of the bioaccumulation of persistent organic pollutants in aquatic food webs. *Chemosphere*, 48(7), 645-651.

Wallberg, P., and Andersson, A. (2000). Transfer of carbon and a polychlorinated biphenyl through the pelagic microbial food web in a coastal ecosystem. *Environmental Toxicology and Chemistry*, 19(4 I), 827-835.

Wania, F. and Mackay, D. (1995). A global distribution model for persistent organic chemicals. *The Science of the Total Environment* 160/161, 211-232.

Wania, F. and Mackay, D. (1996). Tracking the distribution of persistent organic pollutants. *Environmental Science and Technology* 30 (9), 390A-396A.

Wania, F. and McLachlan, M. S. (2001). Estimating the influence of forests on the overall fate of semivolatile organic compounds using a multimedia fate model. *Environmental Science Technology* 35 (3), 582-590.

Wania, F., and Mackay, D. (1993). Global fractionation and cold condensation of low volatility organochlorine compounds in polar regions. *Ambio*, 22(1), 10-18.

Wegmann, F., Scheringer, M. and Hungerbühler, K. (2006). First investigations of mountainous cold condensation effects with the CliMoChem model. *Ecotoxicology and Environmental Safety* 63, 42- 51.

Wells, M.L. and Goldberg, E.D. (1992). Marine submicron particles. *Marine Chemistry*, 40(1-2), 5-18

Williams, R. M. 1982. A model for the dry deposition of particles to natural water surfaces. *Atmospheric Environment*. 16 (8), 1933-1938.

Zhang, L., Bidleman, T., Perry, M. J., and Lohmann, R. (2012). Fate of chiral and achiral organochlorine pesticides in the north atlantic bloom experiment. *Environmental Science and Technology*, 46(15), 8106-8114.

Zhang, L., Dickhut, R., DeMaster, D., Pohl, K., and Lohmann, R. (2013). Organochlorine Pollutants in Western Antarctic Peninsula Sediments and Benthic Deposit Feeders. *Environmental Science and Technology*. 2013 47 (11), 5643-5651

Zinder, B., Schumann, T., and Waldvogel, A. (1988). Aerosol and hydrometeor concentrations and their chemical composition during winter precipitation along a mountain slope - II. enhancement of below-cloud scavenging in a stably stratified atmosphere. *Atmospheric Environment*, 22(12), 2741-2750.

Chapter 2

Objectives

The overall objective of the present PhD thesis is **to study the coupling of persistent organic pollutants between the lower atmosphere and surface ocean in the Arctic and Southern Oceans**. Specific objectives of the present thesis are:

- i. To report the simultaneous measurements of hexachlorocyclohexanes (HCHs), hexachlorobenzene (HCB) and polychlorinated biphenyls (PCBs) in the atmosphere, surface waters and phytoplankton from the North-West Atlantic and Arctic Ocean, and from the Southern Ocean surrounding the Antarctic Peninsula. In the case of the Southern Ocean, to contribute to the generation of the largest data set on POP occurrence for the region.
- ii. To investigate and measure the air-water diffusive exchange and the dry deposition of PCBs, HCHs and HCB in the Arctic and Southern Oceans.
- iii. To assess, for the first time from field studies in the marine environment, the influence of the “biological pump” on the sequestration of atmospheric POPs, and its influence on the atmospheric residence times of POPs in the Polar Oceans.
- iv. To propose the “degradative pump” as a key process controlling the atmospheric deposition of HCHs in the Arctic and Southern Ocean.
- v. To identify the relative importance of secondary sources from Antarctica, and long range transport on the occurrence of POPs in the Southern Ocean and Antarctic atmosphere.

Chapter 3.

**The Oceanic Biological Pump Modulates the
Atmospheric Transport of Persistent Organic
Pollutants to the Arctic**



The results obtained in the present chapter were published as Galbán-Malagón et al., 2012 in *Nature Communications*, 3, 2012, 862.

Chapter 3: PCBs in the North Atlantic and the Arctic Ocean

Abstract

Semivolatile persistent organic pollutants have the potential to reach remote environments, such as the Arctic ocean, through atmospheric transport and deposition. Here we show that this transport of polychlorinated biphenyls to the Arctic ocean is strongly retarded by the oceanic biological pump. A simultaneous sampling of atmospheric, seawater and plankton samples was performed in July 2007 in the Greenland Current and Atlantic sector of the Arctic ocean. The atmospheric concentrations declined during atmospheric transport over the Greenland Current with estimated half-lives of 1–4 days. These short half-lives can be explained by the high air-to-water net diffusive flux, which is similar in magnitude to the estimated settling fluxes in the water column. Therefore, the decrease of atmospheric concentrations is due to sequestration of atmospheric polychlorinated biphenyls by enhanced air–water diffusive fluxes driven by phytoplankton uptake and organic carbon settling fluxes (biological pump).

Chapter 3: PCBs in the North Atlantic and the Arctic Ocean

1. Introduction

The occurrence, transport and impact of persistent organic pollutants (POPs), such as polychlorinated biphenyls (PCBs), in the Arctic Ocean (AO) has been an issue of concern due to the enhanced bioaccumulation potential of POPs in cold environments and their impact on the Arctic ecosystem and the health of human inhabitants¹⁻³. The processes driving the transport of POPs to the AO and their occurrence have been the subject of several studies over the last two decades¹⁻¹⁶, including the presence of POPs in the atmosphere, seawater and to a lesser extent plankton of the AO. Chemicals such as PCBs are highly hydrophobic, as measured by the octanol–water partition coefficients (K_{OW}) ranging between 10^4 and 10^8 , and are semivolatile. Therefore, PCBs and other POPs can effectively undergo volatilization from primary and secondary sources, and via atmospheric transport, accumulate in aquatic organisms once deposited in the Arctic. Regardless of the multi-phase cycling and partitioning of PCBs during their transport to the Arctic, none of the previous studies performed in high-latitude oceanic regions had sampled simultaneously the gas, aerosol, seawater (dissolved and particulate) and plankton phases, nor has quantified the role of the biological pump as a control of transport of POPs to the Arctic. The biological pump is known as the process by which primary producers (phytoplankton) fix carbon dioxide, and a fraction of the new organic matter produced is exported to the deep ocean by settling particles¹⁷. In the context of POPs, the biological pump has been used to name the air–deep ocean transport of POPs², driven by the process of accumulation of POPs in phytoplankton organic matter, which depletes the dissolved concentrations of POPs, thus enhancing the air-to-water flux of pollutants. Part of the organic matter sinks carrying POPs to deep waters². While this process has received considerable attention^{2,9,18,19}, its role as a modulator of the Arctic pollution and atmospheric transport has not been assessed in the field.

In previous Arctic field studies, Sobek and Gustafsson and Gioia *et al.*¹¹ reported concentration gradients of dissolved PCBs in seawater off northern Europe, extending from the North Sea to off-shore waters of western Scandinavian, to Eastern Svalbard and to the ice-covered Arctic regions. These

Chapter 3: PCBs in the North Atlantic and the Arctic Ocean

authors found decreasing concentrations at higher latitudes and evidence of fractionation processes with increasing concentrations of less chlorinated PCBs at high latitudes, which are less prone to cold trapping and being sequestered by settling particles rich in organic matter (biological pump). Gas-phase concentrations have also been reported to decrease from Northern Europe to the Arctic Atlantic sector¹¹, with higher concentrations near the ice-margin zone, presumably due to enhanced volatilization induced by ice melting, which could be currently enhanced due to climate change¹². However, the North-West Atlantic Ocean, a region with dominating south west air masses carrying pollutants from industrial/population influenced areas upwind, has not been studied before in terms of PCB occurrence and cycling, and none of the previous studies reported concentrations of POPs in air, water and plankton simultaneously.

Previous studies have suggested that there are several processes affecting the atmosphere-land and atmosphere-ocean exchange that may reduce the transport potential of POPs to the polar regions. These include sequestration by high organic carbon (OC) soils²⁰⁻²¹, the role of forests as filters of POPs²², and based on the results of modelling studies^{2,18}, the oceanic biological pump. Models suggest that plankton uptake and settling fluxes of organic matter reduces the atmospheric half-lives of POPs by enhancing atmospheric deposition fluxes, thus sequestering atmospheric POPs to the deep ocean.

Water column biogeochemical processes are key factors driving the occurrence and settling of PCBs and other POPs in the Arctic and other oceanic regions^{9,18,19}. The accumulation of hydrophobic POPs in planktonic organisms and the subsequent settling of particle and plankton bound PCBs have the potential to deplete dissolved-phase concentrations of POPs. The resulting enhanced air–water disequilibria of gas and dissolved-phase concentration drives a net diffusive absorption flux from the atmosphere to the water column¹⁸. When this happens, the atmospheric transport is strongly retarded, and even reduced, because atmospheric deposition fluxes deplete the atmospheric levels of POPs². However, field evidence for the influence of the biological pump on the atmospheric occurrence and transport of POPs has not been previously reported.

The objectives of the work presented here were to study the occurrence,

Chapter 3: PCBs in the North Atlantic and the Arctic Ocean

long-range transport potential, atmospheric deposition and the role of the biological pump on the cycling of PCBs in the sub-Arctic and AO. A simultaneous sampling of atmospheric (gas and aerosol phase), seawater (dissolved and particulate phases) and plankton samples was performed in July 2007 in the Greenland Current (GC) and Atlantic sector of the AO. The gas-phase concentrations of PCBs declined during atmospheric over the GC with estimated half-life ranging from 1 to 4 days. The atmospheric depositional fluxes are quantified showing a high air-to-water net diffusive flux of PCBs driven by large air–water disequilibrium in their concentrations. This flux is similar in magnitude to the estimated settling flux of PCBs in the water column. The results show the first evidence from a field study of the important role that the biological pump has modulating the atmospheric transport over the ocean. The meta-analysis of the air–water disequilibrium reported in the literature for various POP families suggests that this phenomenon is generalized in high latitude/high productivity oceanic regions.

2. Results

2.1 Occurrence of PCBs in the GC and AO

Simultaneous sampling of the atmosphere (gas and aerosol phases), seawater (dissolved and particulate phases) and plankton was carried out between Iceland and the Arctic ice-margin zone and Svalbard archipelago in July 2007 as part of the ATOS I cruise on board *R/V Hespérides*. The sampling area can be divided in two different zones; the GC between Iceland and Greenland sailing flowing northeast, and the Atlantic sector of the AO (Supplementary Fig. S1 on Appendix A.1), as the *R/V Hespérides* is not an icebreaker, ice-covered regions were not sampled during the ATOS I cruise. Figure 1 shows the latitudinal trends of PCB concentrations in the gas, aerosol, dissolved, particulate and plankton phases in the GC and AO (See supplementary Tables S1a, S1b and S2 for individual congener concentrations on Appendix A.2).

In brief, higher dissolved concentrations were found near Iceland, and lower concentrations were found near the Svalbard islands (close to the ice margin), but with some variability in this region. Dissolved PCB concentrations

Chapter 3: PCBs in the North Atlantic and the Arctic Ocean

were below 1 pg L^{-1} for most samples, consistent with other studies^{11,13}, even though this is the first report of PCB concentrations in the GC. Particulate phase concentrations in ice-free surface seawater from the GC and AO showed considerable variability ($0.01\text{--}12.29$ and $0.004\text{--}9.73 \text{ pg L}^{-1}$, respectively). Finally, PCB concentrations in phytoplankton showed an increasing trend with latitude but also with a remarkable variability in concentrations close to the ice margin.

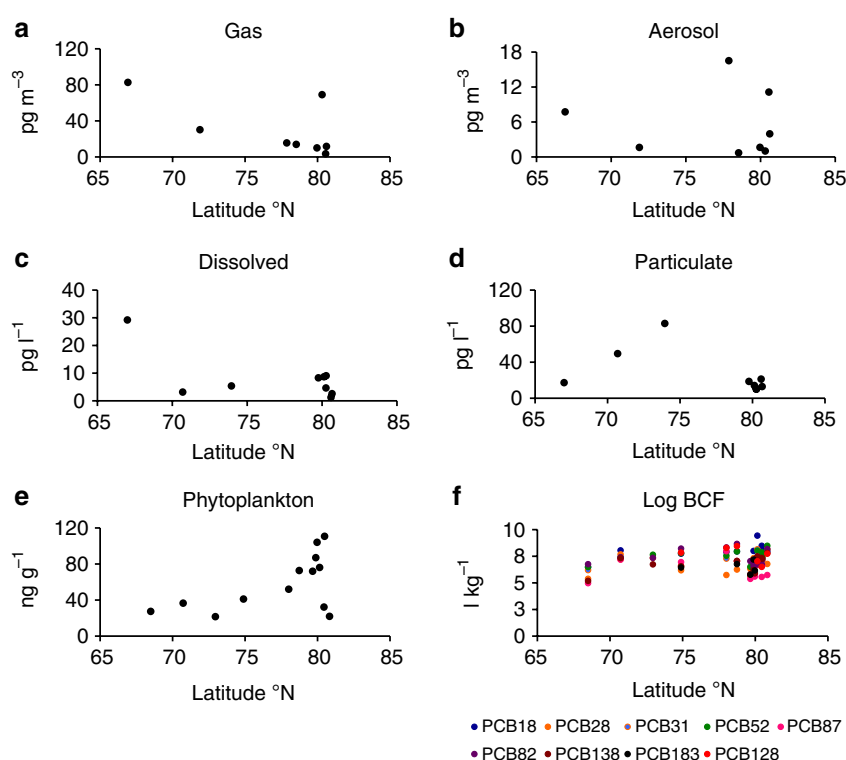


Figure 1. PCB concentrations versus latitude in the (a) gas, (b) aerosol, (c) dissolved, (d) water particulate and (e) phytoplankton phases. Bioconcentration factor (BCF) measured for selected PCBs are shown in the f panel. The concentrations of PCBs are the sum of congeners 18, 17, 31, 33, 52, 49, 44, 99/101, 87, 110, 82, 151, 153, 132/105, 158, 187, 183, 128, 177, 171/156, 180, 169, 201/199, 195 and 208.

2.2 Decreasing PCB concentrations during atmospheric transport.

The sum of total PCB concentrations (27 congeners) in the gas phase (C_G) ranged from 15.7 to 86.9 and 3.5 to 81.7 pg m^{-3} in the GC and AO atmospheres, respectively. The aerosol-phase concentration ranged between 1.6 to 17.3 and 0.7 to 11 pg m^{-3} in air over the GC and AO atmospheres, respectively. The aerosol-bound concentrations of PCBs represents on average 23% of the total atmospheric concentration due to enhanced sorption of POPs to aerosols at low temperatures. The measured gas-phase concentrations of PCBs are comparable to

Chapter 3: PCBs in the North Atlantic and the Arctic Ocean

those reported in Bear Island (North Atlantic-Sub Arctic Region)⁶ for the low chlorinated congeners, and those reported by Gioia *et al.*¹¹ for the eastern North Atlantic (3.5–22 pg m⁻³ for Σ_7 PCBs). The higher concentrations found by the latter in the ice-margin zone, and the climate change modulation of atmospheric POP concentrations recently described¹², is consistent with the higher variability reported here for some congeners in the ice-margin zone, and when air masses came from coastal and ice-covered areas. The summer of 2007 holds the record for the melting of sea-ice around the North Pole²³, which may have contributed to enhanced volatilization of POPs to the atmosphere as has been suggested recently for periods with minimum ice cover extent¹². For some of the sampling periods (those in the GC and one close to the ice margin), the estimated air masses²⁴ were consistently from the southwest (North Americas origin, Supplementary Fig. S2 on Appendix A.1). Among this subset of measurements, higher PCB concentrations were found in the southernmost sample near Iceland (Fig. 1a, Supplementary Fig. S1 on Appendix A.1), suggesting that atmospheric concentrations reduced during transport northwards. Indeed, measured concentrations in the gas phase showed a significant statistical decrease northwards (Friedmann test $p < 0.000005$). The application of the Wilcoxon rank test to the data set shows that the differences of atmospheric concentrations between the sampling points are significant and establishes a gradient in the concentrations with latitude, where C_G at 67°N is higher ($p < 0.05$) than at 74°N and significantly higher ($p < 0.05$) than at 78 and 81°N. It is possible to estimate the travel time (t , days) needed for the atmospheric transport from 67°N to 81°N using the measured wind speed and wind direction (Supplementary Table S3). If gas-phase concentrations are plotted against t , the atmospheric residence time (R_t), or half-lives, can be estimated by fitting equation (3.1) to the measured gas-phase concentrations (see Supplementary Methods S1 on Appendix A.3 for details).

$$C_t = C_0 e^{-\frac{t}{R_t}} \quad [3.1]$$

Where C_0 and C_t are the gas concentrations near Iceland (initial) and after a time period t . R_t can be related to physical–chemical properties that are relevant in the environmental partitioning of POPs, such as the octanol–water partition coefficient ($\log K_{OW}$) by $R_t = 1/(0.943 - 0.195 \log K_{OW})$ (Fig. 2 and Supplementary

Chapter 3: PCBs in the North Atlantic and the Arctic Ocean

Table S4 on Appendix A.2). Examples of R_t estimations are 4, 2.6 and 1.4 days for PCB congeners 18, 87 and 187, respectively.

3. Discussion

The estimated R_t for gas-phase PCBs over the GC, ranging from 1 to 4 days (Fig. 2), are consistent with those predicted in this region during the summer using a model of the atmospheric residence time of POPs² (Supplementary Fig. S3 on appendix A.1). In the latter modelling study, the short atmospheric residence times were driven by the important role that the biological pump has enhancing the air–water exchange of PCBs in this region. Indeed, vertical settling of water column OC and associated pollutants depletes the photic zone dissolved concentrations, driving a net absorption flux of POPs from the atmosphere². R_t range from a few days for the less hydrophobic congeners to around 1–2 day for the more hydrophobic PCBs (Fig. 2), consistent with the influence of the biological pump sequestering more effectively the more hydrophobic POPs from the atmosphere¹⁸. The air–deep water transport is the result of coupled air–water, phytoplankton uptake and settling fluxes¹⁸. The limiting step, or bottle neck, for this transfer is the diffusive air–water exchange¹⁸. Thus, even though the affinity to phytoplankton (or K_{OW}) is orders of magnitude higher for the more hydrophobic PCB congeners, the transfer of PCBs between air and deep water is limited by the air–water mass transfer coefficient that only change by a factor of 2–4 among congeners. Further support for air–water enhanced fluxes driven by the biological pump, as an explanation for the rapid decrease of atmospheric concentrations, is provided by the field measurements of dissolved, particulate and plankton concentrations and estimated air–water–plankton exchange fluxes of PCBs.

Chapter 3: PCBs in the North Atlantic and the Arctic Ocean

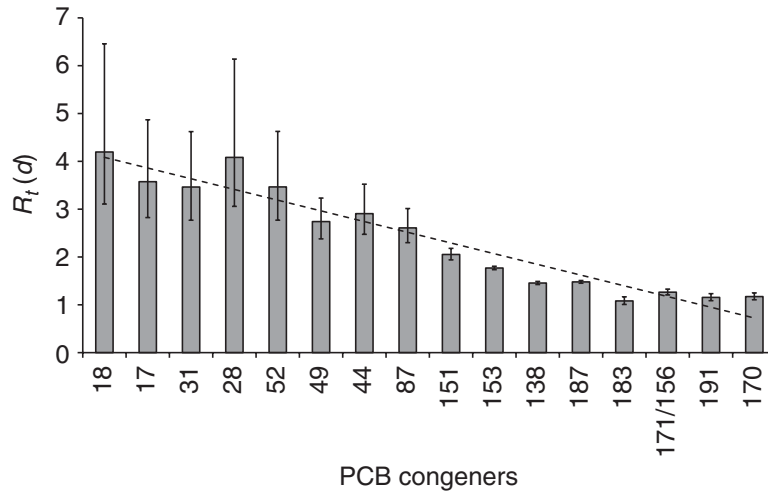


Figure 2. Atmospheric residence times, R_t (in days), estimated for each congener using equation (1) during their transport over the Greenland Current and Arctic ocean.

Bioconcentration factors of PCBs (BCF) in plankton were estimated by²⁵

$$BCF = \frac{C_P}{C_W} \quad [3.2]$$

Where C_P and C_W are the plankton and dissolved-phase concentrations, respectively. The study of bioconcentration of POPs, such as PCBs, in the lower levels of the trophic web is important as well to understand the factors that control the bioaccumulation and magnification of PCB concentrations in the Arctic food web, where due to the low temperatures, some POPs have longer persistence and magnification potential, leading to high concentrations in the higher predators with the associated impact on health³⁻⁴.

The BCF for phytoplankton, shown in Fig. 1, increased slightly at the northern sector of the GC, and showed higher variability near the Svalbard archipelago (Fig. 1). These trends in BCF values are due in part to changes in phytoplankton community and abundance, which was dominated by colonies of *Phaeocystis pouchetti*, and followed by diatoms, the abundance of which showed a dependence with temperature²⁶⁻²⁷. Indeed, PCB concentrations in phytoplankton were significantly correlated with biomass abundance ($C_P = 2.99 \times \text{Phaeocystis Biomass} + 43.5$, $R^2 = 0.76$, $p < 0.01$), and the variability in seawater and plankton-phase concentrations was higher in the ice-margin zone. The influence of the ice-margin zone on the concentration of PCBs in water (and thus particle and phytoplankton phase concentrations) is an issue that has not been

Chapter 3: PCBs in the North Atlantic and the Arctic Ocean

resolved. As in this study, some reports have not observed changes in water concentrations due to ice melting^{11,26}, but the influence of ice melting on atmospheric concentrations is more conclusive^{11,12}. A modification of gas-phase concentrations due to volatilization during ice melting has the potential to modify the seawater concentrations in proximate areas by air–water exchange inputs. The GC and Fram Strait are always regions with high phytoplankton primary productivity and chlorophyll concentrations during spring–summer. Chlorophyll *a* concentrations were 2.3 mg m⁻³ (range 0.3–6.7 mg m⁻³)²⁸ for the cruise stations and were high for all the GC and North Atlantic region as discerned from satellite images (See supplementary Fig. S4 on Appendix A.1). Primary productivity and the gross community production were also high during the sampling period^{28,29}. Periods with high phytoplankton growth can induce lower BCF values for the more hydrophobic compounds in comparison with the BCF values for low growth conditions²⁵, thus introducing further variability in the water column concentrations, consistent with the observations.

Bauerfeind and co-workers³⁰ have shown that most sinking fluxes of OC in the Eastern Fram Strait occur during the summer (the June–September period accounts for more than 60% of the annual export of OC) and the export of OC at 300-m depth accounts for ~10% of the gross primary productivity. It is then possible to estimate the removal of PCBs associated to sinking particles using these reported summer fluxes of OC and biogenic material for the Arctic summer (May to September), and the PCB concentrations measured in particles and plankton. Thus, the settling fluxes of PCBs (F_{Settling} , ng per m² per day) are given by:

$$F_{\text{Settling}} = F_{\text{Biogenic}} C_p \quad [3.3]$$

Where F_{Biogenic} is the sinking flux of biogenic material as reported elsewhere (from 35 to 40 mg per m² per day)³⁰ and C_p are the PCB concentrations measured in plankton. Figure 3 shows the estimated sinking fluxes for the GC and Fram Strait, respectively (See supplementary Table S5 on Appendix A.2). These fluxes can be compared with the atmospheric deposition fluxes of PCBs, which are the sum of net diffusive air–water exchange (F_{AW}) and dry deposition (F_{DD}), estimated in the traditional manner by:

Chapter 3: PCBs in the North Atlantic and the Arctic Ocean

$$F_{AW} = k_{AW} \left(\frac{C_G}{H'} - C_W \right) \quad [3.4]$$

$$F_{DD} = v_D C_A \quad [3.5]$$

Where C_G and C_A are the gas and aerosol-phase PCBs concentrations, respectively, H' is the dimensionless Henry's Law constant, k_{AW} is the air–water mass transfer coefficient, and v_D is the deposition velocity (0.1 cm s^{-1}) of aerosol-bound POPs. Estimated values and details of methodology and assessment of uncertainty for the F_{AW} and F_{DD} can be found elsewhere^{2,11,18,19} and in Supplementary Methods S2 on Appendix A.3

The estimated diffusive air–water exchange shows a significant net deposition of most PCB congeners in both the GC and Arctic region (Fig. 3 and Supplementary Table S6 on Appendix A.2). The dry deposition fluxes (Fig. 3 and Supplementary Table S7 on Appendix A.2) of aerosol-bound PCBs are lower than the net diffusive fluxes, but account for up to 30% of the total deposition fluxes for some congeners due to the low temperatures enhancing the sorption of PCBs to aerosols, thus increasing the dry deposition fluxes. The comparison of atmospheric deposition and sinking fluxes (Fig. 4) shows that approximately the same amount of PCBs that enter the ocean from the atmosphere are settling to the deep ocean, taking into account the factor of 2–3 uncertainty in these estimations for individual compounds (see Supplementary Fig. S6 on Appendix A.1). Therefore, the air–water–plankton–deep water system was presumably close to steady state during the sampling period with a significant coupling between the biological pump and atmospheric deposition. The high fluxes of biogenic matter during the Arctic summer depletes the water column concentrations driving a strong air-to-water fugacity gradient in the GC, which increase the diffusive flux from the atmosphere to water. This removal from the atmosphere as a depositional flux is on average of the order of $0.44 \text{ ng per m}^2 \text{ per day}$ for individual PCB congeners. A flux of this magnitude will remove an important fraction of atmospheric PCBs during their transport to the Arctic. Those PCB congeners with higher BCF values show a stronger association with phytoplankton organic matter, with higher potential for being transported to deep waters and depleting water column concentrations, thus driving a higher air–water diffusive flux. Indeed, there is a significant correlation between F_{AW} and BCF for the data set

Chapter 3: PCBs in the North Atlantic and the Arctic Ocean

generated in this study ($F_{AW} = -0.15 \text{ LogBCF} + 1.07$, $R^2 = 0.26$, $p < 0.05$, Supplementary Fig. S5 on Appendix A.1).

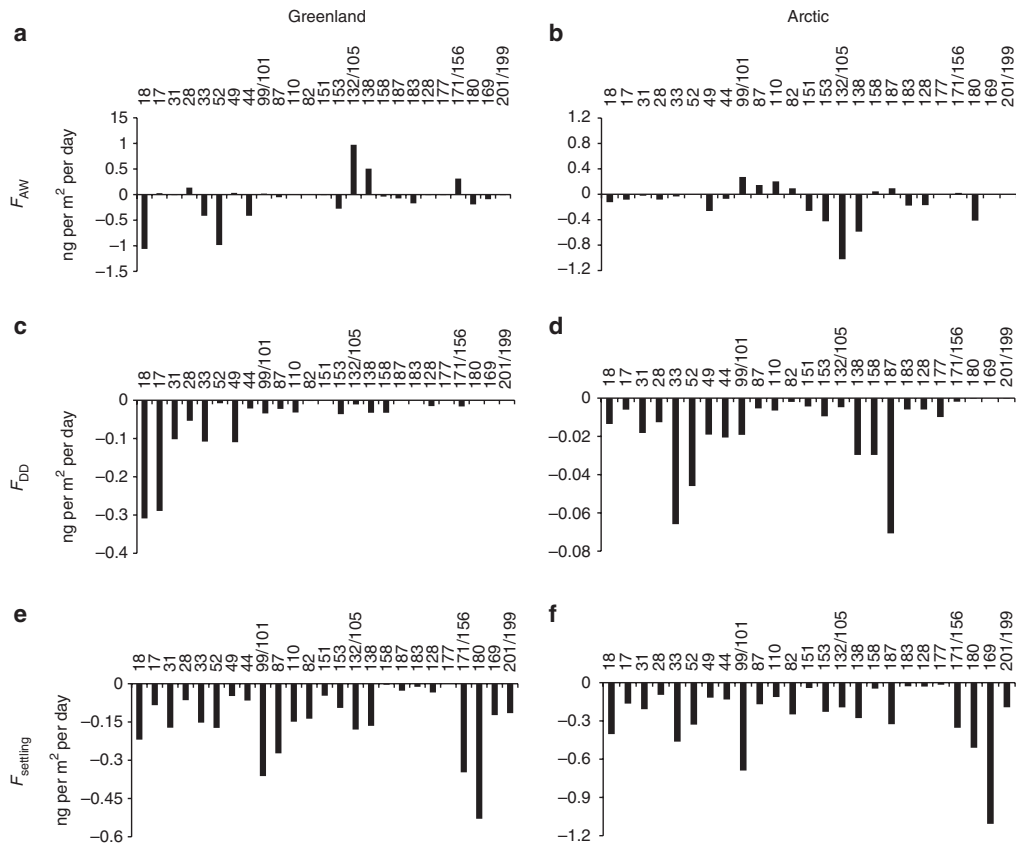


Figure 3. Atmospheric deposition and settling fluxes. net diffusive air–water exchange fluxes (F_{AW} , ng per m² per day) for the (a) Greenland Current and (b) Arctic ocean. Dry deposition fluxes (F_{DD} , ng per m² per day) for the (c) Greenland Current and (d) Arctic ocean. settling fluxes ($F_{settling}$, ng per m² per day) of PCBs for the (e) Greenland Current and (f) Arctic ocean.

Chapter 3: PCBs in the North Atlantic and the Arctic Ocean

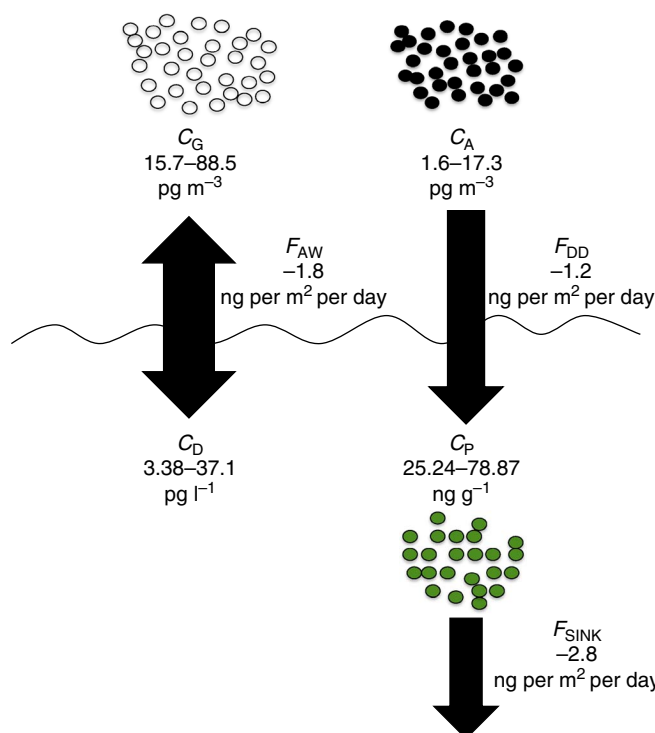


Figure 4 Sequestration of PCBs in the Greenland Current. schematics of the coupled fluxes of ΣPCBs^* involved in the sequestration of atmospheric pollutants by the biological pump. C_G (gas-phase concentration), C_A (aerosol-phase concentration), C_D (dissolved-phase concentration), C_P (phytoplankton-phase concentrations), F_{AW} (net air-to-water diffusive flux), F_{DD} (dry deposition flux) and F_{SINK} (settling flux). *sum of PCBs 18, 17, 31, 33, 52, 49, 44, 99/101, 87, 110, 82, 151, 153, 132/105, 158, 187, 183, 128, 177, 171/156, 180, 169, 201/199, 195 and 208.

The atmospheric deposition fluxes can be used to give estimates of atmospheric residence times that complement those derived from the decrease of atmospheric concentrations (Fig. 2). Taking PCB congeners 153 and 180 as examples (see Supplementary Fig. S6 on Appendix A.1), the total atmospheric concentrations (gas+aerosol) are in the range 0.9–4.7 and 1.2–4.0 pg m^{-3} , respectively. Considering a height of 500 m for the boundary layer, then the atmospheric inventory of PCBs 153 and 180 in the atmospheric boundary layer is 0.45–2.3 and 0.6–2.0 ng m^{-2} , respectively. The atmospheric residence time can be estimated by $R_t = \text{inventory} / \text{net deposition}^2$. The total net deposition is 0.33 and 0.2 $\text{ng per m}^2 \text{ per day}$ for PCBs 153 and 180, respectively. Then the atmospheric residence time estimated from the atmospheric concentrations (inventory) and deposition fluxes are in the ranges 1.4–7 days and 1.8–6 days for PCBs 153 and 180, respectively. These ranges of atmospheric residence times are of the same magnitude, when considering the uncertainties, than those predicted for high-chlorinated PCBs from the decrease of concentrations during atmospheric

Chapter 3: PCBs in the North Atlantic and the Arctic Ocean

transport (Fig. 2), and supports the fact that the high air–water disequilibrium can account for the rapid reduction of atmospheric concentrations over productive oceans. This also suggests that the depletion of atmospheric PCBs by other processes is not relevant in comparison to atmospheric deposition. One potential candidate process might be degradation due to reaction with OH radicals, but this is negligible in this region due to low OH concentrations².

An important issue is whether there is remineralization of PCBs in the surface ocean, or the role that remineralization of organic matter has in the fate of PCBs and other POPs. There is no field, laboratory, nor modelling evidence of effective degradation processes for PCBs in surface seawater even in warmer regions^{19,31}. Therefore, PCBs should be considered as persistent compounds in the oceanic water column, although sinking organic matter will be partly remineralized during sedimentation. When this happens, the fugacity capacity of the settling particles will decrease, and a fraction of PCBs will be redissolved in the meso-pelagic zone or in deep waters. Owing to sampling limitations for POPs, there are no measurements of PCBs from deep waters in the Arctic to evaluate the importance of this process. Subduction of cold surface waters has also been identified as a potential process for removing POPs from the surface ocean in the Greenland Sea³², but this process will only be effective regionally during winter when temperatures are low.

This study provides the first field evidence of the role that the biological pump has sequestering atmospheric POPs over productive oceanic regions, and confirms that the biological pump reduces and minimizes the transport of PCBs to the Arctic during the summer. This is the first field study that reports the occurrence of PCBs in the atmosphere, seawater and plankton, simultaneously, enabling for an assessment of coupled air–water–deep water fluxes that cannot be performed with other data sets. However, the biological pump drives air and water away from equilibrium conditions for hydrophobic compounds, and thus it is possible to perform a meta-analysis of published data sets of gas and dissolved-phase concentrations of organic pollutants to further confirm the important role that the biological pump has driving a marked air–water disequilibrium in concentrations. We compiled data sets describing the gas- and dissolved-phase

Chapter 3: PCBs in the North Atlantic and the Arctic Ocean

concentrations of organic pollutants in oceanic regions characterized by a high primary productivity and relevant for assessing the transport of POPs to the Arctic. These regions are mainly the North Atlantic and Atlantic sector of the Arctic and the regions proximate to the Bering Strait, but not the central Arctic that is covered by sea-ice, or coastal arctic regions that have land influenced dynamics in terms of POP cycling. Fugacity (Pa) is a useful descriptor for assessing the air–water disequilibrium. The fugacity ratio of POPs between air and water (f_A/f_W) is given by,

$$\frac{f_W}{f_A} = \frac{C_W H'}{C_G} \quad [3.6]$$

For the data set generated in this study, the fugacity ratios were higher than 3, showing an air–water disequilibrium driven by the biological pump with a significant net deposition. If this process is important at the hemispheric scale, then high fugacity ratios should have been observed in other assessments of POPs in the North Atlantic, North Pacific and the regions in the AO that show a high primary productivity. Figure 5a shows the PCB air–water fugacity ratios for this study and those reported by Gioia *et al.*¹¹ in the North Atlantic. In both cases, there is a high air–water fugacity gradient consistent with an air–water disequilibrium. Consistent with this study, Gioia *et al.*¹¹ reported higher fugacity gradients (or fluxes) for the more hydrophobic PCB congeners (higher K_{OW}), indicating that the biological pump has depleted the more hydrophobic compounds. Further confirmation of the role of the biological pump can be obtained from assessment of the relative abundance of the different congeners. The less hydrophobic low-chlorinated congeners are more abundant at higher latitudes^{11,13}, a pattern that is consistent with the lower efficiency of the biological pump in removing these POPs from the water column¹⁸.

The biological pump may also modulate the air–water disequilibrium and atmospheric transport of other POPs than PCBs. The compilation of the few existing studies on POPs, such as phthalates³³, polybrominated diphenyl ethers and other brominated organics^{34–35}, shows ubiquitous high air–water fugacity gradients in the high productivity regions around the AO (Fig. 5b). Therefore, all the field studies reporting simultaneous air and water concentrations of

Chapter 3: PCBs in the North Atlantic and the Arctic Ocean

hydrophobic POPs show a significant disequilibrium between air and water fugacities. This further confirms the important role that the biological pump has in sequestering atmospheric POPs in the high-latitude oceanic regions, as there is no other potential mechanism that can account for these high air–water fugacity ratios. Conversely, in oligotrophic regions such as the oceanic gyres, several studies have reported volatilization of PCB in the subtropical gyres of both the south and north basins of the Atlantic and Pacific^{31,36,37}, where the biological pump has a negligible role^{2,18}. In addition, these subtropical regions are characterized by higher atmospheric degradation of PCBs due to reaction with OH radical (lowering their fugacity in the gas phase)², and with warmer environments that enhances volatilization. Therefore, the modulation of atmospheric transport by the biological pump does not occur everywhere over the ocean, but only in the high productivity regions as those in high latitudes.

The sequestration of atmospheric POPs by the biological pump at high latitudes is likely to be a seasonal phenomenon. Sinking fluxes of biogenic material are ten times lower during the winter³⁰, thus as predicted elsewhere², the atmospheric residence times during winter are expected to be much longer due to a lack of sequestration by the biological pump, with a consequent efficient transport to the AO. This will be facilitated by the fact that during the winter the Arctic atmosphere is more permeable to the Atlantic Ocean atmosphere³⁸. However, transport of PCBs during the winter can not be quantified here because gas-phase concentrations in the temperate urban/industrial, rural and coastal regions upwind also depend on temperature, showing minimal concentrations during winter^{39–40}. The temporal and geographical extent of the biological pump in northern latitudes may be modified by climate change, affecting the balance, cycling and occurrence of POPs in the AO⁴¹. The modulation of atmospheric transport by the biological pump is presumably also occurring in other oceanic regions globally, and both its strength and variability in space and time is currently not accounted for in models of regional/global transport of POPs.

Chapter 3: PCBs in the North Atlantic and the Arctic Ocean

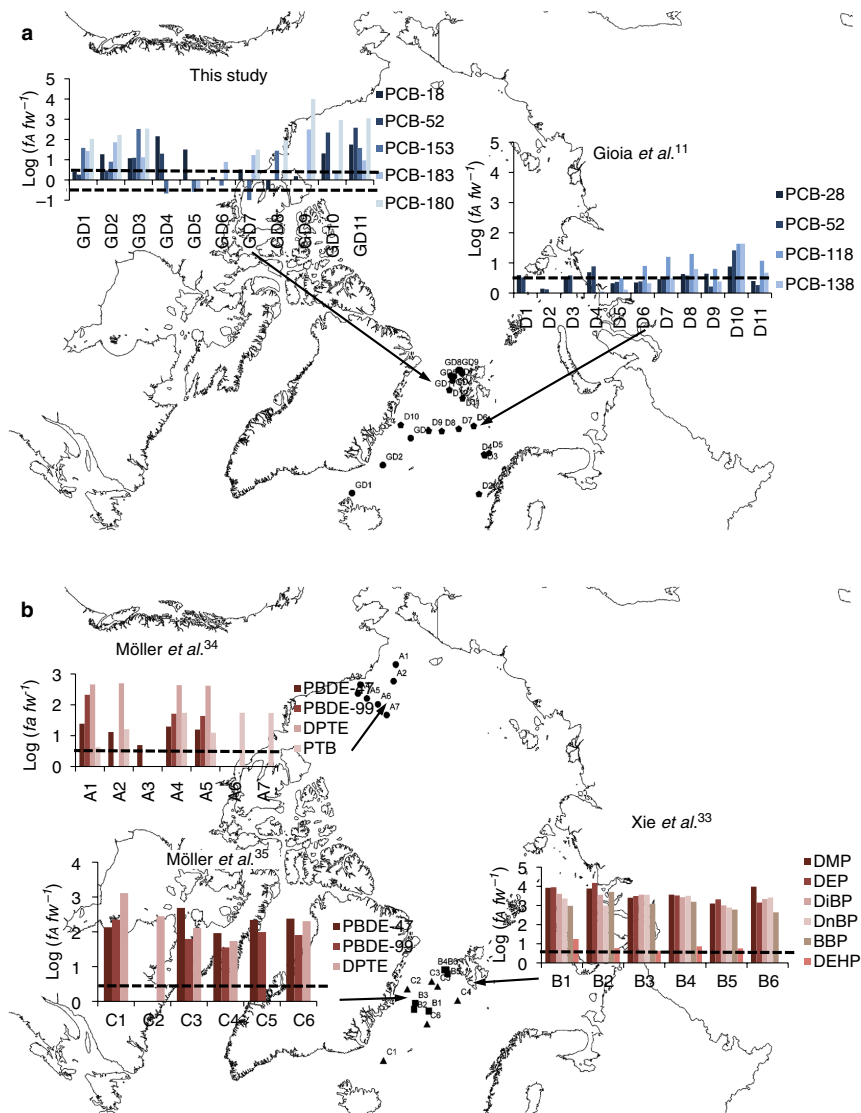


Figure 5. Air–water fugacity ratios in the Arctic region. Map of the Arctic ocean, North Atlantic and North Pacific showing (a) air-to-water fugacity ratios ($\log f_{a/w}$) for PCBs, estimated from the gas and dissolved phase concentrations from this study and those reported in Gioia *et al.*¹¹ and (b) air-to-water fugacity ratios ($\log f_{a/w}$) for other hydrophobic organic pollutants in high productivity regions from the north Atlantic and Arctic ocean³³⁻³⁵. For all these hydrophobic chemicals, there is a strong disequilibrium between air and water (high) consistent with the role of the biological pump lowering water column concentrations of organic compounds. The acronyms for the chemicals stand for DmP (Dimethyl phthalate), DEP (Diethyl phthalate), DiBP (Di-*i*-butyl phthalate), DnBP (Di-*n*-butyl phthalate), BBP (*n*-Butylbenzyl phthalate), DEHP (Diethylhexyl phthalate), PBDE (poly-brominated diphenyl ether), PTB (pentabromotoluene), DPTE (2,3-dibromopropyl-2,4,6-tribromophenyl ether) and PCB (polychlorinated biphenyl).

Chapter 3: PCBs in the North Atlantic and the Arctic Ocean

4. Methods

Sampling: Air sampling was performed using a high-volume sampler (MCV: CAV-A/HF, Collbató, Spain) operating at $40 \text{ m}^3 \text{ h}^{-1}$ located in the upper-deck of *R/V Hespérides* (mean \pm SE sampled air volume $1124 \pm 381 \text{ m}^3$). The high-volume sampler was only operated when the air mass was coming from the ocean, thus avoiding potential ship contamination. With the aim of sample aerosol and gas phase separately we used a precombusted (4 h at $450 \text{ }^\circ\text{C}$) and preweighed Quartz Microfibre Filter (QMA 203x254 mm $1 \text{ }\mu\text{m}$ nominal pore size, Whatman, England) for the particulate phase followed by a Polyurethane Foam (PUF) plugs (100 mm diameter x 120 mm, Klaus Ziemer GmbH, Germany). Both polyurethane foams (PUF) and QMA filters were precleaned before the sampling. PUF was precleaned using soxhlet with Hex:DCM (1:1) during 24 h and QMA filters were precombusted for 4 hours at 450°C .

Surface seawater samples (4 m depth) was sampled using the on board continuous sampling system and transferred into an overflowing 15 L stainless steel container during all the sampling period to avoid contamination from the ship. Seawater was pumped from this 15 L recipient with a peristaltic pump fitted with teflon tubes through Whatman glass fiber filters (142mm diameter, $0.7 \text{ }\mu\text{m}$ pore size) to obtain the particulate phase and through solvent-rinsed stainless steel columns, packed with XAD-2 resin (SUPELCO,USA) to obtain the dissolved phase. The XAD columns had been previously cleaned with Methanol and dichloromethane and were kept in Methanol (MeOH) at 277K.

Phytoplankton sampling was performed using a net trawl with a pore size of $200 \text{ }\mu\text{m}$. Sampling depth was from below the maximum of chlorophyll density depth (MCD) to surface. Then the phytoplankton was filtered through a glass fiber filter (47 mm $0.7 \text{ }\mu\text{m}$ pore size). Copepods were removed from the sampler before filtering. GFF filters were pretreated as described as for QMA filters.

Sample extractions: Prior to the extraction, 10 ng of PCBs 65 and 200 were added to samples to be used as surrogates to control the analyte extraction recovery and losses during sample handling. PUFs and filters corresponding to the gas, aerosol, particulate and phytoplankton were soxhlet extracted for during 24 h. For the PUF extraction Ac:Hex (3:1) was used, while Hex:DCM (1:1) was used

Chapter 3: PCBs in the North Atlantic and the Arctic Ocean

for the aerosol, particulate and phytoplankton filters. All the samples were then concentrated using a rotary evaporation unit. Dissolved seawater samples were extracted eluting XAD columns using 200mL of MeOH followed by 300mL of DCM. Afterwards the MeOH fraction was liquid-liquid extracted with hexane. The Hex and DCM fractions were merged and concentrated using rotary evaporation. All solvents used: Acetone (AC), hexane (HEX), MeOH and dichloromethane (DCM) were gas chromatography quality branded (Merck, KGaA).

Clean up and fractionation was done for all extracts (PUF, aerosol, dissolved seawater and particulate matter) using glass columns filled with neutral alumina (3g 3% deactivated) and anhydrous sodium sulfate (1g). The extract was eluted and fractionated using Hex (12mL) for the first fraction containing the PCBs. Finally the Hexanic fraction was concentrated under a gentle N₂ stream to 150 µL and sealed in amber vials. The phytoplankton samples were cleaned using Silica, Alumina and Anhydrous Sodium Sulfate and eluted using Hex:DCM (1:2 40 mL) followed by MeOH:DCM(1:2 40 mL). The Hex:DCM fraction was used to analyze PCBs concentrations on phytoplankton. More information about the analytical process is presented on Appendix A.1 in the supporting info and has been described elsewhere ¹⁸.

Quantification of PCBs: Analysis were conducted using an Agilent 7890 coupled to a uECD detector (Agilent Technologies) using a Wcot Sil 8CB 60 m capillary column (inner diameter 0.25mm, film thickness 0.25µm). Setting program starts from 90 °C holding during 1 min, then temperature raises from 90°C to 190 °C at 20°C/min and from 190°C to 310°C at 3°C minute holding 310 °C during 18 min. Retention time was used for the identification of the analytes. Internal standard quantification method was used adding 5ng of PCB 30 and 142 prior to injection.

Quality assurance and Control: Detection limits (DL) were calculated using mean plus 3 times standard deviation of noise in the blank samples and mean plus 10 times standard deviation for quantification limits (QL). The median and range of Detection Limits (DL) for selected PCBs in different matrix are 0.015 (0.004-0.07), 0.015 (0.004-0.07), 0.007 (0.001-0.048), 0.008 (0.002-0.167) and 0.019 (0.01-0.069) ng on column for gas, aerosol, dissolved, particulate and

Chapter 3: PCBs in the North Atlantic and the Arctic Ocean

phytoplankton respectively. Detection limits and quantification limits (QL) values for single PCBs are presented on Appendix A.2 in the supporting information.

References.

1. Wania, F. & Mackay, D. Tracking the distribution of persistent organic pollutants. *Environ. Sci. Technol.* **30**, 390–397 (1996).
2. Jurado, E. & Dachs, J. Seasonality in the “grasshopping” and atmospheric residence times of persistent organic pollutants over the oceans. *Geophys. Res. Lett.* **35**, L17805 (2008).
3. AMAP. *PCB in the Russian Federation: Inventory and Proposal for Priority Remedial Actions. Executive Summary. Arctic Monitoring and Assessment Programme*, OSLO and Centre for International Projects: <http://www.amap.no/ol-docs/pcb-es.pdf> (2000).
4. Macdonald, R. W. *et al.* Contaminants in the Canadian arctic: 5 years of progress in understanding sources, occurrence and pathways. *Sci. Total. Environ.* **254**, 93–234 (2000).
5. Hung, H. *et al.* Temporal and spatial variabilities of atmospheric polychlorinated biphenyls (PCBs), organochlorine (OC) pesticides and polycyclic aromatic hydrocarbons (PAHs) in the Canadian arctic: Results from a decade of monitoring. *Sci. Total. Environ.* **342**, 119–144 (2005).
6. Kallenborn, R., Christensen, G., Evenset, A., Schlabach, M. & Stohl, A. Atmospheric transport of persistent organic pollutants (POPs) to Bjørnøya (Bear island). *J. Environ. Monitor.* **9**, 1082–1091 (2007).
7. Wu, X. *et al.* Atmospheric HCH concentrations over the marine boundary layer from Shanghai, China to the Arctic ocean: role of human activity and climate change. *Environ. Sci. Technol.* **44**, 8422–8428 (2010).
8. Hung, H. *et al.* Atmospheric monitoring of organic pollutants in the Arctic under the Arctic monitoring and assessment programme (AMAP): 1993–2006. *Sci. Total Environ.* **408**, 2854–2873 (2010).
9. Kuzyk, Z. Z. A., MacDonald, R. W., Johannessen, S. C. & Stern, G. A. Biogeochemical controls on PCB deposition in Hudson Bay. *Environ. Sci. Technol.* **44**, 3280–3285 (2010).
10. Helm, P. A. & Bidleman, T. F. Gas-particle partitioning of polychlorinated naphthalenes and non- and mono-ortho-substituted polychlorinated biphenyls in Arctic air. *Sci. Total. Environ.* **342**, 161–173 (2005).
11. Gioia, R. *et al.* Polychlorinated biphenyls in air and water of the North Atlantic and

Chapter 3: PCBs in the North Atlantic and the Arctic Ocean

Arctic Ocean. *J. Geophys. Res-Oceans*. **113**, D19302 (2008).

12. Ma, J., Tian, C., Hung, H. & Kallenborn, R. Revolatilization of persistent organic pollutants in the Arctic induced by climate change. *Nature Clim. Change*. **1**, 255–260 (2011).

13. Sobek, A. & Gustafsson, Ö. Latitudinal fractionation of polychlorinated biphenyls in surface seawater along a 62° N-89° N transect from the Southern Norwegian Sea to the North Pole area. *Environ. Sci. Technol.* **38**, 2746–2751 (2004).

14. Carrizo, D. & Gustafsson, O. Distribution and inventories of polychlorinated biphenyls in the polar mixed layer of seven pan-arctic shelf seas and the interior basins. *Environ. Sci. Technol.* **45**, 1420–1427 (2011).

15. Hargrave, B. T. *et al.* Seasonality in bioaccumulation of organochlorines in lower trophic level arctic marine biota. *Environ. Sci. Technol.* **34**, 980–987 (2000).

16. Sobek, A., Reigstad, M. & Gustafsson, O. Partitioning of polychlorinated biphenyls between Arctic seawater and size-fractionated zooplankton. *Environ. Toxicol. Chem.* **25**, 1720–1728 (2006).

17. Sarmiento, J. L. & Gruber, N. *Ocean Biogeochemical Dynamics* (Princeton University Press, 2006).

18. Dachs, J. *et al.* Oceanic biogeochemical controls on global dynamics of persistent organic pollutants. *Environ. Sci. Technol.* **36**, 4229–4237 (2002).

19. Berrojalbiz, N. *et al.* Persistent organic pollutants in Mediterranean seawater and processes affecting their accumulation in plankton. *Environ. Sci. Technol.* **45**, 4315–4322 (2011).

20. Meijer, S. N. *et al.* Global distribution and budget of PCBs and HCB in background surface soils: implications for sources and environmental processes. *Environ. Sci. Technol.* **37**, 667–672 (2003).

21. Ockenden, W. A. *et al.* The global re-cycling of persistent organic pollutants is strongly retarded by soils. *Environ. Pollut.* **121**, 75–80 (2003).

22. Su, Y. & Wania, F. Does the forest filter effect prevent semivolatile organic compounds from reaching the Arctic? *Environ. Sci. Technol.* **39**, 7185–7193 (2005).

23. Arrigo, K. R., Van Dijken, G. & Pabi, S. Impact of a shrinking Arctic ice cover on marine primary production. *Geophys. Res. Lett.* **35**, GL035028 (2008).

24. Draxler, R. R. & Rolph, G. D. HYSPLIT (HYbrid Single-Particle Lagrangian Integrated Trajectory) Model access via NOAA ARL READY, NOAA Air Resources Laboratory:

Chapter 3: PCBs in the North Atlantic and the Arctic Ocean

<http://ready.arl.noaa.gov/HYSPLIT.php> (2011).

25. Del Vento, S. & Dachs, J. Prediction of uptake dynamics of persistent organic pollutants by bacteria and phytoplankton. *Environ. Toxicol. Chem.* **21**, 2099–2107 (2002).
26. Gustafsson, O. *et al.* Observations of the PCB distribution within and in-between ice, snow, ice-rafted debris, ice-interstitial water, and seawater in the Barents sea marginal ice zone and the north Pole area. *Sci. Total. Environ.* **342**, 261–279 (2005).
27. Calbet, A., Saiz, E., Almeda, R., Movilla, J. I. & Alcaraz, M. Low microzooplankton grazing rates in the Arctic ocean during a phaeocystis pouchetii bloom (summer 2007): fact or artifact of the dilution technique? *J. Plankton Res.* **33**, 687–701 (2011).
28. Lasternas, S. & Agustí, S. Phytoplankton community structure during the record Arctic ice-melting of summer 2007. *Polar. Biol.* **33**, 1709–1717 (2010).
29. Regaudie-de-Gioux, A. & Duarte, C. M. Plankton metabolism in the Greenland Sea during the polar summer of 2007. *Polar. Biol.* **33**, 1651–1660 (2010).
30. Bauerfeind, E. *et al.* Particle sedimentation patterns in the eastern Fram Strait during 2000–2005: Results from the arctic long-term observatory HAUSGARTEN. *Deep-Sea. Res. Part I.* **56**, 1471–1487 (2009).
31. Nizzetto, L., Lohmann, R., Gioia, R., Dachs, J. & Jones, K. C. Atlantic ocean surface waters buffer declining atmospheric concentrations of persistent organic pollutants. *Environ. Sci. Technol.* **44**, 6978–6984 (2010).
32. Lohmann, R., Jurado, E., Pilson, M. E. Q. & Dachs, J. Oceanic deep water formation as a sink of persistent organic pollutants. *Geophys. Res. Lett.* **33**, GL025953 (2006).
33. Xie, Z. *et al.* Occurrence and air-sea exchange of phthalates in the arctic. *Environ. Sci. Technol.* **41**, 4555–4560 (2007).
34. Möller, A. *et al.* Polybrominated diphenyl ethers vs alternate brominated flame retardants and dechloranes from East Asia to the Arctic. *Environ. Sci. Technol.* **45**, 6793–6799 (2011).
35. Möller, A., Xie, Z., Sturm, R. & Ebinghaus, R. Polybrominated diphenyl ethers (PBDEs) and alternative brominated flame retardants in air and seawater of the European Arctic. *Environ. Pollut.* **159**, 1577–1583 (2011).
36. Zhang, L. & Lohmann, R. Cycling of PCBs and HCB in the surface ocean- lower atmosphere of the open Pacific. *Environ. Sci. Technol.* **44**, 3832–3838 (2010).
37. Lohmann, R., Klanova, J., Kukucka, P., Yonis, S. & Bollinger, K. PCBs and OCP on an

Chapter 3: PCBs in the North Atlantic and the Arctic Ocean

East-to-west transect: the importance of major currents and net volatilization for PCBs in the Atlantic Ocean. *Environ. Sci. Technol.* **46**, (2012) Doi: 20.1021/es203459e.

38. Zhang, L., Ma, J., Venkatesh, S., Li, Y. F. & Cheung, P. Modeling evidence of episodic intercontinental long-range transport of lindane. *Environ. Sci. Technol.* **42**, 8791–8797 (2008).

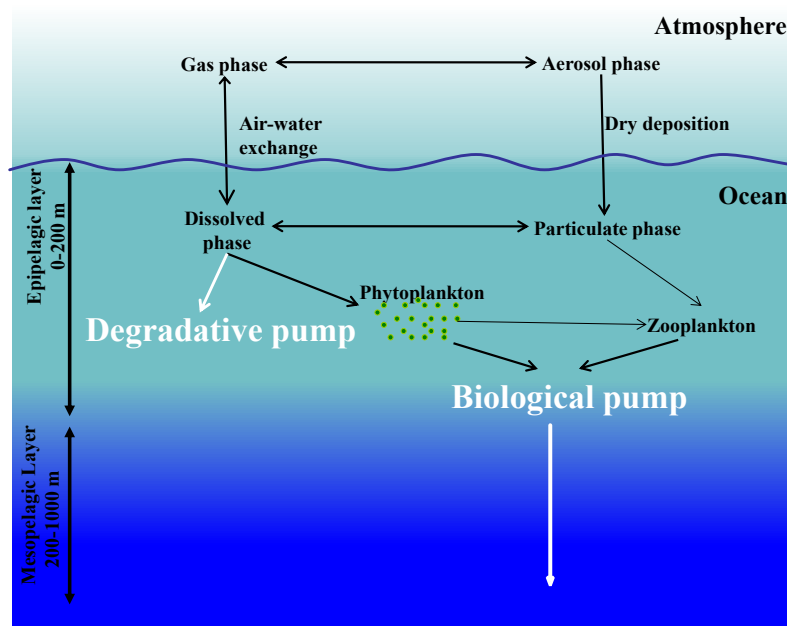
39. Simcik, M. F., Basu, I., Sweet, C. W. & Hites, R. A. Temperature dependence and temporal trends of polychlorinated biphenyls in the Great Lakes atmosphere. *Environ. Sci. Technol.* **33**, 1991–1995 (1999).

40. Brunciak, P. A., Dachs, J., Gigliotti, C. L., Nelson, E. D. & Eisenreich, S. J. Atmospheric polychlorinated biphenyl concentrations and apparent degradation in coastal New Jersey. *Atmos. Environ.* **35**, 3325–3339 (2001).

41. Macdonald, R. W., Harner, T. & Fyfe, J. Recent climate change in the Arctic and its impact on contaminant pathways and interpretation of temporal trend data. *Sci. Total Environ.* **342**, 5–86 (2005).

Chapter 4

The “degradative” and “biological” pumps controls on the atmospheric deposition and sequestration of Hexachlorocyclohexanes and Hexachlorobenzene in the North Atlantic and Arctic Oceans.



The results from the present chapter were published as Galbán-Malagón et al. 2013b in *Environmental Science and Technology*, 2013,47 (13), 7195-7203.

Chapter 4: HCHs and HCB in the North Atlantic and Arctic Ocean.

Abstract

The cycling of Hexachlorobenzene (HCB) and Hexachlorocyclohexanes (HCHs) have been studied in the North Atlantic (Greenland Current) and Arctic Ocean. Concentrations of HCHs and HCB were measured simultaneously in the atmosphere (gas and aerosol phases), seawater (dissolved and particulate phases), and phytoplankton. The atmospheric concentrations of HCHs decrease during transport over the Greenland Current with estimated e-folding times of 1.6 days. This strong decrease in atmospheric concentrations of HCHs is consistent with the estimated atmospheric depositional fluxes driven by strong air-water disequilibrium. The removal of HCHs from the surface ocean by hydrolysis, microbial degradation, and settling of particle-associated HCHs is estimated; the removal fluxes are within a factor of two of the atmospheric inputs for most sampling events, suggesting an important role of the degradative pump in the overall oceanic sink of HCHs. Conversely, the lack of degradation of HCB in surface waters, and its relatively low hydrophobicity, implies a lack of effective removal processes, consistent with the observed air and water concentrations close to equilibrium. This work is the first that estimate the relative importance of the biological and degradative pumps on the atmospheric deposition of non-persistent organic pollutants, and points out the need for further research for quantifying the magnitude of degradative processes in the environment.

Chapter 4: HCHs and HCB in the North Atlantic and Arctic Ocean.

1. Introduction

Organochlorine pesticides (OCPs), such as hexachlorobenzene (HCB) and hexachlorocyclohexanes (HCHs), have been widely used in the past as fungicides and pesticides, and distributed globally through atmospheric transport. HCHs were used in two commercial formulations: technical HCH and Lindane. It is estimated that ~ 10 Mt of technical HCH and 720kt of Lindane were used from 1948 to 2000¹⁻³. The production of HCB has been estimated to be of ~100.000 t⁴. Because of their effects on the human health and the environment they were included in the Long Range Transboundary Air Pollution protocol (LRTAP) of the United Nations Economic Commission for Europe (UN ECE) in 1998, and the Stockholm Convention in 2001⁵⁻⁷. In addition, these chemicals are regularly assessed in Polar environments such as within the Arctic Monitoring and Assessment Programme (AMAP)⁸.

HCHs and HCB share some of the properties of other persistent organic pollutants (POP) in terms of potential for long range transport due to its semi-volatile properties, and in the case of HCB due to its persistence. However, these compounds differ in properties of the widely studied polychlorinated biphenyls (PCBs), usually considered as surrogates of POPs, since they are less hydrophobic, and HCHs are also less persistent in the environment. The distribution of OCPs in the environment has been widely reported close and far from source regions^{4,9,10}. An especially extended body of literature exists for the occurrence and cycling of HCHs in the Arctic showing that atmospheric concentrations of HCHs in the Arctic have decreased over the last decade in response to decreasing primary sources^{2,11-13}. However, HCHs and HCB are still present in soils¹⁴, ice, snow¹⁵, and surface oceans¹⁶⁻²¹ of the Arctic environment. The Arctic has been regarded as one of the ultimate sinks of OCPs, including α -HCH, γ -HCH and HCB^{22,23}, even though recent studies suggest these may be remobilizing from historical reservoirs²⁴.

The understanding of the cycling of HCHs and HCB in the Arctic and adjacent oceans is important due to the large capacity of oceans as a reservoir of organic pollutants and for the role of oceans as sink of POPs²⁵⁻²⁷. HCHs and HCB

Chapter 4: HCHs and HCB in the North Atlantic and Arctic Ocean.

have reached the Arctic and North Atlantic oceans through atmospheric transport and the subsequent deposition. Due to the relatively high solubility of HCHs, ocean currents are also important transport pathways for α -HCH^{16-17, 21}. Several studies have assessed the air-water exchange of HCB and HCHs^{10, 19, 28, 29}, reporting net deposition in most studies, and a reversal in the exchange direction in the Pacific Arctic during the last 15 years³⁰. However, the drivers of air-water exchange have not been comprehensively studied for HCHs and HCB as they have been studied for other POPs. It has been predicted that atmospheric residence times of the more hydrophobic POPs would be reduced by the role of the biological pump sequestering atmospheric pollutants³¹, a process observed recently for PCBs in the Atlantic sector of the Arctic Ocean³². This process is less efficient for chemicals with intermediate hydrophobicities ($3 < \text{Log}K_{OW} < 5$)²⁶, theoretically implying that the biological pump may play a minor role in sequestering HCHs and HCB. Recently, field studies have suggested that the biological pump is not an efficient process for depleting α -HCH, γ -HCH and HCB in surface waters in the North Atlantic²⁰ and in the Mediterranean Sea³³. However, HCHs are known to be degraded in the water column, either by bacteria or abiotically. If degradation in the water column is faster than air-water exchange under certain environmental conditions, a decrease of concentrations in surface waters would be driving air and water far from equilibrium conditions. This “degradative pump”, as opposed to the “biological pump”, could play a role on the cycling of non-persistent organic pollutants. Previous studies suggested that HCHs settling in the water column is a slower pathway compared to degradation^{25, 34}. Moreover, recently, it has been modelled that degradation could be the responsible of the α -HCH depletion in the surface water in the Beaufort Sea³⁵, but there is still little known about the importance of degradation of HCHs on their environmental cycling.

The objectives of this work are: i) to report the simultaneous measurements of HCHs and HCB in five different environmental matrices (gas and aerosol phases, dissolved and particulate phases, and phytoplankton) in the North-West Atlantic and Arctic oceans, ii) to investigate the air-water exchange of HCHs and HCB in the Greenland Current (GC) and the Arctic Ocean (AO) iii)

Chapter 4: HCHs and HCB in the North Atlantic and Arctic Ocean.

to quantify the relative importance of the biological and degradative pumps in the cycling of HCHs and HCB

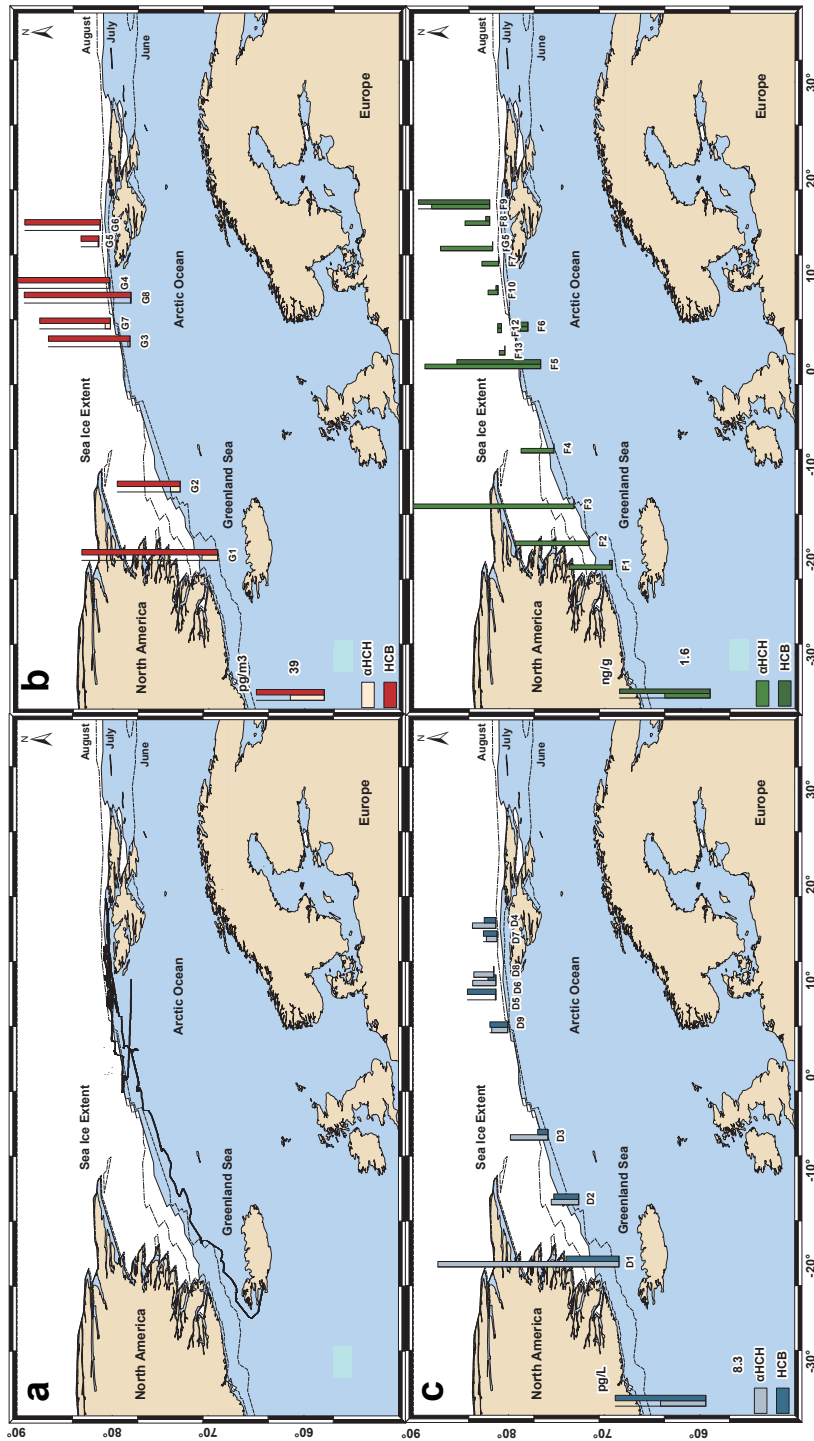


Figure 1. Spatial variability of HCH and HCB concentrations. a) α -HCH and HCB gas phase concentrations (pg m⁻³), c) dissolved phase concentrations (pg L⁻¹) and d) phytoplankton phase concentrations (ng g⁻¹).

Chapter 4: HCHs and HCB in the North Atlantic and Arctic Ocean.

2. Material and methods

2.1 Sampling cruise

The sampling was carried out during the ATOS I cruise on board the *RV Hespérides* on July 2007 in the North Atlantic and Arctic Ocean between Iceland and Svalbard (Figure 1a). The sampling area can be divided into two different regions: Arctic Ocean (AO) and the Greenland Current (GC). Both areas are influenced by high phytoplankton productivity during summer with ice melting affecting more directly the AO (Figure 1). During the cruise, simultaneous samples of air (gas and aerosol phase), surface water (particulate and dissolved phases), and phytoplankton were taken. Ancillary data including physical and chemical characterization of air and water were obtained from the automatic continuous water system and the meteorological station on board of the ship. In addition, vertical profiles of temperature, density and fluorescence were obtained from the CTD casts. Samples' ancillary data are reported in Table S1 on Appendix B.1 in the supporting information.

2.2 Sampling procedures.

Air samples were collected using a high-volume sampler (MCV: CAV-A/HF, Collbató, Spain) deployed over the vessel bridge connected to a wind direction sensor in order to avoid contamination from the ship. Air was sampled only when the wind direction was from the bow (90° to -90°). Sampling flow rate was set at $40 \text{ m}^3 \text{ h}^{-1}$ and the sampling volumes were $1124 \pm 381 \text{ m}^3$. The gas phase was collected on a polyurethane foam (PUF) plugs (100 mm diameter x 120 mm, Klaus Ziemer GmbH, Germany) and the aerosol phase was trapped on a quartz microfiber filters (QM/A) 203x254 mm, 1 μm pore size (Whatman, England).

Seawater dissolved and particulate samples were collected at 5 m depth using the ship on line water system and transferred into a 25 L stainless steel container overflowing during the sampling period. Water was pumped through a glass fibre filter (GF/F) 142 mm \varnothing 0.7 μm pore size (Whatman, England) followed by a stainless steel column filled with cleaned XAD-2 (SUPELCO, USA), collecting the particulate and dissolved phases, respectively³⁶.

Chapter 4: HCHs and HCB in the North Atlantic and Arctic Ocean.

Phytoplankton samples were collected using a net trawl provided with a 50 µm mesh. The sampling depth was chosen based on the CTD chlorophyll density profiles acquired before sampling and deploying the net 10 meters below the depth of the maximum chlorophyll density (MCD) and obtaining integrate samples from this depth to surface. Several net casts were performed ensuring collection of sufficient biomass for subsequent analysis. Phytoplankton was then filtered using a (GF/D) 142 mm Ø 2.7µm pore size (Whatman, England) on board. The aerosol, particulate and phytoplankton filters were stored at -20° C wrapped in aluminium foil inside sealed bags. PUFs were placed in a wrapped aluminium foil and stored inside zip sealed bags. Both XAD-2 columns and PUFs were kept at 4°C until analysis.

Prior to the sampling cruise, PUFs had been pre-cleaned using a Soxhlet extraction with acetone:hexane (3:1) for 24 h. They were then dried, wrapped in aluminium foil and sealed using 2 ziplock bags. Filters were pre-combusted for 4 hours at 450°C. Filters were pre-weighed and wrapped in aluminium foil before sampling. XAD-2 resin was cleaned by eluting the column with 200 mL of methanol, 200 mL of dichloromethane, 250 mL of acetone and plus 200 mL of methanol. XAD-2 columns were sealed and stored at 4°C until sampling. All the stainless steel tools used during the sampling were pre-cleaned by rinsing with acetone before use.

2.3 Chemical analysis.

Prior to extraction a recovery standard was added to all samples (10 ng of PCBs 65, Dr Ehrenstorfer, GMBH, Germany). PUFs were Soxhlet extracted during 24 hours using acetone:hexane (3:1) as solvent. Then, the samples were concentrated by rotary evaporation (R-200, Büchi, Italy) until 1-2 mL, followed by a clean up and fractionation using a glass column filled with 3g of neutral alumina (3% deactivated) and 1 g of anhydrous sodium sulphate. The first fraction was collected using 12 mL of hexane, while the second fraction was collected using 15 mL of hexane:dichloromethane (1:2). All fractions were concentrated

Chapter 4: HCHs and HCB in the North Atlantic and Arctic Ocean.

until 1-2 mL by rotary evaporation. Finally the extracts were concentrated, under a purified N₂ stream, until 150 µL and solvent exchanged to isooctane. Both aerosol and particulate phase filters were Soxhlet extracted using methanol:dichloromethane (1:2). Extracts were transferred into hexane and concentrated to 1-2 mL. The extracts were then purified following the same method described for PUFs.

XAD-2 columns were extracted with 200 mL of methanol followed by 300 mL of dichloromethane. The methanol fraction was liquid-liquid extracted with hexane three times. Both extracts (the dichloromethane and hexane extract) were combined and evaporated in a rotary evaporation to 1-2 mL. The samples were purified as described for PUFs and filters.

Phytoplankton samples were freeze dried for 4 hours. Thirty minutes after the freeze dry step, 10 ng of recovery standard (PCBs 65) was added to the samples. Freeze dried samples were Soxhlet extracted for 24 hours using hexane:dichloromethane (1:2). Samples were purified using a 350 mm long and 8 mm Ø glass column filled with 5 g of silica gel (silica 60, 200 mesh) activated at 250 °C for 24 hours prior to purification, 3 g of deactivated neutral alumina (3%) and 1 g of anhydrous sodium sulphate. Every sample was fractionated into 2 fractions: The first fraction was eluted with 40 mL of hexane:dichloromethane (1:2) and the second with 40 mL of methanol:dichloromethane (1:2). Both fractions were concentrated by rotary evaporation until approximately 1 ml and then the first and second fractions were solvent exchanged to isooctane and ethyl acetate, and further concentrated until 150 µL under a N₂ stream. Prior to injection, 5 ng of PCB 30 was added as internal standards to all samples.

Identification and quantification were done using an Agilent 7890 Gas chromatograph coupled to a µ-ECD detector (Agilent Technologies), provided with a HP-5MS 60m capillary column (inner diameter 0.325 µm, film thickness 0.25 µm). The elution ramp started from 90 °C holding during 1 min, next the temperature raised from 90 to 190 °C (20 °C min⁻¹) and from 190°C to 310°C (3°C min⁻¹) holding 310 °C for 18 min. α-HCH, γ-HCH and HCB were analysed in the merged first and second fraction for the gas and dissolved phase. For the aerosol,

Chapter 4: HCHs and HCB in the North Atlantic and Arctic Ocean.

particulate matter and phytoplankton only the first fraction was injected. Identification and quantification was done using the retention time of the α -HCH, γ -HCH and HCB.

2.4 Quality assurance and quality control.

Detection and quantification limits (DL and QL) were calculated using 2 field blank samples from each matrix. DL was calculated as the average of the blank concentration plus three times the standard deviation, while the QL was derived as the average plus 10 times the standard deviation of the field blanks (Table S2 in Appendix B.1). Recovery of PCB 65 averaged 70% (47-92%) for all matrices (Table S3 in Appendix B.1). Final concentrations were corrected by the recovery of PCB 65.

3. Results and Discussion

3.1 Occurrence of HCHs and HCB in seawater and phytoplankton.

Seawater concentrations did not show a clear spatial trend for the sum of HCH isomers and HCB (Figure 1c, and Figure S2 and Table S4a in Appendix B.2). Dissolved phase γ -HCH concentrations ranged from 2.1 to 6.5 pg L^{-1} and from 0.05 to 2.1 pg L^{-1} in the GC and AO, respectively, while the α -HCH concentrations ranged from 0.03 to 6.3 pg L^{-1} and from 0.002 to 0.81 pg L^{-1} in the GC and AO, respectively. Particulate phase α -HCH concentrations ranged from 0.55 to 0.82 pg L^{-1} and from 0.26 to 0.61 pg L^{-1} for the GC and AC respectively, while particle phase γ HCH concentrations ranged from 0.35 to 0.89 and from 0.02 to 0.48 pg L^{-1} for the GC and AO, respectively. These concentrations are in the same range of those reported in the NE Atlantic and Arctic Oceans¹⁹, but significantly lower (*Kruskal-Wallis*, $p < 0.05$) than those reported in the Greenland, Irminger and Bering seas, and the North Pacific/Arctic Ocean^{20, 21, 28, 30}.

Dissolved phase HCB concentrations ranged from 0.94 to 4.8 pg L^{-1} and 0.03-2.6 pg L^{-1} in the GC and AO, respectively. Seawater particulate phase concentrations were in the range of 0.23-0.39 pg L^{-1} and 0.18-0.36 pg L^{-1} in the GC and the AO. Reported dissolved phase concentrations in the present work are

Chapter 4: HCHs and HCB in the North Atlantic and Arctic Ocean.

similar to those reported for the Arctic Ocean¹⁹, Irminger and Greenland Currents²⁰, and Pacific sector of the Arctic Ocean²¹. However, higher concentrations (*Kruskal-Wallis*, $p < 0.05$) have been reported in other studies^{37, 38}. The HCB particulate phase concentrations are comparable to those reported by Lohmann et al.¹⁹.

HCHs were found in all the phytoplankton samples while HCB was only found in 7 out of the 13 phytoplankton phase samples analysed (Figure 1d, and Figure S1 and table S4b on Appendix B.2). Phytoplankton phase concentrations of α -HCH ranged from 0.13 to 3.1 ng g⁻¹ and from 0.06 to 1 ng g⁻¹ in the GC and AO, respectively, while for γ -HCH, these ranged from 0.42 to 1.8 ng g⁻¹ and from 0.55 to 2.4 ng g⁻¹ for the GC and AO, respectively. HCB concentrations were 0.05-1.4 and 0.04-1.2 ng g⁻¹ in the GC and AO.

There are no previous reports of HCHs and HCB concentrations in phytoplankton for the North Atlantic and Arctic Ocean.

3.2 Atmospheric occurrence of HCHs and HCB.

Atmospheric (gas and aerosol phases) HCHs concentrations are shown in Figure 1 and the complete data set given in table S4c in Appendix B.2. Both α and γ HCH gas phase concentrations showed a one order of magnitude variability with higher concentrations at lower latitudes along the GC and a significant decrease ($p < 0.005$) at higher latitudes in the AO (Figure 1, Figure 2, and Figure S2 in Appendix B.2).

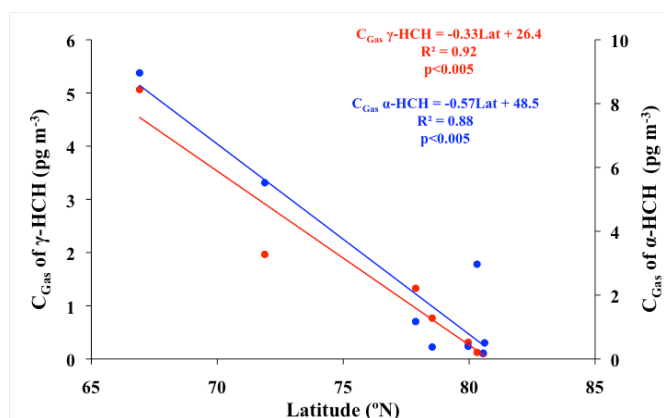


Figure 2. Relationship between the gas phase concentrations (pg m⁻³) of α -HCH and γ -HCH and latitude during the ATOS I cruise

Chapter 4: HCHs and HCB in the North Atlantic and Arctic Ocean.

Conversely, HCB gas phase concentrations were not correlated with latitude (Figure S1). The aerosol phase concentrations mimic the trends observed for the gas phase with HCHs decreasing at higher latitudes and a lack of latitudinal trend for HCB (Figure S1). HCHs were found predominantly in the gas phase (>93% of total atmospheric HCHs). Gas phase concentrations of α -HCH in the GC ranged from 1.17 to 8.96 pg m^{-3} , and from 0.18 to 2.9 pg m^{-3} in the AO, while γ -HCH concentrations were in the range of 1.33 -5 pg m^{-3} and 0.1 -0.77 pg m^{-3} in the GC and AO, respectively. These concentrations of HCHs are in the same range of those described previously in the Atlantic sector of Arctic Ocean¹⁹, the Subpolar North Atlantic Ocean³⁹, the Pacific Ocean sector of the Arctic²¹, the North Pacific Ocean⁴⁰, the Northern Canadian Archipelago⁴¹, and the Irminger and Greenland Current²⁰. However, higher concentrations have been reported for other Arctic regions (Kruskal-Wallis $p < 0.05$)^{10, 28, 42}(Table S5a on Appendix B.2).

HCB was found mainly in the gas phase (approximately 99% of total atmospheric concentrations). Concentrations in the gas phase ranged from 36 to 77 pg m^{-3} and from 0.40 to 61 pg m^{-3} in the GC and OC, respectively. Aerosol phase concentrations were two orders of magnitude lower (Table S4c on Appendix B.2) than those in the gas phase. HCB gas phase concentrations are comparable to concentrations described for the Arctic and Subarctic areas^{19-21, 39, 41, 43} (see Tables S5b in Appendix B.2).

3.3 Field derived atmospheric residence times.

The decrease of concentrations with latitude allows to estimate the atmospheric residence times, or e-folding times, for HCHs. This approach has been previously used and described for PCBs in this region³², and other POPs in other oceanic regions^{44, 45}. The air mass back-trajectories⁴⁶ for the sampling periods show that four samples were influenced by the same source upwind (from the SW) with a wind direction matching the trajectory of the ship (Figures S2a and S2b on Appendix III). Hence, the travel time (t) needed for atmospheric transport to move the air mass from the first sampling period (West of Iceland) to

Chapter 4: HCHs and HCB in the North Atlantic and Arctic Ocean.

the other sampling sites along the Greenland current and Arctic Ocean can be estimated using the wind speed. The least squares fitting of these pairs of gas phase concentrations (C_G , pg m^{-3}) and t will provide the rate of decrease in concentration. Indeed, the variation of atmospheric gas phase concentrations is significantly correlated with t ($p < 0.001$ $R^2 = 83.3\%$) following

$$\ln C_G = -0.61(\pm 0.07)t + 1.92(\pm 0.22) \quad [4.1]$$

The atmospheric e-folding times (Rt , d) equals the inverse of the slope of equation [1], thus $Rt = 1.6$ days (from 1.4 to 1.8 days) for HCHs. There are no statistically differences in the Rt values for α -HCH and γ -HCH. Conversely, HCB does not show a significant decrease in concentrations during its transport to the Arctic. The Rt estimated here for HCHs are higher than field derived Rt for HCHs in the South Atlantic and Indian Ocean but lower than those reported for the East and South China seas⁴⁵. The relatively short e-folding times suggest that the atmosphere in the North Atlantic and the Arctic is rapidly depleted of HCHs. Degradation by OH radical may not be important since OH radical concentrations are low in this region³¹. Air-water exchange should be the main driver of the decrease in atmospheric concentrations of these pollutants.

3.4 Atmospheric deposition of HCHs and HCB.

Atmospheric input fluxes are the sum of diffusive air-water exchange (F_{AW} , $\text{ng m}^{-2} \text{d}^{-1}$) and dry deposition (F_{DD} , $\text{ng m}^{-2} \text{d}^{-1}$) fluxes. Prior to estimating F_{AW} , it is useful to test if there is a significant net air-to-water diffusion of HCHs. This can be achieved by estimating the chemical fugacity in the gas (f_{air} , Pa) and dissolved phases (f_{water} , Pa) by,

$$f_{air} = C_{Gas}RT \quad [4.2]$$

$$f_{water} = C_{Dis}H'RT \quad [4.3]$$

Where R is the ideal gas constant ($8.314 \text{ Pa mol}^{-1} \text{ K}^{-1}$), T is the surface water temperature (K), H' is dimensionless Henry's Law Constant (HLC) corrected by temperature and salinity, and C_{Dis} is the dissolved phase concentration. Estimated fugacity ratios were calculated dividing f_{water} by f_{air} (see

Chapter 4: HCHs and HCB in the North Atlantic and Arctic Ocean.

table S8 in Appendix B.4). Due to uncertainties associated with the air/seawater concentrations and HLC, fugacity ratios need to be assessed within a range of values⁴⁷; ratios between 0.3 and 3 indicate that compounds are close to equilibrium conditions, ratios under 0.3 indicate a significant net deposition and over 3 indicates net volatilization from the sea. The fugacity ratios were lower than 0.3 for HCHs pointing to a significant net air-to-water exchange (Figure S3 and table S7 in Appendix B.4). Previous studies have also reported net deposition in the East Greenland and Irminger Current, and in the Eastern Arctic Ocean^{19, 20, 29, 34, 37, 41-43}. Conversely, fugacity ratios show that HCB is close to air-water equilibrium (Figure S3 and table S7 on Appendix B.4), which is in agreement with previous work in the Beaufort Sea, the Labrador Sea and the Arctic Ocean^{19, 20, 41, 43}. Therefore, the lack of decrease of atmospheric concentrations for HCB is consistent with a lack of strong depositional fluxes. Whether the net deposition of HCH is enough to explain the decreasing concentrations during atmospheric transport can only be assessed after estimating the atmospheric depositional fluxes.

F_{AW} was calculated in the traditional manner by

$$F_{AW} = k_{AW} \left(\frac{C_{Gas}}{H'} - C_{Dis} \right) \quad [4.4]$$

Where k_{AW} is the air-water mass transfer coefficient ($m d^{-1}$). Details of assessment of uncertainty for the F_{AW} and estimations methods for k_{AW} can be found elsewhere^{26, 27}.

Aerosol phase concentrations (C_{Aero}) were used to calculate F_{DD} using the only available field measurement of aerosol deposition velocity of POPs over the ocean ($v_D = 0.1 cm s^{-1}$)⁴⁸ by:

$$F_{DD} = v_D C_{Aero} \quad [4.5]$$

Estimations of F_{AWs} and F_{DDs} for each sampling period are shown in Appendix B.4 (Table S9a) and summarized in Figure 3. The main input of HCHs to the AO and GC is the atmospheric diffusive gas exchange, which is two to three orders of magnitude higher than dry aerosol deposition (Figure 3). The

Chapter 4: HCHs and HCB in the North Atlantic and Arctic Ocean.

estimates of atmospheric depositional fluxes can be used to provide alternative estimates of the e-folding times. With atmospheric concentrations over the GC of about 5 and 3 pg m^{-3} for α -HCH and γ HCH, respectively, and assuming a height for the atmospheric boundary layer of 500 m, the atmospheric inventory is of 2.5 ng m^{-2} and 1.5 $\text{ng m}^{-2} \text{d}^{-1}$ for α -HCH and γ HCH, respectively. The atmospheric residence time of HCHs is given by this atmospheric inventory divided by the atmospheric deposition flux, which is of about 1.7 $\text{ng m}^{-2} \text{d}^{-1}$ and 0.7 $\text{ng m}^{-2} \text{d}^{-1}$ for α -HCH and γ HCH (Figure 3). Then the e-folding times are of 1.5 and 2.1 days for α -HCH and γ HCH, respectively, similar to the 1.6 days estimated above from the decrease of gas phase concentrations.

It is important to elucidate the processes that drive the low concentrations of HCHs in the water column, which induce a high air-to-water disequilibrium and short atmospheric residence times. Previous modelling efforts of the role of the biological pump for chemicals with intermediate hydrophobicity, such as HCHs and HCB, have suggested that it is not strong enough to result in such a high depositional flux^{26, 33}. The determination of concentrations of HCHs and HCB in phytoplankton allow to determine their bioconcentration factors (*BCF*, L Kg^{-1}) by

$$BCF = \frac{C_{Phyto}}{C_{Dis}} \quad [4.6]$$

Where C_{Phyto} (ng kg^{-1}) is the concentration in the phytoplankton phase (see table S4b on Appendix B.3). The obtained *BCFs* for HCB were similar to the temperature corrected $\text{Log}K_{OW}$ (See Table S8 and Figure S4 on Appendix B.4), while *BCFs* for HCHs were significantly higher than those predicted from K_{OW} . The higher *BCF* for HCHs points to a potential higher influence of the biological pump than previously predicted by models. Indeed, the determination of HCHs and HCB in phytoplankton allows to estimate settling fluxes and to compare them, for the first time, with estimated degradation fluxes in surface waters.

Chapter 4: HCHs and HCB in the North Atlantic and Arctic Ocean.

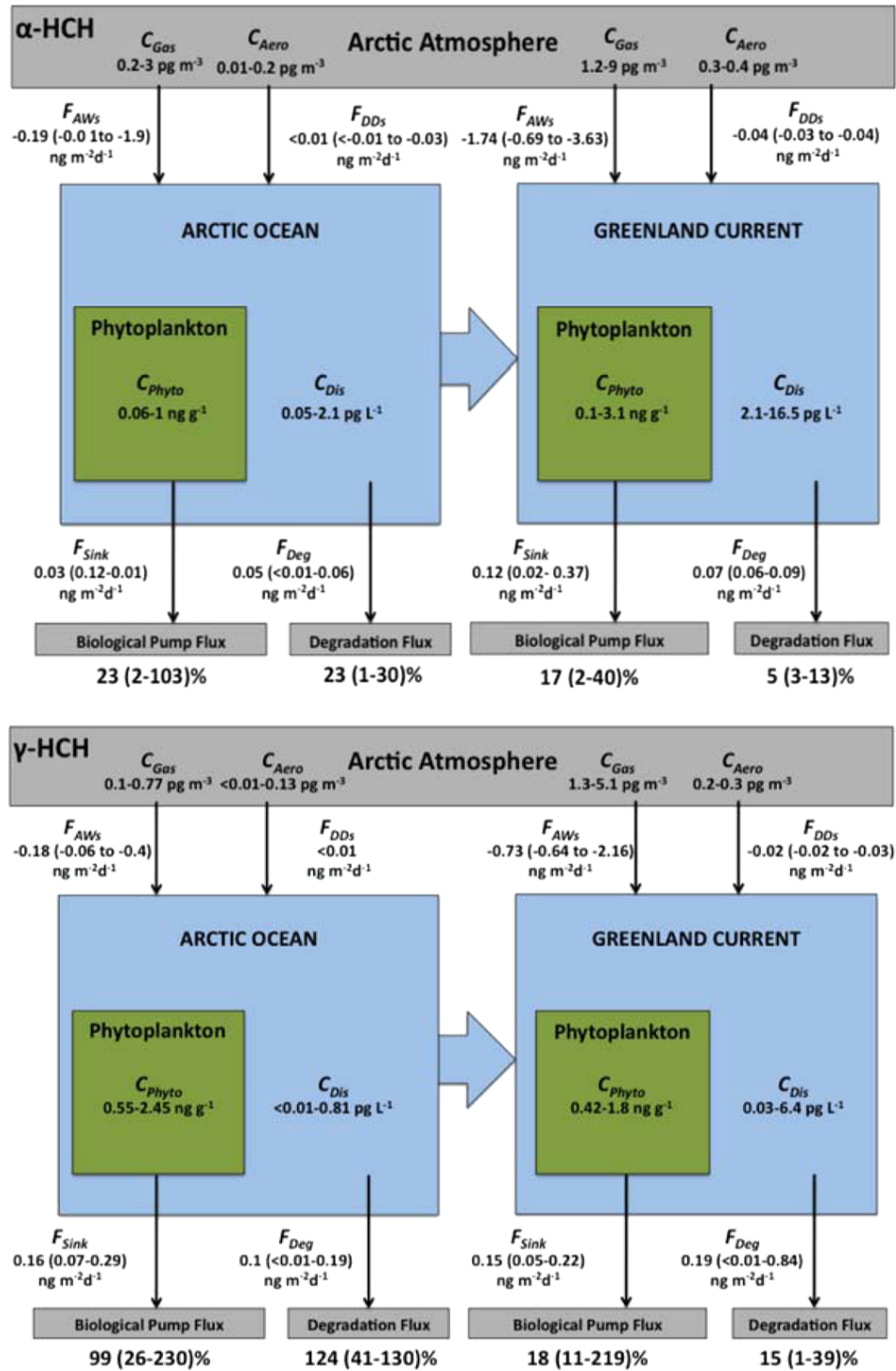


Figure 3. Mass Balance for α -HCH (a) and γ -HCH (b) during ATOS I cruise for the Greenland Current and Arctic Ocean. C_{Gas} is the atmospheric concentration in the gas phase, C_{Aero} is the atmospheric concentration in the aerosol phase, C_{Dis} is the dissolved phase concentration, C_{Phyto} is the concentration in the phytoplankton phase, F_{AW} is the air-to-water diffusive flux, F_{DD} is the dry deposition flux, F_{Sink} is the sinking flux, and F_{Deg} is the total degradation flux for α -HCH and γ -HCH. Figures in % indicate the proportion of the atmospheric input removed by the biological and degradative pumps.

Chapter 4: HCHs and HCB in the North Atlantic and Arctic Ocean.

3.5 Removal fluxes from the water column.

Biotic and abiotic degradation, the biological pump and subduction of water masses are the main mechanisms responsible for removing organic chemicals from surface waters^{25, 26, 33, 34, 48}. Formation of deep water by subduction is not a relevant process during summer in the northern hemisphere, thus it is not considered here. The biological pump is driven by the partitioning of organic chemicals to settling organic matter, including phytoplankton, resulting in a net sinking flux to deeper waters (F_{Sink} , $ng\ m^{-2}\ d^{-1}$), a process especially relevant for hydrophobic POPs in productive regions such as the North Atlantic region adjacent to the Arctic ocean³². Transport through the water column of the less hydrophobic compounds, such as HCHs and HCB, by the biological pump, is not very efficient^{20, 26}. However, the occurrence of HCHs and HCB in Arctic Ocean sediments has been reported previously^{49, 50}, and despite the modest magnitude of the biological pump for HCHs and HCB, it is the responsible for their transport to sediments. F_{Sink} can be estimated by

$$F_{Sink} = F_{Biogenic} C_{Phyto} \quad [7]$$

Where $F_{Biogenic}$ is the biogenic matter sinking fluxes ($g\ m^{-2}d^{-1}$). $F_{Biogenic}$ has been reported elsewhere⁵¹ for the studied region and a value of $0.06\ g\ m^{-2}\ d^{-1}$ was considered here.

The overall degradation fluxes for the mixing layer of the top ocean (F_{Deg} , $ng\ m^{-2}\ d^{-1}$), including microbial degradation ($F_{Deg,m}$, $ng\ m^{-2}\ d^{-1}$) and hydrolysis ($F_{Deg,h}$, $ng\ m^{-2}\ d^{-1}$), have usually not been explicitly estimated for surface waters despite field studies provide evidence of its importance^{29, 32}. Conversely, it has been identified as a key process for deeper waters. Harner et al.³⁴ estimated the microbial degradation constants (k_{ma+} , k_{ma-} and $k_{m\gamma}$) for $\alpha(+)$ -HCH, $\alpha(-)$ -HCH and γ -HCH for the Arctic deep waters from water mass age, assuming they are constant for most of the top 1000 m of the water column. Hydrolysis constants (k_{ha} and $k_{h\gamma}$) for α -HCH and γ -HCH have also been reported^{25, 34}. The bacterial abundance and activity in deep waters is much lower than that observed in the surface mixing layer⁵². Thus, the microbial degradation constants reported at 1000 m depth should be scaled using either the prokaryote biomass

Chapter 4: HCHs and HCB in the North Atlantic and Arctic Ocean.

abundance or activity in the epipelagic zone, which was the zone sampled in the present work (top 26 m), in comparison to that observed in deep waters. Prokaryote biomass production is four to five times higher than in the epipelagic zone ($\approx 250\text{-}265 \text{ mmol C m}^{-2}$) than in the mesopelagic zone ($\approx 50\text{-}75 \text{ mmol C m}^{-2}$)⁵², a similar relation to that of microbial (prokaryote) abundance. It is reasonable to assume that the microbial degradation rates are higher in the upper epipelagic layer than in the mesopelagic layer with a proportionality given by the microbial biomass, thus,

$$K_{ms} = \frac{K_{m1000} B_{ms}}{B_{m1000}} \quad [8]$$

Where K_{ms} and K_{m1000} are the microbial degradation rates at the surface mixing layer and at 1000 m depth, and B_{mh} and B_{m1000} are the microbial biomass in the water-column at surface and at 1000 m depth. These scaling of degradation constants could be done as well using the prokaryote heterotrophic production with similar results for the estimated K_{mh} (see table S9 on Appendix B.4).

Therefore, F_{Deg} in the water column for organic compounds is given by

$$F_{Deg} = F_{Deg_m} + F_{Deg_h} \quad [9]$$

Where

$$F_{Deg_m} = k_{mh} C_{dis} h \quad [10]$$

$$F_{Deg_h} = k_h C_{dis} h \quad [11]$$

Thus

$$F_{Deg\alpha} = (k_{mh\alpha+} 0.5C_{dis} + k_{mh\alpha-} 0.5C_{dis} + k_{h\alpha} C_{dis})h \quad [12]$$

$$F_{Deg\gamma} = (k_{mh\gamma} C_{dis} + k_{h\gamma} C_{dis})h \quad [13]$$

Where $F_{Deg\alpha}$ and $F_{Deg\gamma}$ are the total degradation fluxes ($\text{ng m}^{-2} \text{ d}^{-1}$) of α -HCH and γ -HCH, $k_{mh\alpha+}$, $k_{mh\alpha-}$ and $k_{mh\gamma}$ (d^{-1}) are the scaled microbial degradation rate constants for α -HCH (+ and -) and γ -HCH, respectively, in the mixing layer with depth h (26 m), $0.5C_{dis}$ is the dissolved phase concentration (ng m^{-3})

Chapter 4: HCHs and HCB in the North Atlantic and Arctic Ocean.

corrected by the proportion of α -HCH (+ and -) of the atmospheric input¹⁹. The estimated settling and degradation fluxes for each sampling period are shown in Appendix B.4 (Tables S8 and S9) and summarized in Figure 3.

3.6 Importance of the degradative and biological pumps.

The biological pump drives the fate of the less degradable and hydrophobic compounds, such as PCBs³², but HCHs are more prone to degradation than PCBs^{25, 34} and thus the biological pump may not be the only important removal process of HCHs from the surface water²⁰. In the Arctic ocean, the removal of HCHs by the biological pump account on average 23% and 99% of the atmospheric inputs for α -HCH and γ -HCH, while total degradation fluxes for α -HCH and γ -HCH accounted of average for 23% and 124% of the atmospheric inputs (Figure 3 and table S10 on Appendix B.4). Therefore, in the North Atlantic sector of the Arctic Ocean, diffusive fluxes are enhanced by the low concentrations in seawater driven in part by the high primary production, as measured during the cruise^{53, 54}, inducing an important role of the biological pump, and also in part by degradation fluxes which is enhanced by the elevated microbial proliferation reported during this cruise^{55, 56}. It is not possible to estimate to which degree the low concentrations of HCHs and HCB are due to ice melting freshwater inputs, but these freshwater inputs may introduce nutrients^{57, 58}, which may enhance the microbial degradation and the biological pump.

In the Greenland Current, the higher gas-phase concentrations induced higher atmospheric inputs. Calculated F_{Sink} shows that the biological pump accounts for an average of 17% and 18% of the total atmospheric input fluxes for α -HCH and γ -HCH (Figure 3 and tables S9a,b and S10 on Appendix B.4). The estimated F_{Deg} accounts for an average of 5% and 15% of atmospheric inputs for α -HCH and γ -HCH respectively (figure 3 and table S10 on Appendix B.4). The biological pump and microbial heterotrophic activity are influencing together the water-column depletion of HCHs along the Greenland Current. However, the estimated removal fluxes due to the biological and degradation pump are a factor of two-four lower than the estimated depositional fluxes, but these discrepancies are within the uncertainties associated for the estimates of depositional fluxes,

Chapter 4: HCHs and HCB in the North Atlantic and Arctic Ocean.

biological pump and degradation fluxes, and thus the removal fluxes are not significantly different than the input fluxes. It is also feasible that the important depletion of water column concentrations may have occurred previously to the sampling events, when a higher extent of the biological pump and degradation fluxes were occurring.

Therefore, the sequestration of atmospheric pollutants driving the decrease of atmospheric concentrations is consistent with the predicted removal fluxes in the water column. However, further research should be done in determining the microbial degradation constants of organic pollutants such as HCHs in natural communities in order to quantify with higher accuracy the extent of the degradation pump. Other studies have suggested that the degradation pump could also be important for other non-persistent pollutants such as PAHs³³.

As for HCB, which is a chemical highly persistent in the environment with not known effective degradation processes⁴, the removal due to the degradative pump is negligible. The only removal from the water column will be by sinking, but this contribution is also small. These results are consistent with the lack of significant decrease in HCB concentrations during atmospheric transport, and the close to equilibrium conditions between the gas and dissolved phases (Figure S4 and table S8 on Appendix B.4). HCB was seldom found in the phytoplankton samples with low BCF values, and sinking fluxes account for 3-4% of the maximum atmospheric input estimated when there was a net deposition (figure S5 and table S8 on Appendix B.4). Therefore, both the degradative and biological pumps are not effective removal processes of HCB from surface waters, while they play a significant role for HCHs. The important role of the degradative pump may be responsible in part for the described decrease of HCHs occurrence in oceanic waters²⁹.

Chapter 4: HCHs and HCB in the North Atlantic and Arctic Ocean.

References

1. Li, Y.-F.; Bidleman, T. F.; Barrie, L. A.; McConnell, L. L. Global hexachlorocyclohexane use trends and their impact on the arctic atmospheric environment. *Geophys. Res. Lett.* **1998**, *25* (1), 39-41. DOI 10.1029/97GL03441
2. Li, Y. -F. Global technical hexachlorocyclohexane usage and its contamination consequences in the environment: From 1948 to 1997. *Sci. Total. Environ.* **1999**, *232* (3), 121-158. DOI 10.1016/S0048-9697(99)00114-X
3. Voldner, E.C; Li Y.-F. Global usage of selected persistent organochlorines. *Sci. Total. Environ.* **1995**, *160-161* (15) 201-210. DOI 10.1016/0048-9697(95)04357-7.
4. Barber, J. L.; Sweetman, A. J.; Van Wijk, D.; Jones, K. C. (2005). Hexachlorobenzene in the global environment: Emissions, levels, distribution, trends and processes. *Sci. Total. Environ.* **2005**, *349* (1-3), 1-44. DOI 10.1016/j.scitotenv.2005.03.014
5. UNECE. Protocol on Persistent Organic Pollutants under the 1979 Convention on Long-Range Transboundary Air Pollution; *United Nations Economic Commission for Europe.* **1998**,
6. UNEP Final act of the plenipotentiaries on the Stockholm Convention on persistent organic pollutants; United Nations Environment Program Chemicals. **2001**, www.pop.int
7. De Wit, C. A.; Muir, D. Levels and trends of new contaminants, temporal trends of legacy contaminants and effects of contaminants in the arctic: Preface. *Sci. Total. Environ.* **2010**, *408* (15), 2852-2853. DOI 10.1016/j.scitotenv.2009.06.011
8. Hung, H.; Kallenborn, R.; Breivik, K.; Su, Y.; Brorström-Lundén, E.; Olafsdottir, K.; Thorlacious, J.M.; Leppänen, S.; Bossi, R.; Skow, R.; Manø. S.; Patton, G.W.; Stern, G.; Sverko, E.; Fellin, P. (2010). Atmospheric monitoring of organic pollutants in the arctic under the arctic monitoring and assessment programme (AMAP): 1993-2006. *Sci. Total. Environ.* **2010**, *408* (15), 2854-2873. DOI 10.1016/j.scitotenv.2009.10.044
9. Tanabe, S.; Tatsukawa, R. Vertical transport and residence time of chlorinated hydrocarbons in the open ocean water column. *J. Oceanograp. Soc. Japan.* **1983**, *39* (2), 53-62.
10. Berrojalbiz, N.; Dachs, J.; Del Vento, S.; Ojeda, M. J.; Valle, M. C.; Castro-Jiménez, J.; Mariani, G.; Wollgast, J.; Hanke, G. Persistent organic pollutants in Mediterranean seawater and processes affecting their accumulation in plankton. *Environ. Sci. Technol.* **2011**, *45* (10), 4315-4322.
11. Cabrerizo, A.; Dachs, J.; Barcelo, À D.; Jones, K. C. Climatic and biogeochemical controls on the remobilization and reservoirs of persistent organic pollutants in Antarctica.

Chapter 4: HCHs and HCB in the North Atlantic and Arctic Ocean.

Environ. Sci. Technol. **2013**, 47, 4299-4306.

12. Harner, T.; Jantunen, L. M. M.; Bidleman, T. F.; Barrie, L. A.; Kylin, H.; Strachan, W. M. J.; Macdonald, R. W. Microbial degradation is a key elimination pathway of hexachlorocyclohexanes from the Arctic Ocean. *Geophys. Res. Lett.* **2000**, 27 (8), 1155-1158.
13. Iwata, H.; Tanabe, S.; Sakal, N.; Tatsukawa, R. Distribution of persistent organochlorines in the oceanic air and surface seawater and the role of ocean on their global transport and fate. *Environ. Sci. Technol.* **1993**, 27 (6), 1080-1098.
14. Li, Y.-F.; Bidleman, T. F. Correlation between global emissions of α -hexachlorocyclohexane and its concentrations in the arctic air. *J. Environ. Inform.* 2003, 1 (1), 52!57.
15. Li, Y. -F.; Macdonald, R. W. Sources and pathways of selected organochlorine pesticides to the arctic and the effect of pathway divergence on HCHs trends in biota: A review. *Sci. Total. Environ.* **2005**, 342 (1-3), 87-106. DOI 10.1016/j.scitotenv.2004.12.027
16. Becker, S.; Halsall, C. J.; Tych, W.; Kallenborn, R.; Su, Y.; Hung, H. Long-term trends in atmospheric concentrations of α - and γ -HCH in the Arctic provide insight into the effects of legislation and climatic fluctuations on contaminant levels. *Atmos. Environ.* **2008**, 42 (35), 8225-8233. DOI 10.1016/j.atmosenv.2008.07.058
17. Meijer, S. N.; Shoeib, M.; Jantunen, L. M. M.; Jones, K. C.; Harner, T. (2003). Air-soil exchange of organochlorine pesticides in agricultural soils. 1. field measurements using a novel *in situ* sampling device. *Environ. Sci. Technol.* **2003** 37 (7), 1292-1299. DOI 10.1021/es020540r
18. Herbert, B. M. J.; Villa, S.; Halsall, C. J. Chemical interactions with snow: Understanding the behavior and fate of semi-volatile organic compounds in snow. *Ecotox. Environ. Safe.* **2006**, 63(1), 3-16. DOI 10.1016/j.ecoenv.2005.05.012
19. Macdonald, R.W.; Barrie, L.A.; Bidleman, T.F.; Diamond M.L.; Gregor, D.J.; Semkin, R.G.; Strachan, W.M.J; Li, Y.-F.; Wania, F.; Alae, M.; Alexeeva, L.B.; Backus, S.M.; Bailey, R.; Bewers, J.M.; Gobeil, C.; Halsall, C.J.; Harner, T.; Hoff, J.T.; Jantunen, L.M.M.; Lockhart, W.L.; Mackay, D.; Muir, D.C.G.; Pudykiewicz, J.; Reimer, K.J.; Smith, J.N.; Stern, G.A.; Schroeder, W.H.; Wagemann, R.; Yunker, M.B. Contaminants in the canadian Arctic: 5 years of progress in understanding sources, occurrence and pathways. *Sci. Total. Environ.* **2005**, 254 (2-3), 93-234. DOI 10.1016/S0048-9697(00)00434-4
20. Li, Y.-F.; Macdonald, R. W.; Jantunen, L. M. M.; Harner, T.; Bidleman, T. F.; Strachan, W. M. J. The transport of β -hexachlorocyclohexane to the western Arctic ocean: A contrast to α -HCH. *Sci. Total. Environ.* **2002**, 291 (1-3), 229-246. DOI 10.1016/S0048-9697(01)01104-4

Chapter 4: HCHs and HCB in the North Atlantic and Arctic Ocean.

21. Li, Y.F.; Macdonald, R.W.; Ma, J.; Hung, H.; Venkatesh, S. Historical α -HCH budget in the Arctic ocean: the arctic mass balance box model (AMBBM). *Sci. Total Environ.* **2004**, 324, 115–139. DOI 10.1016/j.scitotenv.2003.10.022
22. Lohmann, R.; Gioia, R.; Jones, K. C.; Nizzetto, L.; Temme, C.; Xie, Z.; Schulz-Bull, D.; Hand, I.; Morgan, E.; Jantunen, L. Organochlorine pesticides and PAHs in the surface water and atmosphere of the north Atlantic and Arctic ocean. *Environ. Sci. Technol.* **2009**, 43 (15), 5633–5639. DOI 10.1021/es901229k
23. Zhang, L.; Bidleman, T.; Perry, M.J.; Lohmann, R. Fate of chiral and achiral organochlorine pesticides in the north Atlantic bloom experiment. *Environ. Sci. Technol.* **2012**, 46 (15), 8106–8114. DOI 10.1021/es3009248
24. Cai, M.; Ma, Y.; Xie, Z.; Zhong, G.; Möller, A.; Yang, H.; Sturm, R.; He, J.; Ebinghaus, R.; Meng, X.Z. Distribution and air-sea exchange of organochlorine pesticides in the north Pacific and the Arctic. *J. Geophys. Res-Atmos.* **2012**, 117 (6), DOI 10.1029/2011JD016910
25. Wania, F.; Mackay, D. Global fractionation and cold condensation of low volatility organochlorine compounds in Polar Regions. *Ambio.* **1993**, 22, 10–18.
26. Wania, F. Assessing the potential of persistent organic chemicals for long-range transport and accumulation in Polar Regions. *Environ. Sci. Technol.* **2003** 37 (7), 1344–1351. DOI 10.1021/es026019e
27. Ma, J.; Hung, H.; Tian, C.; Kallenborn, R. Revolatilization of persistent organic pollutants in the Arctic induced by climate change. *Nat. Clim. Change.* **2011**, 1, 255–260. DOI:10.1038/NCLIMATE1167.
28. Dachs, J.; Lohmann, R.; Ockenden, W. A.; Méjanelle, L.; Eisenreich, S. J.; Jones, K. C. Oceanic biogeochemical controls on global dynamics of persistent organic pollutants. *Environ. Sci. Technol.* **2002**, 36 (20), 4229–4237. DOI 10.1021/es025724k
29. Jurado, E.; Lohmann, R.; Meijer, S.; Jones, K. C.; Dachs, J. Latitudinal and seasonal capacity of the surface oceans as a reservoir of polychlorinated biphenyls. *Environ. Pollut.* **2004**, 128 (1-2), 149–162. DOI 10.1016/j.envpol.2003.08.039
30. Jantunen, L. M.; Bidleman, T. F. Reversal of the air - water gas exchange direction of hexachlorocyclohexanes in the Bering and Chukchi seas: 1993 versus 1988. *Environ. Sci. Technol.* **1995**, 29 (4), 1081–1089.
31. Jantunen, L. M. M.; Bidleman, T. F. Organochlorine pesticides and enantiomers of chiral pesticides in Arctic Ocean water. *Arch. Environ. Con. Tox.* **1998**, 35 (2), 218–228. DOI 10.1007/s002449900370

Chapter 4: HCHs and HCB in the North Atlantic and Arctic Ocean.

32. Lakaschus, S.; Weber, K.; Wania, F.; Bruhn, R.; Schrems, O. (2002). The air-sea equilibrium and time trend of hexachlorocyclohexanes in the Atlantic Ocean between the Arctic and Antarctica. *Environ. Sci. Technol.* **2002**, 36 (2), 138-145. DOI 10.1021/es010211j
33. Jurado, E.; Dachs, J. Seasonality in the "grasshopping" and atmospheric residence times of persistent organic pollutants over the oceans. *Geophys. Res. Lett.* **2008**, 35 (17). DOI 10.1029/2008GL034698
34. Galbán-Malagón, C.; Berrojalbiz, N.; Ojeda, M. J.; Dachs, J. The oceanic biological pump modulates the atmospheric transport of persistent organic pollutants to the Arctic. *Nat. Commun.* **2012**, 3 (862). DOI 10.1038/ncomms1858.
35. Harner, T.; Kylin, H.; Bidleman, T.F.; Strachan W.M.J. Removal of α -hexachlorocyclohexane and enantiomers of γ -hexachlorocyclohexane in the eastern Arctic Ocean. *Environ. Sci. Technol.* **1999**, 33 (8), 1157-64. DOI 10.1021/es980898g
36. Pućko, M.; Stern, G.A.; Macdonald, R.W.; Barber, D.G.; Rosenberg, B.; Walkusz, W. When will α -HCH disappear from the western Arctic ocean? *J. Mar. Syst.* **2011**, DOI 10.1016/J.JMARSYS.2011.09.007.
37. Bauch, D.; Van der Loeff, M. R.; Andersen, N.; Torres-Valdes, S.; Bakker, K.; Abrahamsen, E. P. Origin of freshwater and polynya water in the arctic ocean halocline in summer 2007. *Prog. Oceanogr.* **2011**, 91 (4), 482-495.
38. Dachs, J.; Bayona, J. M. Large volume preconcentration of dissolved hydrocarbons and polychlorinated biphenyls from seawater. intercomparison between C18 disks and XAD-2 column. *Chemosphere.* **1997**, 35 (8), 1669-1679.
39. Hargrave, B. T.; Barrie, L. A.; Bidleman, T. F.; Welch, H. E. Seasonality in exchange of organochlorines between Arctic air and seawater. *Environ. Sci. Technol.* **1998**, 31 (11), 3258-3266. DOI 10.1021/es970266e
40. Kallenborn, R.; Christensen, G.; Evenset, A.; Schlabach, M.; Stohl, A. Atmospheric transport of persistent organic pollutants (POPs) to Bjørnøya (Bear Island). *J. Environ. Monitor.* **2007**, 9 (10), 1082-1091. DOI 10.1039/b707757m
41. Strachan, W. M. J.; Burniston, D. A.; Williamson, M.; Bohdanowicz, H. Spatial differences in persistent organochlorine pollutant concentrations between the Bering and Chukchi seas (1993). *Mar. Pollut. Bull.* **2001**, 43 (1-6), 132-142. DOI 10.1016/S0025-326X(01)00078-9
42. Ding, X.; Wang, X. -M.; Xie, Z.-Q.; Xiang, C. -H.; Mai, B. -X.; Sun, L. -G.; Zheng, M., Sheng, G.-Y.; Fu, J.-M.; Atmospheric hexachlorocyclohexanes in the North Pacific Ocean and the

Chapter 4: HCHs and HCB in the North Atlantic and Arctic Ocean.

adjacent Arctic region: Spatial patterns, chiral signatures, and sea-air exchanges. *Environ. Sci. Technol.* **2007**, *41* (15), 5204-5209. DOI 10.1021/es070237w

43. Wong, F.; Jantunen, L. M.; Pućko, M.; Papakyriakou, T.; Staebler, R. M.; Stern, G. A.; Bidleman, T.F. (2011). Air-water exchange of anthropogenic and natural organohalogenes on international polar year (IPY) expeditions in the Canadian Arctic. *Environ. Sci. Technol.* **2011** *45* (3), 876-881. DOI 10.1021/es1018509

44. Jantunen, L. M.; Helm, P. A.; Kylin, H.; Bidleman, T. F. (2008). Hexachlorocyclohexanes (HCHs) in the Canadian archipelago. 2. Air-water gas exchange of α - and γ -HCH. *Environ. Sci. Technol.* **2008**, *42* (2), 465-470. DOI 10.1021/es071646v

45. Su, Y.; Hung, H.; Blanchard, P.; Patton, G. W.; Kallenborn, R.; Konoplev, A.; Fellin, P.; Li, H.; Geen, C.; Stern, G.; Rosenberg, B.; Barrie, L. A. Spatial and seasonal variations of hexachlorocyclohexanes (HCHs) and hexachlorobenzene (HCB) in the Arctic atmosphere. *Environ. Sci. Technol.* **2006**, *40* (21), 6601-6607. DOI 10.1021/es061065q

46. Del Vento, S.; Dachs, J. Atmospheric occurrence and deposition of polycyclic aromatic hydrocarbons in the northeast tropical and subtropical Atlantic Ocean. *Environ. Sci. Technol.* **2007**, *41* (16), 5608-5613. DOI 10.1021/es0707660

47. Gioia, R.; Li, J.; Schuster, J.; Zhang, Y.; Zhang, G.; Li, X.; Spiro, B.; Bathia, R. S.; Dachs, J.; Jones, K. C. Factors affecting the occurrence and transport of atmospheric organochlorines in the China Sea and the northern Indian and south east Atlantic Oceans. *Environ. Sci. Technol.* **2012**, *46* (18), 10012-10021. DOI 10.1021/es302037t

48. Draxler, R.R.; Rolph, G.D. HYSPLIT (HYbrid Single-Particle Lagrangian Integrated Trajectory) Model access via NOAA ARL READY Website (<http://ready.arl.noaa.gov/HYSPLIT.php>). **2011**, NOAA Air Resources Laboratory, Silver Spring.

49. Bruhn, R.; Lakaschus, S.; McLachlan, M. S. Air/sea gas exchange of PCBs in the southern Baltic Sea. *Atmos. Environ.* **2003**, *37* (24), 3445-3454. DOI 10.1016/S1352-2310(03)00329-7

50. Di Liberto, L.; Angelini, F.; Pietroni, I.; Cairo, F.; Di Donfrancesco, G.; Viola, A.; Argentini, S.; Fierli, F.; Gobbi, G.; Maturilli, M.; Neuber, R.; Snels, M. Estimate of the Arctic convective boundary layer height from lidar observations: A case study. *Adv. Meteorol.* **2012**, DOI: 10.1155/2012/851927.

51. Lohmann, R.; Jurado, E.; Pilson, M. E. Q.; Dachs, J. Oceanic deep water formation as a sink of persistent organic pollutants. *Geophys. Res. Lett.* **2006**, *33* (12), DOI 10.1029/2006GL025953.

Chapter 4: HCHs and HCB in the North Atlantic and Arctic Ocean.

52. Dickson, R.; Rudels, B.; Dye, S.; Karcher, M.; Meincke, J.; Yashayaev, I. Current estimates of freshwater flux through Arctic and subarctic seas. *Prog. Oceanogr.* **2007**, *73* (3-4), 210-230.
53. Straneo, F.; Sutherland, D. A.; Holland, D.; Gladish, C.; Hamilton, G.; Johnson, H.; Rignot, E.; Xu, Y.; Koppes, M. Characteristics of ocean waters reaching Greenland's glaciers. *Ann. Glaciol.* **2012**, *53* (60), 202-210.
54. Moisey, J.; Fisk, A. T.; Hobson, K. A.; Norstrom, R. J. Hexachlorocyclohexane (HCH) isomers and chiral signatures of α -HCH in the arctic marine food web of the northwater polynya. *Environ. Sci. Technol.* **2001**, *35*(10), 1920-1927. DOI 10.1021/es001740a
55. Zaborska, A.; Carroll, J.; Pazdro, K.; Pempkowiak, J. Spatio-temporal patterns of PAHs, PCBs and HCB in sediments of the western Barents sea. *Oceanologia*, **2011**, *53*(4), 1005-1026. DOI 10.5697/oc.53-4.1005
56. Bauerfeind, E.; Nöthig, E.; Beszczynska, A.; Fahl, K.; Kaleschke, L.; Kreker, K.; Klages, M.; Soltwedel, T.; Lorenzen, C.; Wegner, J.; Particle sedimentation patterns in the eastern Fram Strait during 2000-2005: Results from the arctic long-term observatory HAUGSGARTEN. *Deep-Sea Res. Pt. I.* **2009**, *56* (9), 1471-1487. DOI 10.1016/j.dsr.2009.04.011
57. Ngabe, B.; Bidleman, T. F.; Falconer, R. L. Base hydrolysis of α - and γ -hexachlorocyclohexanes. *Environ. Sci. Technol.* **1993**, *27* (9), 1930-1933.
58. Aristegui, J.; Gasol, J.M.; Duarte, C.M.; Herndl, G.J. Microbial oceanography of the dark ocean's pelagic realm. *Limnol. Oceanogr.* **2009**, *54* (5), 1501-29
59. Lasternas, S.; Agustí, S. Phytoplankton community structure during the record arctic ice-melting of summer 2007. *Polar Biol.* **2010**, *33* (12), 1709-1717. DOI 10.1007/s00300-010-0877-x
60. Regaudie-de-Gioux, A.; Duarte, C. M. Plankton metabolism in the Greenland sea during the polar summer of 2007. *Polar Biol.* **2007**, *33* (12), 1651-1660. DOI 10.1007/s00300-010-0792-1
61. Boras, J. A.; Sala, M. M.; Arrieta, J. M.; Sà, E. L.; Felipe, J.; Agustí, S.; Duarte, C.M.; Vaqué, D. Effect of ice melting on bacterial carbon fluxes channelled by viruses and protists in the Arctic Ocean. *Polar Biol.* **2010**, *33* (12), 1695-1707. DOI 10.1007/s00300-010-0798-8
62. Sala, M. M.; Arrieta, J. M.; Boras, J. A.; Duarte, C. M.; Vaqué, D. The impact of ice melting on bacterioplankton in the Arctic Ocean. *Polar Biol.* **2010**, *33* (12), 1683-1694. DOI 10.1007/s00300-010-0808-x
63. Arrigo, K. R.; van Dijken, G.; Pabi, S.. Impact of a shrinking arctic ice cover on marine primary production. *Geophys. Res. Lett.* **2008**, *35* (19), DOI 10.1029/2008GL035028

Chapter 4: HCHs and HCB in the North Atlantic and Arctic Ocean.

64. Tóvar-Sánchez, A.; Duarte, C.M.; Alonso, J.C.; Lacorte, S.; Tauler, R.; Galbán-Malagón, C.J. Impacts of metals and nutrients released from melting multiyear Arctic sea ice. *J. Geophys. Res-Oceans*. **2010**, *115* (C7), DOI 10.1029/2009JC005685

Chapter 5

Polychlorinated Biphenyls, Hexachlorocyclohexanes and Hexachlorobenzene in seawater and phytoplankton from the Southern Ocean (Weddell, South Scotia, and Bellingshausen Seas)



The results from the present chapter were published as Galbán-Malagón et al. 2013a in *Environmental Science and Technology*, 2013,47 (11), 5578-5587.

Chapter 5: POPs in Antarctic Seawater and Phytoplankton

Abstract

The Southern Ocean is one of the most pristine environments in the world but is nonetheless affected by inputs of persistent organic pollutants (POPs). In the present work we report the concentrations of hexachlorocyclohexanes (HCHs), hexachlorobenzene (HCB) and 26 polychlorinated biphenyl (PCBs) congeners in seawater and phytoplankton from samples obtained during three Antarctic cruises in 2005, 2008 and 2009. The levels of PCBs, HCHs and HCB are low in comparison to the few previous reports for this region and studies from other oceans. The long term decline of POP concentrations in the Southern Ocean seawater since early 1980 is consistent with half-lives of 3.4 and 5.7 years for HCHs and PCBs, respectively. There is a large variability of PCBs, HCHs and HCB concentrations in water and phytoplankton within the Bransfield Strait, South Scotia, Weddell and Bellingshausen Seas that masks the differences between the studied Seas. However, the variability of PCBs concentrations in phytoplankton is significantly correlated with phytoplankton biomass with lower concentrations in the most productive waters. This trend is more apparent for the more hydrophobic congeners consistent with the role of settling fluxes of organic matter decreasing the concentrations of hydrophobic POPs in productive waters. The present work reports the most extensive dataset on concentrations in seawater and phytoplankton for the Southern Ocean, and points out to the important biogeochemical drivers, such as settling and degradation, influencing the occurrence of POPs in the ocean.

Chapter 5: POPs in Antarctic Seawater and Phytoplankton

1. Introduction

Persistent organic pollutants (POPs) are bioaccumulative and toxic organic synthetic chemicals, with long half-lives in the environment, which have received increased attention over the last decades. The concern of their impact to ecosystems and human health led to the inclusion of some of them in the Stockholm convention on POPs approved in 2001, whose objective was to reduce the production and use of these harmful compounds¹. Semivolatile POPs, such as polychlorinated biphenyls (PCBs) and other organochlorine compounds, have reached Polar environments through long-range atmospheric transport and deposition²⁻⁸. Due to increased persistence and bioaccumulation potential at low temperatures, there is a need of understanding their fate and impact in Antarctica⁹⁻¹¹.

Even though Antarctica is usually considered a pristine region, also in terms of POPs contamination, there is a long history of scientific assessments of organic pollutants in Antarctica, which started as early as in the late sixties^{12,13}. The atmosphere is the main vector for the introduction of semivolatile POPs to Antarctica through long-range atmospheric transport (LRAT) and deposition⁴. Inputs from oceanic transport are thought to play a minimal role due to the Antarctic Circumpolar Current, which acts as a physical barrier^{6,14}. Transport of pollutants to Antarctica due to oceanic current can only be significant regionally, as described in the Ross Sea due to the modified circumpolar deep water current¹⁵.

The fate and cycling of POPs such as PCBs, hexachlorobenzene (HCB) and hexachlorocyclohexanes (HCHs) have been extensively studied in the Arctic polar environment^{2,5,16-21} and other marine environments. This contrasts with the few assessments on POPs available for Antarctica and the adjacent Southern Ocean^{6,15,23-24}. The study of POPs in Antarctica has been mainly confined to the coastal atmosphere and seawater^{17, 22-35}. The few studies available for biotic matrixes were focused on the occurrence of organic pollutants in krill, penguins, seals and whales^{6, 9-11,32,36-39}, but none of the previous studies reported concentrations for phytoplankton, which is the basis of the trophic food web and

Chapter 5: POPs in Antarctic Seawater and Phytoplankton

plays an important role on the cycling of POPs in the oceanic environment^{7, 22, 40-42}. Recent modeling efforts for the Southern Ocean highlight the importance of phytoplankton in the POPs cycling in Antarctic marine food webs⁴³. However, there is only one report on the concentration for HCB and HCHs in phytoplankton for coastal waters adjacent to western Antarctic Peninsula⁴³.

The absence of field studies in the Southern Ocean implies a gap in the knowledge of the physical and biogeochemical controls on POP occurrence, as reported for other regions^{22,42,45,46}. Recently, it has been shown that POP concentrations in phytoplankton in temperate marine regions and lakes are higher when the abundance of phytoplankton is lower⁴¹⁻⁴². This is due to a coupling of air-water exchange and settling fluxes of particle associated POPs, which leads to the depletion of the more hydrophobic compounds in the photic zone, when the primary productivity or phytoplankton biomass is higher. It is important to explore the validity of these trends in different ecosystems, such as the polar marine environment, which has different physical conditions (temperature, mixing due to high wind speeds, formation of deep oceanic waters...) and different phytoplankton species. In addition, the southern ocean has been poorly characterized in terms of organic pollutants.

The objectives of this study are, i) to report the largest data set of PCBs, HCHs and HCB concentrations in seawater and phytoplankton, covering for the first time a large area of Southern Ocean (South Scotia Sea, the Weddell Sea, the Bransfield Strait, Drake Passage, and Bellingshausen Sea), and ii) to explore the processes influencing the occurrence of legacy POPs in phytoplankton from the Southern Ocean.

2. Materials and Methods

2.1 Sampling

Sampling was conducted on board *R/V Hespérides* during the ICEPOS (2005), ESSASI (2008) and ATOS-II (2009) sampling cruises in austral summer (January-February) around the Antarctic Peninsula (Weddell Sea, Bransfield Strait and Bellingshausen Sea), South Scotia Sea and Drake Passage (See Appendix C.1). This oceanic region is influenced by the Antarctic Circumpolar

Chapter 5: POPs in Antarctic Seawater and Phytoplankton

Current (ACC), specifically by the Antarctic Circumpolar Current Front (ACCF) and the Southern Boundary of the Antarctic Circumpolar Current (ACCSB). Primary production in this area is highly variable⁴⁷ but it is high and spatially extended over large regions compared with surrounding oceanic waters⁴⁸.

Surface dissolved seawater and particulate phases were sampled only during the ESSASI and ATOS-II cruises (Figure 1, upper panels for location of samples), while phytoplankton was sampled in all cruises. Ancillary data (temperature, fluorescence, salinity, radiation...) were provided by the Automatic Data Acquisition System on board of *RV Hespérides* and vertical profiles by CTD deployments (Information available in Appendix C.1, Tables S1, S2a and b). Briefly, surface seawater samples were taken from 5 m depth using the ship on line sampling system and pumped into a precleaned overflowing stainless steel container. From this container, seawater was pumped using a peristaltic pump with a flow rate of 150-200 mL min⁻¹ through a precombusted (4 hours at 450 °C) 142 mm GF/F filters (Whatman GE, UK) and a XAD-2 column separating the particulate and dissolved phases. Sampling volumes ranged from 175 L to 378 L with a median value of 237 L. After sampling, XAD-2 columns were kept at 4 °C and filters were frozen (-20 °C) until extraction and analysis.

Phytoplankton in the photic zone was sampled using a single net trawl system with a 50 µm mesh size. The sampling depth was always from 10 meters below the deep chlorophyll maximum depth (DCM), which ranged from 20 to 100 m depth (averaging 54 m depth, see Appendix C.1), to surface. Several consecutive net trawls were carried out ensuring enough biomass for analysis. Copepodes were removed from the samples and most of the material was phytoplankton with minor contribution of zooplankton. The 50 µm mesh net effectively samples phytoplankton cells, even those smaller than 50 µm in size, due to the aggregation of cells (diatoms, dinoflagellates) and the partial clogging of the net during the sampling. Phytoplankton biomass was transferred into a clean glass and immediately filtered using a precleaned glass system with precombusted (4 hours at 450°C) 47 mm GF/F filters (Whatman GE, UK). After filtering, filters were frozen (-20 °C) until extraction and analysis.

Chapter 5: POPs in Antarctic Seawater and Phytoplankton

2.2 Chemical Analysis

Water samples were extracted following the procedure proposed elsewhere^{41,42,49}. Briefly, the XAD columns were eluted with 200mL of methanol followed by 300 mL of dichloromethane. Surrogate standards were added to each fraction (5 ng of PCBs 65 and 200). The methanol fraction was liquid-liquid extracted with hexane, the eluted hexane was dried with anhydrous sodium sulfate, merged with the dichloromethane fraction and finally concentrated using rotary evaporation. The clean-up step was done using a glass column filled with 3 g of 3 % deactivated neutral alumina and 0.5-1 g of anhydrous sodium sulfate. The extract was fractionated by elution using hexane (12 mL) and a mixture of hexane:dichloromethane 1:2 (15 mL) for the first and second fractions, respectively. The first fraction was used for the analysis of HCHs, HCB and PCBs.

The filters containing the particulate and phytoplankton samples were freeze-dried for 4 h and weighed obtaining the dry weight of biomass. Surrogate standards were added before the extraction (10 ng of PCB congeners 65 and 200). Filters were Soxhlet extracted for 24 h using hexane:dichloromethane (1:2). Extract purification was done using two different methodologies. Particulate phase extracts followed the same clean up procedure performed for the dissolved phase. Phytoplankton clean up was performed using a glass column filled with 0.5 g of anhydrous sodium sulfate over 3 g of 3% deactivated alumina and 5 g of silica gel (silica 60, 200 mesh) activated at 250 °C for 24 h. The fractionation followed the procedure described in Galbán-Malagón et al²². The first fraction was used for the analysis of HCHs, HCB and PCBs.

Seawater samples were analyzed for α -HCH, β -HCH, δ -HCH, γ -HCH, HCB and 41 PCB congeners, even though only 26 of these congeners were detected and quantified (PCBs 18, 17, 31, 28, 33, 52, 49, 99/101, 110, 82, 151, 149, 118, 153, 132/105, 138, 158, 187, 183, 128, 177, 171/156, 180). All samples of phytoplankton were analyzed for PCBs, while HCHs and HCB were only analyzed in samples taken in 2008 and 2009. Analyses for seawater and phytoplankton samples were carried out using a GC- μ ECD (Agilent Technologies) with a HP-5MS capillary column (60 m x 0.25 mm i.d. x 0.25 μ m)

Chapter 5: POPs in Antarctic Seawater and Phytoplankton

internally coated with Poly-di-methyl-syloxane (Agilent Technologies). Splitless injection mode quantification was selected as injection procedure. Oven temperature was programmed from 90 °C (holding time 2 min) to 190 °C at 15 °C min⁻¹ (holding time 1 min) to 203 °C at 3 °C min⁻¹ (holding time 5 min), then to 290 °C at 3 °C min⁻¹ (holding time 1 min), and finally to 310 °C at 5 °C min⁻¹ keeping the final temperature for 10 min.

2.3 Quality control and assurance.

All sampling material (nets, filter holders, Teflon tubes, glass containers...) were cleaned rigorously after sampling to avoid potential contamination between different samples. Sampling devices were made of glass, stainless steel and Teflon and they were rinsed with acetone (3 times) after and before sampling. All the analytical procedure was validated by the recovery rate of the surrogate standards. Three laboratory and three field blanks were analyzed following the same process and in parallel to field samples. Field blanks for the dissolved phase were from XAD-2 columns that were inserted in the sampling system during 30 minutes and analysed following the same procedures as samples. All concentrations were corrected using the recoveries (Table S3 on Appendix C.2) and subtracting the chromatographic signal of blanks previously to quantification process. Concentrations in particulate phase samples are not shown here because they fell below the instrumental limit of quantification (Table S4 on Appendix C.2). Limits of detection and quantification were calculated by averaging the blanks concentration plus three times standard deviation for detection limits and ten times the standard deviation for the quantification limits (Table S5 on Appendix C.2).

2.4 Characteristic decreasing or e-folding times.

E-folding characteristic decreasing time (time needed to decrease the dissolved phase concentrations to e⁻¹ of initial value) for the sum α and γ HCHs and the sum of PCB congeners, since individual congeners were not reported in early studies, was calculated by fitting equation [1] to all the concentrations reported for the studied region:

$$\ln C_w = -k_d t + b \quad [4.1]$$

Chapter 5: POPs in Antarctic Seawater and Phytoplankton

Where k_d is the inverse of the e-folding time T_D (in years), t is time in years and b is the independent term. T_D could not be estimated due to lack of reports of its occurrence during the last decades. The half-lives, defined as the time needed to decrease the dissolved phase concentration to half of its initial concentration, are given by $0.69T_D$.

2.5 Bioconcentration factors

Bioconcentration factors (***BCFs***) were estimated by

$$BCF = \frac{C_P}{C_{WTD}} \quad [4.2]$$

Where C_P is the POP concentration in phytoplankton (pg kg^{-1}) and C_{WTD} is truly dissolved concentration (pg L^{-1}). The sampling of dissolved-phase concentration using XAD-2 adsorbents concentrates the truly dissolved compounds and the chemicals associated with the dissolved organic carbon (DOC). Burkhard⁵⁰ has reviewed the partitioning between DOC and the dissolved phase proposing a DOC-water partitioning coefficient (K_{DOC} , L Kg^{-1}) of $K_{DOC} = 0.08 K_{OW}$ for natural DOC, where K_{OW} is the octanol-water partition coefficient ($\text{Log}K_{OW}$), and a slightly different relationship of $K_{DOC} = 0.11K_{OW}$ when Aldrich humic acid is considered. Here we used the relationship $K_{DOC} = 0.1 K_{OW}$, which has been used previously to estimate C_{WTD} ⁵¹⁻⁵². Therefore, C_{WTD} was estimated as:

$$C_{WTD} = \frac{C_w}{(1 + K_{DOC} DOC)} \quad [4.3]$$

Where C_w is the measured dissolved phase concentration (pg L^{-1}). K_{OW} was corrected by temperature. DOC concentration show a low seasonal and temporal variability even during booms. In the Southern Ocean, ***DOC*** has a mean value of $6 \times 10^{-6} \text{ Kg L}^{-1}$ and range from 40×10^{-6} to $100 \times 10^{-6} \text{ Kg L}^{-1}$ ⁵³

3. Results and Discussion

3.1 Occurrence of organochlorine pesticides (OCPs) in Seawater and phytoplankton

Chapter 5: POPs in Antarctic Seawater and Phytoplankton

The concentrations of Σ HCHs in seawater are shown in Figure 1, and the compound specific values are reported in the supplementary material (Tables S6 and S7 in Appendix C.3). Higher concentrations of Σ HCHs were found in the Bransfield Strait (maximum of 12.3 pg L⁻¹) while the lowest concentration was found in the Bellingshausen Sea (1.2 pg L⁻¹), although there was no statistical significant difference among basins. Concerning individual HCH isomers, the concentration of α -HCH was higher in the transect from the Drake Passage to the Weddell Sea with a value near 1 pg L⁻¹. The β -HCH isomer showed the highest concentrations in the Bransfield Strait (5.9 pg L⁻¹) and the Weddell Sea (5.6 pg L⁻¹) while concentrations were lower in the South Scotia Sea. δ -HCH has never been reported previously in Antarctica and the highest concentration found was of 5.7 pg L⁻¹ in the Bransfield Strait. Conversely, the maximum γ -HCH concentration was found in the Weddell Sea (1.1 pg L⁻¹) and the lowest concentration was found in the Bransfield Strait (0.3 pg L⁻¹). Profiles of isomeric composition of HCHs show that the β -HCH dominates the water samples located in the Weddell and Bransfield Seas and γ -HCH dominates the profiles in the South Scotia and Bellingshausen Seas. Conversely, in the Drake Passage, similar abundances of the four isomers were found. Regarding HCB, the highest and lowest concentrations were found in the Weddell Sea (1.6 pg L⁻¹) and Bellingshausen Sea (0.2 pg L⁻¹), respectively.

There are a few previous studies on the occurrence of HCHs in Antarctic waters (See Table 1). The HCHs concentrations reported here (Table 1) are much lower than early reports from coastal^{31,32} and open sea areas³³. However, the HCHs levels reported in recent reports^{23,24,34,35} show similar or slightly higher concentrations than this study. HCB concentrations reported here are also one order of magnitude lower than the only report available²⁴.

The measured OCP concentrations in phytoplankton are summarized in Table 1 (complete data set in Appendix C.3, Table S8). For example, OCP concentrations in phytoplankton in the Weddell Sea ranged from 0.006 to 0.8 ng g⁻¹ for α -HCH, and between 0.1 to 5.7 ng g⁻¹ for γ -HCH. In the Bellingshausen Sea, the concentrations ranged from 0.008 to 0.4 ng g⁻¹ for α -HCH, and 0.05 to 0.6 ng g⁻¹ for γ -HCH. Finally, in South Scotia Sea, the concentrations in

Chapter 5: POPs in Antarctic Seawater and Phytoplankton

phytoplankton ranged from 0.2 to 0.6 ng g⁻¹ for α -HCH, and between 0.2 to 2.4 ng g⁻¹ for γ -HCH (See Table 1).

In the case of HCB, concentrations in phytoplankton ranged from 0.01 to 7.1 ng g⁻¹, from 0.01 to 3.5 ng g⁻¹, from 0.02 to 11 ng g⁻¹, and from 0.4 to 16 ng g⁻¹ in the Weddell, Bransfield, Bellingshausen and South Scotia Seas, respectively. γ -HCH dominates the HCH isomeric profiles representing from 43% to 68% of total HCHs.

HCHs and HCB concentrations in phytoplankton from the Southern Ocean were previously reported only once in coastal waters of Anvers Island⁴⁴, situated between the Bransfield and the Bellingshausen seas. This study reported concentrations for HCB (0.6-9 ng g⁻¹_{lipid}), α -HCH (0.2 to 1.3 ng g⁻¹_{lipid}) and γ -HCH (0.3 to 5.6 ng g⁻¹_{lipid}) lower than the lipid normalized concentrations in this study (the lipid content for phytoplankton samples ranged from 2 to 2.5% averaging 2.3%).

Chapter 5: POPs in Antarctic Seawater and Phytoplankton

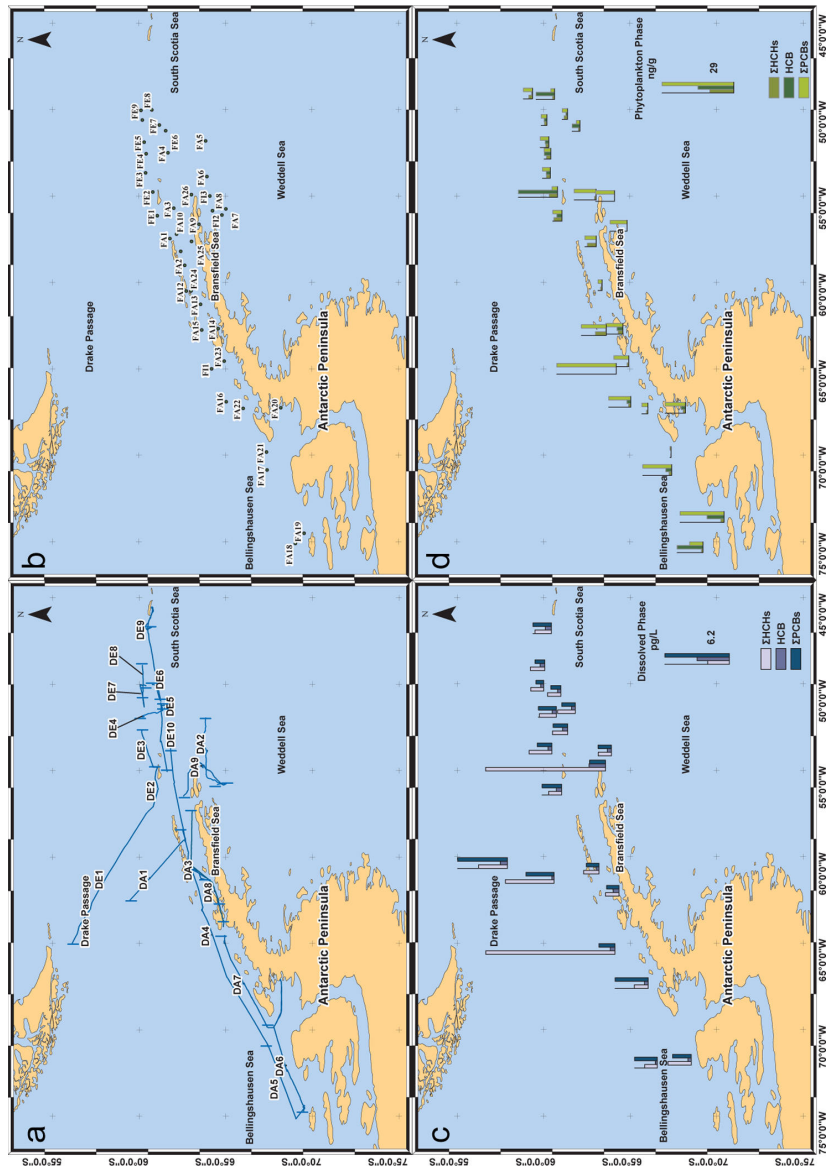


Figure 1: Location of seawater (transects in panel a) and phytoplankton (panel b) samples. Spatial distribution of dissolved phase concentrations of hexachlorocyclohexanes (Σ HCHs), hexachlorobenzene (HCB) and Polychlorinated Biphenyls (Σ_{26} PCBs) in pg L^{-1} (panel c). Concentrations in phytoplankton of Σ HCHs, HCB and Σ_{26} PCBs in ng g^{-1} d.w. (panel d).

3.2 Occurrence of PCBs in seawater and phytoplankton

Dissolved phase Σ_{26} PCBs concentrations ranged from 2.7 to 4.6 pg L^{-1} in the Weddell Sea, from 1.2 to 1.5 pg L^{-1} in the Bransfield Strait, from 1.6 to 3.2 pg L^{-1} in Bellinghousen Sea, and from 0.7 to 1.9 pg L^{-1} in the South Scotia Sea (Table 1 and Tables TS6, TS7 in Appendix C.3). There are no statistically significant differences in concentrations among the Weddell, Bellinghousen and South Scotia seas. Σ_{ICES} PCBs congeners contribution ranged from 22% to 61% of the total PCBs concentrations with a median value of 50% (see table TS6 in

Chapter 5: POPs in Antarctic Seawater and Phytoplankton

Appendix C.3). Profiles of PCBs were generally dominated by the pentachlorinated congeners, except for the sample DA1 which was dominated by trichlorinated congeners. The total PCB concentrations are lower than those reported in previous studies for the open Southern Sea^{15,25,31} and coastal sites³², even though the number of congeners reported in this study is higher. The dissolved phase concentrations at 4 m depth reported here are two orders of magnitude lower than those reported for the surface microlayer¹⁵, consistent with other reports of enrichment of organic pollutants at the marine surface film⁵². Comparing with similar polar areas, the dissolved concentrations in the Southern Ocean are similar to those reported for the Sub-Arctic and Arctic Oceans^{18,21,22}.

Table 1. Comparison of previously reported concentrations of PCBs, HCHs and HCB for seawater (pg L⁻¹) and phytoplankton (ng g⁻¹ dw) in Southern Ocean areas with those reported in this study. Mean and standard deviation (SD) of concentrations are shown.

Matrix	Location	Year	α-HCH		β-HCH		γ-HCH		ΣPCBs		HCB		Reference
			Mean	SD	Mean	SD	Mean	SD	Mean	SD	Mean	SD	
Seawater (ng L ⁻¹)	Tottuki Point	1981	570 ^a		570 ^a		570 ^a		54 ^d				Tanabe et al., 1983
	Langhovde	1981	210 ^e		210 ^e		210 ^e		35 ^d				Tanabe et al., 1983
	Kitano-Ura Cove	1982	570 ^b		570 ^b		570 ^b		69 ^d				Tanabe et al., 1983
	Seawater in Syova Station	1981	503.3 ^a	369.5 ^a	503.3 ^a	369.5 ^a	503.3 ^a	369.5 ^a	55.3 ^d	15.3 ^d			Tanabe et al., 1983
	Dakshin Gangotri Station	1987	90.2 ^b	4.6 ^b	90.2 ^b	4.6 ^b	90.2 ^b	4.6 ^b	100.3 ^e	3.5 ^e			Sen Gupta et al., 1995
	ANT IX	1991	15 ^c				21 ^c						Schreitmüller and Ballschmiter., 1995
	ANT XVII Cruise	1999	4.3	1.3			0.8	0.1					Lakaschus et al., 2002
	Palmer Vicinity	2002	3.1	0.8			3.8	3.9					Dickhut et al., 2005
	Terra Nova Bay	2003	1.41	0.91			2.9	2.2			6.21	4.37	Cincinelli et al., 2009
	Ross Sea (microlayer)	1997-1998							427 ^f	31.1 ^f			Fuoco et al., 2007
	Ross Sea (Sub-superficial water)	1997-1998							48 ^f	4.24 ^f			Fuoco et al., 2007
		1997-1998							67 ^f	15 ^f			Fuoco et al., 2009
		2000-2001							23 ^f				Fuoco et al., 2009
		2001-2002							43.75 ^f	7.18 ^f			Fuoco et al., 2009
		2008	2.5		0.14		0.17						Xie et al., 2011
	Antarctic Cruise	2009	0.953	0.049	0.929	0.055	0.787	0.575	3.727	1.466	0.453	0.327	This Study
	Drake Passage	2009	0.26	0.07	2.885	0.092	2.148	0.516	1.391	0.173	0.976	0.828	This Study
Weddell	2009	0.189	0.09	3.132	4.031	2.26	3.041	1.305	0.186	0.413	0.17	This Study	
Braunfield	2009	0.198	0.08	0.261		0.876	0.365	2.37	0.703	0.281	0.078	This Study	
Bellingshausen	2008	0.24	0.07	0.381	0.326	0.848	0.195	1.34	0.398	0.415	0.096	This Study	
South Scotia Sea	2002	0.45 ^g	0.38 ^g			1.24 ^g	1.65 ^g			2.9 ^g	1.76 ^g	Chirchiole et al., 2004	
Palmer Station		0.18	0.28			1.81	2.11	14.07	12.72	1.64	2.40	This Study	
Weddell		0.30	0.35			1.03	1.14	10.47	14.84	2.29	3.17	This Study	
Braunfield	2008-2009	0.16	0.17			0.41	0.21	11.41	8.66	4.34	4.34	This Study	
Bellingshausen		0.34	0.11			0.79	0.81	2.67	0.86	3.68	4.78	This Study	
South Scotia Sea												This Study	

a: Sum of α, β and γ isomers
 b: Sum of α and β isomers
 c: One Sample result from the Cruise ANT IX
 d: Sum of unspecified number of PCBs
 e: Sum of PCB 101, 136, 151, 118, 153 and 138
 f: Sum of ICES PCBs
 g: ng g⁻¹ Lipid Weight

Chapter 5: POPs in Antarctic Seawater and Phytoplankton

Table 1 summarizes the PCBs concentrations in phytoplankton from the different seas around the Antarctica peninsula (Tables S6, S7). Concentrations of Σ_{26} PCBs in phytoplankton were in the range of 0.5 to 33 ng g⁻¹, 0.4 to 56 ng g⁻¹, 0.5 to 23.4 ng g⁻¹, and 1.5 to 3.8 ng g⁻¹ for the Weddel, Bransfield, Bellingshausen and South Scotia seas, respectively. PCBs profiles were generally dominated by tri and tetra-chlorinated congeners. These concentrations are similar to those reported for the Arctic Ocean²², even though the phytoplankton species dominating in this study were diatoms and dinoflagellates⁵⁴, while for the arctic study was *Phaeocystis pouchetti*. Different species have different shape, outer chemical and physical structure, aggregation strategies, and lipid content, which all may influence the accumulation of POPs in phytoplankton. The similarity in POP concentrations and BCFs, in Arctic and Southern Ocean phytoplankton may indicate a minor role of the phytoplankton species on POP levels since the dissolved phase concentrations are similar at both regions. Generally, there are very few reports of POP concentrations in oceanic phytoplankton^{22, 41-42}. There is a larger number of studies reporting POP concentrations in the particulate-phase from surface waters^{22,41-42,55}, but PCBs were not above LOQ in the particle phase analyzed here. However, concentrations of POPs in the particulate phase cannot be compared with the concentrations in the phytoplankton samples reported in this study, since these are integrated samples for the water column. Phytoplankton does not show a constant abundance with depth, and the maximum of abundance was normally below the thermocline, where the dissolved concentration may be different than at surface.

3.3 Decrease of PCB and OCP in the Southern Ocean seawater

The lower concentrations of HCH and PCBs in this work in comparison to previous studies suggest that there has been an important decrease in the dissolved phase POP concentrations in the Southern Ocean. Figure 2 shows the decrease of HCHs (sum of α and γ isomers of HCH) and PCB concentrations in Antarctic seawater. T_D was of 5 years for HCHs, and 8.75 years for PCBs and estimated half-lives were 3.4 and 5.7 respectively. The uncertainty of T_D for PCBs is higher due to the few studies in this region (See Table 1). The scatter trends could be due in part to the different analytical methods involved. Chiuchiolo et al.⁴⁴ reported half-lives of 2 years for the sum of α and γ isomers of HCHs concentrations in

Chapter 5: POPs in Antarctic Seawater and Phytoplankton

zooplankton^{44,56-58}. Conversely, Tanabe and Tatsukawa⁵⁹ reported longer half-lives (5-10 years) in the oligotrophic ocean (subtropical oceanic gyres). This is probably due to the lower bacterial abundance in these waters (for HCH congeners) and lesser influence of the biological pump as a removing process in oligotrophic waters from oceanic gyres⁴⁰. Our estimated e-folding time and half-lives for PCBs were similar to those described for the Baltic Sea⁶¹ (see table S10 on Appendix C.4). The Baltic Sea presents a higher eutrophy than the Southern Ocean, which would lead to shorter e-folding times due to efficient removal by settling particles. The potential influence of inputs from adjacent land or sediment resuspension may have attenuated this decrease in the Baltic Sea. In the Southern Ocean, the decrease of water column concentrations is the result of an imbalance between atmospheric inputs, which may have decreased due to lower primary sources of HCH and PCBs in source regions, and the loss processes from surface waters. Loss processes are settling to deeper waters due to the role of the biological pump, which is important for PCBs in productive waters^{20,39} or degradation, which is known to be important for HCHs⁶²⁻⁶⁴.

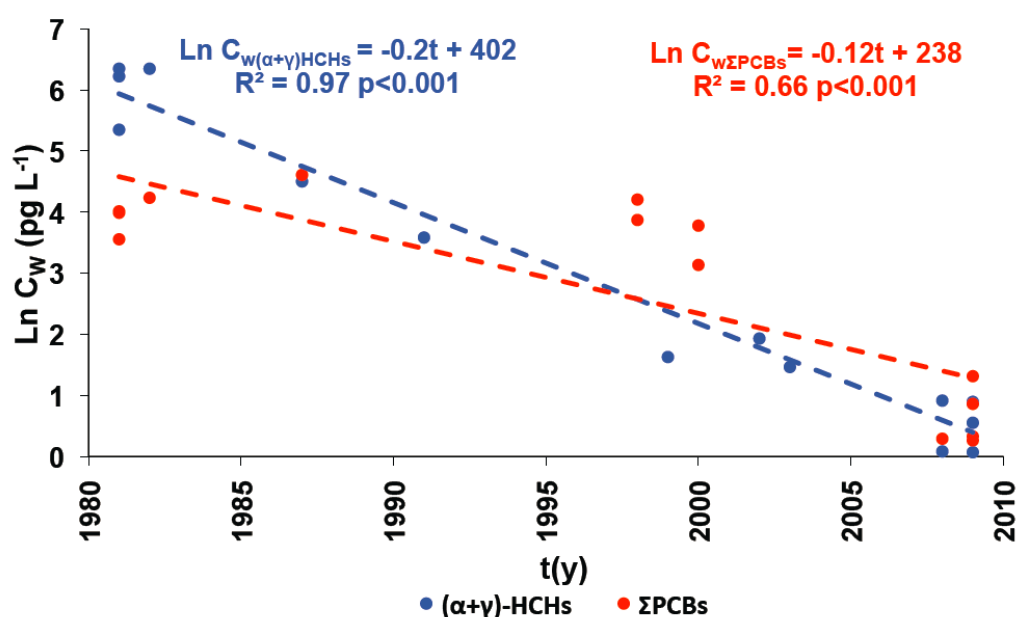


Figure 2. Dissolved phase concentrations of PCBs and HCHs ($\alpha+\gamma$) versus sampling date. Correlations obtained by least squares fitting of equation [1] and used to derive the e-folding time are shown.

Chapter 5: POPs in Antarctic Seawater and Phytoplankton

3.4 Factors driving PCBs, HCHs and HCB concentrations in phytoplankton

There are few previous reports for HCHs, HCB and PCBs concentrations in marine phytoplankton, and also for other aquatic environments. However, there have been some studies focusing on the processes driving the variability of POPs in phytoplankton. For example, lower POP concentrations in phytoplankton at high biomass have been described for the Baltic Sea⁶¹, the Mediterranean Sea⁴² and in lakes⁶⁵⁻⁶⁷. The recent work by Berrojalbiz et al.^{41,42} has provided the framework to interpret this variability of POP concentrations in phytoplankton in terms of inputs to surface waters, mainly diffusive air-water exchange and losses due settling of particle bound POPs and degradative processes. Indeed, POP concentrations in phytoplankton strongly depend on the trophic status and how this affects the inputs and losses of POPs from surface waters^{41,42}. Similar to the approach performed by Berrojalbiz⁴¹, HCHs, HCB and PCBs concentrations in phytoplankton (C_P , ng g⁻¹) were plotted against the phytoplankton biomass density in the water column (B , mg m⁻²) as shown in Figure 3. As C_P and B showed little variability for the other cruises, only the samples from the ATOS-II cruise were plotted (26 out of 39 samples). Consistent with the trends reported by Berrojalbiz⁴¹, C_P values for PCBs were correlated with B by a power function such as,

$$\text{Log}C_P = -m\text{Log}B + a \quad [4.4]$$

Where m and a are the slope and independent term from the least squares linear regression. HCB, PCB 31, 99/101 and 183 are plotted in Figure 3a (and Table S11 on Appendix C.4), where C_P showed a significant inverse correlation with B , especially for the more hydrophobic compounds. If this trend was a manifestation of a simple dilution effect resulting in lower concentrations at high biomass, then the apparent decrease of concentrations (or m value) would be the same for all compounds, however, this trend is not observed for all congeners. In fact, m values obtained by applying equation [4.4] to all congeners specific concentrations are directly correlated with K_{OW} (Table S9 on Appendix C.4) as shown in Figure 3b. Thus, the more hydrophobic the congener, the stronger is the decrease of C_P at high biomass. The fact that the same trend has been observed in the Southern Ocean and the Mediterranean Sea⁴², which have different eutrophy

Chapter 5: POPs in Antarctic Seawater and Phytoplankton

and settling fluxes of organic carbon⁶⁸⁻⁶⁹, suggests that this is a general trend for a wide range of trophic conditions and phytoplankton species. This trend can adequately be explained by the influence of the biological pump influence on the concentrations of PCBs in the photic zone⁴². Higher settling fluxes are associated with high biomass. The flux of particulate organic matter removes preferentially the more hydrophobic POPs from surface water. At the same time, due to phytoplankton growth, phytoplankton uptake can not be maintained by atmospheric inputs since diffusive air-water exchange is not fast enough, especially for more hydrophobic POPs^{40,42}. This imbalance between inputs (air-water diffusive exchange) and outputs (settling fluxes) reduces the concentrations in the water column in regions with higher biomass, especially for more hydrophobic congeners. PCBs and HCB are both persistent in the water column, so they lie in the same line in Figure 3b. In fact, for HCB and low chlorinated PCBs, m is smaller than for the more hydrophobic compounds because the extent of the biological pump is less important for these compounds^{40,42,70}. This depletion of concentrations is not reflected in the dissolved phase at surface because this water mass is isolated from the depth of the maximum of phytoplankton by the thermocline and atmospheric inputs of PCBs maintain the concentrations at surface. Only after intense mixing episodes the decrease of concentrations will be apparent at surface.

Conversely, for HCHs, C_P and B showed significant correlations only for β and γ HCH isomers, while m was not different than zero for α -HCH and δ -HCH (Table TS11 on Appendix C.4). In the case of HCHs, the importance of the biological pump is low due to their low hydrophobicity and the dependence of C_P on B for these compounds is due to, according to Berrojalbiz⁴¹, decreasing concentrations driven by bacterial degradation. HCHs are less persistent than PCBs and HCB, and are more susceptible to biotic and abiotic degradation processes in the water column^{62-64,71-73}. Bacterial abundance increases when phytoplankton biomass is higher. However, due to the low temperatures, degradation will be slower, and the apparent dilution in the Southern Ocean due to degradation is less important (lower m) than that observed in the temperate Mediterranean waters⁴².

Chapter 5: POPs in Antarctic Seawater and Phytoplankton

Nizzetto et al.⁶⁷ has pointed out that these changes of POP concentrations in phytoplankton (and zooplankton) due to the influence of the biological pump may have implications on the accumulation of POPs at higher levels of the food web. *BCFs* in polar regions have previously been calculated for zooplankton, mainly in the Arctic⁷⁴⁻⁷⁷, and here we estimated (Equation [4.2]) the *BCFs* for southern ocean phytoplankton. There is a significant correlation between $\text{Log}BCF$ and $\text{Log}K_{OW}$ for most samples, but the slope is not significantly different from zero for some time periods (see Figures S1a and b in Appendix C.4). These *BCFs* should be examined with caution, because the dissolved phase concentrations were measured at surface, and the phytoplankton phase concentrations were determined for samples that integrate the photic zone of the water column (from below phytoplankton maximum to surface). Nonetheless, the results would point to lower values in *BCF* than predicted from models for the more hydrophobic compounds for some of the sampling periods, which as suggested in other studies⁶⁷ would be due to the role of the biological pump. Further research is needed to elucidate the ecological and physical factors that drive the dynamics of phytoplankton, bacteria and zooplankton and its coupling with the cycle and occurrence of POPs.

Chapter 5: POPs in Antarctic Seawater and Phytoplankton

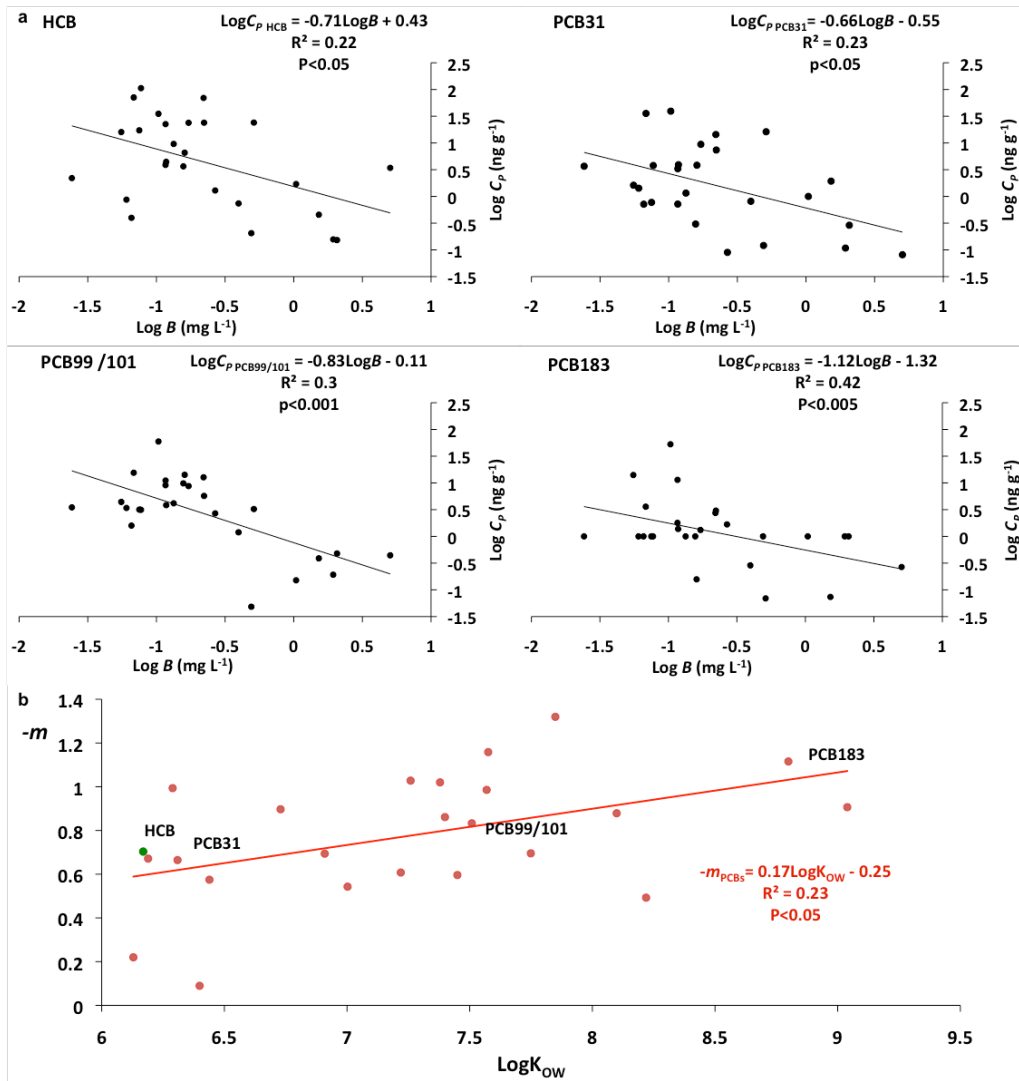


Figure 3: Influence of phytoplankton biomass (B) on POP concentrations in phytoplankton (C_P , $\text{ng g}^{-1} \text{d.w.}$). Panel a shows the least squares regressions of $\text{Log}C_P$ versus B for HCB and PCB congeners 31, 101 and 183. Panel b shows the relationship between m (slope of regressions of $\text{Log}C_P$ versus B as shown in equation [2]) versus the octanol water partition coefficients ($\text{Log}K_{OW}$) for all the PCB congeners and HCB. K_{OW} has been corrected for temperature.

Chapter 5: POPs in Antarctic Seawater and Phytoplankton

References

1. UNEP. Final act of the plenipotentiaries on the Stockholm Convention on persistent organic pollutants; United Nations Environment Program Chemicals. **2001**
2. Kallenborn, R.; Christensen, G.; Evenset, A.; Schlabach, M.; Stohl, A. (2007). Atmospheric transport of persistent organic pollutants (POPs) to Bjørnøya (Bear island). *J. Environ. Monitor.* **2007**, 9(10), 1082-1091.
3. Brown, T. N.; Wania, F. Screening chemicals for the potential to be persistent organic pollutants: A case study of arctic contaminants. *Environ. Sci. Technol.* **2008** 42(14), 5202-5209.
4. Choi, S.-D.; Baek, S.-Y.; Chang, Y.-S.; Wania, F.; Ikonomou, M. G.; Yoon, Y.-J.; Park, B.-K.; Hong, S. Passive air sampling of polychlorinated biphenyls and organochlorine pesticides at the Korean arctic and antarctic research stations: Implications for long-range transport and local pollution. *Environ. Sci. Technol.* **2008**, 42(19), 7125-7131.
5. Wu, X.; Lam, J. C. W.; Xia, C.; Kang, H.; Sun, L.; Xie, Z.; Lam, P. K. S. Atmospheric HCH concentrations over the marine boundary layer from Shanghai, China to the Arctic Ocean: Role of human activity and climate change. *Environ. Sci. Technol.* **2010**, 44(22), 8422-8428.
6. Bengtson-Nash, S. Persistent organic pollutants in Antarctica: Current and future research priorities. *J. Environ. Monitor.* **2011**, 13(3), 497-504.
7. Jurado, E.; Dachs, J. Seasonality in the "grasshopping" and atmospheric residence times of persistent organic pollutants over the oceans. *Geophys. Res. Lett.* **2008**, 35, 17805, doi:10.1029/2008GL034698.
8. Cabreizo, A.; Dachs, J.; Barceló, D.; Jones, K.C. Influence of organic matter content and human activities on the occurrence of organic pollutants in antarctic soils, lichens, grass, and mosses. *Environ. Sci. Technol.* **2012**, 46(3), 1396-1405
9. Poulsen, A.H.; Kawaguchi, S.; Kukkonen, J.V.K.; Leppänen, M.T.; Bengtson-Nash S.M. Aqueous uptake and sublethal toxicity of p,p'-DDE in non-feeding larval stages of antarctic krill (*Euphausia superba*). *Environ. Pollut.* **2012**, 160(1), 185-191.
10. Poulsen, A.H.; Kawaguchi, S.; King, C.K.; King, R.A.; Bengtson-Nash, S.M. Behavioural sensitivity of a key Southern Ocean species (antarctic krill, *Euphausia superba*) to p,p'-DDE exposure. *Ecotoxicol. Environ. Saf.* **2012**, 75, 163-70.
11. Bengtson-Nash, S.; Poulsen, A. H.; Kawaguchi, S.; Vetter, W.; Schlabach, M. Persistent organohalogen contaminant burdens in antarctic krill (*euphausia superba*) from the eastern antarctic sector: A baseline study *Sci. Total Environ.* **2008**, 407(1), 304-314.

Chapter 5: POPs in Antarctic Seawater and Phytoplankton

12. Risebrough, R. W.; Rieche, P.; Peakall, D. B.; Herman, S. G.; Kirven, M. N. Polychlorinated biphenyls in the global ecosystem. *Nature*. **1968** 220(5172), 1098-1102.
13. Risebrough, R.W.; Walker II, W.; Schmidt, T.T.; De Lappe, B.W.; Connors, C.W. Transfer of chlorinated biphenyls to Antarctica. *Nature*, **1976** 264 (5588), 738-739.
14. Bengtson Nash, S.; Rintoul, S. R.; Kawaguchi, S.; Staniland, I.; Hoff, J. V. D.; Tierney, M.; Bossi, R. *Environ. Pollut.* **2010**, 158(9), 2985-2991.
15. Fuoco, R.; Giannarelli, S.; Wei, Y.; Ceccarini, A.; Abete, C.; Francesconi, S.; Termine, M. Persistent organic pollutants (POPs) at Ross sea (Antarctica). *Microchem J*, **2009** 92(1), 44-48.
16. Sobek, A.; Gustafsson, Ö. Latitudinal fractionation of polychlorinated biphenyls in surface seawater along a 62° N-89° N transect from the southern Norwegian Sea to the North Pole area. *Envir. Sci. Technol.*; **2004**, 38(10), 2746-2751
17. Hung, H.; Blanchard, P.; Halsall, C. J.; Bidleman, T. F.; Stern, G. A.; Fellin, P.; Muir, D. C. G.; Barrie, L. A.; Helm, P. A.; Ma, J.; Konoplev, A. Temporal and spatial variabilities of atmospheric polychlorinated biphenyls (PCBs), organochlorine (OC) pesticides and polycyclic aromatic hydrocarbons (PAHs) in the canadian Arctic: Results from a decade of monitoring. *Sci. Total. Environ.* **2005**, 342(1-3), 119-144.
18. Gioia, R.; Lohmann, R.; Dachs, J.; Temme, C.; Lakaschus, S.; Schulz-Bull, D.; Hand, I.; Jones, K. C. Polychlorinated biphenyls in air and water of the North Atlantic and Arctic Ocean. *J. Geophys. Res-Atmos.* **2008**, 113(19), D19302, doi:10.1029/2007JD009750
19. Möller, A.; Xie, Z.; Cai, M.; Zhong, G.; Huang, P.; Cai, M.; Sturm, R.; He, J.; Ebinghaus, R. Polybrominated diphenyl ethers vs alternate brominated flame retardants and dechloranes from East Asia to the Arctic. *Envir. Sci. Technol.* **2011** 45(16), 6793-6799.
20. Ma, J.; Tian, C.; Hung, H.; Kallenborn R. Revolatilization of persistent organic pollutants in the Arctic induced by climate change. *Nature Clim. Chan.* **2011**, 1, 255-260.
21. Carrizo, D.; Gustafsson, Ö. Distribution and inventories of polychlorinated biphenyls in the polar mixed layer of seven Pan-Arctic shelf seas and the interior basins. *Environ. Sci. Technol.* 2011, 45(19): 8377-8384
22. Galbán-Malagón, C.; Berrojalbiz, N.; Ojeda, M.J.; Dachs, J., The oceanic biological pump modulates the atmospheric transport of persistent organic pollutants to the Arctic. *Nat. Commun.* **2012**, 3, Article number 862, doi:10.1038/ncomms1858.
23. Dickhut, R. M.; Cincinelli, A.; Cochran, M.; Ducklow, H. W. Atmospheric concentrations and air-water flux of organochlorine pesticides along the western Antarctic Peninsula. *Environ. Sci. Technol.* **2005** 39(2), 465-470.

Chapter 5: POPs in Antarctic Seawater and Phytoplankton

24. Cincinelli, A.; Martellini, T.; Del Bubba, M.; Lepri, L.; Corsolini, S.; Borghesi, N.; King, M.D.; Dickhut, R. M. Organochlorine pesticide air-water exchange and bioconcentration in krill in the Ross sea. *Environ. Pollut.* **2009**, 157(7), 2153-2158.
25. Fuoco, R.; Giannarelli, S.; Wei, Y.; Abete, C.; Francesconi, S.; Termine, M. Polychlorobiphenyls and polycyclic aromatic hydrocarbons in the sea-surface micro-layer and the water column at Gerlache inlet, Antarctica. *J. Environ. Monitor.* **2005** 7(12), 1313-1319.
26. Kallenborn, R.; Oehme, M.; Wynn-Williams, D. D.; Schlabach, M.; Harris, J. Ambient air levels and atmospheric long-range transport of persistent organochlorines to Signy island, Antarctica. *Sci. Total. Environ.* **1998**, 220(2-3), 167-180.
27. Montone, R. C.; Taniguchi, S.; Weber, R. R. PCBs in the atmosphere of King George island, antarctica. *Sci. Total. Environ.* **2003**, 308(1-3), 167-173.
28. Gambaro, A.; Manodori, L.; Zangrando, R.; Cincinelli, A.; Capodaglio, G.; Cescon, P. Atmospheric PCB concentrations at Terra Nova bay, Antarctica. *Environ. Sci. Technol.* **2005**, 39(24), 9406-9411.
29. Baek, S.-Y.; Choi, S.-D.; Chang, Y.-S. Three-year atmospheric monitoring of organochlorine pesticides and polychlorinated biphenyls in Polar Regions and the South Pacific. *Environ. Sci. Technol.* **2011**, 45(10), 4475-4482.
30. Li, Y.; Geng, D.; Hu, Y.; Wang, P.; Zhang, Q.; Jiang, G. Levels and distribution of polychlorinated biphenyls in the atmosphere close to Chinese Great Wall Station, Antarctica: Results from XAD-resin passive air sampling. *Chinese Sci. Bull.* **2012**, 1-5.
31. Tanabe, S.; Hidaka, H.; Tatsukawa, R. PCBs and chlorinated hydrocarbon pesticides in Antarctic atmosphere and hydrosphere. *Chemosphere.* **1983**, 12(2), 277-288.
32. Sen Gupta, R. S.; Sarkar, A.; Kureishey, T. W. PCBs and organochlorine pesticides in krill, birds and water from Antarctica. *Deep-Sea. Res. Pt. II.* **1996**, 43(1), 119-126
33. Schreitmüller, J. S.; Ballschmiter, K. Air-water equilibrium of hexachlorocyclohexanes and chloromethoxybenzenes in the North and South Atlantic. *Envir. Sci. Technol.* **1995**, 29(1), 207-215.
34. Lakaschus, S.; Weber, K.; Wania, F.; Bruhn, R.; Schrems, O. The air-sea equilibrium and time trend of hexachlorocyclohexanes in the Atlantic Ocean between the Arctic and Antarctica. *Environ. Sci. Technol.* **2002**, 36, (2), 138-145.
35. Xie, Z.; Koch, B.P.; Möller, A.; Sturm, R.; Ebinghaus, R. Transport and fate of hexachlorocyclohexanes in the oceanic air and surface seawater. *Biogeoscience.* **2011**, 2621-2633.

Chapter 5: POPs in Antarctic Seawater and Phytoplankton

36. Corsolini, S. Industrial contaminants in Antarctic biota. *J. Chromatogr. A.* **2009**, 1216(3), 598-612.
37. Corsolini, S.; Ademollo, N.; Romeo, T.; Olmastroni, S.; Focardi, S. Persistent organic pollutants in some species of a Ross sea pelagic trophic web. *Antarct. Sci.* **2003**, 15(1), 95-104.
38. Corsolini, S.; Covaci, A.; Ademollo, N.; Focardi, S.; Schepens, P. Occurrence of organochlorine pesticides (OCPs) and their enantiomeric signatures, and concentrations of polybrominated diphenyl ethers (PBDEs) in the Adélie penguin food web, Antarctica. *Environ. Pollut.* **2006**, 140(2), 371-382.
39. Corsolini, S.; Romeo, T.; Ademollo, N.; Greco, S.; Focardi, S. POPs in key species of marine Antarctic ecosystem. *Microchem. J.* **2002**, 73(1-2), 187-193.
40. Dachs, J.; Lohmann, R.; Ockenden, W. A.; Méjanelle, L.; Eisenreich, S. J.; Jones, K. C. Oceanic biogeochemical controls on global dynamics of persistent organic pollutants. *Environ. Sci. Technol.* **2002**, 36(20), 4229-4237
41. Berrojalbiz, N.; Dachs, J.; Ojeda, M.J.; Valle, M.C.; Castro-Jiménez, J.; Wollgast, J.; Ghiani, M.; Hanke, G.; Zaldivar, J.M. Biogeochemical and physical controls on concentrations of polycyclic aromatic hydrocarbons in water and plankton of the Mediterranean and Black seas. *Global Biogeochem. Cycles* **2011**, 25, GB4003, doi: 10.1029/2010GB003775.
42. Berrojalbiz, N.; Dachs, J.; Del Vento, S.; Ojeda, M.J.; Valle, M.C.; Castro-Jiménez, J.; Mariani, G.; Wollgast, J.; Hanke, G. Persistent organic pollutants in Mediterranean seawater and processes affecting their accumulation in plankton. *Environ. Sci. Technol.* **2011**, 45, 4315-4322.
43. Cropp, R.; Kerr, G.; Bengtson-Nash, S.; Hawker, D. A dynamic biophysical fugacity model of the movement of a persistent organic pollutant in antarctic marine food webs. *Environ. Chem.* **2011**, 8(3), 263-280.
44. Chiuchiolo, A. L.; Dickhut, R. M.; Cochran, M. A.; Ducklow, H. W. Persistent organic pollutants at the base of the Antarctic marine food web. *Environ. Sci. Technol.* **2004**, 38(13), 3551-3557.
45. Nizzetto, L.; Lohmann, R.; Gioia, R.; Dachs, J.; Jones, K.C.; Atlantic Ocean surface waters buffer declining atmospheric concentrations of persistent organic pollutants. *Environ. Sci. Technol.* **2010**, 44(18), 6978-6984.
46. Zhang, L.; Lohmann, R. Cycling of PCBs and HCB in the surface ocean-lower atmosphere of the open pacific. *Environ. Sci. Technol.* **2010**, 44(10), 3832-3838.
47. Tréguer, P.; Jacques, G. Dynamics of nutrients and phytoplankton, and fluxes of carbon, nitrogen and silicon in the antarctic ocean. *Polar Biol.* **1992**, 12(2), 149-162.

Chapter 5: POPs in Antarctic Seawater and Phytoplankton

48. Boyd, P. W.; Robinson, C.; Savidge, G.; Williams, P. J. (1995). Water column and sea-ice primary production during austral spring in the Bellingshausen sea. *Deep-Sea Res. Pt. II.* **1995**, 42(4-5), 1177-1200.
49. Dachs, J.; Bayona, J.M.; Large volume preconcentration of dissolved hydrocarbons and polychlorinated biphenyls from seawater. Intercomparison between C18 disks and XAD-2 column. *Chemosphere.* **1997**, 35(8),1669-1679.
50. Burkhard, L.. Estimating dissolved organic carbon partition coefficients for non-ionic organic chemicals. *Environ. Sci. Technol.* **2000**, 34, 4663-4668.
51. Totten, L.A.; Brunciak, P.A.; Gigliotti, C.L.; Dachs, J. ; Glenn, T.R.; Nelson, E.D.; Eisenreich, S.J. Dynamic Air–Water Exchange of Polychlorinated Biphenyls in the New York–New Jersey Harbor Estuary. *Environ. Sci. Technol.* **2001**, 35, 3834-3840.
52. García-Flor, N.; Guitart, C.; Ábalos, M.; Dachs, J.; Bayona, J. M.; Albaigés, J. Enrichment of organochlorine contaminants in the sea surface microlayer: An organic carbon-driven process. *Mar. Chem.* **2005**, 96(3-4), 331-345.
53. Doval, M.D.; Álvarez-Salgado X.A.; Castro, C.G.; Pérez, F.F. Dissolved organic carbon distributions in the Bransfield and Gerlache Straits, Antarctica, *Deep Sea Res. II*, **2002**, 49 2002, 663-674.
54. Echeveste, P., Agostí, S.; Dachs, J. Cell size dependence of additive versus synergetic effects of UV radiation and PAHs on oceanic phytoplankton. *Environ. Pollut.* **2011**, 159, 1307-1316.
55. Sobek, A.; Reigstad, M.; Gustafsson, Ö., Partitioning of polychlorinated biphenyls between Arctic seawater and size-fractionated zooplankton. *Environ. Toxic. Chem.* **2006**, 25, 1720-1728.
56. Lukowski, A. B.; Ligowski, R. Cumulation of chloroorganic insecticides by antarctic marine diatoms. *Pol. Polar. Res.* **1987**, 8(2), 167-177.
57. Lukowski, A. B.; Ligowski, R. Contamination of Antarctic marine phytoplankton by chlorinated hydrocarbons (BIOMASS III). *Pol. Pol. Res.* **1998**, 9(2-3), 399-408.
58. Cripps, G. C. Hydrocarbons in the seawater and pelagic organisms of the Southern Ocean. (1990). *Polar Biol.* **1990**, 10(5), 393-402.
59. Tanabe, S.; Tatsukawa, R. Vertical transport and residence time of chlorinated hydrocarbons in the open ocean water column. *J. Oceanograp. Soc. Japan.* **1983**, 39(2), 53-62.
60. Sinkkonen, S.; Passivirta, J. Degradation half-life times of PCDDs, PCDFs and PCBs for

Chapter 5: POPs in Antarctic Seawater and Phytoplankton

environmental fate modeling. *Chemosphere*. **2000**, 40, 943–949.

61. Axelman, J. Vertical flux and particulate/water dynamics of Polychlorinated biphenyls (PCBs) in the open Baltic Sea. *Ambio*. **2000**, 29(4-5), 210-216.
62. Harner, T.; Kylin, H.; Bidleman, T. F.; Strachan, W. M. J. Removal of and α -hexachlorocyclohexane and enantiomers of γ -hexachlorocyclohexane in the eastern Arctic Ocean. *Environ. Sci. Technol.* **1999**, 33(8), 1157-1164.
63. Harner, T.; Jantunen, L. M. M.; Bidleman, T. F.; Barrie, L. A.; Kylin, H.; Strachan, W. M. J.; Macdonald, R. W. Microbial degradation is a key elimination pathway of hexachlorocyclohexanes from the Arctic Ocean. *Geophys. Res. Lett.* **2000**, 27(8), 1155-115.
64. Pućko, M.; Stern, G.A.; Macdonald, R.W.; Barber, D.G.; Rosenberg, B.; Walkusz, W. When will α -HCH disappear from the western Arctic Ocean? *J. Mar. Syst.* **2011**, doi: 10.1016/j.jmarsys201109007
65. Dachs, J.; Eisenreich, S.J.; Hoff R.M. Influence of eutrophication on air-water exchange, vertical fluxes and phytoplankton concentrations of persistent organic pollutants. *Environ. Sci. Technol.* **2000**, 34(6), 1095-1102.
66. Larsson, P. Persistent organic pollutants (POPs) in pelagic systems. *Ambio*, **2000**, 29(4-5), 202-209.
67. Nizzetto, L.; Gioia, R.; Li, J.; Borgå, K.; Pomati, F.; Bettinetti, R.; Dachs, J.; Jones, K. C. Biological pump control of the fate and distribution of hydrophobic organic pollutants in water and plankton. *Environ. Sci. Technol.* **2012**, 46(6), 3204-3211.
68. Redaudie-de-Gioux, A.; Vaquer-Sunyer, R.; Duarte, C. Patterns in planktonic metabolism in the Mediterranean Sea. *Biogeosciences* **2009**, 6, 3081-3089.
69. Huang, K.; Ducklow H.; Vernet, M.; Cassar, N.; Bender, M.L. Export production and its regulating factors in the West Antarctica peninsula of the Southern Ocean. *Global Biogeochem. Cycles* **2012**, 26, GB2005, doi: 10.1029/2010GB004028.
70. Jurado, E.; Zaldívar, J.M.; Marinov, D.; Dachs, J. Fate of persistent organic pollutants in the water column: Does turbulent mixing matter? *Mar. Pollut. Bull.* **2007**, 54(4), 441-451.
71. Ngabe, B.; Bidleman, T. F.; Falconer, R. L. Base hydrolysis of α - and γ -hexachlorocyclohexanes. *Environ. Sci. Technol.* **1993**, 27(9), 1930-1933.
72. Lal, R.; Pandey, G.; Sharma, P.; Kumari, K.; Malhotra, S.; Pandey, R.; Raina, V.; Kohler, H.-P. E; Holliger, C.; Jackson, C.; Oakeshott, J. G. Biochemistry of microbial degradation of

Chapter 5: POPs in Antarctic Seawater and Phytoplankton

hexachlorocyclohexane and prospects for bioremediation. *Microbio. Mol. Biol. R.* **2010**, 74(1), 58-80.

73. Grannas, A. M.; Cory, R. M.; Miller, P. L.; Chin, Y.; McKnight, D. M. The role of dissolved organic matter in arctic surface waters in the photolysis of hexachlorobenzene and γ -HCH. *J. Geophys. Res-Bioge.* **2012**, 117(1), G01003, doi: 10.1029/2010JG001518

74. Hargrave, B. T.; Phillips, G. A.; Vass, W. P.; Bruecker, P.; Welch, H. E.; Siferd, T. D. Seasonality in bioaccumulation of organochlorines in lower trophic level arctic marine biota. *Environ. Sci. Technol.* **2000**, 34(6), 980-987.

75. Hoekstra, P. F.; O'Hara, T. M.; Teixeira, C.; Backus, S.; Fisk, A. T.; Muir, D. C. G. Spatial trends and bioaccumulation of organochlorine pollutants in marine zooplankton from the Alaskan and Canadian Arctic. *Environ. Toxicol. Chem.* **2002**, 21(3), 575-583.

76. Fisk, A. T.; Stern, G. A.; Hobson, K. A.; Strachan, W. J.; Loewen, M. D.; Norstrom, R. J. Persistent organic pollutants (POPs) in a small, herbivorous, arctic marine zooplankton (*Calanus hyperboreus*): Trends from April to July and the influence of lipids and trophic transfer. *Mar. Pollut. Bull.* **2001**, 43(1-6), 93-101.

77. Borgå, K.; Fisk, A. T.; Hargrave, B.; Hoekstra, P. F.; Swackhamer, D.; Muir, D. C. G. Bioaccumulation factors for PCBs revisited. *Environ. Sci. Technol.* **2005**, 39(12), 4523-4532.

Chapter 6

Atmospheric Occurrence and Deposition of Hexachlorobenzene and Hexachlorocyclohexanes in the Southern Ocean and Antarctic Peninsula

**Cristóbal Galbán-Malagón, Ana Cabrerizo, Gemma Caballero and Jordi
Dachs**

Submitted for publication to *Atmospheric Environment*.



The results from this chapter were submitted for publication to *Atmospheric
Environment*.

Chapter 6: HCHs and HCB in the Antarctic and Southern Ocean Atmosphere

Abstract

Despite the distance of Antarctica and the Southern Ocean to primary source regions of organochlorine pesticides, such as hexachlorobenzene (HCB) and hexachlorocyclohexanes (HCHs), these organic pollutants are found in this remote region due to long range atmospheric transport and deposition. This study reports the gas- and aerosol- phase concentrations of α -HCH, γ -HCH, and HCB in the atmosphere from the Weddell, South Scotia and Bellingshausen Seas. The atmospheric samples were obtained in two sampling cruises in 2008 and 2009, and in a third sampling campaign at Livingston Island (2009) in order to quantify the potential secondary sources of HCHs and HCB due to volatilization from Antarctic soils and snow. The gas phase concentrations of HCHs and HCB are low, and in the order of very few pg m^{-3} . α -HCH and γ -HCH concentrations were higher when the air mass backtrajectory has “touched” the Antarctic continent, consistent with the net volatilization fluxes of γ -HCH measured at Livingston Island. In addition, the Southern Ocean is an important net sink of HCHs, and to minor extent of HCB, due to high diffusive air-to-water fluxes. These fluxes are presumably driven by the role of the settling fluxes of organic matter-bound HCHs and HCB, but especially due to the role of bacterial degradation, depleting the water column concentrations of HCHs in surface waters. This is the first field study that has studied the coupling between the atmospheric occurrence of HCHs and HCB, the simultaneous air-water exchange, soil/snow-air exchange, and long range atmospheric transport of organic pollutants in Antarctica and the Southern Ocean.

Chapter 6: HCHs and HCB in the Antarctic and Southern Ocean Atmosphere

1. Introduction

Persistent and semivolatile organic pollutants can reach remote oceanic regions through atmospheric transport and deposition (Iwata et al. 1993, Dachs et al. 2002). The study of organochlorine pesticides (OCPs) and other persistent organic pollutants (POPs) in the northern hemisphere and Arctic Ocean has received more attention than the assessment of atmospheric deposition in the southern hemisphere, and especially to its remote regions such as Antarctica and the Southern Ocean (Jantunen et al., 2004, Bengtson-Nash, 2011). OCPs are ubiquitous in the environment and have been detected in all the environmental compartments (water, air, snow, ice and biota) of Polar Regions (Tanabe et al., 1983, Iwata et al., 1993, Cabrerizo et al. 2012, MacDonald et al., 2005). Although there are previous reports of the atmospheric concentrations of OCPs, such as hexachlorobenzene (HCB) and hexachlorocyclohexanes (HCHs), in the Southern Ocean (Tanabe et al., 1983, Larsson et al., 1992, Iwata et al., 1993, Bidleman et al., 1993 and Kallenborn et al., 1998, Jantunen et al., 2004, Montone et al., 2005, Dickhut et al., 2005, Cincinelli et al., 2009, Baek et al., 2011 and Xie et al., 2011), these studies usually cover a small sub-region. Historical production of HCHs and HCB mainly occurred in the northern hemisphere (Breivik et al., 2004), and the occurrence and temporal trends of OCPs in the Arctic reflect its production and usage in the northern hemisphere. Conversely, the occurrence of OCPs in Antarctica reflects their efficiency for long-range atmospheric transport in addition to production trends (Bengtson-Nash, 2011, Dickhut et al., 2005). Since 1990 there was a restriction and reduction of the global production and usage of HCHs and HCB (UNEP 2001). Consequently, the primary sources have been reduced during the last decades (Breivik et al. 2004), which have also lead to a decrease of OCPs seawater concentrations in the Southern Ocean (Galbán-Malagón et al. 2013).

Long range atmospheric transport and deposition are usually considered the main source of POPs to the Antarctic continent and Southern Ocean (Bengtson-Nash et al. 2011, Cabrerizo et al. 2012). Ultimately, these compounds may experience “cold-trapping” at polar regions, where the low temperatures

Chapter 6: HCHs and HCB in the Antarctic and Southern Ocean Atmosphere

further prolong persistence (Wania and Mackay 1995) and enhance their deposition and accumulation in water, soil, snow or biota. In the current scenario of decreasing primary sources, it has been suggested that remobilization of historical polar terrestrial reservoirs (snow, soil) of PCBs and HCB may also be feasible (Ma et al 2011, Cabrerizo et al. 2013) due to changes in climate. Previous attempts to study the cycling of HCHs in Antarctic waters have revealed that net deposition predominates over net volatilization (Dickhut et al., 2005, Cincinelli et al., 2009, Jantunen et al., 2004 and Xie et al., 2004). Conversely, close to air-water equilibrium conditions have been reported for HCB (Cincinelli et al., 2009). Regardless of these pioneering studies, there is a lack of comprehensive studies covering the atmospheric occurrence and deposition in a large region of Antarctica and Southern Ocean. Therefore, the objectives of the present work are: i) to study the occurrence of HCHs and HCB in the atmosphere over the South Scotia Sea, the Weddell Sea, Bransfield Strait and Bellingshausen Sea during two Antarctic oceanic campaigns in 2008 and 2009, ii) to assess the diffusive air-water exchange of HCHs and HCB and the factors driving the air-water cycling of OCPs in the Antarctic Region, and iii) to identify potential local sources of atmospheric HCHs and HCB due to volatilization from soil and snow.

2. Material and Methods

2.1 Sampling and site description

Atmospheric sampling was conducted during the ESSASI and ATOS-II Antarctic cruises in austral summer of 2008 and 2009, respectively, on board of R/V Hespérides. In addition, and simultaneously to the ATOS-II campaign, a field terrestrial sampling campaign was performed at Livingston Island (Southern Shetland Islands) in January-February 2009. The ESSASI campaign sampled the region of the South Scotia Sea between Elephant Island and South Orkneys islands (Figure 1 and Figure S1 in Appenix D.1). The ATOS-II cruise covered the region around the Antarctic Peninsula including the Weddell Sea, the Bransfield Strait and the Bellingshausen Sea (Figure 1 and Figure S1 in Appenix D.1). The terrestrial sampling campaign was carried out at Livingston Island, at the

Chapter 6: HCHs and HCB in the Antarctic and Southern Ocean Atmosphere

surroundings of the Spanish Research Station (Juan Carlos I) (62° 34'S, 61° 13'W, South Shetland Islands) (Figure S2).

During the cruises, simultaneous samples of air (gas and aerosol phase) and surface water (particulate and dissolved phases) were taken. The methods and occurrence of HCHs and HCB in seawater has been described previously in a companion paper (Galbán-Malagón et al. 2013), and we describe here only the sampling and analytical methods for the atmospheric samples and land samples. Ancillary data including physical and chemical characterization of air and water were obtained from the automatic continuous water system and the meteorological station on board of the ship. Samples' ancillary data are reported in Table S1 in Appendix D.1 of the supporting information.

Air samples (gas and aerosol phase) were collected using a high-volume air sampler (MCV: CAV-A/HF, Collbató, Spain) deployed over the vessel bridge connected to a wind direction sensor in order to avoid contamination from the ship. Air was sampled only when the wind direction was from the bow (90° to -90°). Sampling flow rate was set at 40 m³ h⁻¹ and the sampling volumes averaged 1000 m³ and 1400 m³ for the gas phase samples of the ESSASI and ATOS II cruises, respectively. During the ATOS- II cruise, a second high-volume air sampler was operated in parallel for the sampling of aerosol-phase only, with longer sampling periods, so higher volumes of air were sampled (around 1800 m³). This was part of an attempt to determine POPs in aerosols, since aerosol concentrations are extremely low in Antarctica (Weller et al. 2012). The gas phase was collected on a polyurethane foam (PUF) plugs (100 mm diameter x 100 mm, Klaus Ziemer GmbH, Germany) and the aerosol phase was trapped on a quartz microfiber filters (QM/A) 203x254 mm (Whatman, England).

The fugacities of OCPs in soil and snow were measured using the fugacity sampler (Cabrerizo et al. 2009, 2011a and b, 2013) in which the air is forced to flow below a stainless-steel chamber with a surface of 1 m² and separated 3 cm from the soil/snow surface. This sampler allows the air to equilibrate with the surface soil/snow in terms of the chemical fugacity. Four soil-fugacity samplers were operating simultaneously and distributed above soil covered with lichens

Chapter 6: HCHs and HCB in the Antarctic and Southern Ocean Atmosphere

(*Usnea Antarctica*) in Pico Radio Hill (one sampler), bare soil at Polish beach (one sampler) and snow in Sofia Mountain (two samplers) (See Figure S2). In these samplers, the air, after it has been equilibrated with snow or soil, passes through a glass fiber filter to remove dust particles and a polyurethane foam plug (PUF) in which the compounds from the gas phase are retained. In addition to the air equilibrated from the surface (snow and soil), ambient air at a height of 1.5 m is also analyzed. The comparison of the fugacity in the soil/snow, and the fugacity in ambient air, provides the direction of the air-surface exchange. A high-volume air sampler was also deployed at Livingston Island in order to determine HCB and HCHs concentrations in the aerosol phase. Filters and PUFs used in this sampler were quartz fiber filters (GF/F) of 47 mm of diameter and the dimensions of PUFs were 10 x 2 cm. Details of the sampling strategy and conditions at Livingston Island are given elsewhere (Cabrerizo et al. 2013).

Prior to the sampling campaigns, PUFs were pre-cleaned using a Soxhlet extraction with acetone:hexane (3:1) for 24 h. They were then dried under vacuum, and kept well sealed until the sampling. QMA filters used for aerosol sampling were initially pre-combusted at 450°C during 24h, pre-weighed and wrapped in aluminum foil before sampling. After the sampling, PUF and QMA filters were kept at 4°C and -20 °C, respectively, until chemical analysis.

2.2 Analytical Methods

2.2.1 Atmospheric and aerosol extraction and fractionation of OCPs

Briefly, all samples were Soxhlet extracted for 24 h using acetone:hexane (3:1) for gas-phase samples collected on PUFs and using methanol:dichloromethane (1:2) for aerosol-phase samples collected by QMA filters. Prior to extraction, samples were spiked with PCB 65 (Dr Ehrenstorfer, GmbH, Germany), which was used as a recovery standard. Extracts were reduced in a rotary evaporation unit (R-200, Büchi, Italy) until 0.5 ml and fractionated on a 3% deactivated alumina column (3 g), with a top of 1 g of anhydrous sodium sulphate. The first fraction containing PCBs and some OCPs was collected using 12 mL of hexane, while the second fraction containing PAHs and the rest of OCPs

Chapter 6: HCHs and HCB in the Antarctic and Southern Ocean Atmosphere

was collected using 15 mL of hexane: dichloromethane (1:2). All fractions were concentrated until 1 mL by rotary evaporation and solvent exchange to isooctane under a purified N₂ stream until a final volume of 150 µL. α -HCH, γ -HCH and HCB were analyzed in the merged first and second fraction for the gas and dissolved phase. For the aerosol phase samples, only the first fraction was analyzed. Identification and quantification was done using the retention time of the α -HCH, γ -HCH and HCB peaks. The details of the methodology used for analyzing the PUFs from the sampling of the fugacity in soil/snow and ambient air using the fugacity sampler at Livingston Island have been described elsewhere (Cabrerizo et al. 2013).

2.2.2 OCPs Identification and Quantification

OCPs were analyzed by a gas chromatograph coupled to a μ -ECD detector (Agilent Technologies, model 7890), provided with a HP-5MS 60m capillary column (inner diameter 0.325 μ m, film thickness 0.25 μ m). The instrument was operated in splitless mode (close for 1.5min). The oven programmed temperature started from 90 °C (hold for 1 min) to 190 C at 20 °C min⁻¹ and then to 310°C (3°C min⁻¹) (holding time 18 min). Injector and detector temperatures were 280 and 320°C, respectively. Helium and nitrogen were used as carrier (1.5 ml/min and makeup (60 ml/min) gases respectively. Prior to injection, 5 ng of PCB 30 was added as internal standard to all samples.

2.3 Quality Control and Quality Assurance.

All analytical procedures were monitored using strict quality assurance and quality control measures. Sampling equipment were cleaned rigorously prior to sampling and between samples to avoid sample cross contamination. Laboratory and field blanks constituted 20 % of total number of samples processed at a rate of one blank for every. Blank signal accounted for an average of 5(\pm 8)% of the amount detected in samples and was subtracted after quantification for all samples. Limits of detection (LODs) and quantification (LOQs) were estimated from the average plus three times the standard deviation, and average plus ten times the standard deviation from blanks, for LOD and LOQ, respectively. The estimated LODs and LOQs for α -HCH, γ -HCH and HCB were

Chapter 6: HCHs and HCB in the Antarctic and Southern Ocean Atmosphere

0.059-0.16, 0.15-0.46 and 0.14-0.37 pg on column. Instrumental detection limits were also calculated from the lowest standard detected and considering the average sampling volumes, resulting in a value of $<0.001 \text{ pg m}^{-3}$ for the ESSASI samples, and $<0.002 \text{ pg m}^{-3}$ for the ATOS II samples. The recoveries of PCB 65, used as surrogate standard, ranged from 53 to 78 % for ESSASI samples, and from 67 to 76 % for ATOS II samples. Quality control and quality assurance parameters regarding samples taken at terrestrial campaign are reported elsewhere (Cabrerizo et al, 2013)

2.4 Statistical Analysis

Differences in concentrations were analyzed using a non-parametric statistical approach using the *Mann Whitney U test* for the comparison of the ESSASI and ATOS II atmospheric concentrations of α -HCH, γ -HCH and HCB (Figure 2A, B and C). The influence of air-mass backtrajectories on OCP atmospheric concentrations was discerned using the *Kruskal-Wallis test* for 3 or more groups followed by a post hoc *Dunn's Multiple Comparisons test* (Figure 2D, E and F)

3. Results and Discussion

3.1 Atmospheric occurrence of HCHs and HCB

3.1.1 Gas phase concentrations of α -HCH and γ -HCH

During the ESSASI cruise (January-February 2008), gas phase concentrations of α -HCH and γ -HCH ranged from 0.06 to 5.8 pg m^{-3} and from 1.5 to 7.1 pg m^{-3} , respectively. Conversely, the gas phase concentrations from the ATOS II cruise (February 2009) ranged from 0.04 to 0.5 pg m^{-3} , and from 0.07 to 3 pg m^{-3} for α -HCH and γ -HCH, respectively (see Figure 2). The concentrations of α -HCH and γ -HCH in 2008 were higher (*Kruskal Wallis test*, $p<0.05$) than in 2009. These inter-annual differences may be due to the different regions sampled in the different cruises, to differences in the air mass trajectories, or to other factors as discussed below.

Chapter 6: HCHs and HCB in the Antarctic and Southern Ocean Atmosphere

In general, the concentrations of γ -HCH were higher than those of α -HCH in both cruises (see Table 1 and Table S4). During the sampling campaign performed at Livingston Island, only γ -HCH was detected with ambient air concentrations ranging from LOQ to 2.73 pg m^{-3} (Table S5). α -HCH was always below LOQ due to the low sampled volumes of the land-based samples (around 70 m^3). These concentrations are in agreement of previous reported studies for the atmosphere over the coastal Antarctic continent and Islands (Dickhutt et al., 2005 and Cincinelli et al., 2009), or over the Southern Ocean (Jantunen et al., 2004, Dickhutt et al., 2005 and Montone et al., 2005 and Xie et al., 2011). However, the concentrations reported in this study are significantly lower than the concentrations reported over Antarctic land and waters during early sampling efforts in the 1980s and 1990s (Tanabe et al., 1983., Larsson et al., 1992, Iwata et al., 1993 and Bidleman et al., 1993) (See Table 1 for a comparison of HCHs and HCB concentrations reported in this study in comparison to previous reports), suggesting a decrease in atmospheric concentrations in agreement with the reported temporal trends for seawater concentrations of HCH (Galbán-Malagón et al. 2013, Lakaschus et al. 2002). This decrease in atmospheric concentrations reflects the restriction in the use/emissions of these chemicals from source regions. Latitudinal gradients have been reported previously for α -HCH and γ -HCH (Bidleman et al., 1993). However, in the present study, in which a smaller latitudinal range was sampled, this trend was not significant, consistent with other recent reports (Jantunen et al., 2004).

Chapter 6: HCHs and HCB in the Antarctic and Southern Ocean Atmosphere

Table 1. Atmospheric concentrations (gas-phase) of HCH and HCB reported for the Southern Ocean and Antarctic region (pg m⁻³).

Location	Year	α -HCH		γ -HCH		HCB		Reference
		Mean	SD	Mean	SD	Mean	SD	
Sabrina Coast	1981	120		120				
Balleny Islands	1981	170		170				
Syowa Station	1982	49		49				Tanabe et al., 1983 ^a
Amundsen Bay	1982	44		44				
Cape Evans (Ross Island)	1989			66.75	43.69			
	1990			72.00				Larsson et al., 1992
Southern Ocean	1990	26.00		12.00				Iwata et al., 1993
Gondwana cruise (New Zealand to Antarctica)	1990	4.15	1.19	5.80	5.60	62.60	20.00	Bidleman et al., 1993
Signy Island	1995	3.50	2.44	33.01	20.13			Kallenborn et al., 1998
Transect Brazil-Antarctica	1995	3.77	0.64	3.00	4.60	23.90	1.79	Montone et al., 2005
Agulhas Cruise (South Africa-Antarctica)	1997-1998	1.01	0.31					Jantunen et al., 2004
Antarctic Peninsula	2001-2002	0.32	0.10	0.78	0.80	20.59	6.51	Dickhut et al., 2005
Terra Nova Bay	2003-2004	0.22	0.08	0.56	0.32	11.36	5.35	Cincinelli et al., 2009
King George Island	2005							
	2006	2.28	0.27	2.85	0.46			Baek et al., 2011
	2007	1.72						
Southern Ocean Cruise	2008	0.75	0.21	0.70	0.28			Xie et al., 2011
South Scotia Sea	2008	1.70	2.16	1.63	1.52	49.71	8.19	
Bellingshausen	2009	0.26	0.18	1.14	1.61	32.19	18.63	
Bransfield	2009	0.14	0.09	0.12	0.07	35.03	14.55	
Weddell	2009	0.16	0.14	0.87	0.88	11.93	15.77	This Study
Livingston Island (Polish Bluff)	2009			0.93	0	11.97	2.67	
Livingston Island (Radio Peak)	2009			2.27	0.68	10.30	4.81	
Livingston Island (Sofia Mountain)	2009			0.79	0.77	11.79	1.82	

Chapter 6: HCHs and HCB in the Antarctic and Southern Ocean Atmosphere

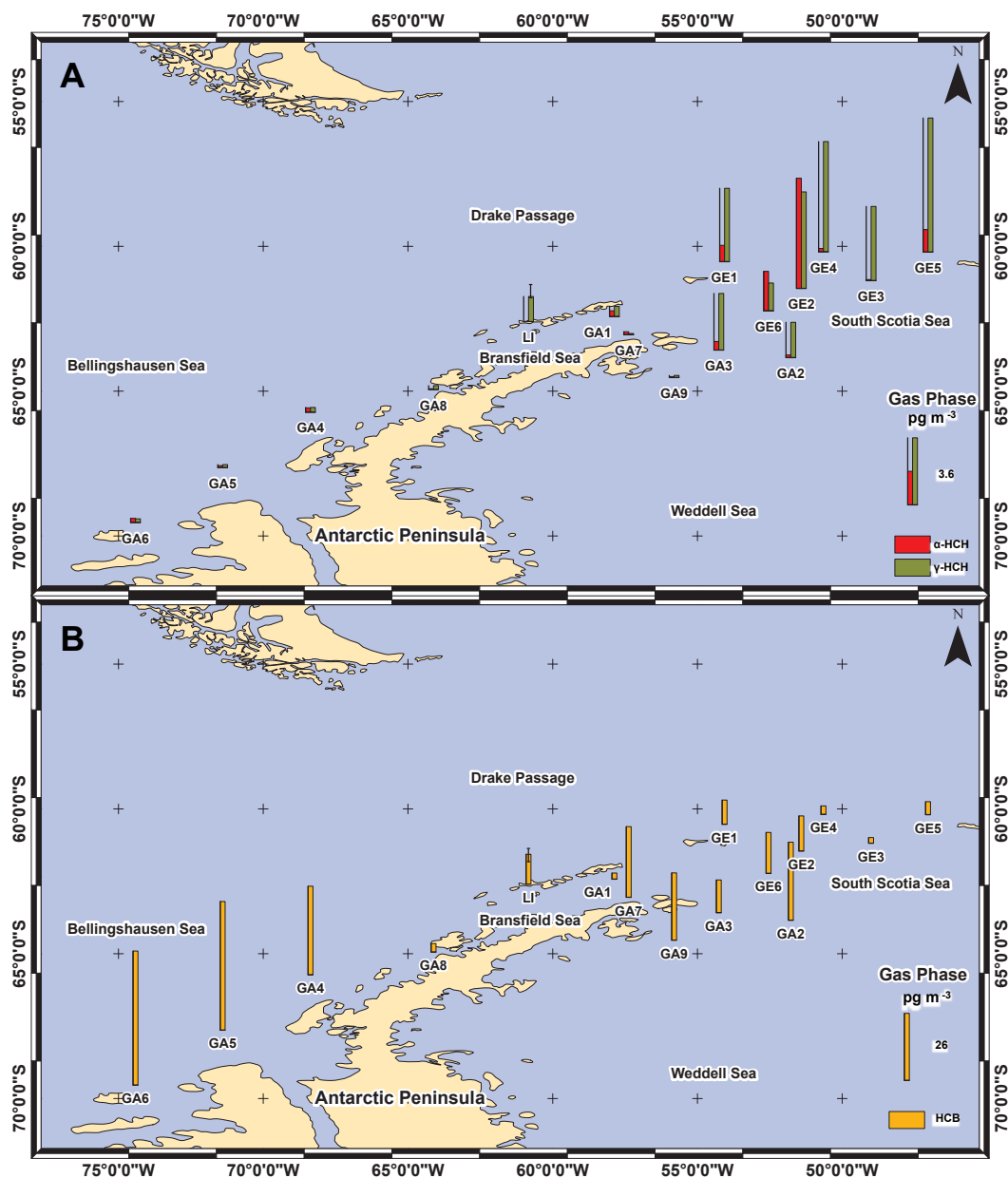


Figure 1. Gas phase concentrations (pg m^{-3}) of HCHs (A) and HCB (B) in samples taken during the ESSASI (GE) and ATOS II (GA) cruises in 2008 and 2009, respectively. Average and range is also shown for the gas-phase samples taken at Livingston Island.

3.1.2 Gas phase concentrations of HCB

Over the Southern Ocean, ambient air concentration of HCB were in the range of $2.2\text{-}15.8 \text{ pg m}^{-3}$, $2.4\text{-}30.1 \text{ pg m}^{-3}$, $25.9\text{-}51.8 \text{ pg m}^{-3}$ and $12.6\text{-}49.7 \text{ pg m}^{-3}$ in the South Scotia, Weddell, Bransfield and Bellingshausen Seas, respectively. The highest concentrations were found in the Bransfield and Bellingshausen Seas, while the lowest concentrations were found in the Weddell Sea during the ATOS

Chapter 6: HCHs and HCB in the Antarctic and Southern Ocean Atmosphere

II cruise. The results of the *Kruskal Wallis test* ($p < 0.05$) indicate that there are no significant differences between the concentrations measured in 2008 and 2009 (Figure 2). At Livingston Island, the HCB gas phase concentrations ranged from 4.19 to 15.73 pg m^{-3} (Table S5), comparable to those determined over the ocean. The gas-phase concentrations of HCB reported here are in the same range than those reported in the atmosphere from the open and coastal Southern Ocean (See Table 1) (Montone et al., 2005, Bidleman et al., 1993, Dickhut et al., 2005), and from the Antarctic continent and islands (Dickhut et al., 2005 and Cincinelli et al., 2009). HCB concentrations are also comparable to those measured in the Arctic Ocean (Galbán-Malagón, 2013, Lohmann et al., 2008, Su et al., 2006 and Wong et al., 2011). Gas phase concentrations over the ocean were not correlated with temperature.

3.1.3 Aerosol phase concentration of α -HCH, γ -HCH and HCB

The aerosol phase concentrations over the Southern Ocean during the ATOS 2 cruise ranged from 0.01 to 0.1 pg m^{-3} , 0.03 to 0.1 pg m^{-3} and from 0.04 to 0.08 pg m^{-3} for α -HCH, γ -HCH and HCB, respectively (Table 1). At Livingston Island, the aerosol-phase HCB concentration was in the range of 0.0035-0.004 pg m^{-3} . To the best of our knowledge, there are no previous studies reporting aerosol-phase concentrations of HCHs and HCB for the Southern Ocean or Antarctica. However, these concentrations were lower than the aerosol-phase concentrations measured in the Arctic and Subarctic atmosphere (Galbán-Malagón et al. 2013b).

Chapter 6: HCHs and HCB in the Antarctic and Southern Ocean Atmosphere

3.2 Influence of the air-mass backtrajectories on atmospheric concentrations of HCHs and HCB

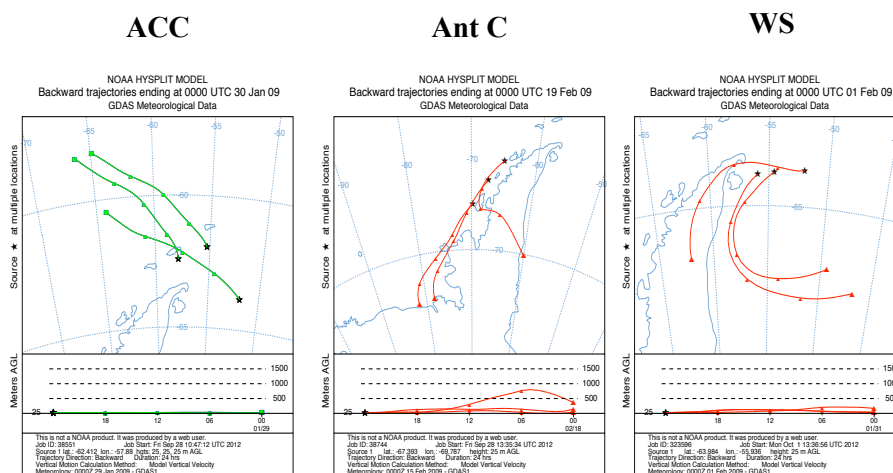


Figure 3. Characteristic air-mass back trajectories for sampling periods influenced by the Antarctic Circumpolar water Current (ACC), the Weddell Sea (WS) and the Antarctic Continent (AC).

The air-mass back-trajectories were assessed using the NOAA HYSPLIT model (Draxler and Rolph, 2011). The back trajectories were estimated at 25 meters height and were computed for the initial, middle and final time of the sampling period to ensure clear and coherent information about the air mass origin during sampling, since air masses can be highly variable close to the Antarctic continent. The three characteristic air mass backtrajectories encountered are shown in Figure 2 (all the backtrajectories are shown in Figures S4 and S5 in Appendix D.2) and belongs to the Antarctic Circumpolar Water Current (ACC) accompanying air masses, those coming from the Antarctic Continent (AntC), and air masses coming from the Weddell Sea (WS). Non-parametric tests were performed to establish differences in gas phase concentrations between the different sampling events revealing that for α -HCH and γ -HCH, gas phase concentrations were significantly different ($p < 0.05$) for those samples influenced by WS and AntC air masses, but the concentrations for these groups of sampling events were not significantly different than when the sampling events were influenced by the ACC air masses (right panels of Figure 3). Generally, concentrations of HCHs were higher when the air mass has “touched” the Antarctic continent or they came from the NW seawater in the ACC, while

Chapter 6: HCHs and HCB in the Antarctic and Southern Ocean Atmosphere

concentrations were lower when the air mass came from the Weddell Sea. In the case of HCB, there were no significant differences between the gas-phase concentrations for the different air mass backtrajectories (right panels of Figure 2). The analysis of the air-mass backtrajectories did not allow to discern a direct source of HCHs or HCB originating in South America, thus affecting the Antarctic atmosphere as a result of a lack of direct transport from mid-latitudes to higher-latitudes (Dickhut et al., 2005). This result agrees with the trends described recently for perfluorinated compounds (Del Vento et al., 2012).

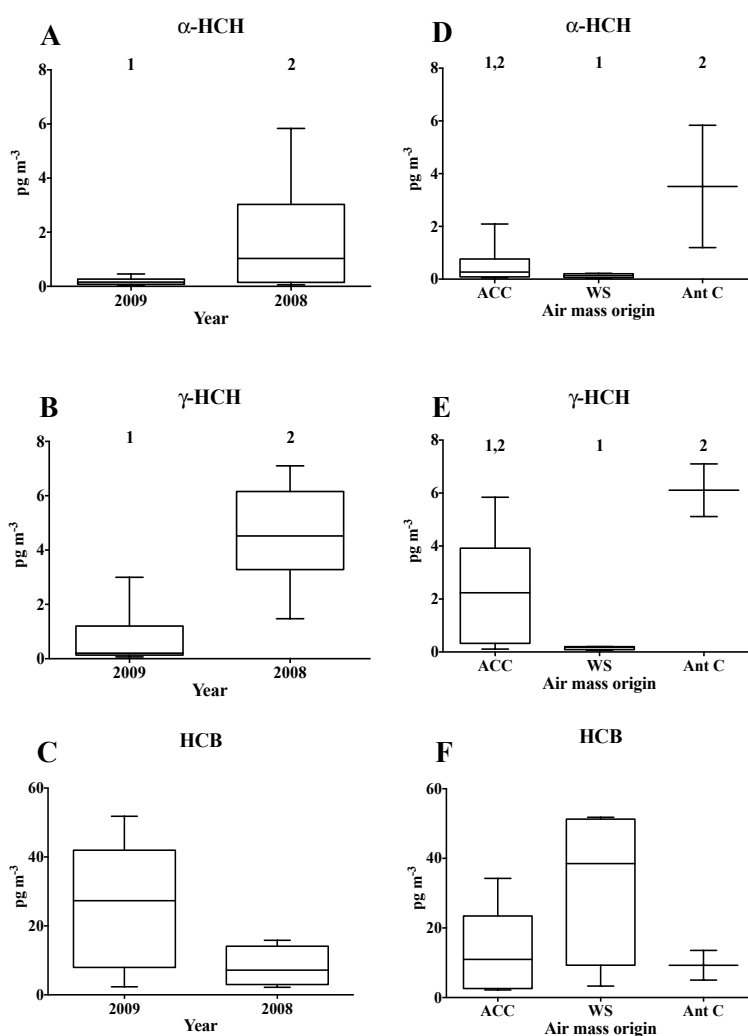


Figure 3. Box-Plot comparing gas-phase concentrations during the ESSASI (2008) and ATOS II (2009) cruises for α -HCH (A), γ -HCH (B) and HCB (C). Box-Plot comparing the influence of the air mass origin (based on backtrajectory analysis) for α -HCH (D), γ -HCH (E) and HCB (F). For figures A, B and C differences ($p < 0.05$) are marked numbers 1 and 2 over the box in the case of the figures D, E and F. 1, 2 over the box means that there are no statistical differences with 1 and 2. ACC: Antarctic Circumpolar Water Current influence, WS: Weddell Sea origin and AntC: Antarctic Continent Influence.

3.3 Antarctica as a secondary source of HCHs and HCBs

Chapter 6: HCHs and HCB in the Antarctic and Southern Ocean Atmosphere

The potential influence of the Antarctic continent as a secondary source of HCHs and/or HCB inducing higher gas phase concentrations, as observed in the AntC dominated air masses in comparison to WS air masses (Figure 2), require further attention. Recently, it has been suggested (Ma et al., 2011, Cabrerizo et al., 2013, Kang et al., 2012) that Arctic and Antarctic seawater, snow and/or soils are becoming important secondary sources, remobilizing POPs and modulating the trends of legacy pollutants in the Arctic and Antarctic atmosphere. Indeed, this process could be more intense during periods of high wind speeds influenced by the katabatic winds coming from the continents (speed > 10 m s⁻¹), enhancing the release of contaminants to the atmosphere (Hallsall et al., 2004). The deployment of fugacity samplers at Livingston Island allows determining the soil-air and snow-air fugacity ratios and thus the determination of the occurrence of local sources of atmospheric HCHs and HCB from Antarctica. The ambient air fugacity (f_A , Pa) and the snow or soil fugacity (f_S , Pa) were calculated by (Mackay, 1979):

$$f_A = \frac{10^{-12} C_{Gas} RT}{MW} \quad [6.1]$$

$$f_S = \frac{10^{-12} C_{SA} RT}{MW} \quad [6.2]$$

Where C_{Gas} is the measured ambient air gas-phase concentration at 1.5 m height (pg m⁻³), R is the gas constant (8.314 Pa m³ mol⁻¹ K⁻¹), T is the air temperature (K), MW is the chemical molecular weight (g mol⁻¹), and C_{SA} (pg m⁻³) is the gas phase concentration that has been equilibrated with the soil or snow surface (Table S5 in Appenix D.3) as measured using the fugacity sampler (Cabrerizo et al. 2009, 2013). The re-volatilization of HCHs and HCB from the surface reservoirs can be confirmed by comparing f_A and f_S . When f_S is higher than f_A there is a net volatilization of the chemical. In contrast, if f_A is higher than f_S there is a net deposition of the chemical. However, since there is an uncertainty in the measurements, equilibrium would be represented by $\log f_S/f_A$ in the range of +0.23 and -0.52 (Cabrerizo et al., 2009, 2011b, 2013). Figure 4 shows that HCB and γ -HCH in snow and soil were close to equilibrium with the over-lying atmosphere but with a tendency for a net volatilization for more than half of the

Chapter 6: HCHs and HCB in the Antarctic and Southern Ocean Atmosphere

sampling periods. These results suggest that during the austral summer, Antarctica is a secondary source of γ -HCH and HCB to the atmosphere, especially due to volatilization from snow. The “signal” from the Antarctic secondary sources may be more important for HCHs than HCB, as suggested by the comparison of gas-phase concentrations for different air-mass backtrajectories, because HCB is more persistent in the atmosphere than γ -HCH and thus long-range atmospheric transport may be more effective in comparison to secondary sources.

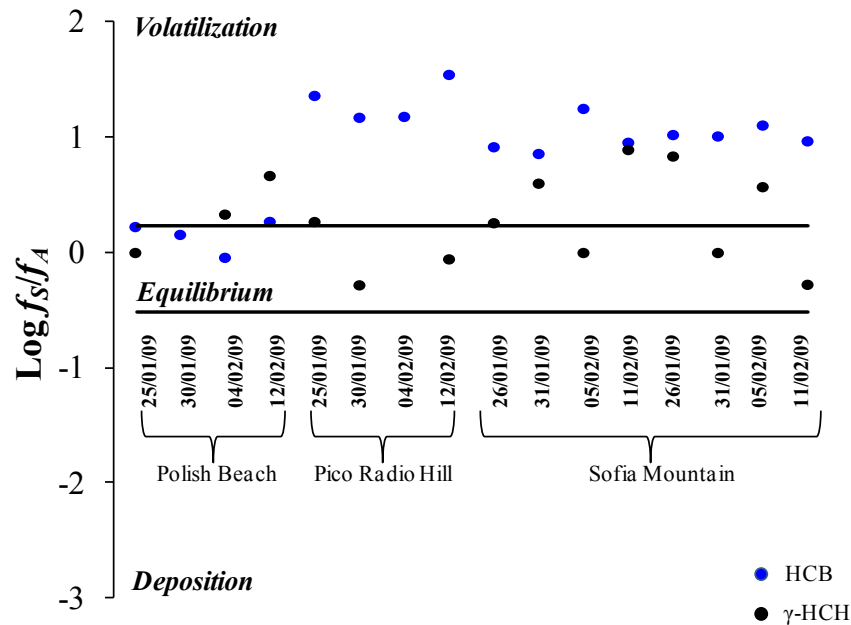


Figure 4. Surface/Air fugacity ratio ($\text{Log } f_s/f_A$) of HCB and γ -HCH for the different sampling sites and periods at Livingston Island (Antarctica). The black lines indicate the surface-air equilibrium range for $\text{Log } f_s/f_A$ (+0.23, -0.52).

3.4 Air-Sea diffusive exchange and dry deposition processes

The low concentrations over the Weddell Sea, and the high variability of concentrations when the air-masses are from oceanic regions, suggest that atmospheric deposition may be an important removal process for atmospheric HCHs and HCB. The net direction of the diffusive air-water exchange can be determined by comparing the chemical fugacity in water (f_w , Pa) and air (f_A , Pa).

$$f_w = \frac{10^{-12} C_{Dis} H' RT_w}{MW} \quad [6.3]$$

Chapter 6: HCHs and HCB in the Antarctic and Southern Ocean Atmosphere

Where C_{Dis} is the truly dissolved concentration estimated from the measured dissolved concentrations corrected by dissolved organic carbon (DOC) as reported elsewhere (Galbán-Malagón et al., 2013), R is the ideal gas constant ($8.314 \text{ Pa mol}^{-1} \text{ K}^{-1}$), T_w is the water surface temperature (K), H' is the surface temperature and salinity corrected dimensionless Henry's Law Constant (HLC) for each compound (Table S2 in Appendix C), and MW is the molecular weight of the studied compound. f_A over the ocean was estimated from equation [1] using the C_{Gas} measured during the cruises. More information about the truly dissolved concentration and HLC corrections is given in the supporting info (Appendix D.3).

Fugacity ratios (f_w/f_A) should be considered with caution due to the uncertainties associated with the C_{Gas} , C_{Dis} and HLC . The uncertainties associated to C_{Gas} and C_{Dis} were estimated to be 0.15 (15% error in analytical measure). Another source of uncertainty is the estimation of HLC , and a factor of 3 was chosen (Li et al., 2003). Following the approach of Brühn et al., 2003, if $f_w/f_A < 0.76$ indicates net deposition, $f_w/f_A > 3.23$ indicates net volatilization, and $0.76 \leq f_w/f_A \leq 3.23$ indicates that the gas-phase and dissolved-phase are close to equilibrium. f_w/f_A are shown in Figure 5A. During the ESSASSI cruise, the fugacity ratios indicate a net deposition for α -HCH and γ -HCH, while HCB showed conditions of close to air-water equilibrium to net deposition (South Scotia Sea). In the case of the sampling events during the ATOS II cruise (Weddell, Bransfield and Bellingshausen seas), there was a net deposition of HCHs and HCB for all the sampling events except for 2 samples (Table S5 on Appendix D.3). The fugacity ratios reported here for HCHs agree with those reported in the Antarctic Peninsula coastal waters (Dickhutt et al., 2005), the Ross Sea (Cincinelli et al., 2009) and Southern Ocean (Jantunen et al., 2004 and Xie et al., 2011) indicating that there is a strong disequilibrium between the air and water in the Southern/Antarctic Ocean. Conversely, HCB has been reported to be close to equilibrium in the Ross Sea (Cincinelli et al., 2009) but this study shows that there is significant air-water disequilibrium in some areas, especially for those samples from the ATOS II cruise that covered the marine regions around the Antarctic Peninsula (Weddell Sea, Bransfield Strait and Bellingshausen Sea).

Chapter 6: HCHs and HCB in the Antarctic and Southern Ocean Atmosphere

The magnitude of the net diffusive air-water fluxes (F_{AW} , $\text{ng m}^{-2} \text{d}^{-1}$) were estimated using the two-film model as follows

$$F_{AW} = k_{AW} \left(\frac{C_{Gas}}{H'} - C_{Dis} \right) \quad [6.4]$$

Where k_{AW} (m d^{-1}) is the estimated air-water mass transfer coefficient. The diffusive air-water fluxes are shown in Figure 5B. The highest depositional fluxes of α -HCH and γ -HCH were estimated for the Bransfield Strait ($0.3 \text{ ng m}^{-2} \text{d}^{-1}$ and $1.9 \text{ ng m}^{-2} \text{d}^{-1}$, respectively) and the lowest were found in the Weddell Sea for α -HCH ($0.02 \text{ ng m}^{-2} \text{d}^{-1}$) and in the Bellingshausen Sea for γ -HCH ($0.04 \text{ ng m}^{-2} \text{d}^{-1}$). HCB fluxes were significantly higher than those measured for HCHs (Kruskal-Wallis $p < 0.05$) in the South Scotia and the Bellingshausen Seas. The highest HCB diffusive flux was obtained in the South Scotia Sea samples ($5.5 \text{ ng m}^{-2} \text{d}^{-1}$) and the lowest in the Bransfield Sea ($0.1 \text{ ng m}^{-2} \text{d}^{-1}$).

The dry deposition was calculated from the aerosol-phase concentrations by:

$$F_{DD} = 10^{-3} C_A v_D \quad [6.5]$$

Where C_A is the aerosol-phase concentration (pg m^{-3}) and v_D is the particle deposition velocity of 258 m d^{-1} (or 0.3 cm s^{-1}) measured in Antarctica (Grönlund et al., 2002). Dry deposition fluxes ranged from 0.003 to 0.009, from 0.008 to 0.03, and from 0.01 to 0.02 $\text{ng m}^{-2} \text{d}^{-1}$ for α -HCH, γ -HCH and HCB respectively (see Table S7 on Appenix D.3).

Chapter 6: HCHs and HCB in the Antarctic and Southern Ocean Atmosphere

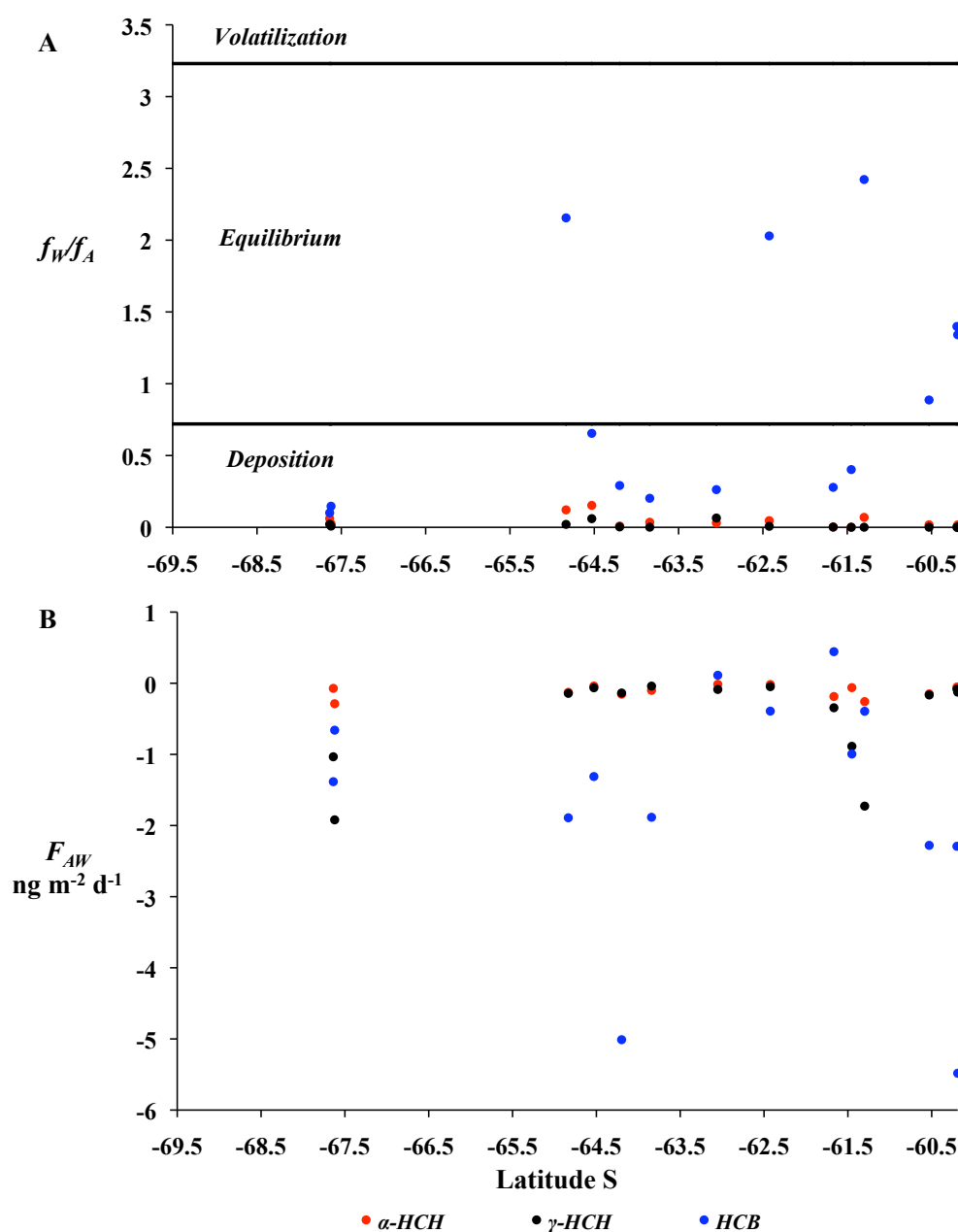


Figure 5. (A) Water-air fugacity ratio (f_w/f_A) and (B) air-water diffusive exchange fluxes ($\text{ng m}^{-2} \text{d}^{-1}$) for the air-water pairs of samples obtained during the ESSASI and ATOS II cruises against latitude for α -HCH (red dots), γ -HCH (black dots) and HCB (blue dots). f_w/f_A values over 3.23 means volatilization, f_w/f_A values under 0.72 means deposition, and f_w/f_A values between 3.23 and 0.72 means that concentrations in the gas and dissolved phases were close to equilibrium.

The seawater around the Antarctic Peninsula has low concentrations of POPs due to the distance from sources and isolation of Antarctic waters by the Antarctic Circumpolar Current (ACC) (Bengtson-Nash et al., 2010, Rintoul, 2000). The low concentrations of POPs in surface waters can also be due to loss processes in the water-column like the biological pump (Dachs et al., 2002, Galbán-Malagón et al. 2012) and the degradative pump (Galbán-Malagón et al.,

Chapter 6: HCHs and HCB in the Antarctic and Southern Ocean Atmosphere

2013b). Figure 6 schematizes the major processes affecting the occurrence of HCH and HCB in the Antarctic atmosphere and waters. The biological pump occurs when the settling flux of organic matter-bound POPs depletes the dissolved concentrations at sea surface, inducing higher air-water diffusive exchanges (Dachs et al. 2002, Galbán-Malagón 2012). This process is highly efficient for the transport of hydrophobic POPs, such as some PCBs (Dachs et al., 2002, Galbán-Malagón et al., 2012), but is not very efficient for the less hydrophobic PCBs and compounds like HCHs and HCB (Zhang et al., 2012, Berrojálbiz et al., 2011 and Galbán-Malagón et al., 2013b). Conversely, in the degradative pump, the depletion of the dissolved phase concentrations is due to degradation. Degradation of HCHs is driven by hydrolysis and bacterial degradation (Harner et al., 1999 and 2000, Helm et al., 2002) and it is the most important removal process in the Arctic water column (Li et al., 2004), followed by ocean currents. A recent modelling study has also suggested that microbial degradation and hydrolysis could be the responsible of α -HCH depletion in surface waters from the Beaufort Sea (Pucko et al., 2011), and it has been demonstrated that degradation is an important process in the cycling of HCHs in the upper water column of the North Atlantic and Arctic Oceans (Galbán-Malagón et al. 2013b). Degradation constants have been reported for α -HCH and γ -HCH in the Arctic Ocean (Harner et al., 1999 and Harner et al., 2000) at a 1000 m depth, and these constants can be scaled for surface waters using the bacterial biomass as reported elsewhere (Galbán-Malagón et al., 2013b, see Appendix D.3 for estimation of degradative fluxes). Degradation fluxes accounts, on average, for 12% and 28% of α -HCH and γ -HCH atmospheric inputs to the open Southern Ocean, but this percentage is higher in areas near to coast line, where up to 40% for α -HCH, and around 100% of γ -HCH of atmospheric inputs are lost by degradation in the photic zone (See tables S6, S7 and S8 Appendix C). Therefore, in the Southern Ocean, the strong net diffusive fluxes are driven in part by the degradative pump depleting the dissolved phase concentrations. It has been reported that bacterial production is strongly correlated with the phytoplankton biomass in the Southern Ocean (Ortega-Retuerta et al., 2008), thus during periods of high phytoplankton growth and abundance, the degradative pump would be more efficient in the depletion of HCHs in the water-

Chapter 6: HCHs and HCB in the Antarctic and Southern Ocean Atmosphere

column. This loss process occurs in parallel to the losses due to the biological pump, which are small for compounds such as HCHs. In the case of HCB, there is not any known process that could degrade HCB in the surface waters. So depletion of HCB concentrations in surface waters could be related to the exportation of HCB associated to particles (Barber et al., 2005 and Lohmann et al., 2009) but this removal process is considered small for HCB due to its low K_{OW} , consistent with air and water fugacities closer to equilibrium.

4. Conclusions

This work describes and discusses the first comprehensive study of the atmospheric occurrence and transport, soil/snow-air exchange and water-air exchange of HCHs and HCB for the Antarctic Peninsula and Southern Ocean (Figure 6). Despite the importance of secondary sources of HCHs from land-compartments (soils, snow) affecting the levels of some sampling events, long range atmospheric transport is the main input of HCHs and HCB to the Antarctic Peninsula region. The high air-water net diffusive deposition of HCHs to the Southern Ocean is enhanced by the role of the degradative pump depleting the water column concentrations. Conversely, for HCB, which is persistent in the water column, air and water are closer to equilibrium conditions. Further research is needed to close the mass balance of these compounds in the region, and delimitate the role of zooplankton and macrozooplankton in Antarctic waters, which recently has been revealed as an important transport pathway through the water-column in Arctic waters (Pucko et al., 2013)

Chapter 6: HCHs and HCB in the Antarctic and Southern Ocean Atmosphere

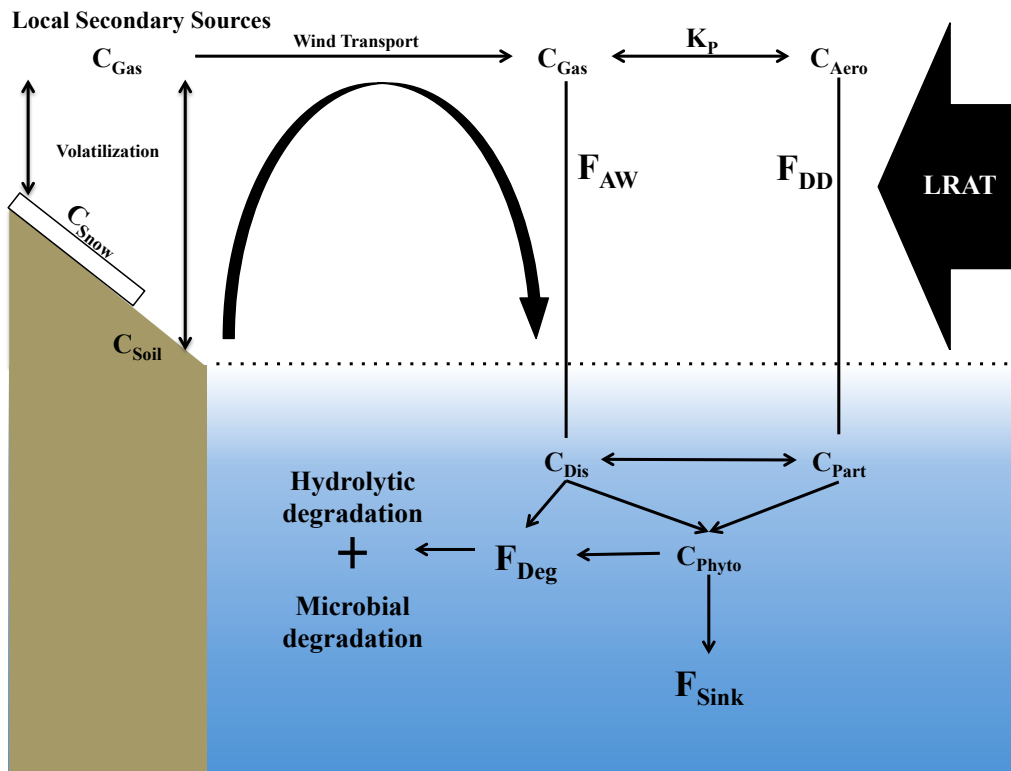


Figure 6. Scheme of POPs cycling in Antarctica and Southern Ocean showing the influence of local secondary sources, such as soils and snow (C_{Soil} and C_{Snow}), and the long range atmospheric transport (LRAT), to gas-phase (C_{Gas}) and aerosol phase (C_{Aero}) HCB and HCHs. Main input fluxes to the surface waters are the diffusive air-water exchange (F_{AW}) and to lower extent dry deposition (F_{DD}). Ultimate sinks are the transportation through the water column by settling particles (F_{Sink} , Biological Pump) and the microbial and hydrolysis degradation (F_{Deg}). C_{Dis} is the dissolved phase concentrations, C_{Part} is the particulate phase concentration and C_{Phyto} is the Phytoplankton concentration.

Chapter 6: HCHs and HCB in the Antarctic and Southern Ocean Atmosphere

References

- Breivik, K., Alcock, R., Li, Y. F., Bailey, R. E., Fiedler, H., Pacyna, J. M. 2004. Primary sources of selected POPs: Regional and global scale emission inventories. *Environ. Pollut.* 128(1-2), 3-16. DOI: 10.1016/j.envpol.2003.08.031
- Baek, S.-Y., Choi, S.-D., Chang, Y.-S. 2011. Three-year atmospheric monitoring of organochlorine pesticides and polychlorinated biphenyls in Polar Regions and the South Pacific. *Environ. Sci. Technol.* 45(10), 4475-4482.
- Barber, J. L., Sweetman, A. J., Van Wijk, D., and Jones, K. C. 2005. Hexachlorobenzene in the global environment: Emissions, levels, distribution, trends and processes. *Sci. Total Environ.* 349(1-3), 1-44.
- Bengtson Nash, S., Rintoul, S. R., Kawaguchi, S., Staniland, I., Hoff, J. V. D., Tierney, M., Bossi, R. 2010. Perfluorinated compounds in the Antarctic region: Ocean circulation provides prolonged protection from distant sources. *Environ. Pollut.* 158(9), 2985-2991.
- Bengtson-Nash, S. 2011. Persistent organic pollutants in Antarctica: Current and future research priorities. *J. Environ. Monitor.* 13(3), 497-504.
- Berrojálbiz, N., Dachs, J., Del Vento, S., Ojeda, M.J., Valle, M.C., Castro-Jiménez, J., Mariani, G., Wollgast, J., Hanke, G. 2011. Persistent organic pollutants in Mediterranean seawater and processes affecting their accumulation in plankton. *Environ. Sci. Technol.* 45 (10), 4315-4322.
- Bidleman, T. F., Walla, M. D., Roura, R., Carr, E., Schmidt, S. 1990. Organochlorine pesticides in the atmosphere of the Southern Ocean and Antarctica, January-March. *Mar. Pollut. Bull.* 1993, 26, 258-262 (24).
- Bruhn, R., Lakaschus, S., McLachlan, M. S. 2003. Air/sea gas exchange of PCBs in the southern Baltic Sea. *Atmos. Environ.* 37(24), 3445-3454.
- Cabrerizo, A., Dachs, J., Barceló, D. 2009. Development of a soil fugacity sampler for determination of air-soil partitioning of persistent organic pollutants under field controlled conditions. *Environ. Sci. Technol.* 43 (21) 8257– 8263
- Cabrerizo, A., Dachs, J., Barceló, D., Jones, K. C. 2011. Factors influencing the soil-air partitioning and the strength of soils as a secondary source of polychlorinated biphenyls to the atmosphere. *Environ. Sci. Technol.* 2011, 45 (11) 4785– 4792
- Cabrerizo, A., Dachs, J., Jones, K. C., Barceló, D. 2011b. Soil-air exchange controls on background atmospheric concentrations of organochlorine pesticides. *Atmos. Chem. Phys.* 11, 12799– 12811.

Chapter 6: HCHs and HCB in the Antarctic and Southern Ocean Atmosphere

Cabrerizo, A., Dachs, J., Barceló, D., Jones, K. C. 2012. Influence of organic matter content and human activities on the occurrence of organic pollutants in Antarctic soils, lichens, grass and mosses. *Environ. Sci. Technol.*, 46(9), 1396-1405. DOI: 10.1021/es203425b

Cabrerizo, A., Dachs, J., Barceló, D., Jones, K. C. 2013. Climatic and biogeochemical controls on the remobilization and reservoirs of persistent organic pollutants in Antarctica. *Environ. Sci. Technol.*, 47(9), 4299-4306. DOI: 10.1021/es400471c

Cincinelli, A., Martellini, T., Del Bubba, M., Lepri, L., Corsolini, S., Borghesi, N., King, M.D., Dickhut, R. M. 2009. Organochlorine pesticide air-water exchange and bioconcentration in krill in the Ross sea. *Environ. Pollut.* 157(7), 2153-2158.

Dachs, J., Lohmann, R., Ockenden, W. A., Méjanelle, L., Eisenreich, S. J., Jones, K. C. 2002. Oceanic biogeochemical controls on global dynamics of persistent organic pollutants. *Environ. Sci. Technol.* 36(20), 4229-4237.

Del Vento, S., Halsall, C., Gioia, R., Jones, K., Dachs, J. 2012. Volatile per- and polyfluoroalkyl compounds in the remote atmosphere of the western Antarctic Peninsula: an indirect source of perfluoroalkyl acids to Antarctic waters? *Atmos. Pollut. Res.* 3, 450-455, DOI: 10.5094/APR.2012.051.

Dickhut, R. M., Cincinelli, A., Cochran, M., Ducklow, H. W. 2005. Atmospheric concentrations and air-water flux of organochlorine pesticides along the western Antarctic Peninsula. *Environ. Sci. Technol.* 39(2), 465-470.

Draxler, R.R. and Rolph, G.D., 2011. HYSPLIT (HYbrid Single-Particle Lagrangian Integrated Trajectory) Model access via NOAA ARL READY Website (<http://ready.arl.noaa.gov/HYSPLIT.php>). NOAA Air Resources Laboratory, Silver Spring.

Galbán-Malagón, C., Berrojalbiz, N., Ojeda, M. J., Dachs, J. 2012. The oceanic biological pump modulates the atmospheric transport of persistent organic pollutants to the Arctic. *Nature Commun.* 3, 862, DOI: 10.1038/ncomms1858.

Galbán-Malagón, C. J., Del Vento, S., Berrojalbiz, N., Ojeda, M.J., Dachs, J. 2013a. Polychlorinated Biphenyls, Hexachlorocyclohexanes and Hexachlorobenzene in Seawater and Phytoplankton from the Southern Ocean (Weddell, South Scotia, and Bellingshausen Seas). *Environ. Sci. Technol.* DOI: 10.1021/es400030q

Galbán-Malagón, C.J. Berrojalbiz, N., Gioia, R., Dachs, J. 2013b. The “degradative” and “biological” pump control on the atmospheric deposition and sequestration of hexachlorocyclohexanes and hexachlorobenzene in the North Atlantic and Arctic Oceans. *Environ. Sci. Technol.*

Chapter 6: HCHs and HCB in the Antarctic and Southern Ocean Atmosphere

Grönlund, A., D. Nilsson, I.K. Koponen, A. Virkkula, M.E. Hansson. 2002. Aerosol dry deposition measured with eddy-covariance technique at Wasa and Aboa, Dronning Maud Land, Antarctica. *Annals Glaciol.* 35, 355-361.

Halsall C.J. 2004. Investigating the occurrence of persistent organic pollutants (POPs) in the Arctic: their atmospheric behaviour and interaction with the seasonal snow pack. *Environ. Pollut.* 128, 163–75.

Harner, T., Jantunen, L. M. M., Bidleman, T. F., Barrie, L. A., Kylin, H., Strachan, W. M. J., Macdonald, R. W. 2000. Microbial degradation is a key elimination pathway of hexachlorocyclohexanes from the arctic ocean. *Geophys. Res. Lett.* 27(8), 1155-115.

Harner, T., Kylin, H., Bidleman, T. F., Strachan, W. M. J. 1999. Removal of α -hexachlorocyclohexane and enantiomers of γ -Hexachlorocyclohexane in the eastern Arctic Ocean. *Environ. Sci. Technol.* 33(8), 1157-1164.

Helm, P. A., Diamond, M. L., Semkin, R., Strachan, W. M. J., Teixeira, C., Gregor, D. 2002. A mass balance model describing multiyear fate of organochlorine compounds in a high arctic lake. *Environ. Sci. Technol.* 36(5), 996-1003.

Iwata, H., Tanabe, S., Sakai, N., & Tatsukawa, R. (1993). Distribution of persistent organochlorines in the oceanic air and surface seawater and the role of ocean on their global transport and fate. *Environ. Sci. Technol.* 27(6), 1080-1098.

Jantunen, L.M., Kylin, H., Bidleman, T.F. 2004. Air–water gas exchange of α -hexachlorocyclohexane enantiomers in the South Atlantic Ocean and Antarctica. *Deep-Sea Res. Pt. II.* 51(22-24), 2661-2672, DOI: 10.1016/j.dsr2.2004.02.002.

Kallenborn, R., Oehme, M., Wynn-Williams, D. D., Schlabach, M., Harris, J. 1998. Ambient air levels and atmospheric long-range transport of persistent organochlorines to Signy island, Antarctica. *Sci. Total. Environ.* 220(2-3), 167-180.

Kang, J-H., Son, M-H., Hur S.D., Hong, S., Motoyama, H., Fukui, K. and Chang, Y-S. 2012. Deposition of organochlorine pesticides into the surface snow of East Antarctica. *Sci. Total Environ.* Vol 433,290-295, DOI: 10.1016/j.scitotenv.2012.06.037.

Larsson, P., Järnmark, C. and Södergren, A. 1992. PCBs and chlorinated pesticides in the atmosphere and aquatic organisms of Ross Island, Antarctica. *Mar. Pollut. Bull.* 25(9–12), 281-287, DOI: 10.1016/0025-326X(92)90683-W.

Li, N., Wania, F., Lei, Y.D., Daly, G.L., 2003. A comprehensive and critical compilation, evaluation and selection of physical-chemical property data for selected polychlorinated biphenyls. *J. Phys. Chem. Ref. Data.*

Chapter 6: HCHs and HCB in the Antarctic and Southern Ocean Atmosphere

Li, Y.F., Macdonald, R.W., Ma, J., Hung, H., and Venkatesh, S. 2004. α -HCH budget in the arctic ocean: the arctic mass balance box model (AMBBM). *Sci. Total Environ.* 324, pp. 115–139

Lohmann, R., Gioia, R., Jones, K. C., Nizzetto, L., Temme, C., Xie, Z., Schulz-Bull, D., Hand, I., Morgan, E., Jantunen, L. 2009. Organochlorine pesticides and PAHs in the surface water and atmosphere of the north atlantic and arctic ocean. *Environ. Sci. Technol.* 43(15), 5633-5639.

Ma, J., Hung, H., Tian, C., Kallenborn, R. 2011. Revolatilization of persistent organic pollutants in the arctic induced by climate change. *Nature Climate Change*, 1(5), 255-260.

Macdonald, R.W., Barrie, L.A., Bidleman, T.F., Diamond M.L., Gregor, D.J., Semkin, R.G., Strachan, W.M.J, Li, Y.-F., Wania, F., Alae, M., Alexeeva, L.B., Backus, S.M., Bailey, R., Bewers, J.M., Gobeil, C., Halsall, C.J., Harner, T., Hoff, J.T., Jantunen, L.M.M., Lockhart, W.L., Mackay, D., Muir, D.C.G., Pudykiewicz, J., Reimer, K.J., Smith, J.N., Stern, G.A., Schroeder, W.H., Wagemann, R., Yunker, M.B. 2005. Contaminants in the canadian Arctic: 5 years of progress in understanding sources, occurrence and pathways. *Sci. Total. Environ.* 254 (2-3), 93-234. DOI 10.1016/S0048-9697(00)00434-4

Mackay, D. 1979 Finding fugacity feasible. *Environ. Sci. Technol.* 13 (10), 1218-1223.

Montone, R.C., Taniguchi, S., Boian, C., Weber, R.R. 2005. PCBs and chlorinated pesticides (DDTs, HCHs and HCB) in the atmosphere of the southwest Atlantic and Antarctic oceans. *Mar. Pollut. Bull.* 50 (7), 778-782, DOI: 10.1016/j.marpolbul.2005.03.002.

Ortega-Retuerta, E., Reche, I., Pulido-Villena, E., Agustí, S., Duarte, C. M.. 2008. Exploring the relationship between active bacterioplankton and phytoplankton in the Southern Ocean. *Aquatic Microbial Ecology.* 52(1), 99-106

Pučko, M., Stern, G.A., Macdonald, R.W., Barber, D.G., Rosenberg, B., Walkusz, W. 2011 When will α -HCH disappear from the western Arctic Ocean? *J. Mar. Syst.* DOI: 10.1016/j.jmarsys.2011.09.007

Pučko, Monika, Walkusz, W., Macdonald, R. W., Barber, D. G., Fuchs, C., & Stern, G. A. (2013). Importance of Arctic Zooplankton Seasonal Migrations for α -Hexachlorocyclohexane Bioaccumulation Dynamics. *Environ. Sci. Technol.* 47(9), 4155-4163. DOI: 10.1021/es304472d

Rintoul, S.R., 2000. Southern ocean currents and climate. *Papers P. R. Soc. Tasmania.* 133, 41-50.

Chapter 6: HCHs and HCB in the Antarctic and Southern Ocean Atmosphere

Su, Y., Hung, H., Blanchard, P., Patton, G. W., Kallenborn, R., Konoplev, A., Fellin, P., Li, H., Stern, G., Rosenberg, B., Barrie, L. A. 2006. Spatial and seasonal variations of hexachlorocyclohexanes (HCHs) and hexachlorobenzene (HCB) in the Arctic atmosphere. *Environ. Sci. Technol.* 40(21), 6601-6607.

Schmidtko, S., G. C. Johnson and J. M. Lyman, 2013. MIMOC: A Global Monthly Isopycnal Upper-Ocean Climatology with Mixed Layers. *J. Geophys. Res.* **118**. DOI: 10.1002/jgrc.20122.

Tanabe, S., Hidaka, H., Tatsukawa, R. 1983. PCBS and chlorinated hydrocarbon pesticides in antarctic atmosphere and hydrosphere. *Chemosphere.* 12(2), 277-288.

UNEP. 2001. Final act of the plenipotentiaries on the Stockholm Convention on persistent organic pollutants, United Nations Environment Program Chemicals. www.pop.int.

Wania F, Mackay D. 1995. A global distribution model for persistent organic chemicals. *Sci Total Environ.* 160-161, 211-232.

Wania F, Mackay D. 1999 The evolution of mass balance models of persistent organic pollutant fate in the environment. *Environ. Pollut.* 100(1-3), 223-240.

Weller, R., Minikin, A., Petzold, A., Wagenbach, D., König-Langlo, G. 2012. Characterization of long-term and seasonal variations of black carbon (BC) concentrations at Neumayer, Antarctica. *Atmos. Chem. Phys. Discuss.*, 12(9), 25355-25387. DOI: 10.5194/acpd-12-25355-2012

Wong, F., Jantunen, L. M., Pućko, M., Papakyriakou, T., Staebler, R. M., Stern, G. A., Bidleman, T.F.. 2011. Air-water exchange of anthropogenic and natural organohalogens on international polar year (IPY) expeditions in the canadian arctic. *Environ. Sci. Technol.* 45(3), 876-881.

Xie, Z., Koch, B.P., Möller, A., Sturm, R., Ebinghaus, R. 2011. Transport and fate of Hexachlorocyclohexanes in the oceanic air and surface seawater. *Biogeoscience.* 2621-2633.

Zhang L, Bidleman T, Perry MJ, Lohmann R. 2012. Fate of chiral and achiral organochlorine pesticides in the north Atlantic bloom experiment. *Environ. Sci. Technol* 46(15):8106-14.

Chapter 7

Factors affecting the atmospheric occurrence and deposition of Polychlorinated Biphenyls in the Southern Ocean



The results from this chapter were accepted for publication in *Atmospheric Chemistry and Physics Discussions*.

Chapter 7: PCBs in the Antarctic and Southern Ocean Atmosphere

Abstract

Persistent organic pollutants, such as polychlorinated biphenyls, reach the Southern Ocean atmosphere through long-range atmospheric transport. In this study we report the largest data set available for the atmospheric occurrence of PCBs in the Southern Ocean surrounding the Antarctic Peninsula from samples obtained during three cruises in 2005, 2008 and 2009. The gas phase concentrations of total PCBs ($\Sigma_{25}\text{PCBs}$) ranged from 1 to 70 pg m^{-3} , while the aerosol phase concentrations were significantly lower (0.04 to 0.4 pg m^{-3}). The aerosol phase is enriched in the more hydrophobic congeners consistent with the model predictions of gas-particle partitioning. There is a net air to water diffusive flux of PCBs to the Southern Ocean, up to 50 times higher than the dry deposition flux of aerosol-bound PCBs. The air-water disequilibrium is higher for the more hydrophobic congeners consistent with the role of the biological pump removing PCBs from the water column by settling of PCBs bound to organic matter. The atmospheric half-lives of PCB 52 and 180 are of 3.8 and 1 days, respectively, as predicted from the measured atmospheric concentration and depositional fluxes. The volatilization of PCBs from Antarctic soils during the Austral summer drives higher gas phase concentrations in the atmosphere over Antarctica during the warmer periods. This temperature dependence is not observed for PCBs over the adjacent Southern Ocean, probably due to the importance of long-range atmospheric transport and atmospheric deposition modulating the atmospheric occurrence of PCBs.

Chapter 7: PCBs in the Antarctic and Southern Ocean Atmosphere

1. Introduction

Polychlorinated biphenyls (PCBs) are distributed in the global atmosphere (Gioia et al. 2008, Gioia et al. 2012, Bogdal et al., 2012) due to their persistence, semivolatility, and potential for long-range atmospheric transport. In addition, their low degradability, toxicity, and ability to bioaccumulate/biomagnify along food chains raise concern on their impact on ecosystem health (Jones and De Voogt, 1999). Its introduction into the environment is the result of their use for decades, mainly in the Northern Hemisphere (Breivik et al. 2004). The Stockholm Convention on Persistent Organic Pollutants (POPs) approved in 2001 bans the use, production and export of several families of POPs, including PCBs (chm.pop.int).

PCBs are considered as a surrogate of the behaviour of hydrophobic organic contaminants because PCBs comprise congeners with a wide range of physical chemical properties. The fate, transport and sinks of PCBs in different global regions and environments have received considerable attention during the last decades (see for example Lohmann et al. 2007). The occurrence of PCBs have also been reported in remote regions such as Antarctica and the Southern Ocean atmosphere (Tanabe et al., 1983, Iwata et al., 1996, Kallenborn et al., 1998, Fuoco et al., 1996, Montone et al., 2003 and 2005, Gambaro et al., 2005), seawater (Tanabe et al., 1983, Galbán-Malagón et al. 2013), soils (Cabrerizo et al. 2012, Kang et al., 2012) and biota (Larsson et al., 1992, Bengtson-Nash et al., 2008, Galbán-Malagón et al., 2013a, Cabrerizo et al., 2012,). The atmospheric long-range transport of PCBs occurs through successive steps of volatilization and deposition (hops) and PCBs can reach eventually Polar Regions like the Arctic and Antarctica (Wania and Mackay 1996, Jurado and Dachs, 2008). This process is known as “grasshopping” and POPs with physical-chemical properties like those of PCBs are known as hoppers (Wania and Mackay, 1996, Lohmann et al. 2007). Therefore, the quantification of atmospheric deposition and volatilization processes is important to understand and predict the long-range atmospheric transport of POPs and their impact to remote regions.

Chapter 7: PCBs in the Antarctic and Southern Ocean Atmosphere

The low temperatures in Polar Regions favours partitioning of organic pollutants to soils, vegetation and seawater through “cold trapping” (Wania and Mackay 1996). However, this process is not irreversible, and re-volatilization as the consequence of declining levels in the atmosphere due to lower primary emissions, or climate change, can occur in Polar Regions (Ma et al. 2011, Cabrerizo et al. 2013). In addition, the Southern Ocean is characterized by high primary productivity and biomass during the Austral summer (Tréguer and Jacques 1998, Boyd 1992), driving high settling fluxes of organic matter and organic matter-bound hydrophobic pollutants to deep waters, and enhancing the atmospheric deposition of POPs such as PCBs by a process known as biological pump (Dachs et al. 2002, Jurado and Dachs, 2008). The influence of the biological pump on air-water diffusive fluxes of PCBs has been assessed in lakes (Dachs et al. 1999, 2000, Meijer et al. 2009, Nizzetto et al. 2012), the Mediterranean Sea (Berrojalbiz et al. 2011), and the Arctic Ocean (Galbán-Malagón et al. 2012). A recent companion study has shown that the biological pump can also affect the levels of PCBs in the Southern Ocean water column (Galbán-Malagón et al. 2013), but its influence on the PCB occurrence in the Southern Ocean atmosphere is still limited to estimates from environmental models (Dachs et al. 2002, Jurado and Dachs, 2008).

Previous reports on PCBs concentrations in the Antarctic and the Southern Ocean atmosphere are scarce compared to the Arctic and its surrounding oceans (Bengtson-Nash et al., 2011). These studies pointed out that the atmospheric concentrations in Antarctica are influenced by meteorological conditions, like temperature (Ockenden et al., 2001) and by the synoptic atmospheric circulation in the Antarctic region (Montone et al., 2003). Also, the direct transport of PCBs from South America was evidenced by temporal series at Signy Island (Kallenborn et al., 1998). However, the previous studies on the atmospheric occurrence of PCBs in Antarctica covered small geographic areas and most were restricted to sites near Antarctic scientific bases (Larsson et al., 1992, Kallenborn et al., 1998, Ockenden et al., 2001, Gambaro et al., 2005, Baek et al., 2011, Li et al., 2012 and Cabrerizo et al., 2013). In the present study, we report the atmospheric gas and aerosol phase PCBs occurrence from samples taken during

Chapter 7: PCBs in the Antarctic and Southern Ocean Atmosphere

three Antarctic cruises (2005, 2008 and 2009) covering a large region including the Bransfield Strait, the Weddell, Bellingshausen and South Scotia Seas. In addition, a terrestrial campaign was carried out, simultaneously to the 2009 cruise, at Livingston Island in which PCBs were measured in the gas and aerosol phase over land. Therefore, the objectives are i) to report the largest data set available of PCB concentrations in the Southern Ocean atmosphere, and ii) assess the different factors driving the occurrence of PCBs, such as long-range atmospheric transport, volatilization from Antarctic snow and soils, and atmospheric deposition to seawater.

2. Materials and Methods

2.1 Sampling

The atmospheric samples (gas and aerosol phase) were collected on board the *R/V Hespérides* during three Antarctic surveys around the Antarctic Peninsula (ICEPOS, February 2005 and ATOS II, January-February 2009), and in the South Scotia Sea (ESSASI, January 2008). In addition, a terrestrial sampling campaign was carried out in January-February 2009 at Livingston Island (Southern Shetlands, Antarctica) where atmospheric samples (gas and aerosol phase) were collected at two sites. The air samples were collected using a high-volume air sampler (MCV: CAV-A/HF, Collbató, Spain). The sampling sites were Polish Beach (13 m of altitude), a bare soil area located near the coast, and Pico Radio Hill (131 m of altitude) with soil covered by lichens. Atmospheric conditions during the sampling periods were obtained from the meteorological stations deployed on board the ship and at Livingston Island. Details of sampling events, locations and ancillary data for each sample are given in Figures S1 and S2, and Table S1 in Appendix E.1. The sampling methodology has been described previously (Galbán-Malagón et al., 2012, Cabrerizo et al., 2013). For the sampling of oceanic air, the high-volume sampler was deployed over the vessel bridge connected to a wind direction sensor in order to avoid contamination from the ship. Sampling flow rate was set at $40 \text{ m}^3 \text{ h}^{-1}$ and the sampling volumes averaged 600 m^3 , 1000 m^3 and 1400 m^3 for the gas phase samples of the ICEPOS, ESSASI

Chapter 7: PCBs in the Antarctic and Southern Ocean Atmosphere

and ATOS II cruises, respectively, and 800 m³ for the samples taken at Livingston Island. During the ATOS II cruise, a second high-volume air sampler was operated in parallel for the sampling of aerosol phase only, with longer sampling periods, so higher volumes of air were sampled (around 1800 m³). The gas phase was collected on a polyurethane foam (PUF) plugs (100 mm diameter x 100 mm, Klaus Ziemer GmbH, Germany) and the aerosol phase was filtered on a quartz microfiber filters (203x254 mm, QMA, Whatman, England).

Previous to the sampling campaigns, PUFs were cleaned in the laboratory by soxhlet extraction with acetone:hexane (3:1), dried under vacuum, packed in aluminium foil envelopes and introduced into two zip-sealed bags until sampling. The QMA filters were placed inside aluminium foil envelopes and were combusted for 6 hours at 450°C. After combustion, filters were kept inside two zip-sealed bags until sampling. After sampling, the PUFs and QMA filters were packed similarly and kept at 4°C and -20°C, respectively, until their analysis in the laboratory.

2.2 Chemical Analysis

Briefly, all gas phase samples collected on PUFs were Soxhlet extracted for 24 h using acetone:hexane (3:1 v/v), while QMA filters were extracted using methanol:dichloromethane (1:2 v/v). Prior to extraction, samples were spiked with PCB 65 and PCB 200 (Dr Ehrenstorfer, GmbH, Germany), which were used as recovery standards. Extracts were reduced in a rotary evaporation unit (R-200, Büchi, Italy) until 0.5 ml, and fractionated on a 3% deactivated alumina column (3 g) with 1 g of anhydrous sodium sulphate on top. The first fraction containing PCBs was collected using 12 mL of hexane, a second fraction containing other compounds was collected using 15 mL of hexane: dichloromethane (1:2 v/v). All fractions were concentrated until 1 mL by rotary evaporation and solvent exchange to isooctane under a purified N₂ stream until a final volume of 150 µL. Identification and quantification was done using the retention time of individual PCB congeners. The details of the methodology used for analyzing the samples taken at Livingston Island has been described elsewhere (Cabrerizo et al. 2013).

Chapter 7: PCBs in the Antarctic and Southern Ocean Atmosphere

PCBs were analyzed by a gas chromatograph coupled to a μ -ECD detector (Agilent Technologies, model 7890), provided with a HP-5MS 60m capillary column (inner diameter 0.325 μm , film thickness 0.25 μm). The instrument was operated in splitless mode (close for 1.5 min). The oven programmed temperature started from 90 $^{\circ}\text{C}$ (hold for 1 min) to 190 $^{\circ}\text{C}$ at 20 $^{\circ}\text{C min}^{-1}$, and then to 310 $^{\circ}\text{C}$ (3 $^{\circ}\text{C min}^{-1}$) (holding time 18 min). Injector and detector temperatures were 280 and 320 $^{\circ}\text{C}$, respectively. Helium and nitrogen were used as carrier (1.5 mL min^{-1}) and makeup (60 mL min^{-1}) gases respectively. Prior to injection, 5 ng of PCB 30 and PCB 142 were added as internal standards to all samples. The analysed congeners were PCB 18, 17, 31, 28, 33, 52, 49, 99+101, 110, 151, 149, 118, 153, 132+105, 138, 158, 187, 183, 128, 177, 171, 156 and 180. Organic and elemental carbon in the aerosol phase was determined using the thermal-optical transmittance in a Sunset Laboratory Carbon Analyzer using the NIOSH temperature protocol (Birch et al. 1996).

2.3 Quality Control and Quality assurance

One blank was collected every five field samples and followed the same extraction process than samples. During quantification, the chromatographic blank signal was subtracted from the sample's signal. Blank levels were always below 5% of sample values. The range of recoveries for PCBs 65 and 200 for the gas phase samples were 51-75% and 51-81 for the ICEPOS cruise, 53-78% and 57-87% for the ESSASI cruise, and 67-76% and 51-81% for the ATOS II cruise. The recoveries for samples taken at Livingston Island were 53-76% and 58-101% for PCB 65 and 200, respectively. The recoveries for the aerosol phase samples were in the range 52-78% and 69-115% for PCB 65 and 200, respectively (Table S2 in Appendix E.2). Instrumental detection limits (IDLs) were calculated using the less concentrated quantifiable standard divided by the averaged volume of samples. IDLs ranged from 0.001 to 0.023 pg m^{-3} . Limits of detection and quantification (LODs and LOQs) were from 0.006 to 0.85, and from 0.019 to 2.83 pg on column. More information about the IDLs, LOQs and LODs is given on Table S3 in Appendix E.2.

Chapter 7: PCBs in the Antarctic and Southern Ocean Atmosphere

2.4 Atmospheric back trajectories

The air mass back trajectories were retrieved from the NOAA HYSPLIT model to study the source region of the atmospheric samples (Draxler and Rolph, 2011). Three 24 hours back trajectories were calculated for each sample corresponding to the initial, middle and final sampling time. Back trajectories were estimated for each sampling period at 25 m height, an example of the dominant source back trajectories is given in Figure S3 in Appendix E.3.

3. Results and Discussion

3.1 Occurrence of PCBs in the Southern Ocean Atmosphere

Concentrations of Σ_{25} PCBs in the gas and aerosol phase are depicted in Figure 1A and B, respectively. Figure 2A and B shows the average profiles of PCB congeners in the aerosol and gas phase samples, respectively, and the congener specific concentrations for each sampling event are given in Tables S4-S9 in Appendix E.4. Gas phase concentrations of Σ_{25} PCBs ranged from 7.1 to 45.2 pg m^{-3} , 6.2 to 78.9 pg m^{-3} , and 5.2 to 39.9 pg m^{-3} for the ICEPOS, ESSASSI and ATOS II cruises, respectively. The gas phase concentrations at Livingston Island ranged from 2.1 to 3.1 pg m^{-3} , and from 4 to 29 pg m^{-3} at Polish Beach and Pico Radio Hill, respectively. The contribution of the seven ICES congeners to the Σ_{25} PCBs concentrations averaged 52%, 51.7% and 50.5% and 45.7% for the ICEPOS, ESSASSI, ATOS II and Livingston Island samples, respectively. A *Kruskall-Wallis test* revealed that the median values of the samples were different among the different cruises ($p < 0.01$). A *post hoc Dunn's test* showed that Σ_{25} PCBs at Polish Beach were significantly lower ($p < 0.05$) than the concentrations measured in the South Scotia Sea atmosphere, but not significantly different than the concentrations in the other campaigns (Figure S4 in Appendix E.4). These gas phase PCBs concentrations are lower than those reported in the early 1980s (180 pg m^{-3}) for the Southern Indian and Pacific Oceans (Tanabe et al., 1983), but comparable to those reported in other regions of the Southern Ocean (Larsson et al., 1992, Iwata et al., 1993, Kallenborn et al., 1998, Montone et al., 2005 and 2003, Gambaro et al., 2005, Baek et al., 2011 and Li et al., 2012).

Chapter 7: PCBs in the Antarctic and Southern Ocean Atmosphere

However, the number of congeners is not the same for the different studies, and since we report the concentrations for a higher number of congeners (see Table 1), atmospheric PCBs concentrations may have decreased during recent decades.

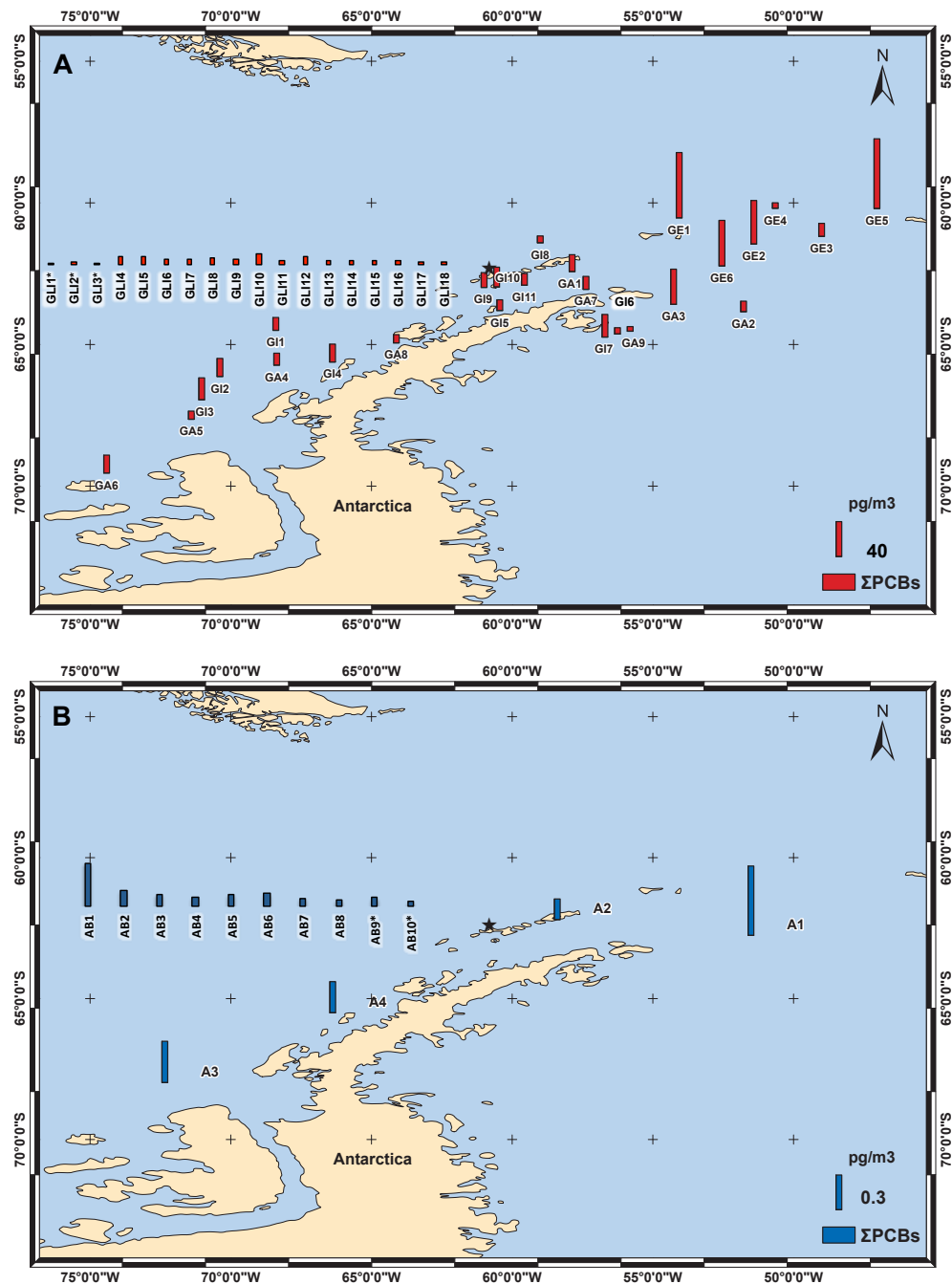


Figure 1. Atmospheric occurrence of PCBs. Spatial distribution of gas (A) and aerosol (B) phase concentrations of polychlorinated biphenyls ($\Sigma_{25}\text{PCBs}$, pg m^{-3}) around the Antarctic Peninsula in 2005 (ICEPOS), 2008 (ESSASI) and 2009 (ATOS II cruise and Livingston Island samples). G11-G111 are samples taken during the ICEPOS cruise (2005), GE1-GE6 are samples taken during the ESSASI cruise (2008), GA1-GA9 are samples taken during the ATOS II cruise, and GL11-GL18 are samples in Livingston Island (* indicate the samples taken at Polish Beach). A1-A4 are aerosol phase samples taken during ATOS II cruise and AB1-AB10 are samples taken at Livingston Island (* indicate aerosol phase samples taken at Polish Beach).

Chapter 7: PCBs in the Antarctic and Southern Ocean Atmosphere

Table 1. Comparison of the gas phase PCBs concentrations (pg m^{-3}) reported in the literature for the Antarctic atmosphere with those reported in this study.

Location	Year	Mean	SD	Σ PCBs	Reference
Sabrina Coast	1981	180			Tanabe et al., 1983 ^a
Balleny Islands	1981	64			Tanabe et al., 1983 ^a
Syowa Station	1982	81			Tanabe et al., 1983 ^a
Amundsen Bay	1982	96			Tanabe et al., 1983 ^a
Cape Evans (Ross Island)	1989	32.33	34.02		Larsson et al., 1992 ^b
	1990	6.00			Larsson et al., 1992 ^b
Southern Ocean (Daisan-Nisin Maru Cruise)	1990	28.00			Iwata et al., 1993 ^c
Signy Island	1995	67.28	41.28		Kallenborn et al., 1998 ^d
King George Island	1996	35.33	27.01		Montone et al., 2003 ^e
Transect Brazil-Antarctica	1995	62.43	8.89		Montone et al., 2005 ^e
Halley Land Base	1998	2.78			Oeckenden et al., 2001 ^f
Weddell Sea	1998	42.66			Oeckenden et al., 2001 ^f
Terra Nova Bay	2004	1.58			Gambaro et al., 2005 ^g
King George Island	2005	18.70	10.59		Baek et al., 2011 ^h
	2006	20.83	10.07		Baek et al., 2011 ^h
King George Island (Great Wall Station)	2009-2010	4.45	2.36		Li et al., 2012 ⁱ
Livingston Island (Radio Hill and Sofia Mt)	2009	9.15	3.61		Cabrero et al., 2013 ^j
Bellingshausen Weddell	2005	25.82	13.16		This Study
Bransfield	2005	16.93	16.43		This Study
South Scotia Sea	2005	20.97	3.73		This Study
Bellingshausen	2008	45.84	29.91		This Study
Bransfield	2009	20.89	16.59		This Study
Weddell	2009	13.38	7.61		This Study
	2009	13.49	5.06		This Study

a: Sum of unspecified PCBs congeners

b: Sum of PCBs 95, 101, 110, 149, 153 and 138

c: Sum of PCBs 8, 15, 16, 17, 18, 20, 28, 31, 32, 33, 34, 37, 41, 42, 44, 49, 51, 52, 53, 58, 60, 66, 69, 70, 74, 87, 91, 95, 101, 118, 128, 138, 144 and 149

d: Sum of PCBs 18, 28, 31, 47, 52, 66, 74, 99, 101, 105, 114, 118, 128, 138, 149, 153, 156, 167, 170, 180, 187 and 189

e: Sum of PCBs 18, 52, 44, 101, 118, 153, 138, 187, 128 and 180

f: Sum of PCBs 28, 52, 101, 153, 132, 138 and 180

g: Sum of PCBs 1, 2, 3, 4+10, 9+7, 6, 8, 5, 12, 15, 19, 18, 17, 24+27, 16+32, 29, 26, 25, 28+31, 33+20, 22, 46+69, 62, 49, 47+48, 44+59, 42, 71, 67, 63, 74, 70, 66, 56+60, 77, 93+95, 91, 92, 84+90/101, 119, 83, 97, 123+107/109, 118, 136, 151, 135+144, 149, 134, 146, 141, 137, 164, 167, 179, 176, 178, 185, 174, 177, 197 and 194,

h: Sum of all the PCBs except PCB 11

i: Sum of PCBs 28, 52, 77, 81, 101, 105, 114, 123, 126, 128, 138, 153, 156, 157, 167, 169, 180, 189 and 209

j: Sum of PCBs 18, 17, 31, 28, 33, 52, 49, 44, 74, 70, 95, 99+101, 87, 118, 110, 151, 149, 153, 132+105, 138, 158, 128, 169, 187, 183, 177, 171+156, 180, 191, 170, 201/199, 195, 194, 205, 206, 208 and 209

Chapter 7: PCBs in the Antarctic and Southern Ocean Atmosphere

Only four and ten of the aerosol phase samples taken during the ATOS II cruise and at Livingston Island, respectively, had levels of PCBs above LOQ (see Figure 1B, and Table S8 in Appendix E.4). Aerosol phase concentration ranges for Σ_{25} PCBs were 0.2 to 0.7 pg m^{-3} during the ATOS II cruise, and 0.06 to 0.4 pg m^{-3} and 0.04 to 0.07 pg m^{-3} at Pico Radio Hill and Polish Beach in sites from Livingston Island, respectively. There were no significant differences among the aerosol phase Σ_{25} PCBs concentrations over the southern Ocean and those in the Livingston Island atmosphere (*Kruskall-Wallis test*). Aerosol phase concentrations accounted for 1 to 4% of the total atmospheric (gas+aerosol) burden. This is the first time that PCBs concentrations in the aerosol phase are reported for Antarctica and the Southern Ocean. These concentrations are significantly lower (*Kruskal-Wallis, $p < 0.05$*) than the aerosol phase PCB concentrations reported for other oceanic regions like the North Atlantic and Arctic Ocean (Galbán-Malagón et al., 2012). The pattern of PCB congeners in the aerosol phase has a higher contribution of the more chlorinated congeners in comparison to the gas phase (Figure 2).

Chapter 7: PCBs in the Antarctic and Southern Ocean Atmosphere

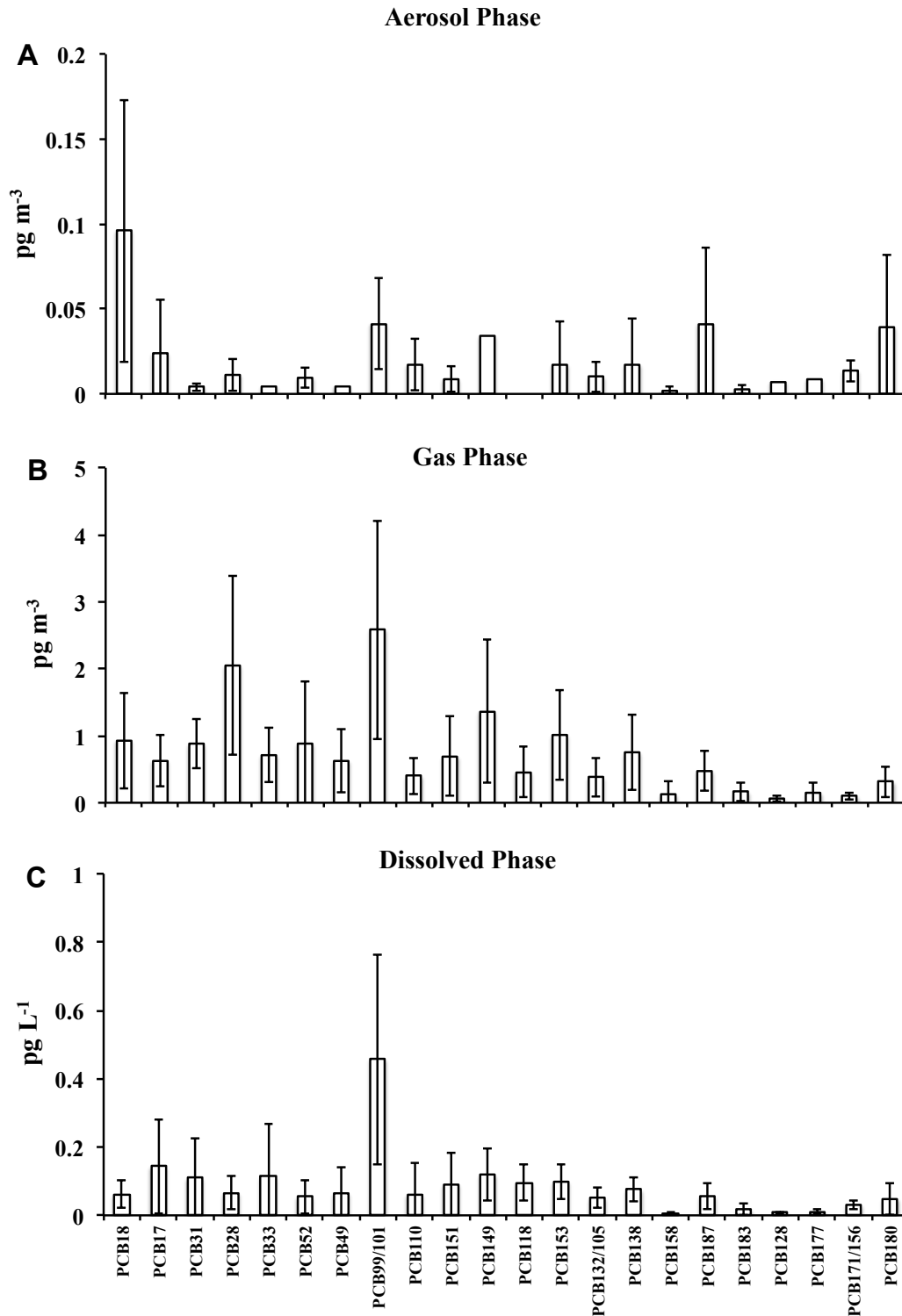


Figure 2. Congener specific occurrence of PCBs. Average profiles of PCB congeners in the aerosol (A, pg m^{-3}), gas (B, pg m^{-3}) and dissolved phase (C, pg L^{-1}) in the Southern Ocean. Dissolved phase concentrations are taken from Galbán-Malagón et al., 2013a

Chapter 7: PCBs in the Antarctic and Southern Ocean Atmosphere

3.2 Gas-particle partitioning of PCBs

The understanding and quantification of gas-particle partitioning is important to predict and assess the atmospheric deposition, atmospheric degradation/transformation processes, and the long-range atmospheric transport of PCBs in the environment (Bidleman 1988, Scheringer, 1997). Since this is the first report of aerosol phase concentrations in the Southern Ocean atmosphere, it is useful to evaluate the gas-particle partitioning of PCBs in this remote atmosphere in order to compare it with model predictions. A common approach to predict the aerosol-gas partition coefficients is (Finizio et al. 1998),

$$K_p = \frac{C_A}{C_G TSP} = 1.8 \times 10^{-12} f_{OC} \left(\frac{\gamma_{Oct} MW_{OCT}}{\gamma_{OM} MW_{OM}} \right) K_{OA} \quad (7.1)$$

Where C_A and C_G are the aerosol and gas phase concentrations (pg m^{-3}) of PCB congeners, TSP is the concentration of total suspended particles ($\mu\text{g m}^{-3}$), f_{OC} is the fraction of organic carbon in the aerosol, γ_{Oct} and γ_{OM} are the activity coefficients of PCBs in octanol and the aerosol organic matter, MW_{OCT} (g mol^{-1}) and MW_{OM} (g mol^{-1}) are the molecular weight of octanol and aerosol organic matter, and K_{OA} is the temperature corrected octanol-air partition coefficient.

Measured K_p was calculated using the measured C_A , C_G , and TSP values for the Southern Ocean and Livingston Island atmosphere (Figure 3). These values can be compared with the predicted K_p obtained from the right side term of equation 6.1, assuming that the ratio $\gamma_{Oct} MW_{OCT} / \gamma_{OM} MW_{OM}$ equals the unity (Finizio et al., 1998), an assumption that does not affect the discussion below. f_{OC} was measured in the aerosols taken at Livingston Island and it ranged from below detection limit to $0.31 \mu\text{g m}^{-3}$. The average was $0.28 \mu\text{g m}^{-3}$ for all samples above LOQ. Measured and predicted K_p (see equation 6.1) for each sampling period are shown in Tables S15, S16 and S17 in Appendix E.5.

Measured and predicted K_p were significantly correlated among them in the four sampling periods for which the aerosol phase concentrations over the Southern Ocean are available (Figure 3, upper panels), and for the pairs of aerosol and gas phase concentrations taken at the coastal site of Polish Beach (Figure 3, lower panels) at Livingston Island. Conversely, at Pico Radio Hill, which is a site

Chapter 7: PCBs in the Antarctic and Southern Ocean Atmosphere

further in land, the measured K_P did not correlate with the predicted K_P (figure S10 in Appendix E.5). The slopes of the correlation between measured and predicted K_P was always significantly lower than unity (Figure 3), similar to those reported in continental environments (Mandalakis and Stephanou 2007, Radonić et al., 2011), but lower than the slopes reported for PCBs in urban atmospheres (Harner and Bidleman, 1998). The low slopes observed over the ocean and coastal sites can be due to various factors. First, γ_{OM} can be different for the different PCB congeners inducing a slope lower than unity when measured K_P is regressed against predicted K_P (see equation 6.1). Another possibility is that PCBs in the gas and aerosol phase are not in equilibrium. This lack of equilibrium can be driven by recent entries and losses of PCBs to the atmosphere. At the Polish Beach and Pico Radio Hill sites there was a net volatilization of PCB from soils as reported in a companion work (Cabrerizo et al. 2013). The lack of correlation between predicted and measured K_P at Pico Radio Hill would be due to the fresh inputs of PCBs from soil, which have had no time to equilibrate with the aerosol phase. Conversely, the atmosphere at the coastal is more influenced by the ocean, and while there is a volatilization of PCBs from soils at Polish Beach, over the adjacent seawaters there is a net deposition to close to air-water equilibrium (see below). Indeed, the occurrence of PCBs in the aerosol and gas phase is the result of the interactions of various factors such as volatilization from local secondary sources, long-range atmospheric transport, and deposition.

Chapter 7: PCBs in the Antarctic and Southern Ocean Atmosphere

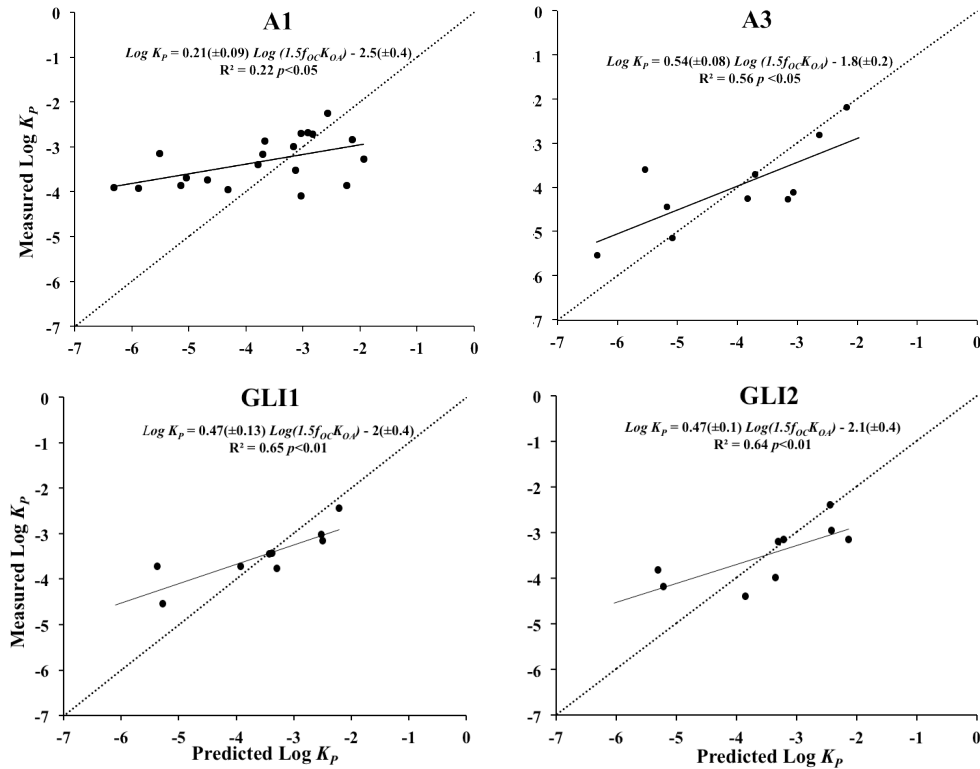


Figure 3. Gas-particle partition of PCBs. Measured versus predicted particle-gas partition coefficients ($\text{Log } K_p$) estimated for samples taken over the Southern Ocean (samples A1 and A3 in upper panels) and at Livingston Island (samples GLI1 and GLI2 in lower panels).

3.3 Air-water diffusive exchange and dry deposition of PCBs

Diffusive air-water exchange is the dominant process for the transfer of PCBs from the atmosphere to seawater (Jurado et al. 2004). The air-water fugacity ratios ($f_w f_A^{-1}$) describes the direction of the net diffusive flux. The PCB fugacity in air (f_A , Pa) and water (f_w , Pa) are given by

$$f_A = \frac{10^{-12} C_G RT_w}{MW} \quad (7.2)$$

$$f_w = \frac{10^{-12} C_{TD} H' RT_w}{MW} \quad (7.3)$$

Where C_{TD} (pg m^{-3}) is the truly dissolved-phase concentration in seawater, which has been obtained by correcting the apparent dissolved phase concentrations measured during the ESSASSI and ATOS II campaigns (Galbán-

Chapter 7: PCBs in the Antarctic and Southern Ocean Atmosphere

Malagón, et al., 2013), using the Dissolved Organic Carbon (DOC) as a surrogate for the colloidal phase as commonly done (Nizzeto et al., 2011, Rowe et al., 2007, Totten et al., 2001 and García-Flor et al., 2009). Values of C_{TD} are given in Figure 2C and Table S11 on Appendix E.4, while the discussion of these concentrations has been given in a companion paper (Galbán-Malagón et al. 2013). H' is the dimensionless Henry's Law Constant corrected for temperature and salinity (Table S10 in Appendix E.5), R is the ideal gas constant ($8.314 \text{ Pa mol}^{-1} \text{ K}^{-1}$), T_w (K) is the water surface temperature, and MW (g mol^{-1}) is the molecular weight of the studied compound. The uncertainties associated to the fugacity ratio are derived from uncertainties on C_G , C_{TD} and H' (Bruhn et al., 2003). Uncertainties associated to measured gas and dissolved phase were estimated to be of 15%. The uncertainty on the Henry's Law Constant is especially relevant (Bruhn et al., 2003): a 30% uncertainty on H' has been assumed in this study (Li et al. 2003). Therefore, the logarithm of $f_w f_A^{-1}$ ranging from -0.11 to 0.5 indicates that the compounds are close to air-water equilibrium, fugacity ratios below -0.11 indicate that the direction of the exchange between air and water is net deposition, and over 0.5 indicates a net volatilization.

The calculated water-air fugacity ratios showed that deposition dominates over volatilization for most compounds and sampling periods (Figure 4A), and thus there was a net absorption of PCBs during the ESSASI (South Scotia Sea) and ATOS II (Weddell, Bransfield and Bellingshausen seas) cruises (Figure 4A, and Table S12 in Appendix E.5). At the seawater adjacent to the coastal Polish Beach site, air and water were close to equilibrium conditions.

The low PCB levels in seawater, driving the air-water disequilibrium, are the consequence of two factors i) the isolation of Antarctic water masses (Rintoul et al., 2000, Bengtson-Nash et al., 2010) from oceanic waters at northern latitudes which have higher concentrations (Nizzeto et al. 2010), and ii) the action of the biological pump that actively sequesters surface water contaminants lowering their concentrations in the photic zone (Galbán-Malagón et al., 2013a). The influence of the biological pump on air-water dis-equilibrium is evidenced by plotting $\text{Log } f_w f_A^{-1}$ versus the temperature corrected octanol-water partition constant ($\text{log } K_{OW}$), showing a lower value of $f_w f_A^{-1}$ for the more hydrophobic congeners ($p < 0.05$) (Figure 4B and Figures S6 and S7 in Appendix E.4). This

Chapter 7: PCBs in the Antarctic and Southern Ocean Atmosphere

trend is consistent with the role of settling organic carbon lowering the dissolved phase concentrations for the more hydrophobic congeners, thus increasing the air-water fugacity gradients, pointing out the important role of phytoplankton as one of the controlling factors in the biogeochemical cycling of PCBs in the highly productive Southern Ocean around the Antarctic Peninsula (Dachs et al. 2002, Galbán-Malagón et al., 2013a).

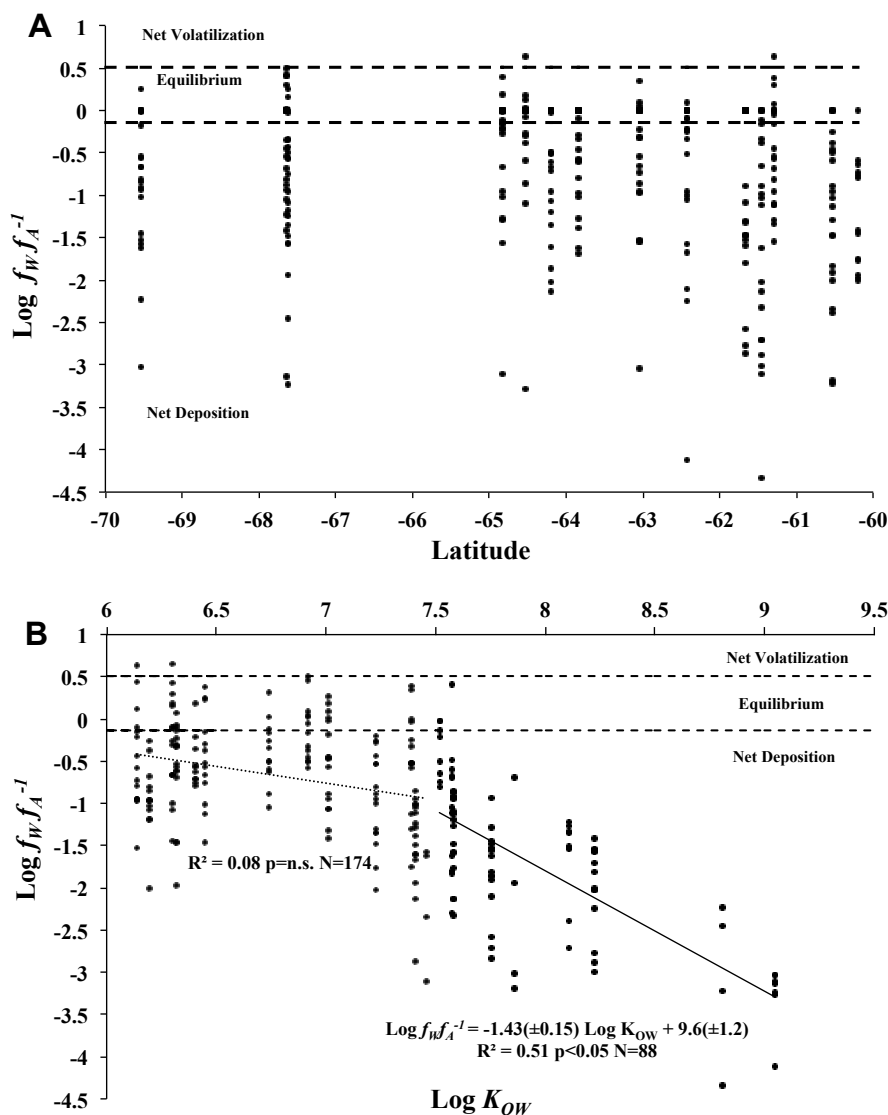


Figure 4. Air-water dis-equilibrium of PCBs. Estimated congener specific air/water fugacity ratios ($\log f_w/f_A$) calculated for the ESSASI and ATOS II cruises versus latitude (A), and versus the temperature corrected octanol water partition coefficient, $\text{Log } K_{OW}$ (B).

Chapter 7: PCBs in the Antarctic and Southern Ocean Atmosphere

The air-water net diffusive fluxes (F_{AW} , $\text{ng m}^{-2} \text{d}^{-1}$) were estimated for the oceanic samples using the two-film model as follows,

$$F_{AW} = k_{AW} \left(C_{TD} - \frac{C_G}{H'} \right) \quad (7.4)$$

Where k_{AW} (m d^{-1}) is the air-water mass transfer velocity that depends on the compound's physical-chemical properties, wind speed and T_W (Dachs et al. 2002, Jurado et al. 2004). F_{AW} for each sampling period and PCB congener are given in Table S13 in Appendix E.4. F_{AW} for Σ_{25} PCBs ranged from -0.32 to -7.67 $\text{ng m}^{-2} \text{d}^{-1}$ and from -0.89 to -7.01 $\text{ng m}^{-2} \text{d}^{-1}$ during the ESSASI and ATOS II cruises, respectively. Figure 5A shows F_{AW} for each PCB congener and no significant differences with latitude were observed. Figure 5B shows the average diffusive fluxes for individual PCB congeners. Even though the fugacity gradient is higher for the more hydrophobic congeners (Figure 4B), F_{AW} do not significantly increases for the more chlorinated congeners because the abundances of the less chlorinated congeners is higher in the gas phase, and k_{AW} is higher for lighter congeners.

Chapter 7: PCBs in the Antarctic and Southern Ocean Atmosphere

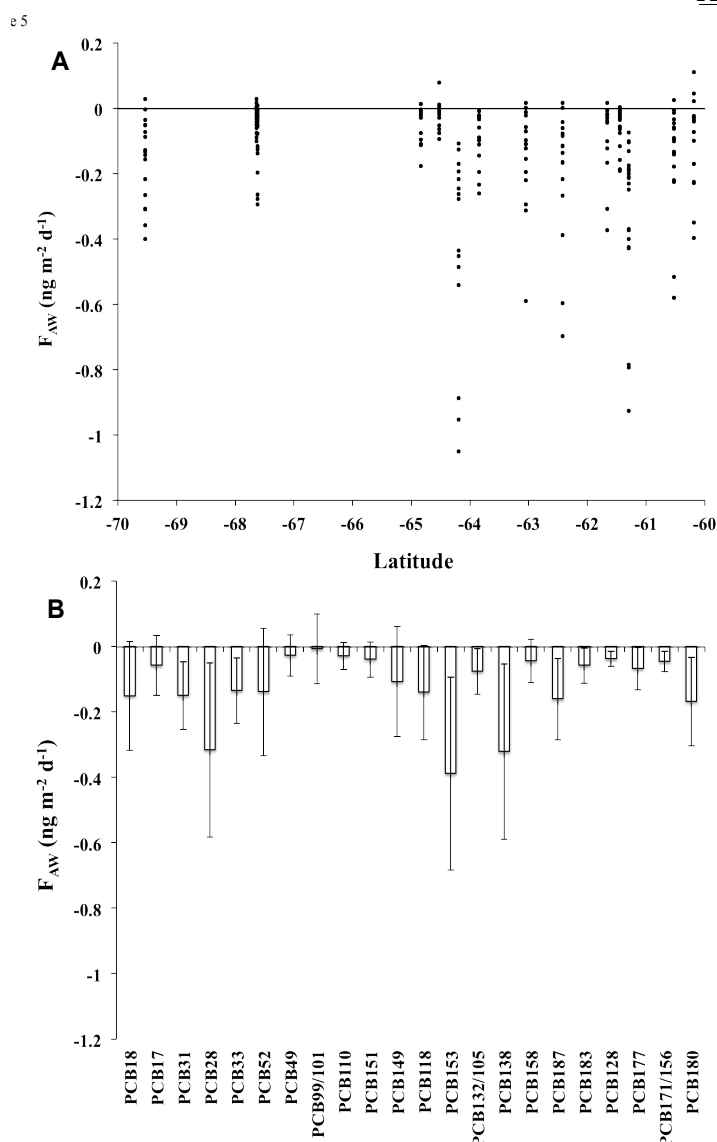


Figure 5. Air-water exchange of PCBs. Net diffusive air-water exchange ($\text{ng m}^{-2} \text{d}^{-1}$) fluxes during the ESSASI and ATOS II cruises versus latitude (A), and congener-specific diffusive fluxes for the Southern Ocean (B).

Atmospheric dry deposition was estimated by

$$F_{DD} = -v_D C_A \quad (7.5)$$

Where v_D is the aerosol deposition velocity, which for the Antarctic atmosphere a value of 258 m d^{-1} has been reported (Grönlund et al., 2002). Dry deposition fluxes for $\Sigma_{25}\text{PCBs}$ ranged from -0.05 to $-0.2 \text{ ng m}^{-2} \text{d}^{-1}$, and from -0.01 to $-0.1 \text{ ng m}^{-2} \text{d}^{-1}$ in the Southern Ocean (Weddell Sea, Bransfield Strait, Bellingshausen Sea) and in Livingston Island, respectively. These dry deposition

Chapter 7: PCBs in the Antarctic and Southern Ocean Atmosphere

fluxes are from 9 to 50 times lower than air-water diffusive fluxes. In addition, the dry deposition fluxes calculated here for the Southern Ocean are also one to two orders of magnitude lower than the dry deposition fluxes estimated for the Arctic atmosphere (Galbán-Malagón et al., 2012). As discussed above, the measured gas-particle partitioning is consistent with the model predictions. Thus, the low dry deposition fluxes are solely due to the very low concentrations of PCBs in the aerosol phase, as a consequence of the low amounts of aerosol organic carbon in the atmosphere.

To better understand the fate of PCBs once they are deposited to seawater, it could be useful to compare these atmospheric deposition fluxes with the sediment accumulation fluxes of PCBs reported recently for the Bellingshausen Sea (Zhang et al. 2013). The ratio of air-water diffusive exchange of the ICES PCB congeners measured here to the sediment accumulation fluxes for the four sites reported by Zhang and co-workers are 9, 12, 14 and 1800 (dimensionless). Therefore, atmospheric deposition of PCBs to the Bellingshausen Sea is from one to three orders of magnitude higher than the accumulation in sediment. The biological pump is likely to be the major removal process of PCBs from surface waters as showed by the trend depicted in Figure 4B, and by the decrease of PCB concentrations in phytoplankton at high biomass (Galbán-Malagón et al. 2013). Once in the mesopelagic zone, an important fraction of organic matter is remineralized driving the re-dissolution of PCBs in deep waters. In addition, remineralization of organic matter and partitioning to the dissolved phase can also occur at the sediment-water interface. Therefore, a small amount of PCBs that enter the Southern Ocean will be accumulated in the sediments.

3.4 Temperature dependence of gas phase concentrations

Higher temperatures favours the displacement of the air-water, air-snow and air-soil partitioning towards the atmospheric side, thus inducing higher gas phase concentrations of POPs. Recently, higher gas phase concentrations of PCBs for the warmer periods have been described in the atmosphere at Livingston Island, consistent with the measured volatilization of PCBs from soils and snow

Chapter 7: PCBs in the Antarctic and Southern Ocean Atmosphere

(Cabrerizo et al. 2013). Similarly, hexachlorocyclohexanes, (HCHs) also show higher concentrations at higher temperatures in the Antarctic atmosphere (Kang et al., 2012, Galbán-Malagón et al., 2013b). Other studies carried out in the Arctic have also shown that volatilization from seasonal snowpack is enhanced during high wind speed events, affecting the concentrations in the gas phase (Hallsall et al., 2004). Figure 6 (right panels) shows the significant correlation of gas phase concentrations of PCBs with air temperature at Pico Radio Hill site (data from Cabrerizo et al., 2013). Conversely, over the Southern Ocean, gas phase concentrations of PCBs are not correlated with temperature (Figure 6, left panels). The absence of this relationship over the Southern Ocean agrees with previous results from Polar Regions in the Arctic (Oehme et al., 1996, Stern et al., 1997, Galbán-Malagón et al., 2012) and in Antarctica (Kallenborn et al., 1998) for PCBs. The lack of temperature dependence of atmospheric concentrations is consistent with an important contribution of long-range atmospheric transport (Wania et al. 1998). During transport, the atmospheric concentrations are modulated by dilution, and the net deposition to the ocean. Conversely, the temperature dependent gas phase concentrations dependency on temperature tends to occur when the surface contamination and/or temperature are high (Wania et al., 1998), supporting a volatilization, and thus an important contribution from local secondary sources as described for Livingston Island (Cabrerizo et al. 2013), especially for the less hydrophobic compounds.

Chapter 7: PCBs in the Antarctic and Southern Ocean Atmosphere

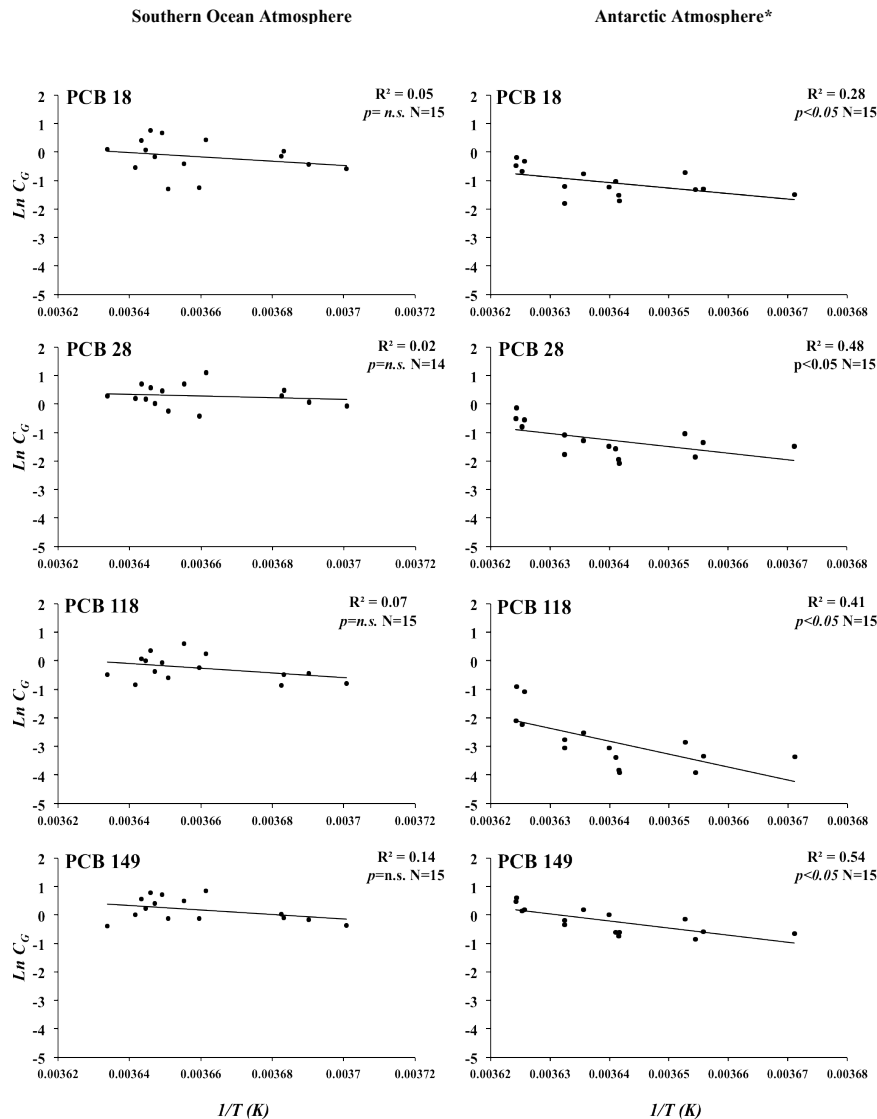


Figure 6. Temperature dependence of atmospheric concentrations of PCBs. Natural logarithm of atmospheric gas phase concentrations concentration of PCBs ($\text{Ln } C_G$, pg m^{-3}) versus inverse of air temperature ($1/T$, K^{-1}) in the Southern Ocean Atmosphere (left panels) and in the Antarctic atmosphere at Livingston Island (right panels). *Data taken from Cabrerizo et al., 2013.

3.5 Factors affecting the atmospheric occurrence of PCBs in the Southern Ocean

The 24 hours air-mass back-trajectories for the air (gas and aerosol phase) samples showed three main origins (Figures from S2) i) oceanic air masses from the west following the Antarctic circumpolar water current (ACC), ii) air masses from the Weddell Sea (WS), and iii) air mass that had “touched” the Antarctic continent or islands (AntC) during the previous 24 hours. There are no significant differences between the PCB concentrations measured in air samples influenced

Chapter 7: PCBs in the Antarctic and Southern Ocean **Atmosphere**

by the three characteristic air masses (Figure S7 in Appendix E.4). This observation is consistent with the trends observed during the same cruises for perfluorinated compounds (Del Vento et al., 2012) and hexachlorobenzene (Galbán-Malagón et al. 2013b). However, for compounds such as hexachlorocyclohexane (HCHs), which are degraded/sequestered faster during transport, there was a significant influence of the AntC air masses supporting higher levels of HCHs (Galbán-Malagón et al., 2013b).

The lack of differences among the concentrations for the different air mass back trajectories is due to the large variability in gas phase concentrations for AntC air masses, suggesting that the influence of secondary sources of PCBs on the Antarctic continent cannot be ruled out. However, the air mass analysis cannot provide the information on the relative influence of secondary sources because of the high air-to water diffusive fluxes, which modify the atmospheric concentrations during transport. The atmospheric half-lives of PCBs over the southern Ocean can be estimated using the atmospheric deposition fluxes reported above. The average atmospheric concentrations of PCBs 52 and 180 are 1.4 and 0.5 pg m^{-3} . Assuming an atmospheric mixing layer height of 500 m, the atmospheric inventory of PCBs 52 and 180 is 0.72 and 0.25 ng m^{-2} , respectively. Their calculated atmospheric deposition flux is 0.14 and 0.17 $\text{ng m}^{-2} \text{d}^{-1}$, respectively, as shown in Figure 5B. The atmospheric e-folding time or time needed to decrease the concentration to 1/e of initial concentrations, is given by the ratio of the inventory and atmospheric flux. The e-folding times for PCB52 and PCB180 are 5.2 and 1.5 days, which are similar to those predicted in this region when considering the influence of the biological pump sequestering atmospheric PCBs (Jurado and Dachs, 2008). These values are also comparable with those determined over other productive oceanic regions (Galbán-Malagón et al. 2012). The half-lives, the time to half the initial concentrations, are shorter, and yield 3.8 and 1 days for PCB52 and PCB180, respectively. During the Austral summer, when the warming of soil and snow induces volatilization of PCBs, especially the less hydrophobic compounds (Cabrerizo et al. 2013), there is a continuous cycling of PCBs from the continent to the ocean. However, Once volatilized, lighter PCB congeners will have higher capacity for long-range

Chapter 7: PCBs in the Antarctic and Southern Ocean Atmosphere

atmospheric transport as they are sequestered by the biological pump to a lower degree.

4. Conclusions

The present study reported the largest data set on the atmospheric occurrence of PCBs in the Southern Ocean surrounding the Antarctic Peninsula. Concentrations are low in comparison to other oceanic regions and the estimations of atmospheric deposition show a net flux from the atmosphere to the ocean. The large air-to-water disequilibrium for the more hydrophobic compounds is consistent with the role of the biological pump driving the sequestration of atmospheric PCBs in the region. The concentrations in the aerosol phase are extremely low due to the small concentrations of organic aerosol in the Antarctic atmosphere, and dry deposition accounts for a small fraction of the total deposition fluxes. Atmospheric concentrations are not correlated with temperature over the Southern Ocean, contrasting with the clear temperature dependence of gas phase PCB concentrations over land. These distinct trends suggest the major contribution of long-range atmospheric transport and local secondary sources for the marine and terrestrial atmosphere, respectively.

Chapter 7: PCBs in the Antarctic and Southern Ocean Atmosphere

References

Baek, S. -Y., Choi, S. -D. and Chang, Y. -S. Three-year atmospheric monitoring of organochlorine pesticides and polychlorinated biphenyls in Polar Regions and the South Pacific. *Environ. Sci. Technol.*, 45(10), 4475-4482, 2011.

Bengtson Nash, S. M., Poulsen, A. H., Kawaguchi, S., Vetter, W., and Schlabach, M. Persistent organohalogen contaminant burdens in Antarctic krill (*Euphausia superba*) from the Eastern Antarctic sector: A baseline study. *Sci. Total Environ.*, 407(1), 304-314, 2008.

Bengtson-Nash, S. Persistent organic pollutants in Antarctica: Current and future research priorities. *J. Environ. Monitor.*, 13(3), 497-504, 2011.

Bengtson-Nash, S., Rintoul, S. R., Kawaguchi, S., Staniland, I., Hoff, J. V. D., Tierney, M., and Bossi, R. Perfluorinated compounds in the Antarctic Region: Ocean circulation provides prolonged protection from distant sources. *Environ. Pollut.*, 158(9), 2985-2991, 2010.

Berrojalbiz, N., Dachs, J., Del Vento, S., Ojeda, M. J., Valle, M. C., Castro-Jiménez, J., Mariani, G., Wollgast, J. and Hanke, G. Persistent organic pollutants in Mediterranean seawater and processes affecting their accumulation in plankton. *Environ. Sci. Technol.*, 45(10), 4315-4322, 2011.

Bidleman, T. F. Atmospheric processes. *Environ. Sci. Technol.*, 22(4), 361-367, 1988.

Bidleman, T. F. Atmospheric transport and air-surface exchange of pesticides. *Water Air Soil Pollut.*, 115(1-4), 115-166, 1999.

Birch, M. E.; Cary, R. A. Elemental carbon-based method for monitoring occupational exposures to particulate diesel exhaust. *Aerosol Sci. Technol.*, 25, 221-241., 1996.

Bogdal, C., Scheringer, M., Abad, E., Abalos, M., van Bavel, B., Hagberg, J., and Fiedler, H. Worldwide distribution of persistent organic pollutants in air, including results of air monitoring by passive air sampling in five continents. *TRAC-Trend. Anal. Chem.* 46, 251-161, doi: 10.1016/j.trac.2012.05.011, 2012.

Boyd, P. W.; Robinson, C.; Savidge, G.; Williams, P. J. Water column and sea-ice primary production during Austral spring in the Bellingshausen sea. *Deep-Sea Res. Pt. II.*, 42(4-5), 1177-1200., 1995

Breivik, K., Alcock, R., Li, Y., Bailey, R. E., Fiedler, H., and Pacyna, J. M. Primary sources of selected POPs: Regional and global scale emission inventories. *Environ. Pollut.*, 128(1-2), 3-16, doi: 10.1016/j.envpol.2003.08.031, 2004.

Chapter 7: PCBs in the Antarctic and Southern Ocean Atmosphere

Cabrerizo, A., Dachs, J., Barceló, D., and Jones, K. C. Climatic and biogeochemical controls on the remobilization and reservoirs of persistent organic pollutants in Antarctica. *Environ. Sci. Technol.*, 47(9), 4299-4306. 2013

Cabrerizo, A., Dachs, J., Barceló, D., and Jones, K. C. Influence of organic matter content and human activities on the occurrence of organic pollutants in Antarctic soils, lichens, grass, and mosses. *Environ. Sci. Technol.*, 46(3), 1396-1405. 2012

Dachs, J., Eisenreich, S. J., and Hoff, R. M. Influence of eutrophication on air-water exchange, vertical fluxes, and phytoplankton concentrations of persistent organic pollutants. *Environ. Sci. Technol.*, 34(6), 1095-1102, 2000.

Dachs, J., Eisenreich, S. J., Baker, J. E., Ko, F. -C., and Jeremiason, J. D. Coupling of phytoplankton uptake and air-water exchange of persistent organic pollutants. *Environ. Sci. Technol.*, 33(20), 3653-3660, 1999.

Dachs, J., Lohmann, R., Ockenden, W. A., Méjanelle, L., Eisenreich, S. J., and Jones, K. C. (2002). Oceanic biogeochemical controls on global dynamics of persistent organic pollutants. *Environ. Sci. Technol.*, 36(20), 4229-4237, 2002.

Doval, M. D., Álvarez-Salgado, X. A., Castro, C. G., and Pérez, F. F. Dissolved organic carbon distributions in the Bransfield and Gerlache straits, Antarctica. *Deep-Sea Res. Pt. II.*, 49(4-5), 663-674, 2002.

Fuoco, R., Colombini, M. P., Ceccarini, A., and Abete, C. Polychlorobiphenyls in Antarctica. *Microchem. J.*, 54(4), 384-390, 1996.

Galbán-Malagón, C. J., Cabrerizo, A., Caballero, G., and Dachs, J. Atmospheric occurrence and deposition of hexachlorobenzene and hexachlorocyclohexanes in the Southern Ocean and Antarctic Peninsula. Submitted for publication to *Atmos. Environ.*, 2013b

Galbán-Malagón, C. J., Del Vento, S., Berrojalbiz, N., Ojeda, M. J., and Dachs, J. Polychlorinated biphenyls, hexachlorocyclohexanes and hexachlorobenzene in seawater and phytoplankton from the Southern Ocean (Weddell, South Scotia, and Bellingshausen seas). *Environ. Sci. Technol.*, 47(11), 5578-5587. 2013a

Galbán-Malagón, C., Berrojalbiz, N., Ojeda, M.J. and Dachs, J. The oceanic biological pump modulates the atmospheric transport of persistent organic pollutants to the Arctic. *Nat. Comm.*, 3, doi: 10.1038/ncomms1858, 2012.

Gambaro, A., Manodori, L., Zangrando, R., Cincinelli, A., Capodaglio, G., and Cescon, P. Atmospheric PCB concentrations at Terra Nova bay, Antarctica. *Environ. Sci. Technol.*, 39(24),

Chapter 7: PCBs in the Antarctic and Southern Ocean Atmosphere

9406-9411, 2005.

García-Flor, N., Guitart, C., Ábalos, M., Dachs, J., Bayona, J. M., and Albaigés, J. Enrichment of organochlorine contaminants in the sea surface microlayer: An organic carbon-driven process. *Mar. Chem.*, 96(3-4), 331-345, 2005.

Grönlund, A., Nilsson, D., Koponen, I. K., Virkkula, A., and Hansson, M. E. Aerosol dry deposition measured with eddy-covariance technique at Wasa and Aboa, Dronning Maud land, Antarctica. *Ann. Glaciol.*, 35, 355-361, 2002.

Halsall, C. J. Investigating the occurrence of persistent organic pollutants (POPs) in the arctic: Their atmospheric behaviour and interaction with the seasonal snow pack. *Environ. Pollut.*, 128(1-2), 163-175, 2004.

Harner, T., and Bidleman, T. F. Measurement of octanol-air partition coefficients for polycyclic aromatic hydrocarbons and polychlorinated naphthalenes. *J. Chem. Eng. Data*, 43(1), 40-46, 1998.

Harner, T., and Bidleman, T. F. Octanol-air partition coefficient for describing particle/gas partitioning of aromatic compounds in urban air. *Environ. Sci. Technol.*, 32(10), 1494-1502, 1998.

Iwata, H., Tanabe, S., Sakai, N., and Tatsukawa, R. Distribution of persistent organochlorines in the oceanic air and surface seawater and the role of ocean on their global transport and fate. *Environ. Sci. Technol.*, 27(6), 1080-1098, 1993.

Jones, K. C., and De Voogt, P.. Persistent organic pollutants (POPs): State of the science. *Environ. Pollut.*, 100(1-3), 209-221, 1998.

Jurado, E., and Dachs, J. Seasonality in the "grasshopping" and atmospheric residence times of persistent organic pollutants over the oceans. *Geophys. Res. Lett.*, 35(17), doi: 10.1029/2008GL034698, 2008.

Jurado, E., Jaward, F. M., Lohmann, R., Jones, K. C., Simó, R., and Dachs, J. Atmospheric dry deposition of persistent organic pollutants to the Atlantic and inferences for the global oceans. *Environ. Sci. Technol.*, 38(21), 5505-5513, 2004.

Kallenborn, R., Oehme, M., Wynn-Williams, D. D., Schlabach, M., and Harris, J. Ambient air levels and atmospheric long-range transport of persistent organochlorines to Signy Island, Antarctica. *Sci. Total. Environ.*, 220(2-3), 167-180, 1998.

Chapter 7: PCBs in the Antarctic and Southern Ocean Atmosphere

Kang, J. -H, Son, M. -H., Hur, S. -D., Hong, S., Motoyama, H., Fukui, K., and Chang, Y. -S. Deposition of organochlorine pesticides into the surface snow of East Antarctica. *Sci. Total Environ.*, 433, 290-295, 2012.

Larsson, P., Jarnmark, C., and Sodergren, A. PCBs and chlorinated pesticides in the atmosphere and aquatic organisms of Ross Island, Antarctica. *Mar. Pollut. Bull.*, 25(9-12), 281-287, 1992.

Li, Y., Geng, D., Liu, F., Wang, T., Wang, P., Zhang, Q., and Jiang, G. Study of PCBs and PBDEs in King George Island, Antarctica, using PUF passive air sampling. *Atmos. Environ.*, 51, 140-145, 2012.

Ma, J., Hung, H., Tian, C. and Kallenborn, R., Revolatilization of persistent organic pollutants in the Arctic induced by climate change *Nat. Climate Change.* 1, 255–260. doi:10.1038/nclimate1167. 2011.

Mandalakis, M., E.G. Stephanou. Atmospheric concentration characteristics and gas-particle partitioning of PCBs in a rural area of Eastern Germana. *Environ. Pollut.* 147, 211-221, 2007.

Meijer, S. N., Dachs, J., Fernandez, P., Camarero, L., Catalan, J., Del Vento, S., Van Droodge, B., Jurado, E., and Grimalt, J. O. Modelling the dynamic air-water-sediment coupled fluxes and occurrence of polychlorinated biphenyls in a high altitude lake. *Environ. Pollut.*, 140(3), 546-560, 2006.

Meijer, S. N., Ockenden, W. A., Sweetman, A., Breivik, K., Grimalt, J. O., and Jones, K. C. Global distribution and budget of PCBs and HCB in background surface soils: Implications for sources and environmental processes. *Environ. Sci. Technol.*, 37(4), 667-672, 2003.

Montone, R. C., Taniguchi, S., and Weber, R. R. PCBs in the atmosphere of King George Island, Antarctica. *Sci. Total Environ.*, 308(1-3), 167-173, 2003.

Montone, R. C., Taniguchi, S., Boian, C., and Weber, R. R. PCBs and chlorinated pesticides (DDTs, HCHs and HCB) in the atmosphere of the Southwest Atlantic and Antarctic Oceans. *Mar. Pollut. Bull.*, 50(7), 778-786, 2005.

Nizzetto, L., Gioia, R., Li, J., Borgå, K., Pomati, F., Bettinetti, R., Dachs, J. and Jones, K. C. Biological pump control of the fate and distribution of hydrophobic organic pollutants in water and plankton. *Environ. Sci. Technol.*, 46(6), 3204-3211, 2012.

Chapter 7: PCBs in the Antarctic and Southern Ocean Atmosphere

Nizzetto, L., MacLeod, M., Borgå, K., Cabrerizo, A., Dachs, J., Guardo, A. D., Ghirardello, D., Hansen, K. M., Jarvis, A., Lindroth, A., Ludwig, B., Monteith, D., Perlinger, J. A., Scheringer, M., Schwendenmann, L., Semple, K. T., Wick, L. Y., Zhang, G. and Jones, K. C. Past, present, and future controls on levels of persistent organic pollutants in the global environment. *Environ. Sci. Technol.*, 44(17), 6526-6531, 2010.

Ockenden, W. A., Lohmann, R., Shears, J. R., and Jones, K. C. The significance of PCBs in the atmosphere of the Southern Hemisphere. *Environ. Sci. Pollut. Res.*, 8(3), 189-194, 2001.

Oehme, M. Seasonal changes and relations between levels of organochlorines in Arctic ambient air: First results of an all-year-round monitoring program at Ny-Alesund, Svalbard, Norway. *Environ. Sci. Technol.*, 30(7), 2294-2304, 1996.

Pankow, J. F. An absorption model of the gas/aerosol partitioning involved in the formation of secondary organic aerosol. *Atmos. Environ.*, 28(2), 189-193, 1994.

Pankow, J. F. Further discussion of the octanol/air partition coefficient (K_{OA}) as a correlating parameter for gas/particle partitioning coefficients. *Atmos. Environ.*, 32(9), 1493-1497, 1998.

Radonić, J., Miloradov, M. V., Sekulić, M. T., Kiursk, J., Djogo, M., and Milovanović, D. The octanol-air partition coefficient, K_{OA} , as a predictor of gas-particle partitioning of polycyclic aromatic hydrocarbons and polychlorinated biphenyls at industrial and urban sites. *J. Serb. Chem. Soc.*, 76(3), 447-458, 2011.

Rintoul, S.R., Southern Ocean currents and climate. *Pap. Proc. R. Soc. Tasman.* 133,41-50. 2000.

Rowe, A. A., Totten, L. A., Xie, M., Fikslin, T. J., and Eisenreich, S. J. Air-water exchange of polychlorinated biphenyls in the Delaware River. *Environ. Sci. Technol.*, 41(4), 1152-1158, 2007.

Scheringer, M. Characterization of the environmental distribution behavior of organic chemicals by means of persistence and spatial range. *Environ. Sci. Technol.*, 31(10), 2891-2897, 1997.

Stern, G. A., Halsall, C. J., Barrie, L. A., Muir, D. C. G., Fellin, P., Rosenberg, B., Rovinsky, F.Y.A., Kononov, E.Y.A. and Pastuhov, B. Polychlorinated biphenyls in Arctic air. 1. temporal and spatial trends: 1992-1994. *Environ. Sci. Technol.*, 31(12), 3619-3628, 1997

Tanabe, S., Hidaka, H., and Tatsukawa, R. PCBs and chlorinated hydrocarbon pesticides in Antarctic atmosphere and hydrosphere. *Chemosphere*, 12(2), 277-288, 1983.

Chapter 7: PCBs in the Antarctic and Southern Ocean Atmosphere

Totten, L. A., Brunciak, P. A., Gigliotti, C. L., Dachs, J., Glenn IV, T. R., Nelson, E. D., and Eisenreich, S. J. Dynamic air-water exchange of polychlorinated biphenyls in the new york-new jersey harbor estuary. *Environ. Sci. Technol.*, 35(19), 3834-3840, 2001.

Tréguer, P., and Jacques, G. Dynamics of nutrients and phytoplankton, and fluxes of carbon, nitrogen and silicon in the antarctic ocean. *Polar Biol.*, 12(2), 149-162. 1992

Wania, F., and Mackay, D. Tracking the distribution of persistent organic pollutants. *Environ. Sci. Technol.*, 30(9), 390A-397^a, 1996.

Wania, F.; Haugen, J. E.; Lei, Y. D.; Mackay, D. Temperature Dependence of Atmospheric Concentrations of Semivolatile Organic Compounds. *Environ. Sci. Technol.* 1013-1021, 1998.

Wania, F., Axelman, J., and Broman, D. A review of processes involved in the exchange of persistent organic pollutants across the air-sea interface. *Environ. Pollut.*, 102(1), 3-23, 1998.

Yamasaki, H., Kuwata, K., and Miyamoto, H. Effects of ambient temperature on aspects of airborne polycyclic aromatic hydrocarbons. *Environ. Sci. Technol.*, 16(4), 189-194, 1982.

Zhang, L., Dickhut, R., Demaster, D., Pohl, K., and Lohmann, R. Organochlorine pollutants in Western Antarctic Peninsula sediments and benthic deposit feeders. *Environ. Sci. Technol.*, 47 (11), 5643-5651, 2013.

Chapter 8

Conclusions

The Conclusions from the present thesis were:

- Atmospheric HCHs and PCBs concentrations found were in the lower range of concentrations reported for Polar Oceans confirming the continued decreasing tendency of atmospheric concentrations of HCHs and PCBs since its production and commercialization control. Atmospheric concentrations of HCHs and PCBs found in the Antarctic Peninsula surrounding waters were lower compared to the Arctic and those reported for the South Scotia Sea. Conversely HCB concentrations did not present this decreasing tendency and were in the same range of concentrations reported in the last 20 years in the Arctic and Antarctica.

- Aerosol concentrations of HCHs, HCB and PCBs found were the first reported in the Arctic and Antarctic Oceans atmosphere. Aerosol concentrations did not represent more than the 4% of total atmospheric concentrations (sum of aerosol and gas phase concentrations), which agrees with model predictions.

- Dissolved seawater concentrations for HCHs and PCBs were in the lower range of those found in the Arctic and Antarctica. Antarctic Peninsula surrounding waters concentrations were lower than concentrations found in the South Scotia Sea and Arctic Ocean. HCB concentrations found in the Arctic surface waters were one order of magnitude higher than those measured in the Antarctic surface waters. Particulate HCH, HCB and PCBs concentrations found were in the same range of the concentrations given in the literature for the Arctic.

- Phytoplankton HCHs, HCB and PCBs concentrations given in the present thesis were the first presented for the Arctic and Antarctica showing that concentrations in the Arctic were higher than concentrations from the Antarctic phytoplankton. However, HCB was not found in all the phytoplankton samples in the Arctic.

Conclusions

- Long-range atmospheric transport has been pointed as the main input of HCHs, HCB and PCBs to the Arctic and Antarctic Ocean atmosphere due to lack of correlation with environmental temperature. In the case of the Arctic the biological pump is able to reduce and modulate the transport due to active sequestration of POPs from surface waters enhancing the atmospheric deposition to surface waters. In the case of Antarctica it has been found that secondary local sources, like soil or snow, are important inputs of HCHs, HCB and PCBs in the Antarctic islands atmosphere.

- Field derived atmospheric residence times for PCBs and HCHs had been estimated following different approaches and all the results obtained were in agreement with the model predictions for PCBs revealing that atmospheric residence times is higher for less hydrophobic PCBs than for the more hydrophobic PCBs.

- The assessment of gas-particle partition constant in the Antarctic atmosphere showed a strong correlation among the field derived gas-particle partition coefficients estimated and model predictions. However, field derived gas-particle coefficients estimated inland did not presented this tendency. These differences could be due to the input of PCBs volatilized from soils and snow for inland samples where their influence is higher than the long range atmospheric transport. In the case of coastal and oceanic samples there is a strong net deposition of the more hydrophobic compounds from the gas phase to the oceans, which compensates the slightly inputs of PCBs from secondary sources.

- The air to water diffusive exchange fluxes were dominant during all the sampling campaigns, being the principal input of POPs to the Arctic and Antarctic surface waters. Dry deposition was identified as a secondary input that represents less than 5% of total atmospheric inputs. However, HCB showed a close to equilibrium state in the Arctic and Antarctic Polar Oceans. These results points that HCB is close to the equilibrium between the studied phases in the Arctic and Antarctic atmosphere.

- Estimated bioconcentration factors obtained in the present work for the hydrophobic PCBs were lower than the estimated from models pointing that the biological pump sequestration of POPs from the water column is occurring during high productivity periods as well as higher Bioconcentrations factors found for less chlorinated PCBs and HCHs. For the HCB bioconcentrations factors were

Conclusions

in the same range of values predicted from models pointing that HCB is in equilibrium between the phytoplankton and the dissolved seawater.

- The estimated diffusive exchange fluxes of PCBs between the air and water, and the PCBs sinking fluxes by means of the biological pump in the water column points that the sequestration of PCBs in the upper water column depletes the concentrations in surface waters and enhances the input of PCBs from the atmospheric compartment especially during productive periods. The sequestration in the water column process is more efficient for the more hydrophobic compounds and also it has been demonstrated that in the case of less hydrophobic and degradable compounds like HCHs there are another biogeochemical factors that control their cycling in Polar surface waters.

- For HCHs it was suggested that microbial communities are able to degrade these compounds. In the present thesis we concluded that this factor is occurring during high productivity periods coupled to the biological pump revealing the action of a degradative pump. The degradation of HCHs coupled to the biological pump action points that there is an active depletion process in polar oceans surface waters. These results were confirmed by the lower atmospheric residence time found in the Arctic and Antarctic atmosphere compared with PCBs with similar characteristics prediction models.

Appendix A

Supplementary Information to Chapter 3.

The Oceanic Biological Pump Modulates the Atmospheric Transport of Persistent Organic Pollutants to the Arctic

Appendix A.1: Supplementary Figures

Supplementary Figure S1. Cruise course during the ATOS-1 sampling campaign and sample locations ...221

Supplementary Figure S2a. Backtrajectories for dominating air masses for each sample in July 2007...222

Supplementary Figure S2b. Backtrajectories for dominating air masses for each sample in July 2007...223

Supplementary Figure S3. Modelled atmospheric residence time PCBs in the North Atlantic...224

Supplementary Figure S4. Surface chlorophyll concentrations for the sampling period...225

Supplementary Figure S5. Diffusive air-water flux (F_{AW}) versus bioconcentration factors (LogBCF) ...226

Supplementary Figure S6. Schematics of the PCB 153 and 180 air-water-deep water fluxes...227

Appendix A.2: Supplementary Tables:

Supplementary Table S1a. Concentrations of PCBs in the different sampled matrixes ...228

Supplementary Table S1b Concentrations of PCBs in the different sampled matrixes...229

Supplementary Table S2 Summary of concentrations for the different phases...230

Supplementary Table S3 Ancillary data for each sample...231

Supplementary Table S4. Predicted atmospheric residence times from atmospheric concentrations...232

Supplementary Table S5. Averaged summer sinking fluxes...233

Supplementary Table S6. Diffusive net flux estimations for PCBs...234

Supplementary Table S7. Dry deposition flux estimations for PCBs...235

Supplementary Table S8. Air-water fugacity ratios for PCBs ...236

Supplementary Table S9 Limits of quantifications and limits of detection for the

Appendix A

studied PCBs...237

Supplementary Table S10 Physico-chemical properties...238

Appendix A.3 Supplementary methods

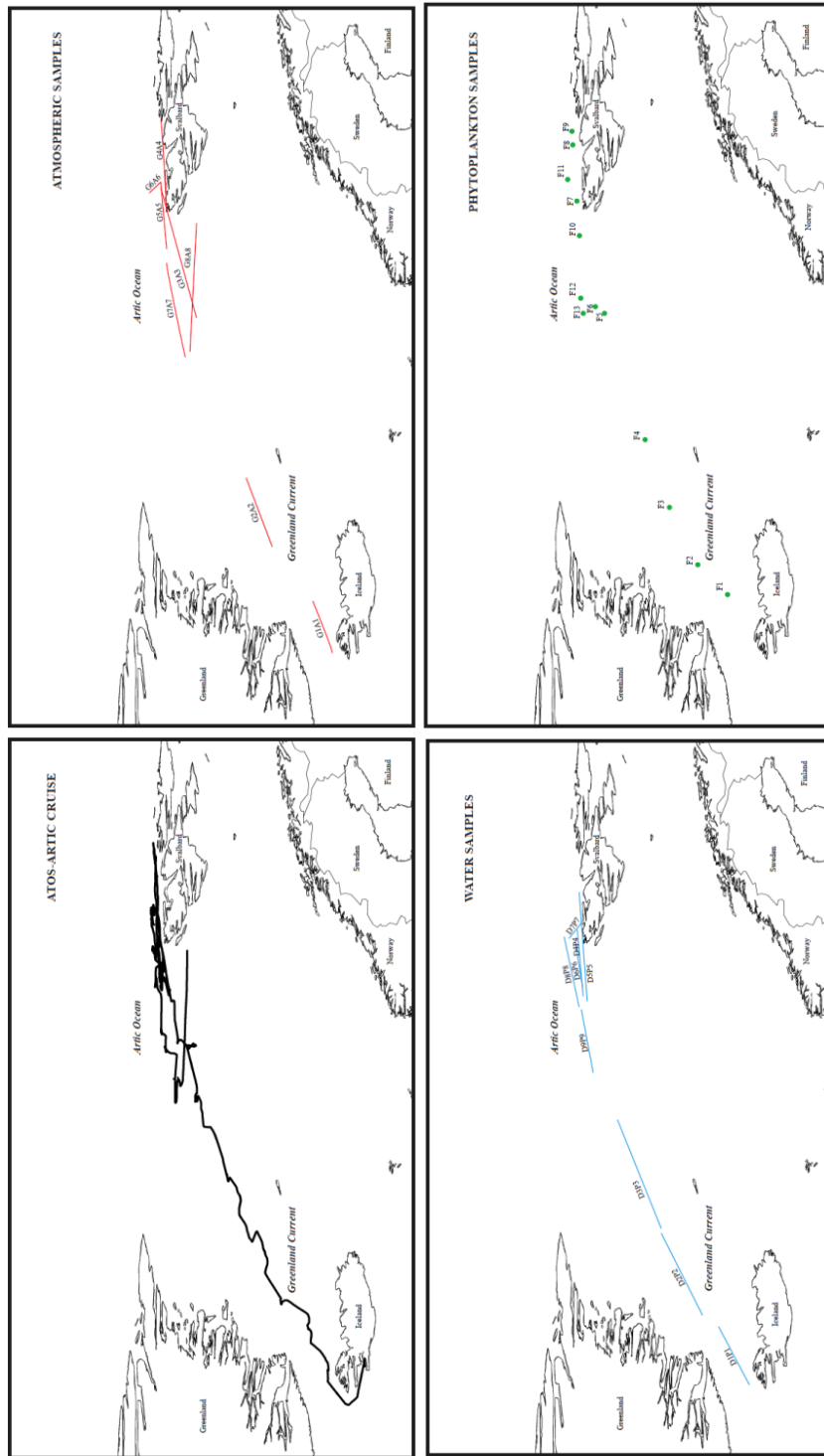
Supplementary Method S1: Atmospheric transport statistical analysis and Regression analysis...239

Supplementary Method S2: Estimation of air-water diffusive exchange and dry deposition fluxes of PCBs...241

Supplementary Method S3: Estimation of fugacity ratios...244

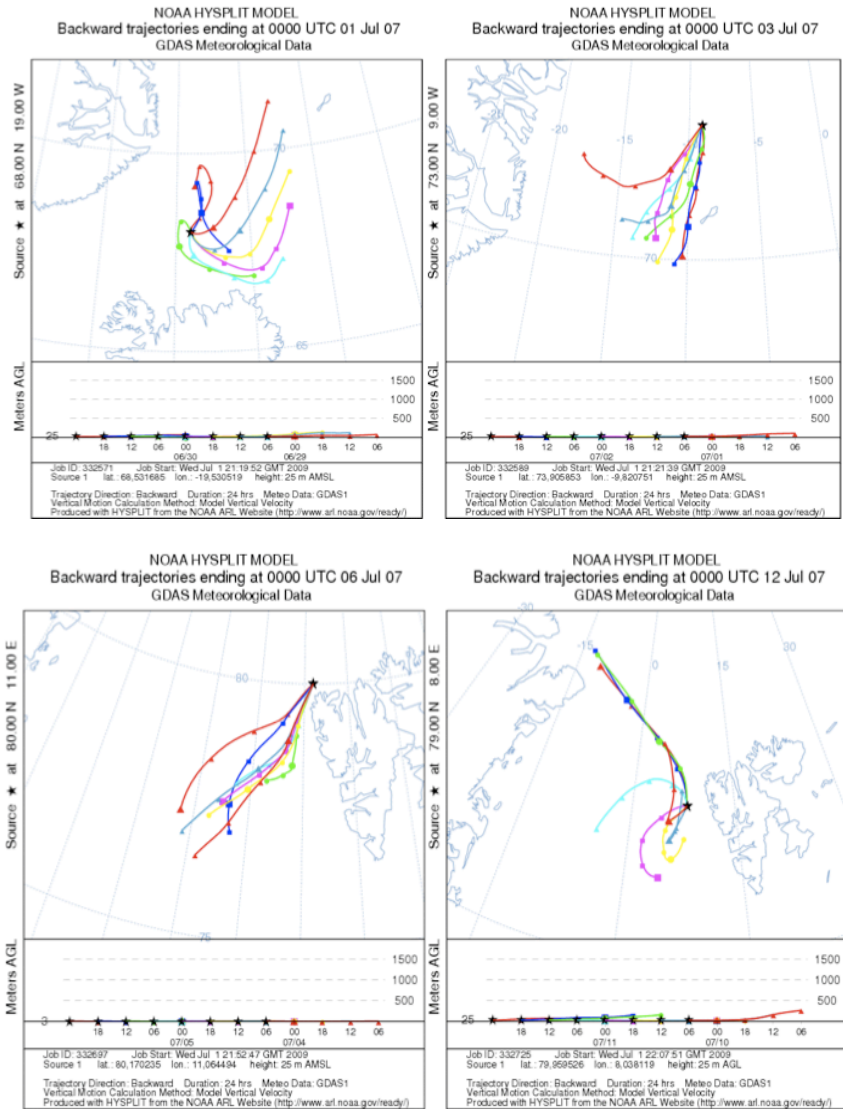
Additional References...245

Appendix A.1: Supplementary Figures

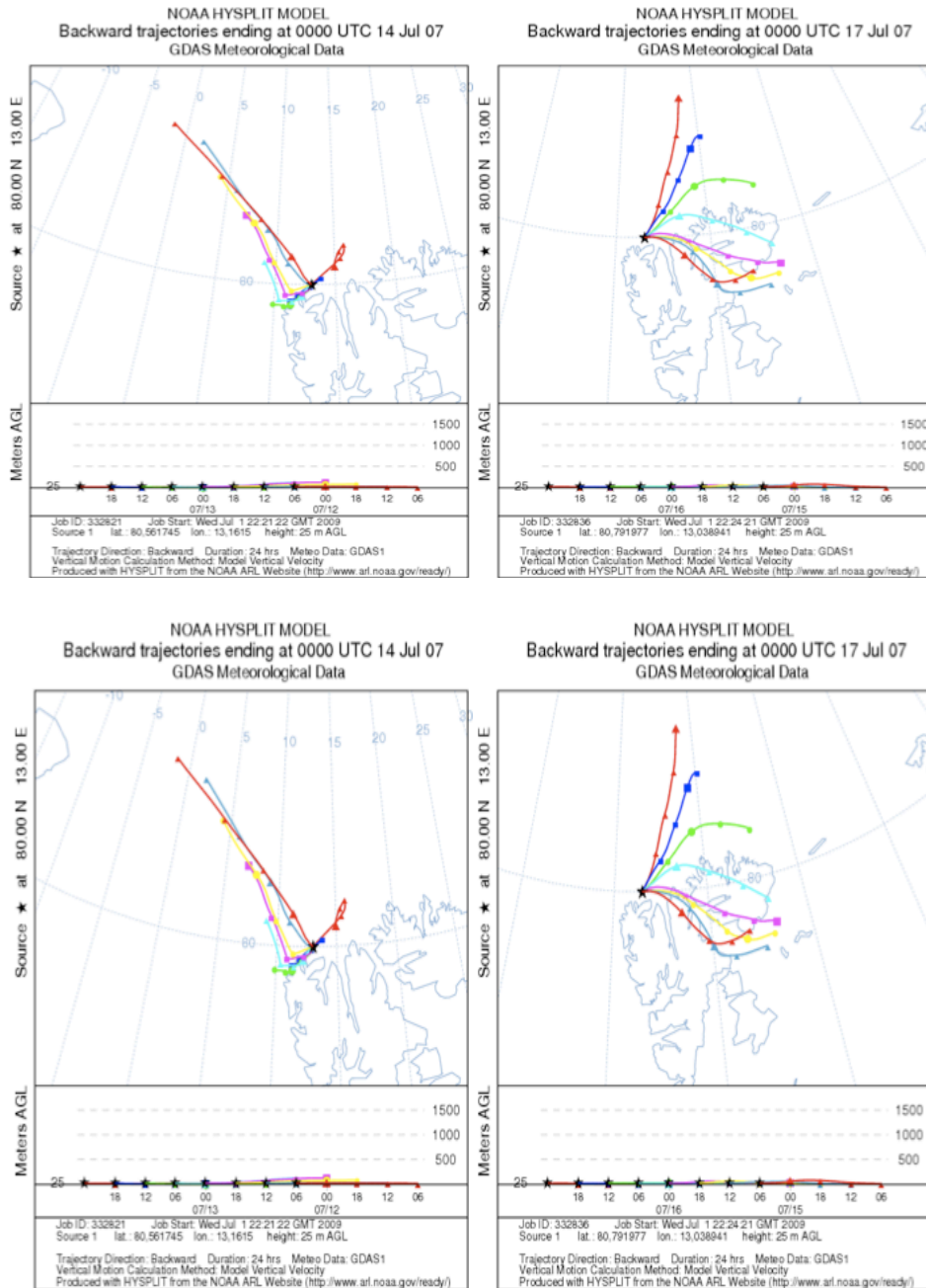


Supplementary Figure S1. Cruise course during the ATOS-1 sampling campaign and sample locations. Cruise course during ATOS-ARTIC sampling campaign on board *RV Hespérides* in July 2007 (upper panel left) and sampling locations for the atmospheric samples (upper panel right), water samples (lower panel left), phytoplankton samples (lower panel, right).

Backtrajectories



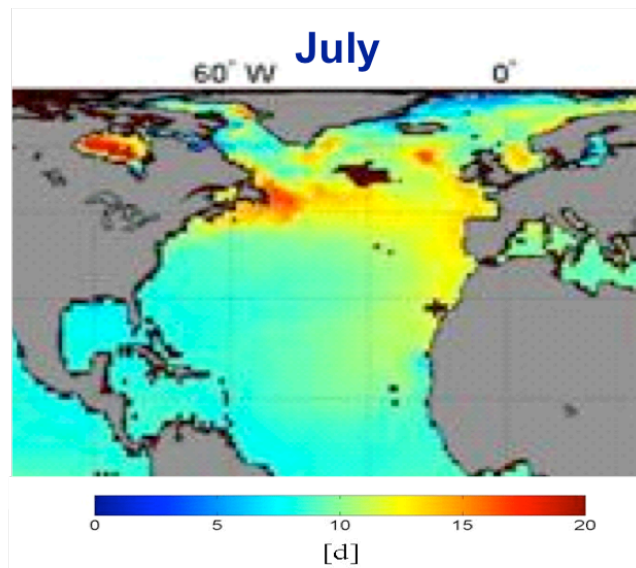
Supplementary Figure S2a. Backtrajectories for dominating air masses for each sample in July 2007



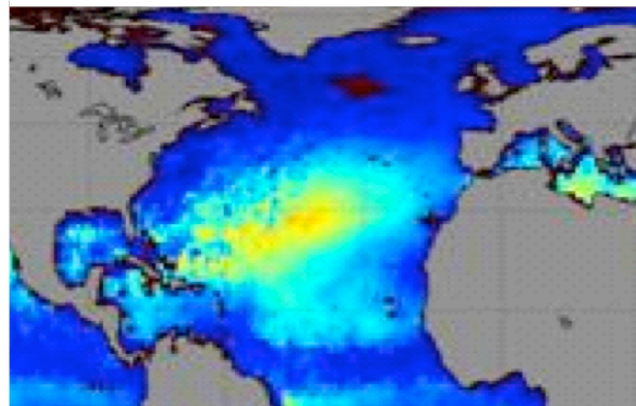
Supplementary Figure S2b. Backtrajectories for dominating air masses for each sample in July 2007

Appendix A

PCB 28

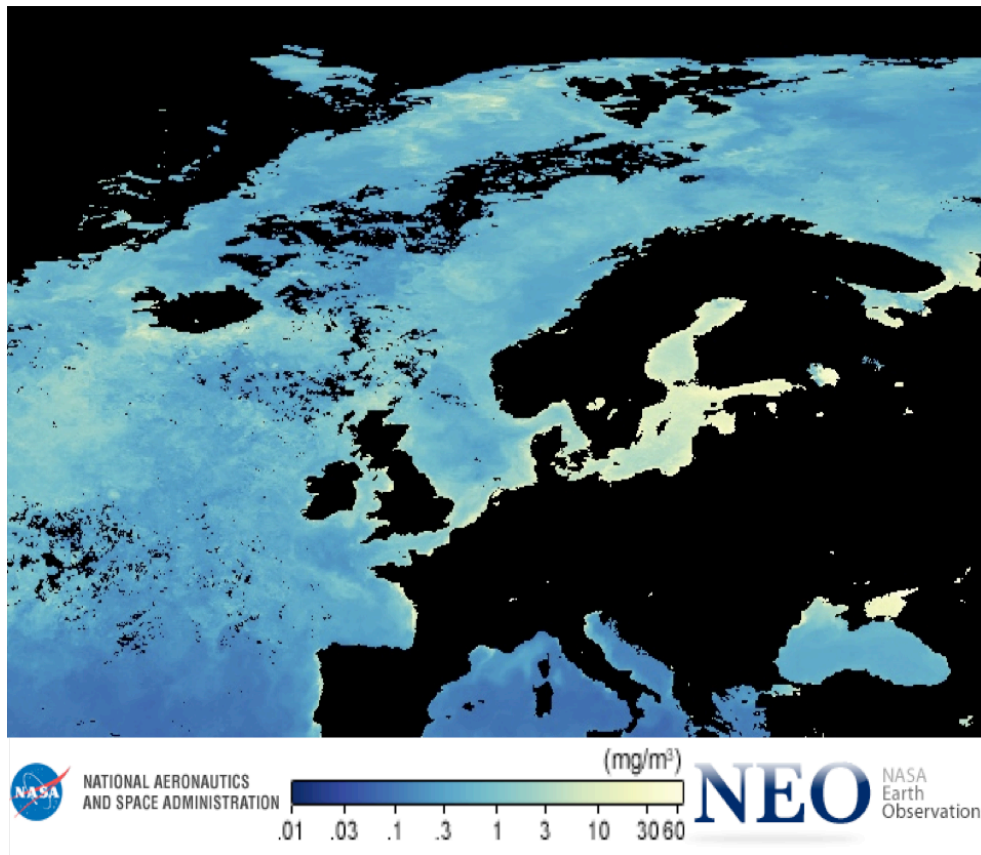


PCB 180



Jurado and Dachs, 2008 GRL

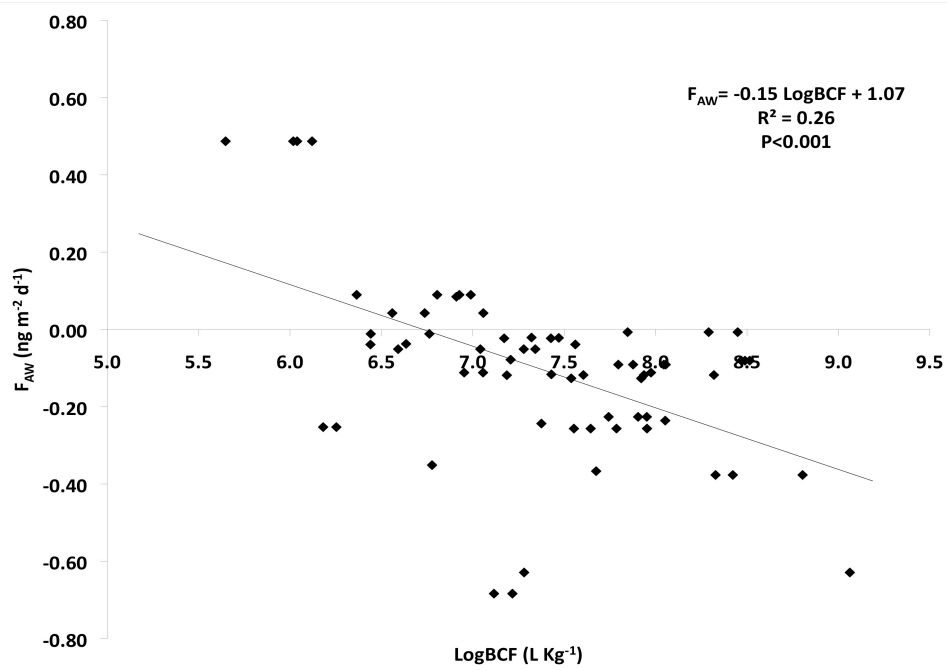
Supplementary Figure S3. Modelled atmospheric residence time for PCBs in the North Atlantic. Atmospheric residence times of PCB 28 (upper panel) and PCB 180 (lower panel) as predicted using a model that accounts for the influence of the biological pump on atmospheric concentrations. Results shown are for July for a climatological year as reported elsewhere².



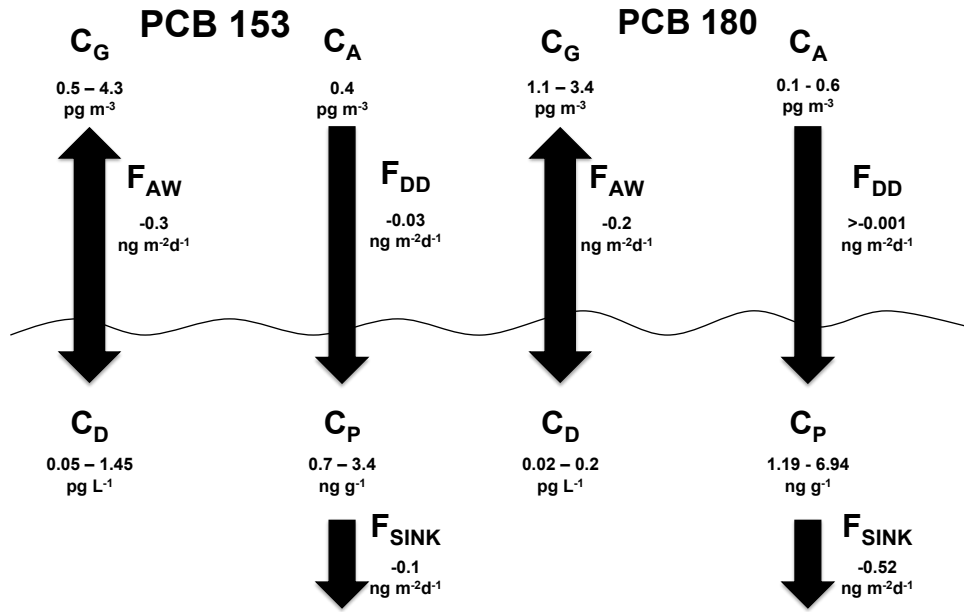
Supplementary Figure S4. Surface chlorophyll concentrations for the sampling period.

Reproduced from <http://neo.sci.gsfc.nasa.gov>

Appendix A



Supplementary Figure S5. Diffusive air-water flux (F_{AW}) versus the bioconcentration factor (LogBCF). The diffusive air-water flux versus the BCF is shown for all the PCB congeners and for the sampling events corresponding to the Greenland Current.



Supplementary Figure S6. Schematics of the PCB 153 and 180 air-water-deep water fluxes

Appendix A

Appendix A.2 Supplementary Tables

Supplementary Table S1a. Concentrations of PCBs in the different sampled matrixes. Concentrations of PCBs in the gas, aerosol, dissolved, particles and phytoplankton phases during our sampling cruise. GC: Greenland Current AO: Arctic Ocean nd: not detected

Sample Type	Sample	PCB18	PCB17	PCB31	PCB28	PCB33	PCB52	PCB49	PCB44	PCB99/101	PCB87	PCB110	PCB82	PCB151
GC Atmospheric Gas (pg m ⁻³)	G1	12.7788	3.7077	1.1311	1.9858	5.6430	6.1896	4.8752	nd	6.4376	5.2701	nd	nd	1.3128
	G2	2.1319	1.3098	0.9031	3.7109	1.2780	2.4551	0.1096	6.9754	nd	1.6672	nd	nd	0.7037
	G3	4.4945	nd	0.3829	0.1065	nd	6.9281	0.4522	2.3964	nd	nd	nd	nd	0.0304
	G4	0.9957	0.5357	nd	0.9579	nd	nd	4.3295	1.4508	0.8702	0.3110	0.0250	0.7133	0.1897
AO Atmospheric Gas (pg m ⁻³)	G5	0.7541	1.0576	0.3882	0.0541	0.1109	nd	0.7759	1.2582	1.1041	0.4594	nd	nd	1.0006
	G6	0.0268	0.0181	0.1784	0.2444	0.1109	nd	1.1298	1.6399	0.1030	nd	nd	nd	nd
	G7	0.1512	0.0567	0.1550	nd	nd	nd	0.1200	0.1966	nd	nd	nd	nd	5.3800
	G8	1.8985	0.4744	1.5823	1.7842	0.2767	2.6410	0.9359	2.2158	nd	0.1549	nd	nd	0.1485
GC Atmospheric Aerosol (pg m ⁻³)	A1	nd	nd	2.0306	0.4071	2.3908	0.1684	1.0808	nd	nd	0.3135	nd	0.0234	nd
	A2	nd	nd	0.4623	nd	0.2207	0.0125	0.1791	nd	0.2207	0.0541	nd	nd	nd
	A3	3.5750	3.3485	1.0443	0.8344	1.1383	nd	2.5473	0.2487	0.3978	0.4144	0.3702	nd	nd
AO Atmospheric Aerosol (pg m ⁻³)	A4	0.0580	0.0652	0.1521	0.0435	nd	0.5579	0.1666	0.1087	0.2536	0.0867	0.0685	0.0365	0.5006
	A5	0.0677	0.0395	0.1297	0.0508	nd	0.1523	0.0564	0.0451	0.1887	0.1059	0.0506	0.0092	0.0506
	A6	0.3434	0.1042	0.4073	0.4571	0.7626	0.8857	0.3647	0.5613	nd	0.0835	0.1060	nd	nd
	A7	nd	nd	0.1512	0.0321	nd	0.2949	nd	nd	nd	0.0321	nd	nd	nd
GC Dissolved Seawater (pg L ⁻¹)	D1	1.0314	2.6285	1.0854	4.2253	0.0335	0.6099	nd	nd	1.9173	2.3850	1.2180	0.2011	0.2392
	D2	0.0252	0.0484	0.0588	0.0225	0.0235	0.1607	0.0457	0.0561	0.9668	0.1074	0.1148	0.1041	0.0484
	D3	0.0375	0.0176	0.1810	0.5464	0.0002	0.0463	0.0264	0.0517	0.0076	0.1139	0.6160	0.0118	0.0395
	D4	0.0069	0.0117	0.0666	0.0991	0.0181	0.0673	0.3277	1.6297	1.6297	0.5429	0.8923	0.3022	0.0396
AO Dissolved Seawater (pg L ⁻¹)	D5	0.1569	0.3650	0.6209	0.1501	nd	0.6516	0.2559	0.7847	2.1459	0.5685	0.2013	0.1979	0.1023
	D6	0.0540	0.0358	0.1891	0.0473	0.0331	0.5853	0.4088	0.3620	0.0000	0.5364	1.5109	0.3017	0.5304
	D7	0.0194	0.0065	0.0156	0.0096	0.0108	0.0125	0.1116	0.0092	0.0570	0.3460	0.2579	0.0041	0.0121
	D8	0.0234	0.0051	0.0008	0.3012	0.0041	0.0025	0.0722	0.0016	0.0152	0.5183	0.4456	0.0196	0.0048
GC Seawater Particulate (pg L ⁻¹)	P1	nd	nd	0.9496	0.0179	0.6540	1.6126	nd	0.4412	7.5209	0.8824	0.0802	1.7382	nd
	P2	2.9887	0.1420	0.8151	0.7904	0.4569	2.8281	0.4666	1.9373	19.8396	2.5338	nd	6.1072	nd
	P3	0.7412	0.0977	0.7757	0.4712	0.7182	4.3610	0.7719	2.7069	31.9783	4.4875	nd	11.3576	nd
	P4	1.4764	0.0865	0.6111	0.7033	0.3786	1.4115	0.1284	0.6818	9.7154	0.7689	nd	1.4256	nd
AO Seawater Particulate (pg L ⁻¹)	P5	0.1385	nd	0.7914	0.0923	0.0133	1.1805	nd	0.3907	4.9800	0.3907	nd	0.7060	nd
	P6	0.7558	0.2083	0.9347	0.3662	0.3021	1.3540	3.3657	1.9163	2.7796	0.2237	0.0608	0.5958	nd
	P7	0.9420	0.4098	0.5558	0.4380	1.5119	0.4474	1.2041	8.7425	1.0745	0.0836	1.8271	nd	nd
	P8	0.5906	0.2544	0.4488	0.0352	0.6201	1.5116	0.3860	0.0927	4.7398	0.4087	0.1675	1.0416	nd
GC Phytoplankton (ng g ⁻¹)	F1	3.0288	0.6706	1.7100	0.0310	nd	1.8944	nd	0.7963	3.4786	0.2235	0.3493	1.1486	nd
	F2	2.8487	1.3018	0.9467	1.0651	0.8115	3.8123	nd	nd	4.5139	1.6484	5.1226	2.6796	nd
	F3	nd	nd	3.9747	nd	3.5138	1.6014	nd	nd	1.6475	nd	nd	0.2650	nd
	F4	2.0751	0.7096	0.7064	0.8294	0.0126	2.2700	0.6023	0.8515	4.9795	1.0218	1.8795	1.9584	0.5866
AO Phytoplankton (ng g ⁻¹)	F5	3.0092	1.5229	3.4373	0.2997	3.2905	2.2966	nd	nd	8.0122	10.7523	0.0917	2.5199	nd
	F6	3.3572	3.6738	1.9892	0.9797	10.0657	3.2557	nd	0.6780	11.6249	1.2963	2.5329	5.4122	1.0573
	F7	18.8591	1.6275	9.4631	0.5034	nd	7.1644	1.1577	0.5537	18.3054	2.7013	0.9060	1.6611	0.0336
	F8	2.1006	1.4004	2.2288	1.2327	2.5937	5.2071	1.4103	0.4043	3.6785	0.1972	1.2623	1.7357	0.3353
AO Phytoplankton (ng g ⁻¹)	F9	4.1143	2.8286	2.2000	3.5714	6.8857	5.6000	3.9714	1.6000	8.8571	1.9143	0.4000	4.0286	0.2000
	F10	5.4146	0.9634	1.8171	0.9756	nd	3.1098	nd	6.5244	1.0976	7.8902	0.5976	1.1098	nd
	F11	1.9760	1.9087	0.4790	0.3219	2.4476	1.7066	0.4566	0.3293	4.3114	0.2320	0.6362	1.3473	0.0299
	F12	3.1408	2.2599	1.7040	1.2202	0.0000	4.3971	1.1552	2.2744	12.3610	1.6895	3.0036	5.5307	1.2058
F13	1.3673	1.7558	0.9284	0.7518	0.9072	2.4672	0.6660	0.8375	8.6731	1.0141	1.9273	4.0616	0.8123	

Supplementary Table S1b. Concentrations of PCBs in the different sampled matrixes of PCBs in the gas, aerosol, dissolved, particles and phytoplankton phases during our sampling cruise. GC: Greenland Current AO: Artic Ocean nd: not detected

Sample Type	Sample	PCB153	PCB132/105	PCB138	PCB158	PCB187	PCB183	PCB128	PCB177	PCB171/156	PCB180	PCB191	PCB169	PCB170	PCB201/199	ΣPCBs	ΣPCBs _{Res}
GC Atmospheric Gas (pg m ⁻³)	G1	4.2986	6.3117	3.3870	nd	3.3270	6.3370	nd	0.0600	0.4051	3.4471	5.9357	0.8041	0.7441	88.5403	28.7085	
	G2	3.1779	0.7705	0.4742	0.6656	1.3630	0.4488	0.0882	0.0548	0.1144	1.1152	6.8912	0.8697	0.3535	0.1676	37.9800	11.0842
	G3	0.5046	nd	0.1124	nd	0.1826	nd	nd	nd	nd	nd	nd	nd	nd	nd	15.6901	7.7509
AO Atmospheric Gas (pg m ⁻³)	G4	0.6134	nd	0.5378	0.1066	0.2047	0.0300	nd	nd	0.0077	nd	0.1840	nd	0.0029	nd	12.9337	3.2853
	G5	0.1988	nd	1.0118	0.0512	0.5600	0.2688	0.5006	nd	0.5741	nd	nd	nd	0.7424	nd	12.0029	3.8000
	G6	0.1972	nd	9.1210	nd	0.1595	nd	nd	nd	0.0631	nd	nd	nd	nd	nd	3.4866	0.6991
	G7	7.0321	6.6134	9.1210	nd	4.2363	3.1153	1.0747	nd	3.8412	2.2316	5.2032	1.2628	nd	nd	112.7212	47.9149
G8	0.6303	0.1709	0.9972	nd	0.2650	0.0128	nd	nd	nd	0.3451	nd	nd	nd	nd	14.9925	6.4241	
GC Atmospheric Aerosol (pg m ⁻³)	A1	nd	0.2059	0.0094	0.2527	nd	0.1871	nd	0.1871	nd	0.4913	nd	nd	nd	8.6370	1.0761	
	A2	nd	0.1333	nd	0.2624	nd	0.1541	nd	0.1583	nd	0.1583	nd	nd	nd	2.4491	0.1708	
	A3	0.4199	0.3315	0.2831	0.6189	nd	0.1879	nd	nd	nd	0.5802	0.5305	0.2597	nd	18.4499	2.6799	
	A4	0.1141	0.0183	0.0502	0.0365	1.3238	0.0959	nd	0.0137	nd	0.0548	nd	nd	nd	4.7582	1.6421	
AO Atmospheric Aerosol (pg m ⁻³)	A5	0.1059	0.0184	0.0598	0.0552	0.3130	0.0414	0.0092	0.0138	nd	0.0598	nd	nd	0.0276	0.0184	1.7842	0.6173
	A6	nd	2.6015	nd	1.3154	nd	0.0542	0.3159	nd	0.1060	nd	nd	nd	0.1081	1.10139	3.9759	nd
	A7	nd	0.1645	nd	0.1323	nd	nd	nd	0.1078	0.1040	nd	nd	nd	nd	1.3629	0.1361	
	A8	nd	0.0620	nd	0.1795	nd	nd	0.1432	nd	0.1090	nd	nd	nd	nd	1.1132	0.1090	
GC Dissolved Seawater (pg L ⁻¹)	D1	0.0586	7.5902	7.8427	1.0565	0.0849	0.3472	0.3016	nd	2.4490	0.1814	nd	0.0681	nd	37.0542	16.1931	
	D2	0.2443	0.1039	0.1332	0.0184	0.1508	0.0116	0.0030	0.0159	0.5115	0.0536	0.0991	0.0409	nd	0.0205	1.7349	
	D3	0.0053	2.4642	0.4689	0.0112	0.0003	0.0547	0.0032	0.0035	0.0035	0.5177	0.0208	0.0085	0.0144	0.0044	5.8555	
	D4	1.4511	0.0575	0.0708	0.2813	0.1413	0.1455	0.0062	1.8130	0.0406	0.0202	0.1538	nd	0.0236	0.0343	8.5590	
	D5	0.6926	0.1058	0.5970	0.0512	0.5459	0.0068	0.2115	0.0785	0.1533	0.1331	0.0205	nd	nd	0.0409	9.9000	
	D6	1.3860	1.0992	2.0615	0.0642	0.3394	0.0369	0.2848	nd	0.3305	0.1972	0.1770	0.0229	nd	12.4553	4.4423	
	D7	0.0053	0.0048	0.0788	0.0532	0.0152	0.0628	0.0006	0.0110	0.0808	0.0089	0.0005	0.0218	0.0051	0.0005	1.3343	
	D8	nd	0.8686	0.0112	nd	0.0031	0.0232	0.0005	0.0086	0.1492	0.0042	nd	nd	nd	nd	2.5855	
	D9	0.0127	0.2705	0.0020	0.0500	nd	0.0040	0.0002	0.1247	0.0103	0.0038	nd	nd	nd	nd	4.6327	
GC Seawater Particulate (pg L ⁻¹)	P1	nd	1.2001	nd	0.1822	nd	nd	0.5198	nd	0.4412	nd	nd	nd	nd	17.2865		
	P2	nd	3.4021	nd	0.3957	nd	nd	1.8783	nd	0.8860	nd	nd	nd	0.3808	50.6123		
	P3	nd	8.3985	nd	1.2608	nd	0.3345	nd	0.3294	nd	0.3294	nd	nd	nd	84.3883		
	P4	nd	0.4914	nd	0.1372	nd	nd	nd	0.3320	nd	nd	nd	nd	nd	19.4676		
AO Seawater Particulate (pg L ⁻¹)	P6	0.3012	0.2448	nd	0.0471	nd	nd	nd	nd	0.1789	nd	nd	nd	0.0000	10.2248		
	P7	0.8780	0.7651	0.3261	0.8780	nd	nd	0.0544	nd	0.1848	nd	nd	nd	0.1848	14.7416		
	P8	0.4002	0.5790	0.5790	0.0710	nd	nd	nd	nd	0.1087	nd	nd	nd	0.1714	5.0549		
	P9	0.1764	0.2703	0.3443	nd	nd	nd	nd	nd	0.3832	nd	nd	nd	0.1277	22.5399		
GC Phytoplankton (ng g ⁻¹)	F1	0.7404	1.2462	1.2098	nd	0.0028	nd	nd	nd	6.9433	nd	0.2962	2.5370	0.9276	29.9218		
	F2	1.4624	3.0685	2.7895	0.0507	0.6509	nd	nd	nd	4.1589	nd	nd	nd	nd	9.6284		
	F3	nd	1.0945	2.5576	nd	nd	nd	nd	nd	4.3664	nd	nd	1.0829	1.1060	40.8538		
	F4	1.4065	2.5670	1.6998	nd	0.3690	0.1514	0.2271	nd	5.0457	9.7603	1.6336	0.2744	2.5323	25.2419		
	F5	1.1315	3.2538	nd	nd	nd	0.6300	nd	nd	1.1988	6.4220	0.0000	0.8991	1.9327	53.6014		
	F6	3.3871	2.6941	5.3524	0.4062	0.7766	0.3166	0.9080	0.1673	3.3035	6.1290	0.1613	1.5950	0.5854	52.6972		
	F7	6.6611	1.7114	2.1980	2.6510	nd	0.0671	0.0761	nd	0.3691	0.6544	nd	nd	nd	82.3059		
	F8	1.1834	1.7554	1.5582	0.0592	1.1933	nd	0.0197	0.2268	nd	1.7258	nd	0.0099	nd	80.7383		
AO Phytoplankton (ng g ⁻¹)	F9	2.7429	3.5714	3.8286	0.2857	1.6000	nd	nd	nd	2.6857	0.3143	nd	45.9429	0.7143	35.6312		
	F10	1.3537	3.2805	3.2805	0.2439	22.5732	0.5732	nd	nd	0.2073	3.3537	0.6220	25.5854	0.0610	113.4286		
	F11	0.9506	1.6018	1.8713	0.1497	0.7859	nd	0.0299	0.1572	0.4117	0.4865	0.0898	nd	nd	89.4146		
	F12	4.0433	4.1949	5.4368	0.5632	1.1191	nd	0.7004	0.3394	11.4079	22.7998	nd	5.6029	1.2058	24.8278		
	F13	2.5530	3.5621	4.2482	0.3078	0.4490	0.1766	0.5651	0.1110	8.5166	15.8829	0.0000	4.3037	1.7306	114.9170		
															8.5271		
															55.1047		

Appendix A

Supplementary Table S2. Summary of concentrations for the different phases. Σ PCBs:

Sum of concentrations of detected PCBs, Σ PCBs_{SICES}: Sum of PCBs

28,52,99/101,138,153 and 180.

Sample Type	Σ PCBs		Σ PCBs _{SICES}	
	AVERAGE	MEDIAN (MIN-MAX)	AVERAGE	MEDIAN (MIN-MAX)
GC Atmospheric Gas	46.861	37.95 (15.701-86.932)	15.684	11.804 (7.760-28.109)
AO Atmospheric Gas	24.661	12.446 (3.487-81.734)	12.317	3.285 (0.699-47.915)
GC Atmospheric Aerosol	8.893	7.748 (1.637-17.295)	1.309	1.076 (0.171-2.680)
AO Atmospheric Aerosol	3.682	1.669 (0.709-11.014)	1.296	0.617 (0.109-3.976)
GC Dissolved Seawater	13.712	7.207 (3.379-37.054)	5.406	1.88 (1.671-16.193)
AO Dissolved Seawater	5729.000	4.657 (1.310-10.726)	2.383	1.865 (0.259-4.913)
GC Seawater Particulate	42.205	34.091 (17.286-83.349)	25.202	20.508 (10.682-49.110)
AO Seawater Particulate	14.078	13.672 (10.225-21.741)	7.210	6.723 (3.959-12.781)
GC Phytoplankton	46.597	45.83 (25.242-78.871)	18.315	17.704 (9.628-34.857)
AO Phytoplankton	75.049	79.01 (23.885-110.729)	28.386	27.371 (10.696-55.105)

Supplementary Table S3. Ancillary data for each sample. Ancillary data, location and dates for the different sampling matrix. G: gas, A: aerosol, D: dissolved seawater, P: particulate, F: phytoplankton, MCD: maximum chlorophyll depth, Rad: radiation, Press: atmospheric pressure and *u*: windspeed.

Air Sample (gas and aerosols)	Start Date	Stop Date	Start Lat °N	Final Long °E	Stop Lat °N	Stop Long °E	Volume m ³	Air Temp °C	Wind Dir °	<i>u</i> m s ⁻¹	Press atm
G1+A1	31/06/07	17/07	66.91	-23.79	68.53	-19.53	633	4.29	159.05	4.68	1.33
G2+A2	27/07	37/07	71.89	-15.22	73.91	-9.82	1259	2.17	136.76	3.20	1.34
G3+A3	6/7/07	9/7/07	77.88	2.71	80.17	11.06	1183	1.82	226.95	7.43	1.34
G4+A4	11/7/07	14/7/07	80.61	18.23	79.96	8.04	1402	2.15	200.11	4.81	1.34
G5+A5	14/7/07	17/7/07	79.96	8.04	80.56	13.16	1700	0.96	90.35	6.79	1.34
G6+A6	17/7/07	19/7/07	80.56	13.31	80.79	13.04	1379	0.43	58.40	7.67	1.33
G7+A7	23/7/07	25/7/07	80.31	7.22	78.53	-0.47	1379	0.96	35.27	7.85	1.33
G8+A8	25/7/07	26/7/07	78.53	-0.48	78.00	10.11	936	4.05	229.24	5.98	1.33
Water Samples (dissolved and particulates)	Volume L	Water Temp °C	Salinity pps	Mass g							
D1+P1	31/06/07	17/07	67.00	-22.530	69.569	-17.686	246.350	3.238	32.380	0.00279	
D2+P2	27/07	37/07	70.694	-17.108	73.919	-10.608	253.000	2.561	32.254	0.00233	
D3+P3	37/07	57/07	73.947	-10.267	77.385	-1.636	276.258	3.268	33.755	0.00239	
D4+P4	8/7/07	11/7/07	79.753	7.718	80.419	16.377	308.955	2.501	33.428	0.00233	
D5+P5	12/7/07	13/7/07	80.271	13.931	79.825	8.048	293.118	3.327	33.445	0.00231	
D6+P6	14/7/07	17/7/07	80.128	8.849	80.330	10.290	676.000	2.750	33.039	0.00114	
D7+P7	17/7/07	19/7/07	80.594	13.394	80.804	13.039	371.048	1.924	32.636	0.00186	
D8+P8	20/7/07	23/7/07	80.665	12.281	80.313	7.218	424.650	1.529	32.846	0.00162	
D9+P9	23/7/07	25/7/07	80.258	7.061	79.335	2.103	672.243	-0.464	31.684	0.00101	
Phytoplankton Samples	Time (hh:mm)	Longitude °N	Latitude °E	Biomass g	Depth m	MCD M	Rad W m ⁻²	Water T °C	Salinity pps	Conductivity mS cm ⁻¹	Fluorescence V
F1	17/07	10:50	68.49	-19.49	0.3161	45.00	327.66	3.21	32.30	29.64	nd
F2	27/07	9:30	70.73	-17.16	0.1183	30.00	257.45	2.10	31.69	28.24	nd
F3	37/07	11:00	72.95	-12.65	0.1733	36.00	224.68	3.4	31.82	28.71	0.48
F4	47/07	9:50	74.89	-7.44	0.3171	42.00	135.74	2.22	32.70	29.15	0.15
F5	67/07	9:30	78.01	2.55	0.1635	45.00	510.22	3.80	34.84	32.27	0.38
F6	77/07	12:45	78.74	3.03	0.1674	25.00	352.34	2.77	33.69	30.43	0.39
F7	97/07	12:30	80.14	11.33	0.0596	30.00	575.75	5.24	34.69	33.44	0.31
F8	107/07	9:00	80.44	15.67	0.1014	37.00	248.08	1.62	32.92	28.83	0.31
F9	117/07	17:00	80.48	16.89	0.0350	35.00	168.51	1.34	33.18	29.32	0.26
F10	157/07	10:30	79.88	8.57	0.0820	40.00	608.52	1.34	7.20	35.09	0.26
F11	197/07	13:00	80.83	13.02	0.1336	49.00	173.19	1.32	31.94	27.15	0.29
F12	237/07	11:20	79.97	3.62	0.1385	25.00	201.27	1.33	-0.83	31.53	0.34
F13	247/07	11:30	79.66	2.42	0.1982	40.00	220.00	-0.80	31.41	25.72	0.34

Appendix A

Supplementary Table S4. Predicted atmospheric residence times from atmospheric concentrations. Atmospheric residence times for each PCB congener obtained from the measured gas phase concentrations (in days) during PCB transport over the Greenland Current.

Compound	$0.943-0.195 \log K_{ow}$	R_t
	d^{-1}	d (max - min)
PCB18	0.24	4.2 (6.5-3.1)
PCB17	0.28	3.6 (4.9-2.8)
PCB31	0.29	3.5 (4.6-2.8)
PCB28	0.24	4.1 (6.1-3.1)
PCB52	0.29	3.5 (4.6-2.8)
PCB49	0.36	2.7 (3.2-2.4)
PCB44	0.34	2.9 (3.5-2.5)
PCB87	0.38	2.6 (3.0-2.3)
PCB151	0.49	2.1 (2.2-1.9)
PCB153	0.57	1.8 (1.8-1.7)
PCB138	0.69	1.5 (1.5-1.4)
PCB187	0.68	1.5 (1.5-1.5)
PCB183	0.92	1.1 (1.2-1.0)
PCB171/156	0.79	1.2 (1.3-1.2)
PCB191	0.87	1.2 (1.2-1.1)
PCB170	0.85	1.2(1.2-1.1)

Supplementary Table S5. Averaged summer sinking fluxes. Averaged summer sinking fluxes estimated using the sinking fluxes for biogenic matter proposed by Bauerfiend et al., 2009 for the Arctic Ocean. uc: unable to calculate due to concentrations in the phytoplankton below quantification limit.

	Averaged												
Summer Estimated Sinking Flux (ng m ⁻² d ⁻¹)	PCB18	PCB17	PCB31	PCB28	PCB33	PCB52	PCB49	PCB44	PCB99/101	PCB87	PCB110	PCB82	PCB151
F1	0.2423	0.0536	0.1368	0.0825	Uc	0.1516	uc	0.0637	0.2783	0.0179	0.0279	0.0916	uc
F2	0.2279	0.1041	0.0757	0.0852	0.0649	0.3050	uc	uc	0.3611	0.1319	0.4098	0.2144	uc
F3	uc	uc	0.3180	uc	0.2811	0.1281	uc	uc	0.1318	uc	uc	0.0212	uc
F4	0.1660	0.0568	0.0565	0.0664	0.0010	0.1774	0.0482	0.0681	0.3984	0.0817	0.1504	0.1567	0.0469
F5	0.2407	0.1218	0.2750	0.0240	0.2632	0.1037	uc	uc	0.6410	0.8602	0.0073	0.2016	uc
F6	0.2686	0.2939	0.1591	0.0784	0.8053	0.2605	uc	0.0540	0.9300	0.1037	0.2026	0.4330	0.0846
F7	1.5087	0.1302	0.7570	0.0403	Uc	0.5732	0.0926	0.0443	1.4644	0.2161	0.0725	0.1329	0.0027
F8	0.1680	0.1120	0.1783	0.0986	0.2075	0.4166	0.1128	0.0323	0.2943	0.0158	0.1010	0.1389	0.0268
F9	0.3291	0.2263	0.1760	0.2857	0.5509	0.4480	0.3177	0.1280	0.7086	0.1531	0.0320	0.3223	0.0160
F10	0.4332	0.0771	0.1454	0.0780	Uc	0.2488	uc	0.5220	0.0878	0.6312	0.0478	0.0888	uc
F11	0.1581	0.1527	0.0383	0.0257	0.1958	0.1365	0.0365	0.0263	0.3449	0.0186	0.0509	0.1078	0.0024
F12	0.2513	0.1808	0.1363	0.0976	Uc	0.3518	0.0924	0.1819	0.9889	0.1352	0.2403	0.4425	0.0965
F13	0.1094	0.1405	0.0743	0.0601	0.5526	0.1974	0.0533	0.0670	0.6938	0.0811	0.1542	0.3249	0.0650
Summer Estimated Sinking Flux (ng m ⁻² d ⁻¹)	PCB153	PCB132/105	PCB138	PCB158	PCB187	PCB183	PCB128	PCB177	PCB171/156	PCB180	PCB169	PCB201/199	
F1	0.0592	0.0997	0.0968	uc	0.0002	uc	uc	uc	0.5555	uc	0.2030	0.0279	
F2	0.1170	0.2455	0.2232	0.0041	0.0521	uc	uc	uc	0.3327	uc	uc	uc	
F3	uc	0.0876	0.2046	uc	Uc	uc	uc	uc	0.3493	uc	0.0866	uc	
F4	0.1125	0.2054	0.1360	uc	0.0295	0.0121	0.0182	uc	0.4037	0.5452	0.1307	0.2026	
F5	0.0905	0.2603	Uc	uc	Uc	uc	0.0504	uc	0.0959	0.5138	0.0719	uc	
F6	0.2710	0.2155	0.4282	0.0325	0.0621	0.0253	0.0726	0.0134	0.2643	0.4903	0.1276	0.2241	
F7	0.5329	0.1369	0.1758	0.2121	Uc	uc	0.0054	uc	uc	0.0295	uc	uc	
F8	0.0947	0.1404	0.1247	0.0047	0.0955	uc	0.0016	0.0181	uc	0.1381	0.0008	0.0355	
F9	0.2194	0.2857	0.3063	0.0229	0.1280	uc	uc	uc	0.2149	0.0251	3.6754	uc	
F10	0.1083	0.0224	0.2624	0.0195	1.8059	0.0459	uc	uc	0.0166	0.2683	2.0468	0.0137	
F11	0.0760	0.1281	0.1497	0.0120	0.0629	uc	0.0024	0.0126	0.0329	0.0389	uc	0.0096	
F12	0.3235	0.3356	0.4349	0.0451	0.0895	uc	0.0560	0.0271	0.9126	1.8224	0.4482	0.6822	
F13	0.2042	0.2850	0.3399	0.0246	0.0359	0.0141	0.0452	0.0089	0.6813	1.2706	0.3443	uc	

Appendix A

Supplementary Table S6. Diffusive net air-water flux estimations for PCBs. Compound specific net air-water diffusive fluxes for PCBs and for each sampling period. Negative values indicates net deposition flux and positive values indicates water-to-air net volatilization flux . uc: unable to calculate due to lack of concentrations in one of the two phases.

Net Flux (ng m ⁻² d ⁻¹)	PCB18	PCB17	PCB31	PCB28	PCB33	PCB52	PCB49	PCB44	PCB99/101	PCB87	PCB110	PCB82	PCB151
G1+D1	-2.125	0.318	0.186	1.138	-0.988	-0.974	uc	uc	0.019	0.076	uc	uc	-0.013
G2+D2	-0.236	-0.116	-0.078	-0.367	-0.126	-0.243	0.000	-0.705	Uc	-0.118	uc	uc	-0.023
G2+D3	-0.226	-0.118	-0.051	-0.253	-0.127	-0.257	-0.003	-0.684	Uc	-0.112	uc	uc	-0.023
G3+D4	-1.659	uc	-0.087	0.027	uc	-2.468	0.104	0.148	Uc	uc	uc	uc	0.029
G4+D4	-0.202	-0.092	uc	-0.144	uc	uc	-0.538	0.260	0.006	0.144	0.331	0.111	-0.001
G4+D5	-0.145	0.043	uc	-0.118	uc	uc	-0.538	0.005	0.793	0.090	0.076	0.076	0.029
G5+D6	-0.218	-0.287	-0.006	0.011	uc	uc	0.065	-0.187	0.005	0.203	uc	uc	0.104
G6+D7	0.001	-0.002	-0.054	-0.083	-0.034	uc	-0.270	-0.420	0.018	uc	uc	uc	uc
G7+D8	-0.057	uc	-0.054	uc	uc	uc	-0.036	-0.015	Uc	uc	uc	uc	-1.178
G8+D8	-0.538	uc	-0.408	-0.357	uc	-0.736	-0.203	-0.545	Uc	0.299	uc	uc	-0.020
G8+D9	0.359	0.624	0.401	-0.359	uc	-0.519	2.239	-0.313	Uc	1.692	uc	uc	0.321
Net Flux (ng m ⁻² d ⁻¹)	PCB153	PCB132/105	PCB138	PCB158	PCB187	PCB183	PCB128	PCB177	PCB171/156	PCB180	PCB169	PCB201/199	
G1+D1	-0.858	2.455	2.000	uc	-0.274	-0.480	Uc	uc	0.765	-0.417	uc	-0.020	
G2+D2	-0.351	-0.022	-0.021	-0.039	-0.037	-0.021	-0.007	0.000	0.085	-0.078	-0.090	-0.002	
G2+D3	-0.377	0.487	0.042	-0.039	-0.066	-0.011	-0.007	-0.003	0.090	-0.081	-0.091	-0.005	
G3+D4	0.485	uc	0.006	uc	0.080	uc	Uc	uc	Uc	uc	uc	uc	
G4+D4	0.254	uc	-0.070	0.096	0.037	0.055	Uc	uc	0.001	uc	uc	uc	
G4+D5	0.066	uc	0.113	0.009	0.214	-0.0002	Uc	uc	0.043	uc	uc	uc	
G5+D6	0.520	uc	0.820	0.032	0.149	-0.023	0.024	uc	Uc	-0.027	uc	uc	
G6+D7	-0.076	uc	uc	uc	-0.022	uc	Uc	uc	Uc	-0.013	uc	uc	
G7+D8	-2.891	-1.023	-3.215	uc	uc	-0.745	-0.366	uc	Uc	-1.204	uc	uc	
G8+D8	-0.181	0.398	-0.145	uc	uc	0.0001	Uc	uc	Uc	-0.072	uc	uc	
G8+D9	-0.1949	2.621	1.633	uc	0.336	uc	Uc	uc	Uc	0.402	uc	uc	

Supplementary Table S7. Dry deposition flux estimations for PCBs. Estimated dry deposition of aerosol bound PCBs for each sampling period. uc: unable to calculate due to concentrations below the detection limit.

	PCB18	PCB17	PCB31	PCB28	PCB33	PCB52	PCB49	PCB44	PCB99/101	PCB87	PCB110	PCB82	PCB151
Dry Dep Flux (ng m ⁻² d ⁻¹)													
A1	uc	uc	0.1754	0.0352	0.2066	0.0146	0.0934	uc	uc	0.0271	uc	0.0020	uc
A2	uc	uc	0.0399	uc	0.0191	0.0011	0.0155	uc	uc	0.0047	uc	uc	uc
A3	0.3089	0.2893	0.0902	0.0721	0.0983	uc	0.2201	0.0215	0.0344	0.0358	0.0320	uc	uc
A4	0.0050	0.0056	0.0131	0.0038	uc	0.0482	0.0144	0.0094	0.0221	0.0075	0.0059	0.0032	0.0043
A5	0.0058	0.0034	0.0112	0.0044	uc	0.0132	0.0049	0.0039	0.0163	0.0091	0.0044	0.0008	0.0044
A6	0.0297	0.0090	0.0352	0.0395	0.0659	0.0765	0.0315	0.0485	uc	0.0072	0.0092	uc	uc
A7	uc	uc	0.0131	0.0028	uc	uc	0.0255	uc	uc	0.0028	uc	uc	uc
A8	uc	uc	0.0185	uc	uc	uc	uc	uc	uc	0.0002	uc	uc	uc
Dry Dep Flux (ng m ⁻² d ⁻¹)													
A1	uc	0.0008	0.0008	0.0218	uc	uc	0.0162	uc	0.0162	0.0005	uc	uc	uc
A2	uc	uc	uc	0.0227	uc	uc	0.0133	uc	uc	0.0002	uc	uc	uc
A3	0.0363	0.0210	0.0210	0.0535	uc	uc	0.0162	uc	uc	0.0006	0.0003	uc	uc
A4	0.0099	0.0043	0.0043	0.0032	0.1144	0.0083	uc	0.0012	uc	0.0001	uc	<0.0001	uc
A5	0.0091	0.0052	0.0052	0.0048	0.0270	0.0036	0.0008	0.0012	uc	0.0001	uc	<0.0001	uc
A6	uc	uc	uc	0.1137	uc	uc	0.0047	0.0273	uc	0.0001	uc	<0.0001	uc
A7	uc	uc	uc	0.0114	uc	uc	uc	uc	0.0093	0.0001	uc	uc	uc
A8	uc	uc	uc	0.0155	uc	uc	0.0124	uc	0.0000	0.0001	uc	uc	uc

Supplementary Table S8. Air-water fugacity ratios for PCBs. Fugacity ratio ($\log(f_{air}/f_{DMS})$) for each PCBs congener. uc: unable to calculate due to lack of concentrations in one of the two phases. Values higher than 0.47 imply a net deposition diffusive flux.

Compound	PCB18	PCB17	PCB31	PCB28	PCB33	PCB52	PCB49	PCB44	PCB99/101	PCB87	PCB110	PCB82	PCB151
G1+D1	0.402	-0.489	-0.594	-1.048	1.628	0.263	uc	uc	-0.416	-0.373	uc	uc	0.075
G2+D2	1.271	0.834	0.616	1.532	1.180	0.471	-0.420	1.309	uc	0.506	uc	uc	0.535
G2+D3	1.075	1.246	0.101	0.125	3.343	1.096	-0.197	1.327	uc	0.458	uc	uc	0.598
G3+D4	2.159	uc	0.190	-0.653	uc	1.299	-0.659	-0.617	uc	uc	uc	uc	-0.741
G4+D4	1.505	1.061	uc	0.301	uc	uc	0.322	-0.835	-0.447	-0.926	-2.165	-3.182	0.054
G4+D5	0.138	-0.442	uc	0.112	uc	uc	0.423	-0.525	-1.324	-0.767	-1.529	-3.009	-0.369
G5+D6	0.519	0.906	-0.222	-0.597	uc	uc	-0.500	-0.222	uc	-0.723	uc	uc	-0.139
G6+D7	-0.469	-0.104	0.544	0.765	0.511	uc	0.239	1.350	-0.652	uc	uc	uc	uc
G7+D8	0.186	0.486	1.770	uc	uc	uc	-0.557	1.336	uc	uc	uc	uc	2.454
G8+D8	1.312	1.430	2.784	0.366	1.335	2.344	0.504	2.395	uc	0.028	uc	uc	0.951
G8+D9	1.750	uc	1.867	0.424	uc	2.581	1.559	0.695	uc	0.021	uc	uc	1.374

Compound	PCB153	PCB132/105	PCB138	PCB158	PCB187	PCB183	PCB128	PCB177	PCB171/156	PCB180	PCB169	PCB201/199
G1+D1	1.585	-0.432	-0.367	uc	1.710	1.430	uc	uc	-0.424	2.031	uc	1.804
G2+D2	0.903	0.587	0.641	1.547	1.174	1.862	1.999	0.986	-0.360	2.224	2.492	1.833
G2+D3	2.520	-0.829	0.036	1.710	3.783	1.122	1.891	1.563	-0.434	2.538	2.837	2.401
G3+D4	-0.669	uc	0.292	uc	0.331	uc	uc	uc	uc	uc	uc	uc
G4+D4	-0.584	uc	0.972	-0.456	0.381	-0.408	uc	uc	0.627	uc	uc	uc
G4+D5	-0.281	uc	0.022	0.262	-0.232	0.893	uc	uc	0.022	uc	uc	uc
G5+D6	-0.996	uc	-0.141	-0.037	0.522	1.229	0.885	uc	uc	1.501	uc	uc
G6+D7	1.447	uc	uc	uc	1.373	uc	uc	uc	uc	1.956	uc	uc
G7+D8	uc	0.654	3.081	uc	3.439	2.496	3.991	uc	uc	4.003	uc	uc
G8+D8	uc	0.048	1.908	uc	2.243	0.362	uc	uc	uc	2.962	uc	uc
G8+D9	1.582	0.057	2.683	uc	uc	0.966	uc	uc	uc	3.050	uc	uc

Supplementary Table S9. Limits of Quantification and limits of detection for studied PCBs. DL:Limit of detection, QL: Limit of quantification

ng on column	GAS		AEROSOL		DISSOLVED		PARTICULATE		PHYTOPLANKTON	
	DL	QL	DL	QL	DL	QL	DL	QL	DL	QL
PCB18	0.055	0.139	0.011	0.026	0.008	0.012	0.016	0.036	0.051	0.124
PCB17	0.015	0.029	0.010	0.026	0.016	0.039	0.029	0.078	0.033	0.079
PCB31	0.036	0.093	0.004	0.007	0.007	0.019	0.004	0.008	0.056	0.153
PCB28	0.034	0.090	0.004	0.008	0.003	0.004	0.009	0.022	0.018	0.046
PCB33	0.021	0.049	0.026	0.071	0.009	0.020	0.021	0.054	0.047	0.122
PCB52	0.016	0.035	0.008	0.016	0.024	0.060	0.010	0.018	0.031	0.074
PCB49	0.016	0.035	0.048	0.134	0.007	0.011	0.033	0.078	0.013	0.018
PCB44	0.017	0.038	0.008	0.017	0.045	0.121	0.010	0.018	0.024	0.046
PCB99/101	0.013	0.021	0.024	0.062	0.036	0.086	0.057	0.144	0.068	0.187
PCB87	0.008	0.016	0.013	0.035	0.016	0.035	0.026	0.066	0.013	0.018
PCB110	0.004	0.005	0.007	0.018	0.004	0.004	0.007	0.012	0.033	0.082
PCB 82	0.018	0.047	0.007	0.018	0.006	0.012	0.009	0.020	0.023	0.046
PCB151	0.016	0.037	0.016	0.044	0.012	0.024	0.007	0.007	0.015	0.026
PCB153	0.014	0.022	0.017	0.044	0.013	0.025	0.009	0.011	0.022	0.061
PCB132/105	0.010	0.017	0.008	0.018	0.005	0.005	0.009	0.015	0.015	0.023
PCB138	0.008	0.014	0.005	0.009	0.007	0.013	0.002	0.004	0.017	0.037
PCB158	0.009	0.023	0.005	0.012	0.005	0.011	0.009	0.020	0.010	0.018
PCB187	0.004	0.005	0.004	0.009	0.008	0.020	0.009	0.020	0.011	0.017
PCB183	0.027	0.070	0.005	0.009	0.008	0.020	0.004	0.008	0.027	0.065
PCB177	0.071	0.112	0.002	0.002	0.207	0.585	0.002	0.004	0.020	0.051
PCB171/156	0.009	0.015	0.002	0.002	0.004	0.004	0.007	0.016	0.013	0.023
PCB180	0.007	0.014	0.002	0.002	0.005	0.011	0.167	0.465	0.015	0.037
PCB191	0.025	0.061	0.010	0.019	0.003	0.003	0.013	0.033	0.023	0.041
PCB169	0.016	0.021	0.005	0.009	0.016	0.040	0.007	0.016	0.010	0.018
PCB170	0.009	0.010	0.003	0.004	0.005	0.011	0.004	0.009	0.010	0.018
PCB201/199	0.008	0.014	0.004	0.009	0.005	0.011	0.007	0.016	0.013	0.023

Appendix A

Supplementary Table S10. Physicochemical properties. Values of octanol-water partition coefficients, Henry's Law constant and enthalpy of phase change for PCBs reported in the literature and used in this study.

Compound	Log Kow 298K	Ref	AH (Kj/mol)	H (Pa·m ³ /mol) 298K	Ref
PCB18	5.600		35.0	25.3	
PCB17	5.760		39.0	32.1	
PCB33	5.870		42.0	29.2	
PCB49	6.380		25.0	39.9	
PCB87	6.370	Hansch et al. 1995 ⁴²	33.0	36.5	
PCB151	6.850		37.0	73.5	
PCB 132/105	7.040		61.0	59.4	
PCB128	7.320		118.0	32.7	
PCB171/156	7.570		101.0	37.0	
PCB31	5.780		41.0	30.7	
PCB28	5.660		33.0	36.5	
PCB52	5.910	Li et al. 2003 ⁴³	31.0	31.3	
PCB153	6.870		66.0	54.0	
PCB138	7.220		87.0	45.2	
PCB180	8.510		144.0	37.3	Bamford et al. 2002 ⁴⁹
PCB44	6.260		26.0	28.1	
PCB 82	6.730	Ran et al. 2002 ⁴⁴	42.0	40.3	
PCB183	8.270		100.0	61.5	
PCB158	7.690		80.0	49.9	
PCB99/101	6.980	Hardy. 2002 ⁴⁵	16.0	51.8	
PCB110	6.200	Sangster. 1993 ⁴⁶	38.0	42.0	
PCB187	7.046		96.0	65.9	
PCB177	6.921	Makino. 1998 ⁴⁷	112.0	50.6	
PCB191	7.325		149.0	28.8	
PCB169	7.010	Yeh & Hong. 2002 ⁴⁸	162.0	23.4	
PCB201/199	7.320		145.0	97.5	

Appendix A.3: Supplementary Methods

Supplementary Method S1: Atmospheric transport statistical analysis and Regression analysis

In order to investigate the differences of the gas phase concentrations at different times (C_t as C_0 , $C_{2,3}$, $C_{3,6}$ and $C_{4,5}$) during the Greenland current transect, were all samples are influenced by the same Air Mass from the SW (See Fig S2a and S2b), the non-parametric Friedman test for dependent variables was performed. Travelling times of the dominant air mass during all the transects were considered as the independent variable and the compound concentrations as the dependent. Differences were observed for the four sampling points ($p < 0.0005$). Observed concentrations in C_0 are higher than observed concentrations in $C_{2,3}$, $C_{3,6}$ and $C_{4,5}$ (Wilcoxon test $p < 0.05$), Concentrations in $C_{2,3}$ are higher than observed in $C_{3,6}$ and $C_{4,5}$ and (Wilcoxon test $p < 0.05$) and $C_{3,6}$ and $C_{4,5}$ did not differ among them (Wilcoxon test $p = 0.074$).

Atmospheric concentration decay was modeled in the classical form following the equation:

$$C_t = C_0 e^{-\frac{t}{R_t}} \quad [\text{A.1}]$$

Where C_0 and C_t are the initial and final concentrations (ng m^{-3}), t is the time in days (d) and R_t^{-1} is the decay rate, while R_t is the residence time in the atmosphere. Then:

$$\ln C_t = \ln C_0 - \frac{t}{R_t} \quad [\text{A.2}]$$

Thus, a correlation matrix was done between the natural logarithm of the concentrations in each sample ($\ln C_t$), the sampling time transpired from the “source point” (first sampling station) in days (t), the temperature corrected octanol-water partition constant in logarithmic form ($\text{Log}K_{ow}$) and the product of $\text{Log}K_{ow}$ and t ($t\text{Log}K_{ow}$). The correlation matrix showed that the $\ln C_t$ was correlated with all the mentioned variables ($p < 0.001$) when only one variable was introduced in the least square regression. Conversely, multiple parameter least squares linear regressions were tested using the three descriptors (t , $\text{Log}K_{ow}$, $t\text{Log}K_{ow}$), revealing that only t and $t\text{Log}K_{ow}$ fitting parameters were significative ($p < 0.001$). The obtained equation was

$$\ln C_t = 0.943t - 0.195t\text{Log}K_{ow} - 5.687 \quad [\text{A.3}]$$

Appendix A

thus:

$$C_t = LnC_0 e^{(0.943-0.195LogK_{ow})t} \quad [A.4]$$

Where the independent term equals to LnC_0

$$LnC_0 = -5.687$$

Comparing equation1 (A.1) with (A.4) results that the residence time (inverse of decay rate constant) R_t^{-1} is defined in the transect as follows:

$$-\frac{t}{R_t} = (0.943-0.195LogK_{ow})t \quad [A.5]$$

thus

$$R_t = \frac{1}{-0.943+0.195LogK_{ow}} \quad [A.6]$$

The estimated atmospheric residence times for each studied compound are shown in Supplementary Table S4 (See Appendix A.4) and in Figure 2 of the main text.

Supplementary Method S2: Estimation of air-water diffusive exchange and dry deposition fluxes of PCBs

Diffusive air-water exchange (F_{AW}) of individual PCB congeners was calculated in the traditional manner by:

$$F_{AW} = k_{AW} \left(\frac{C_G}{H'} - C_W \right) \quad [A.7]$$

Where C_G and C_W are the gas- and dissolved-phase PCB concentrations, respectively, H' is the dimensionless Henry's Law constant corrected for temperature and salinity as described above, and k_{AW} is the air-water mass transfer coefficient. k_{AW} may be estimated as the result of transfer through two layers at each side of the air-water interface:

$$\frac{1}{k_{AW}} = \frac{1}{k_A H'} + \frac{1}{k_W} \quad [A.8]$$

Where k_A and k_W are the POP mass transfer coefficients ($m\ d^{-1}$) in the air and water films, respectively. k_W may be calculated from the mass transfer coefficient of CO_2 in the water side (k_{w,CO_2} , $m\ d^{-1}$), which is a function of wind speed at 10 m height (U_{10} , $m\ s^{-1}$).

$$k_{w,CO_2} = k_{w,CO_2} U_{10}^2 + 0.061 U_{10} \quad [A.9]$$

$$k_W = k_{w,CO_2} \left(\frac{Sc_{POP}}{600} \right)^{-0.5} \quad [A.10]$$

Where Sc_{POP} is the Schmidt number of the POP and 600 accounts for the Schmidt number of CO_2 at 298K, respectively. Similarly, k_A may be estimated from the mass transfer coefficient of H_2O in the air side (k_{A,H_2O} , $m\ d^{-1}$) that is also dependent on the wind speed

$$k_{A,H_2O} = 0.2 U_{10} + 0.3 \quad [A.11]$$

$$k_A = k_{A,H_2O} \left(\frac{D_{POP,a}}{D_{H_2O,a}} \right)^{0.61} \quad [A.12]$$

Where $D_{POP,a}$ and $D_{H_2O,a}$ are the diffusivity coefficients of the POP and H_2O in air, respectively. From equations A.9-A.12, it is obvious that wind speed has a great influence on the magnitude of k_{AW} . On the other hand, temperature influences the magnitude of k_{AW} through its influence on diffusivities, Schmidt numbers and H' . The nonlinear influence of wind speed on k_W has been considered by estimating the weibul parameters of the wind speed distribution, and correcting the equation A.9 following Simó & Dachs 2002⁵⁰.

Appendix A

In order to estimate the air-water fugacity ratios and diffusive exchanges it is important to have accurate values of the Henry's Law Constant (H). It is difficult to establish which of the experimental or observational values presented in the bibliography for the H are the best option^{49,51-56} (i.e Burkhard et al., 1985, Bamford et al., 2000, 2002; ten Huschler et al., 1992, 2006; Tateya et al., 1998; Gioia et al., 2010). In any case, it is important that all the H values for the PCB congeners are consistent among them. In this study, we use the H values proposed by Bamford et al.^{49,52}, (Supplementary Table S10). Another important issue is the enthalpy of phase change used, ΔH_H , since the reported H values are referred to 25°C and sampling temperature ranged from -0.5 to 3.5 °C, a moderate change in these enthalpies induce a significant change in the H values at low temperatures. The ΔH_H selection values were those published on Bamford et al., 2002⁴⁹. Values reported in the most recent papers are higher than those reported previously⁵⁵ (Tateya et al., 1988) which assumed a constant value of ΔH_H for all 209 PCB congeners (28 KJ mol⁻¹). The Bamford et al., 2002⁴⁹ study proposed values for ΔH_H under the 30 KJ mol⁻¹.for few compounds and are higher for other compounds. Zhang⁵⁷ proposed a higher value of 49.9 KJ mol⁻¹ obtained from the experimental results published in ten Hulscher et al., 1992⁵³ for PCBs 9, 28 and 52. Following the recommendations proposed by Totten et al., 2003⁵⁸ we choose the ΔH_H values from Bamford et al., 2002⁴⁹. Other studies have shown lower enthalpies, which would lead to higher HLC at the field temperatures than those used here. The H term introduce an important uncertainty on the estimation of the fugacity gradients and fluxes, which is about 2-3 orders of magnitude.

Therefore, H values were corrected for temperature (equation A.13) and salinity following Schwarzenback et al., 1993⁵⁹. For the T correction we used the surface water temperature^{58,60-61}.

$$\frac{H_{T_0}}{H_{298.15}} = e^{\left[\frac{-\Delta U_{AW}}{R} \left(\frac{1}{T_w} - \frac{1}{298.15} \right) \right]} \quad [A.13]$$

Where H_{T_0} , $H_{T_{298.15}}$ and $H_{T_{0S}}$ are the HLC value temperature corrected, the HLC at 298K and HLC corrected by temperature and salinity, $-\Delta U_{AW}$ is heat of phase change (KJ mol⁻¹) and R is the ideal gas constant (KJ mol⁻¹ K⁻¹). With the temperature and salinity corrected H , H' was calculated following:

$$H' = \frac{H_{T_{0S}}}{RT} \quad [A.14]$$

Appendix A

Where H_{ToS} from equation 9 is the temperature and salinity corrected value of HLC in KJ, T represents the temperature (K) of the water surface and R is the ideal gas constant in KJ mol⁻¹ K⁻¹. Selected values for the different physico-chemical properties are summarized on Supplementary Table S10 on appendix A.3

Dry deposition (F_{DD}) of aerosol bound PCB congeners was estimated as

$$F_{DD} = v_D C_A \quad [A.15]$$

Where C_A is the aerosol phase individual PCB concentrations, and v_D is the deposition velocity of aerosols. There are very few measurements in the literature, and the only field determination of v_D values were made in the field are for the subtropical Atlantic ⁶². This study showed that v_D had a value of 0.1 cm s⁻¹ except in high wind conditions. Therefore, in this study we assume 0.1 cm s⁻¹ as deposition velocity for aerosol bound PCBs.

Appendix A

Supplementary Method S3

Estimation of fugacity ratios

Fugacity gives information about the escaping tendency of a compound from one matrix to another adjacent matrix. Fugacity is widely used as equilibrium criteria, thus if the fugacity in water equals the fugacity in air, then there is air-water equilibrium. For the gas phase and dissolved phase fugacities are given by:

$$f_{Gas} = \frac{C_{Gas}}{MW} RT \quad [A.16]$$

$$f_{Dis} = \frac{C_{Dis}}{MW} H' RT \quad [A.17]$$

Where f_{Gas} and f_{Dis} represent the fugacity in the gas phase and water dissolved phase, which have units of pressure (Pa). C_{Gas} and C_{Dis} are the concentrations in the gas phase and the water dissolved phase in $g\ m^{-3}$, R is the ideal gas constant in $Pa\ m^3\ mol^{-1}\ K^{-1}$, T is the temperature of the surface water (K) and finally H' is the dimensionless temperature and salinity corrected *HLC*. Then the fugacity quotient was obtained by f_{Gas}/f_{water} , which is dimensionless and represents the ratio between fugacity in the dissolved phase and the gas phase. The fugacity ratio provides the direction of the air-sea net exchange²⁰ and depends on H values, as discussed elsewhere^{61,63-65} and above. Due to the uncertainties in the H values, usually a factor of 3 is considered as the uncertainty of the fugacity ratios, thus a value >0.47 ($\log 3$) indicates net deposition, a value <-0.52 ($\log 0.3$) indicates net volatilization and a fugacity ratio between $\log 0.3$ to $\log 3$ indicates that air and water are close to equilibrium. Supplementary Table S8 (See appendix A.2) shows the fugacity ratios for this study, and most of them are higher than 0.47, thus pointing to a net deposition of PCBs in the Greenland current and Arctic Ocean.

Additional References

42. Hansch, C., Leo, A.J., Hoekman, D. *Exploring QSAR, Hydrophobic, Electronic, and Steric Constants*. ACS Professional Reference Book, American Chemical Society, Washington, DC (1995)
43. Li, N., Wania, F., Lei, Y.D., Daly, G.L. A comprehensive and critical compilation, evaluation, and selection of physical- chemical property data for selected polychlorinated biphenyls. *J. Phys. Chem. Ref. Data* 32, 1545–1590 (2003)
44. Ran, Y., He, Y., Hang, G., Johnson, J.L.H., Yalkowsky, S.H. Estimation of aqueous solubility of organic compounds by using the general solubility equation. *Chemosphere* 48, 487–509 (2002)
45. Hardy, M.L. A comparison of the properties of the major commercial PBDPO/PBDE product to those of major PBB and PCB products. *Chemosphere* 46, 717–728 (2002)
46. Sangster, J. *LogK_{OW}, A Databank of Evaluated Octanol-Water Partition Coefficients*. First ed., Montreal, Quebec, Canada (1993)
47. Makino, M. Prediction of *n*-octanol/water partition coefficients of polychlorinated biphenyls by use of computer calculated molecular properties. *Chemosphere* 37, 13–26 (1998)
48. Yeh, M.-F, Hong, C.-S. Octanol-water partition coefficients of non-*ortho*- and mono-*ortho*-substituted polychlorinated biphenyls. *J. Chem. Eng. Data* 47, 209–215 (2002)
49. Bamford, H. A., Ko, F. C. & Baker, J. E. Seasonal and annual air-water exchange of polychlorinated biphenyls across baltimore harbor and the northern chesapeake bay. *Environ. Sci. Technol.* **36**, 4245-4252 (2002)
50. Simó, R., and J. Dachs (2002), Global ocean emission of dimethylsulfide predicted from biogeophysical data, *Global Biogeochem.Cycles* **16**, 1078 (2002)
51. Burkhard, L. P. Estimation of vapor pressures for halogenated aromatic hydrocarbons by a group-contribution method. *Ind. Eng. Chem. Fund.* **24**, 119-120 (1985)
52. Bamford, H. A., Poster, D. L. & Baker, J. E. Henry's law constants of polychlorinated biphenyl congeners and their variation with temperature. *J. Chem. Eng. Data.* **45**, 1069-1074 (2000)
53. Ten Hulscher, T. E. M., Van der Velde, L. E., & Bruggeman, W. A. (1992). Temperature dependence of henry's law constants for selected chlorobenzenes, polychlorinated biphenyls and polycyclic aromatic hydrocarbons. *Environ. Toxicology and Chemistry.* **11**, 1595-1603 (1992)

Appendix A

54. Ten Hulscher, T. E. M., Van Den Heuvel, H., Van Noort, P. C. M., & Govers, H. A. J. (2006). Henry's law constants for eleven polychlorinated biphenyls at 20°C. *J. Chem. Eng. Data.* **51**, 347-351 (2006)
55. Tateya, S., Tanabe, S and Tatsukawa, R. PCBs on the Globe: Possible Trend of Future Levels in the Open Ocean Environment. In: N.W. Schmidtke, Ed., Toxic Contamination in Large Lakes, Lewis Publishers, Chelsea, Michigan. 237–281 (1988)
56. Gioia, R., Jones, K. C., Lohmann, R., Nizzetto, L. & Dachs, J. Field-derived henry's law constants for polychlorinated biphenyls in oceanic waters. *J. Geophys. Res-Oceans.* **115** JC005054 (2010)
57. Zhang, H. M.S. Thesis, University of Minnesota, Minneapolis, MN, (1996)
58. Totten, L. A., Gigliotti, C. L., Offenber, J. H., Baker, J. E., & Eisenreich, S. J. Reevaluation of air-water exchange fluxes of PCBs in green bay and southern lake michigan. *Environmental Science and Technology*, 37(9), 1739-1743 (2003)
59. Schwarzenbach R.P., Gschwend P.M., and Imboden D.M. Environmental organic chemistry. John Wiley & Sons. Chichester (1993)
60. Achman, D. R., Hornbuckle, K. C. & Eisenreich, S. J. Volatilization of polychlorinated biphenyls from green-bay, lake michigan. *Environ. Sci. Technol.* **27**, 75-87 (1993)
61. Bruhn, R., Lakaschus, S. & McLachlan, M. S. Air/sea gas exchange of PCBs in the Southern Baltic Sea. *Atmos. Environ.* **37**, 3445-3454 (2003).
62. Del Vento, S., Dachs, J. Atmospheric occurrence and deposition of polycyclic aromatic hydrocarbons in the NE tropical and subtropical Atlantic ocean. *Environ. Sci. Technol.* **41**, 5608-5613 (2007)
63. Hoff, R. M. An error budget for the determination of the atmospheric mass loading of toxic chemicals in the great lakes. *J. Great Lakes Res.* **20**, 229-239 (1994)
64. Hillery, B. R., et al. Atmospheric deposition of toxic pollutants to the great lakes as measured by the integrated atmospheric deposition network. *Environ. Sci. Technol.* **32**, 2216-2221 (1998)
65. Mackay, D., & Bentzen, E. The role of the atmosphere in great lakes contamination. *Atmos. Environ.*, **31** 4045-4047 (1997).

Appendix B
Supporting information to Chapter 4.
The “degradative” and “biological” pumps
controls on the atmospheric deposition and
sequestration of hexachlorocyclohexanes (HCHs)
and hexachlorobenzene (HCB) in the North
Atlantic and Arctic Oceans

Appendix B.1: Ancillary data and methods

Table S1. Ancillary data for gas (G), aerosol (A), dissolved (D), particulate (P) and phytoplankton (F) samples during ATOS I cruise. Maximum Chlorophyll Depth (DCM)...251

Table S2. Detection and Quantification Limits (DL and QL) for the studied matrixes during the ATOS I cruise...252

Table S3. Average recoveries of the surrogate PCB 65 for the samples from the ATOS I cruise...252

Appendix B.2: Concentrations of HCHs and HCB for the gas, aerosol, dissolved, particulate and phytoplankton phases, and comparison with previous reports.

Table S4a. Concentrations of HCHs and HCB in the dissolved and particulate phases (pg L^{-1}) from the Greenland Current (GC) and Arctic Ocean (AO) sampling events...253

Table S4b. Concentrations of HCHs and HCB in the phytoplankton phase samples (ng g^{-1}) from the Greenland Current (GC) and Arctic Ocean (AO) sampling events...253

Table S4c. Concentrations of HCHs and HCB in the gas and aerosol phase samples (pg m^{-3}) from the Greenland Current (GC) and Arctic Ocean (AO) sampling events...253

Table S5a. Previously reported concentrations of α -HCH and γ -HCH in the gas and dissolved phases for the Arctic region...254

Table S5b. Previously reported concentrations of HCB in the gas, dissolved and particulate phase for the Arctic region...255

Figure S1. Latitudinal distribution of the concentrations of α -HCH, γ -HCH and HCB in the gas, aerosol, dissolved, particulate and phytoplankton phases along the Greenland Current and the Arctic Ocean...256

Appendix B.3 Back-trajectories of the air masses during the sampling cruise.

Appendix B

Figure S2a. Backtrajectories of the air masses estimated for the ATOS I samples G1+A1 (A), G2+A2(B), G3+A3(C) and G4+A4 (D)...257

Figure S2b. Backtrajectories of the air masses estimated for ATOS I samples G5+A5 (E), G6+A6(F), G7+A7(G) and G8+A8 (H)...258

Appendix B.4 Concentrations of HCHs and HCB for the gas, aerosol, dissolved, particulate and phytoplankton phases, and comparison with previous reports.

Table S6. Physical-chemical constants used for the estimations of the fugacities, fluxes and correlations in the present study...259

Table S7. Estimations of water-air fugacity ratios (f_w/f_a), air-water diffusive fluxes (F_{AW}), dry deposition fluxes (F_{DD}) and Sinking fluxes (F_{SINK}) for each one of the sampling events of the ATOS I cruise...260

Table S8. Estimated Bioconcentration Factor (BCFs, $L\ Kg^{-1}$) from the concentrations in the dissolved and phytoplankton phases during the ATOS I cruise...261

Table S9. Total degradation flux ($ng\ m^{-2}\ d^{-1}$) for α -HCHs and γ -HCH...262

Table S10. Comparison of the degradation and sinking fluxes with atmospheric inputs...262

Figure S3. Water-air fugacity ratios for α -HCH, γ -HCH and HCB...263

Figure S4. Box-Plot comparing the measured LogBCF ($L\ Kg^{-1}$) for the studied compounds with the temperature corrected Log K_{OW} ...264

Figure S5. Mass Balance for HCB during ATOS I cruise...265

Figure Surface chlorophyll concentrations in the North Atlantic and Arctic ocean for the sampling period (July 2007)...266

Additional References...267

Appendix B.1: Ancillary data and methods

Table S1. Ancillary data for gas (G), aerosol (A), dissolved (D), particulate (P) and phytoplankton (F) phase samples during the ATOS I cruise. Initial (start) and final (stop) position and date are given for samples taken during transects. DCM stands for Maximum Chlorophyll Depth.

Sample	Start Date	Stop Date	Start Location °N °E	Final Location °N °E	Volume m ³	Air Temperature °C	Wind Direction °	Wind Speed m s ⁻¹	Pressure atm				
G1+A1	31/06/07	01/07/07	66.91 -23.79	68.53 -19.53	633	4.29	159.05	4.68	1.33				
G2+A2	02/07/07	03/07/07	71.89 -15.22	73.91 -9.82	1259	2.17	136.76	3.20	1.34				
G3+A3	06/07/07	09/07/07	77.88 2.71	80.17 11.06	1183	1.82	226.95	7.43	1.34				
G4+A4	11/07/07	14/07/07	80.61 18.23	79.96 8.04	1402	2.15	200.11	4.81	1.34				
G5+A5	14/07/07	17/07/07	79.96 8.04	80.56 13.16	1700	0.96	90.35	6.79	1.34				
G6+A6	17/07/07	19/07/07	80.56 13.31	80.79 13.04	1379	0.43	58.40	7.67	1.33				
G7+A7	23/07/07	25/07/07	80.31 7.22	78.53 -0.47	1379	0.96	35.27	7.85	1.33				
G8+A8	25/07/07	26/07/07	78.53 -0.48	78.00 10.11	936	4.05	229.24	5.98	1.33				
Sample	Start Date	Stop Date	Start Location °N °E	Final Location °N °E	Volume L	Water Temperature °C	Salinity pps	Mass g					
D1+P1	31/06/07	01/07/07	67.00 -22.53	69.57 -17.69	246.350	3.238	32.380	0.00279					
D2+P2	02/07/07	03/07/07	70.69 -17.11	73.92 -10.61	253.000	2.561	32.254	0.00233					
D3+P3	03/07/07	05/07/07	73.95 -10.27	77.39 -1.64	276.258	3.268	33.755	0.00239					
D4+P4	08/07/07	11/07/07	79.75 7.72	80.42 16.38	308.955	2.501	33.428	0.00233					
D5+P5	12/07/07	13/07/07	80.27 13.93	79.83 8.05	293.118	3.327	33.445	0.00231					
D6+P6	14/07/07	17/07/07	80.13 8.85	80.33 10.29	676.000	2.750	33.039	0.00114					
D7+P7	17/07/07	19/07/07	80.59 13.39	80.80 13.04	371.048	1.924	32.636	0.00186					
D8+P8	20/07/07	23/07/07	80.66 12.28	80.31 7.22	424.650	1.529	32.846	0.00162					
D9+P9	23/07/07	25/07/07	80.26 7.06	79.34 2.10	672.243	-0.464	31.684	0.00101					
Sample	Date	Time	Lat °N	Lon °E	Biomass g	Depth m	DCM m	Water Temperature °C	Salinity pps	Radiation W m ⁻²	Pressure atm	Conductivity mΩ cm ⁻¹	Fluorescence V
F1	01/07/07	10:50	68.49	-19.49	0.3161	45	35	3.21	32.303	327.66	1.33	29.644	nd
F2	02/07/07	9:30	70.73	-17.16	0.1183	30	20	2.1	31.690	257.45	1.33	28.235	nd
F3	03/07/07	11:00	72.95	-12.65	0.1733	36	26	2.56	31.822	224.68	1.34	28.710	0.481
F4	04/07/07	9:50	74.89	-7.44	0.3171	42	32	2.22	32.695	135.74	1.34	29.145	0.145
F5	06/07/07	9:30	78.01	2.55	0.1635	45	36	3.8	34.836	510.22	1.35	32.271	0.383
F6	07/07/07	12:45	78.74	3.03	0.1674	25	15	2.77	33.692	332.34	1.34	30.426	0.391
F7	09/07/07	12:30	80.14	11.33	0.0596	30	20	5.24	34.692	575.75	1.34	33.435	0.313
F8	10/07/07	9:00	80.44	15.67	0.1014	37	27	1.62	32.923	248.08	1.33	28.831	0.305
F9	11/07/07	17:00	80.48	16.89	0.035	35	25	1.97	33.176	168.51	1.34	29.321	0.259
F10	15/07/07	10:30	79.88	8.57	0.082	40	30	7.2	35.092	608.52	1.34	35.582	0.259
F11	19/07/07	13:00	80.83	13.02	0.1336	49	39	0.5	31.937	173.19	1.32	27.148	0.293
F12	23/07/07	11:20	79.97	3.62	0.1385	25	15	-0.83	31.527	201.27	1.33	25.784	0.337
F13	24/07/07	11:30	79.66	2.42	0.1982	40	30	-0.8	31.406	220.00	1.33	25.722	0.342

Appendix B

Table S2. Detection and Quantification Limits (DL and QL) for the studied matrixes during the ATOS I cruise

pg on column	Gas		Dissolved		Aerosol		Particulate		Phytoplankton	
	DL	QL	DL	QL	DL	QL	DL	QL	DL	QL
α-HCH	0.01	0.04	0.01	0.01	0.02	0.04	0.01	0.03	0.01	0.03
γ-HCH	0.01	0.02	0.02	0.04	0.02	0.03	0.05	0.15	0.01	0.02
HCb	0.02	0.07	0.01	0.05	0.01	0.05	0.004	0.01	0.04	0.10

Table S3. Average recoveries of the surrogate PCB 65 for the samples from the ATOS I cruise. SD: standard deviation, min: minimum value, and max: maximum value.

		PCB 65			
		mean	sd	min	max
Recovery %	Gas	73%	12%	58%	92%
	Aerosol	75%	9%	66%	88%
	Dissolved	70%	11%	55%	88%
	Particulate	70%	8%	62%	90%
	Phytoplankton	64%	11%	47%	79%

Appendix B.2: Concentrations of HCHs and HCB for the gas, aerosol, dissolved, particulate and phytoplankton phases, and comparison with previous reports.

Tables S4a. Concentrations of HCHs and HCB in the dissolved and particulate phases ($\mu\text{g L}^{-1}$) from the Greenland Current (GC) and Arctic Ocean (AO) sampling events. The position, date and ancillary data of the samples can be found in Appendix B.1.

	GC				AO				
	D1	D2	D3	D4	D5	D6	D7	D8	D9
Dissolved ($\mu\text{g L}^{-1}$)									
α -HCH	16.505	2.502	3.428	2.135	0.051	2.112	0.974	1.823	1.462
γ -HCH	6.350	0.028	1.456	1.417	0.150	0.002	0.417	0.769	0.806
Σ_{HCHs}	22.855	2.530	4.884	3.551	0.201	2.114	1.391	2.592	2.268
HCB	4.816	2.276	0.937	1.059	2.596	0.722	1.251	0.025	1.629
Particulate ($\mu\text{g L}^{-1}$)									
α -HCH	0.824	0.624	0.552	0.562	0.607	0.256	0.499	0.351	0.381
γ -HCH	0.349	0.858	0.517	0.887	0.224	0.024	0.480	0.310	0.266
Σ_{HCHs}	1.174	1.482	1.069	1.449	0.831	0.280	0.980	0.661	0.647
HCB	0.385	0.235	0.282	0.260	0.363	0.184	0.250	0.233	0.197

Table S4b. Concentrations of HCHs and HCB in the phytoplankton phase samples (ng g^{-1}) from the Greenland Current (GC) and Arctic Ocean (AO) sampling events. The position, date and ancillary data of the samples can be found in Appendix B.1. nd: not detected

Phyto (ng g^{-1})	GC						AO						
	F1	F2	F3	F4	F5	F6	F7	F8	F9	F10	F11	F12	F13
α -HCH	0.743	1.276	3.122	0.564	1.994	0.131	0.285	0.424	1.000	0.171	0.898	0.065	0.096
γ -HCH	nd	0.592	1.613	0.416	1.798	1.278	2.131	1.558	1.343	0.549	0.891	2.455	0.873
Σ_{HCHs}	0.743	1.868	4.735	0.981	3.792	1.410	2.416	1.982	2.343	0.720	1.789	2.520	0.969
HCB	0.047	nd	nd	nd	1.443	0.203	nd	0.069	1.229	0.037	nd	0.065	nd

Tables S4c. Concentrations of HCHs and HCB in the gas and aerosol phase samples ($\mu\text{g m}^{-3}$) from the Greenland Current (GC) and Arctic Ocean (AO) sampling events. The position, date and ancillary data of the samples can be found in Appendix B.1. nd: not detected

Gas ($\mu\text{g m}^{-3}$)	GC			AO				
	G1	G2	G3	G4	G5	G6	G7	G8
α -HCH	8.962	5.520	1.172	0.506	0.395	0.182	2.969	0.374
γ -HCH	5.065	1.966	1.328	nd	0.313	0.100	0.124	0.768
Σ_{HCHs}	14.027	7.486	2.500	0.506	0.708	0.282	3.093	1.142
HCB	77.427	35.858	46.460	56.095	10.134	43.051	40.265	60.834
Aerosol ($\mu\text{g m}^{-3}$)								
α -HCH	0.430	0.325	0.519	0.022	0.011	0.050	0.214	0.308
γ -HCH	0.295		0.204	0.130	0.062	0.052	0.002	0.019
Σ_{HCHs}	0.725	0.325	0.204	0.152	0.073	0.050	0.217	0.019
HCB	0.122	0.158	0.315	0.029	0.034	0.059	0.090	0.065

Table S5a. Previously reported concentrations of α -HCH and γ -HCH in the gas and dissolved phases for the Arctic region.

Location	Year	α -HCH			γ -HCH			Ref			
		Mean	sd	Min	Max	Mean	sd		Min	Max	
Chukchi Sea	1990	270.0		240.0	300.0	28.0		26.0	29.0	Iwata et al., 1993	
Bering Sea		300.0		230.0	390.0	42.0		21.0	67.0		
Bering Sea	1993	105.0	16.0			23.0	7.0				
Canadian Archipelago	1999	45.9	12.7	23.0	73.0	9.5	1.2	3.4	10.4	Jantunen and Bidleman, 1995	
	2000	17.0		5.5	27.1	7.8		1.8	17.1	Jantunen et al., 2008	
	2001	14.2		9.8	21.1	5.1		2.6	10.8	Kallenborn et al., 2007	
	2002	14.9		3.2	22.0	4.9		1.2	9.0		
	2003	11.2		9.0	15.0	3.9		2.8	5.5		
Pacific Ocean	2003	6.5	2.6	2.1	10.7	0.8	0.4	0.2	2.1	Ding et al., 2007	
Alert		22.0		1.4	66.0	5.6		0.4	19.0	Su et al., 2006	
Kinngait		28.0		2.7	66.0	4.1		1.2	1.7		
Little Fox Lake	2000-	48.0		17.0	87.0	4.5		1.7	10.0		
Point Barrow	2003	19.0		6.0	37.0	2.7		0.9	5.8		
Valkarkai		64.0		60.0	75.0						
Zepellin		22.0		0.3	61.0	6.2		0.4	23.0		
Arctic	2004	2.7	1.4	0.3	6.5	2.2	2.3	0.4	9.3		Lohmann et al., 2009
Labrador Sea	2007	21.0	5.8			2.3	0.4				
Hudson Bay	2008	30.0	8.9			2.4	0.5				
		7.5	2.3			7.7	3.7				
Beaufort Sea	2008	16.0	2.6			2.1	0.2				
		48.0	13.0			4.6	0.7				
Greenland/Irminger Current	2008	4.9	1.2	2.9	8.9	2.2	1.8	0.6	7.5	Zhang et al., 2012	
Arctic/Pacific	2010	12.67	7.56	5.70	26.80	2.05	1.01	1.00	3.80	Cai et al., 2012	
Greenland Current	2007	5.22	3.90	1.17	8.96	2.79	2.00	1.33	5.06	This Study	
Arctic Ocean		0.9	1.17	0.18	2.97	0.33	0.31	0.10	0.77		

Location	Year	α -HCH			γ -HCH			Ref		
		Mean	sd	Min	Max	Mean	sd		Min	Max
Bering Sea	1990	1400		1300	1600	180		150.00	220	Iwata et al., 1993
Chuchki Sea		1500		1200	1900	190		160.00	230	
Bering Sea	1993	2050	3555	1410	2980	458.97	93.21	290.00	730	
Bering Strait to Greenland Sea	1993	1977.50	698.76	550	2740	381.69	162.92	13.70	700	Jantunen and Bidleman, 1995
Arctic	2004	12.50	16.22	0.5	65	4.48	5.59	0.40	21.00	Jantunen and Bidleman, 1998
Greenland/Irminger Current	2008	57.6	28.9	28.9	90	20.4	9.6	9.60	31.50	Lohmann et al., 2009
Arctic/Pacific	2010	295.1	173.3	67.2	536.0	66.5	42.7	16.0	134.2	Zhang et al., 2012
Greenland Current		6.1	6.9	2.1	16.5	2.3	2.8	0.03	6.4	Cai et al., 2012
Arctic Ocean	2007	1.3	0.8	0.1	2.1	0.4	0.4	0.002	0.8	This Study

Gas (pg m⁻³)

Dissolved (pg L⁻¹)

Table S5b. Previously reported concentrations of HCB in the gas, dissolved and particulate phase for the Arctic region.

Location	Year	mean	sd	Min	Max	Reference
Bear Island	2000	33.37		6.70	68.63	Kallenborn et al., 2007
	2001	21.49		7.23	45.18	
	2002	20.37		9.36	39.70	
	2003	24.81		15.51	47.50	
Alert Kinnigait Little Fox Lake Point Barrow Zepellin	2004	64		20	130	Su et al., 2008
	2003	58		4.4	110	
	2003	88		71	120	
	2003	54		26	120	
	2003	51		2.8	270	
	2004	44	13	22	87.10	
Hudson Bay Beaufort Sea	2008	58	2.60			Wong et al., 2011
	2008	48	6.50			
	2008	71	11			
Greenland/Norwegian Current	2008	14	1	4.10	20.50	Zhang et al., 2012
	GC	53.2	21.6	35.9	77.4	This study
	AO	34.1	27.3	0.4	60.8	
Gas (pg m⁻³)						
Dissolved (pg L⁻¹)						
Location	Year	mean	sd	Min	Max	Reference
Arctic	2004	4.55	2.61	0.85	9.61	Lohmann et al., 2009
	1993	15		12	17	Strachan et al., 2001
	1997	9				Strachan et al., 2000
	1996	7				
Resolute Bay Greenland/Norwegian Current	1998	9				Hargrave et al., 1998
	1993	16		14	18	
	2008	0.2	0.10	0.1	0.8	
GC AO	2007	2.27	1.80	0.94	4.82	Zhang et al., 2012
	2007	1.24	0.97	0.03	2.60	
Particulate (pg L⁻¹)						
Location	Year	mean	sd	Min	Max	Reference
Arctic GC	2004	0.27	0.26	0.05	1.09	Lohmann et al., 2009
	2007	0.29	0.07	0.23	0.39	
AO	2007	0.25	0.07	0.18	0.36	This Study

Appendix B

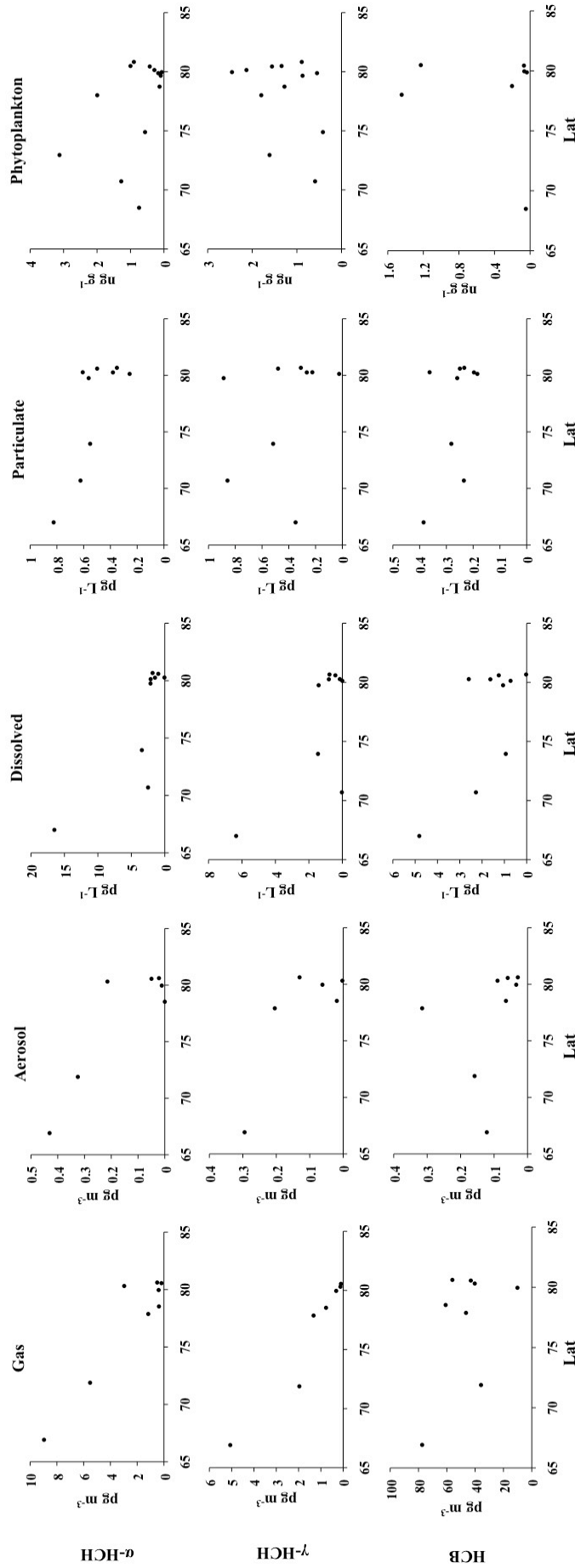


Figure S1. Latitudinal distribution of the concentrations of α -HCH, γ -HCH and HCB in the gas, aerosol, dissolved, particulate and phytoplankton phases along the Greenland Current and the Arctic Ocean.

Appendix B.3: Back-trajectories of the air masses during the sampling cruise.

Backtrajectories

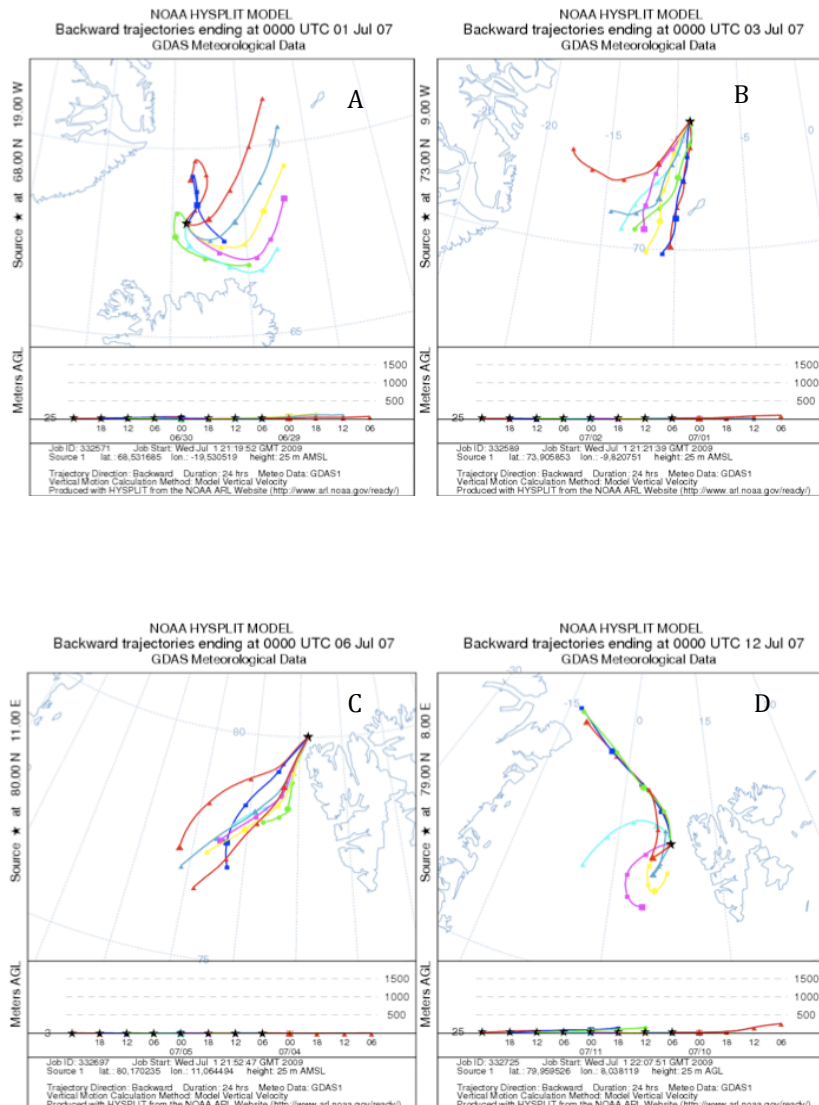


Figure S2a. Backtrajectories of the air masses estimated for the ATOS I samples G1+A1 (A), G2+A2(B), G3+A3(C) and G4+A4 (D). HYSPLIT back-trajectory Model from NOAA was used to estimate the source of the air masses during the sampling period. Each back-trajectory was calculated every 6 hours.

Appendix B

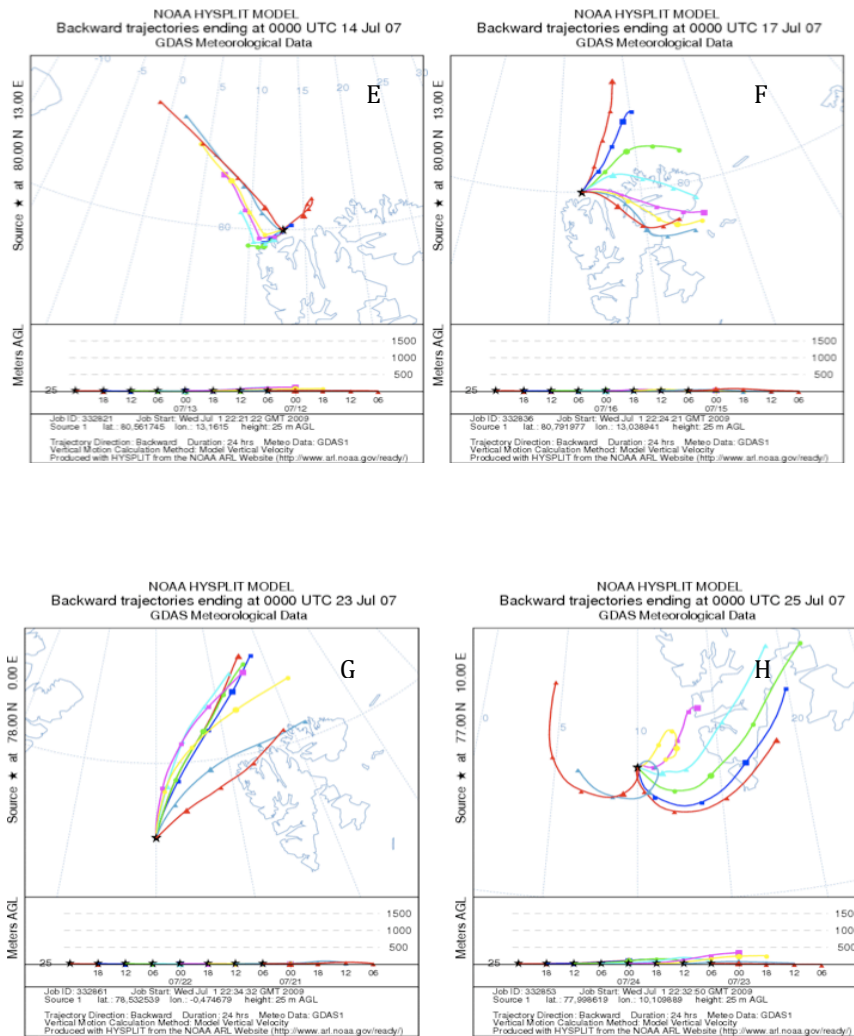


Figure S2b. Backtrajectories of the air masses estimated for ATOS I samples G5+A5 (E), G6+A6(F), G7+A7(G) and G8+A8 (H). HYSPLIT back-trajectory Model from NOAA (Draxler and Rolph, 2011) was used to estimate the source of the air masses during the sampling period. Each back-trajectory was calculated every 6 hours.

Appendix B.4: Supplementary information on the estimation of fluxes and cycling.

Table S6: Physical-chemical constants used for the estimations of the fugacities, fluxes and correlations in the present study.

Compound	Log K _{OW} (298K)	Ref.	AH _{WA} (KJ mol ⁻¹)	Ref.	H (Pa m ⁻³ mol ⁻¹) 298K	Ref.
α-HCH	3.94	Xiao et al. 2004	59.3	Sahsuvar et al., 2003	0.360	Sahsuvar et al., 2003
γ-HCH	3.83	Xiao et al. 2004	61.4	Sahsuvar et al., 2003	0.165	Sahsuvar et al., 2003
HCB	5.64	Shen & Wania 2005	35	Cortés et al., 1998	5	Jantunen and Bidleman 2006

Appendix B

Table S7: Estimations of water-air fugacity ratios (f_w/f_a), air-water diffusive fluxes (F_{AW}), dry deposition fluxes (F_{DD}) and Sinking fluxes (F_{SINK}) for each one of the sampling events of the ATOS-I cruise. Sinking fluxes were estimated using the biogenic matter settling flux reported in Bauerfeind et al., (2009). nd: not determined due to concentrations below quantification limit.

Compound	GC									AO																
	G1D1	G2D2	G2D3	G3D4	G4D4	G4D5	G5D6	G6D7	G7D8	G8D8	G8D9	F1	F2	F3	F4	F5	F6	F7	F8	F9	F10	F11	F12	F13		
f_w/f_a	α -HCH	0.056	0.013	0.019	0.052	0.121	0.361	0.021	0.155	0.011	0.014	0.012														
	γ -HCH	0.016	0.001	0.001	0.013	nd	Nd	0.143	0.021	0.006	0.008	0.006														
	HCB	1.05	1.068	0.441	0.383	0.317	1.018	0.302	0.345	0.008	0.019	1.252														
F_{AW} ($ng\ m^{-2}\ d^{-1}$)	α -HCH	-3.63	-1.75	-1.74	-0.69	-0.20	-0.22	-0.19	-0.10	-1.91	-0.17	-0.18														
	γ -HCH	-2.16	-0.64	-0.64	-0.82	nd	nd	-0.18	-0.06	-0.08	-0.40	-0.40														
	HCB	-0.06	0.00	-0.36	-2.42	-1.43	-0.57	0.08	-1.98	-3.47	-3.19	-1.78														
F_{DD} ($ng\ m^{-2}\ d^{-1}$)	α -HCH	A1	A2	A3		A4	A5	A6	A7	A8																
	γ -HCH	-0.037	-0.028	-0.045		-0.002	-0.001	-0.004	-0.019	-0.027																
	HCB	-0.025	nd	-0.018		-0.011	-0.005	-0.005	0.000	-0.002																
F_{SINK} ($ng\ m^{-2}\ d^{-1}$)	α -HCH	-0.011	-0.014	-0.027		-0.003	-0.003	-0.005	-0.008	-0.006																
	γ -HCH	0.09	0.15	0.37	0.07	0.24	0.02	0.03	0.05	0.12	0.02	0.01														
	HCB	nd	0.07	0.19	0.05	0.22	0.15	0.26	0.19	0.16	0.07	0.11														
		0.01	nd	nd	nd	0.17	0.02	nd	0.01	0.15	nd															

Table S8. Estimated Bioconcentration Factor (BCFs, L Kg⁻¹) from the concentrations in the dissolved and phytoplankton phases during the ATOS I cruise. These are apparent BCFs since the dissolved phase concentrations was measured at 5 m depth, and the phytoplankton phase concentration is an integration from the depth with maximum of biomass to surface. nd: not determined due to one of the concentrations below the quantification limit.

L Kg⁻¹	α-HCH	γ-HCH	HCB
F1	4.6	nd	4
F2	5.7	7.3	nd
F3	5.9	6	nd
F4	5.2	55	nd
F5	5.7	6	6.2
F6	4.5	6	5.3
F7	5.1	6.2	nd
F8	5.3	6	4.8
F9	6.4	6.5	5.9
F10	4.9	8.5	4.7
F11	5.8	6.2	nd
F12	4.6	6.5	5.5
F13	4.8	6	nd

Appendix B

Table S9. Total degradation flux ($\text{ng m}^{-2} \text{d}^{-1}$) for α -HCHs and γ -HCH. The microbial degradation flux was estimated with two approaches obtaining similar results. The first scaled the microbial degradation constant by using the differences in the microbial biomass at different depths, the second approach scaled the degradation constant by using the heterotrophic production at different depths. The total degradation flux also includes the flux due to hydrolysis, which makes a small contribution to the total degradation flux.

F_{DEG}	Compound	D1	D2	D3	D4	D5	D6	D7	D8	D9
corrected by Biomass $\text{ng m}^{-2} \text{d}^{-1}$	α -HCH	0.432	0.065	0.090	0.056	0.001	0.055	0.025	0.048	0.038
	γ -HCH	0.840	0.004	0.193	0.187	0.020	<0.001	0.055	0.102	0.107
corrected by Heterotrophic Production $\text{ng m}^{-2} \text{d}^{-1}$	α -HCH	0.474	0.072	0.098	0.061	0.001	0.061	0.028	0.052	0.042
	γ -HCH	0.951	0.004	0.218	0.212	0.022	<0.001	0.062	0.115	0.121

Table S10. Comparison of the degradation and sinking fluxes with atmospheric inputs. The table gives the percentage of degradation (F_{DEG}) and sinking flux (F_{SINK}) when compared with the atmospheric deposition ($F_{\text{AW}}+F_{\text{DD}}$) for each sampling event.

		%Atmospheric input	D1	D2	D3	D4				
GC	F_{SINK}	α -HCH	2%	9%	40%	25%				
		γ -HCH		11%	18%	219%				
	F_{DEG}	α -HCH	12%	4%	3%	6%				
		γ -HCH	39%	1%	23%	6%				
			D4	D5	D6	D7	D8	D9		
AO	F_{SINK}	α -HCH	35%	55%	11%	107%	2%	6%		
		γ -HCH			36%	174%	231%	26%		
	F_{DEG}	α -HCH	28%	1%	28%	24%	13%	19%		
		γ -HCH				130%	124%	41%		

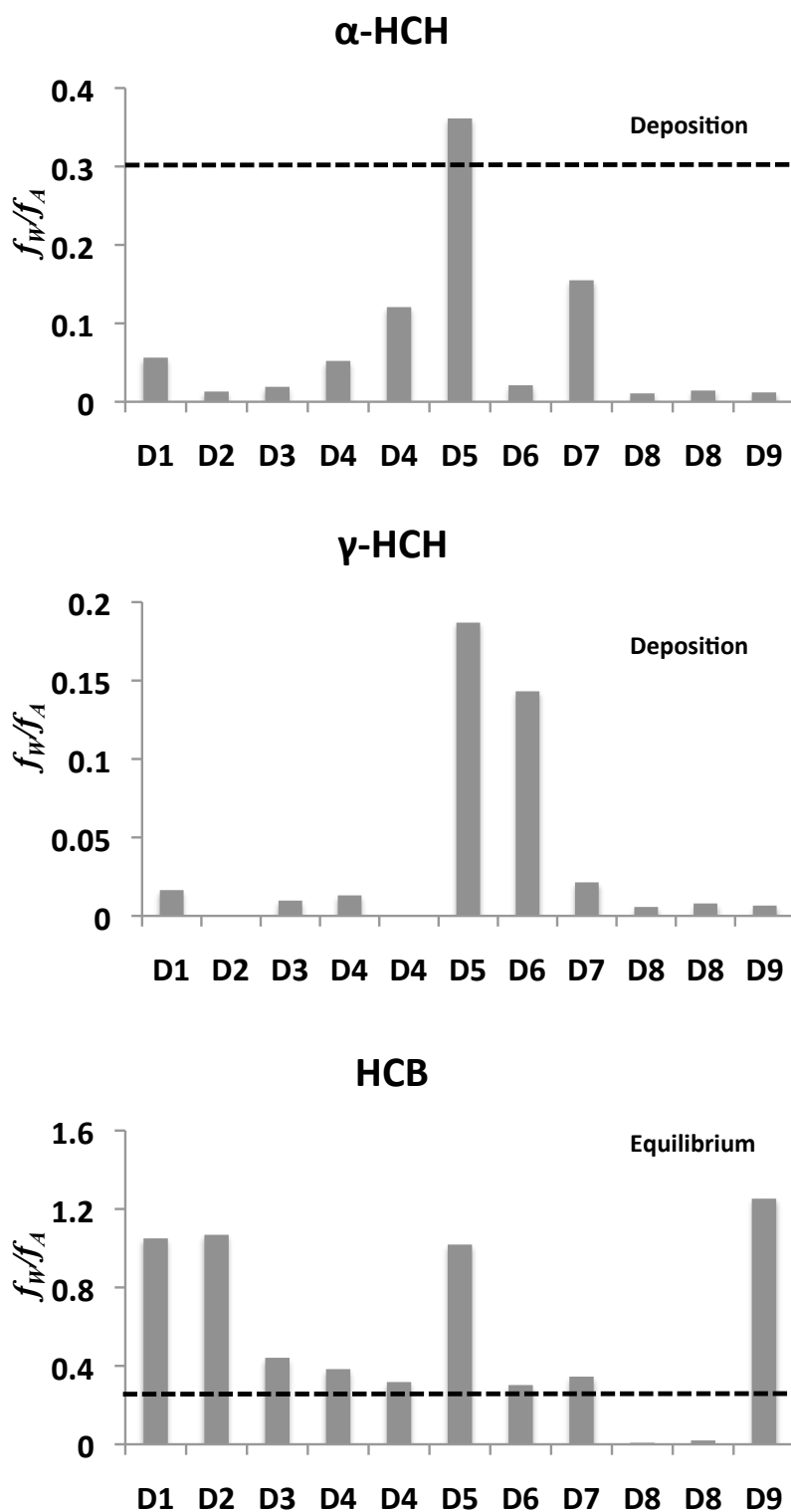


Figure S3. Water-air fugacity ratios for α -HCH, γ -HCH and HCB. Fugacity ratios (f_w/f_A) between 0.3 and 3 show that the studied compounds are close to equilibrium, values below 0.3 indicate that there is a net deposition, and values above 3 indicate a net volatilization.

Appendix B

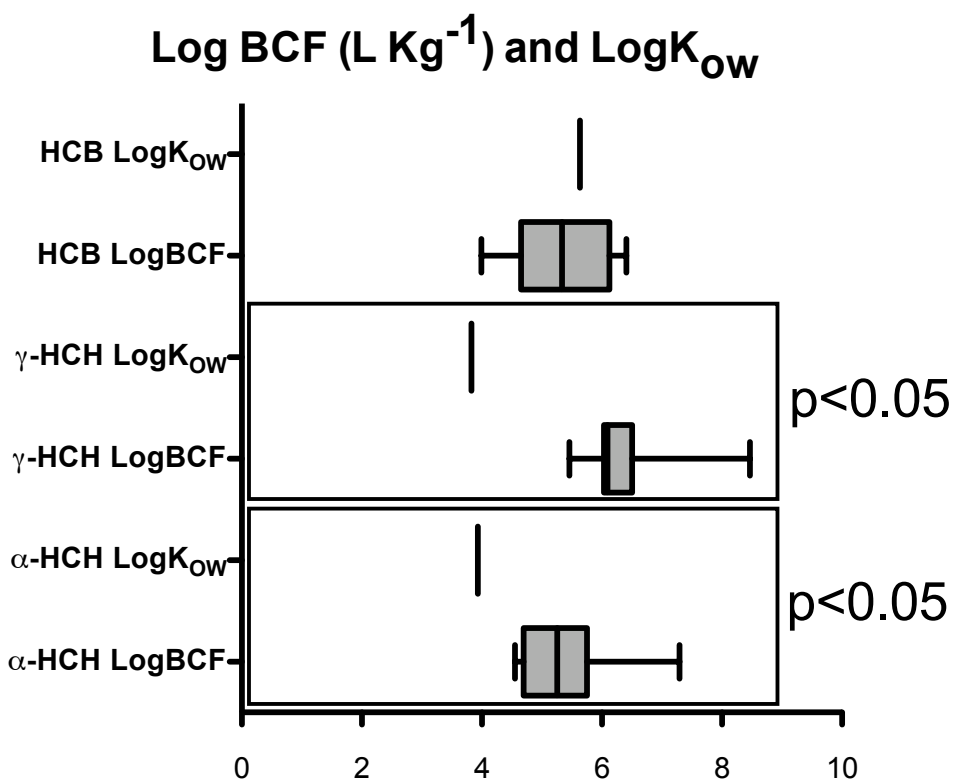


Figure S4. Box-Plot comparing the measured LogBCF ($L\ Kg^{-1}$) for the studied compounds with the temperature corrected LogK_{ow}.

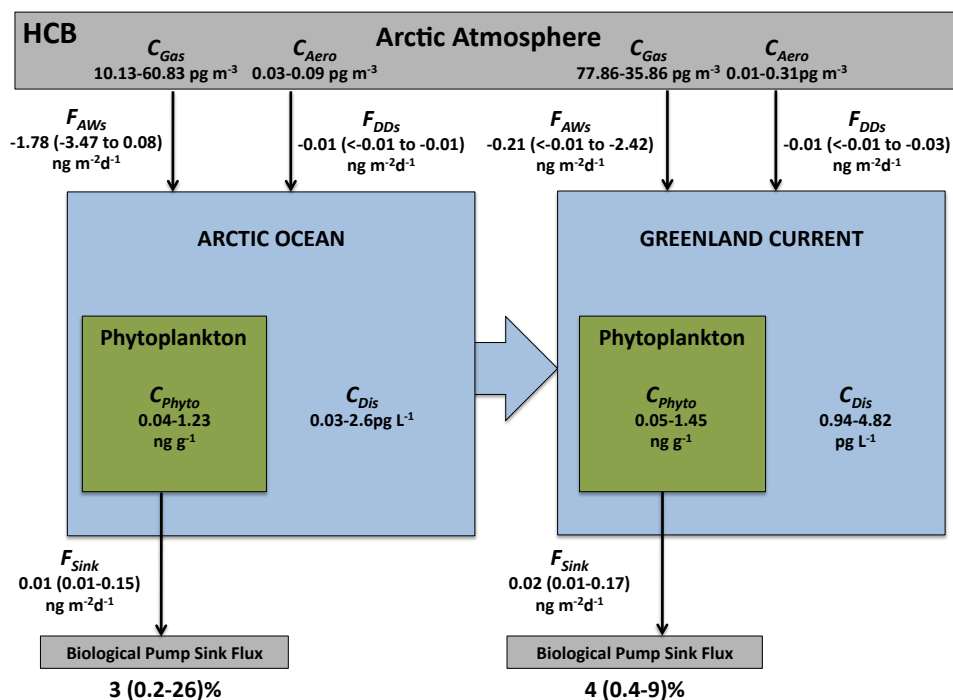


Figure S5. Mass Balance for HCB during ATOS I cruise. Where C_{Gas} is the atmospheric concentration in the gas phase, C_{Aero} is the atmospheric concentration in the aerosol phase, C_{Dis} is the dissolved phase concentration, C_{Phyto} is the concentration in the phytoplankton phase, F_{AW} is the air-to-water diffusive flux, F_{DD} is the dry deposition flux and F_{Sink} is the sink flux of HCB calculated in the Arctic Ocean and Greenland Current. Numbers in percentage (%) represent the proportion of the atmospheric input that are removed by the biological pump.

Appendix B

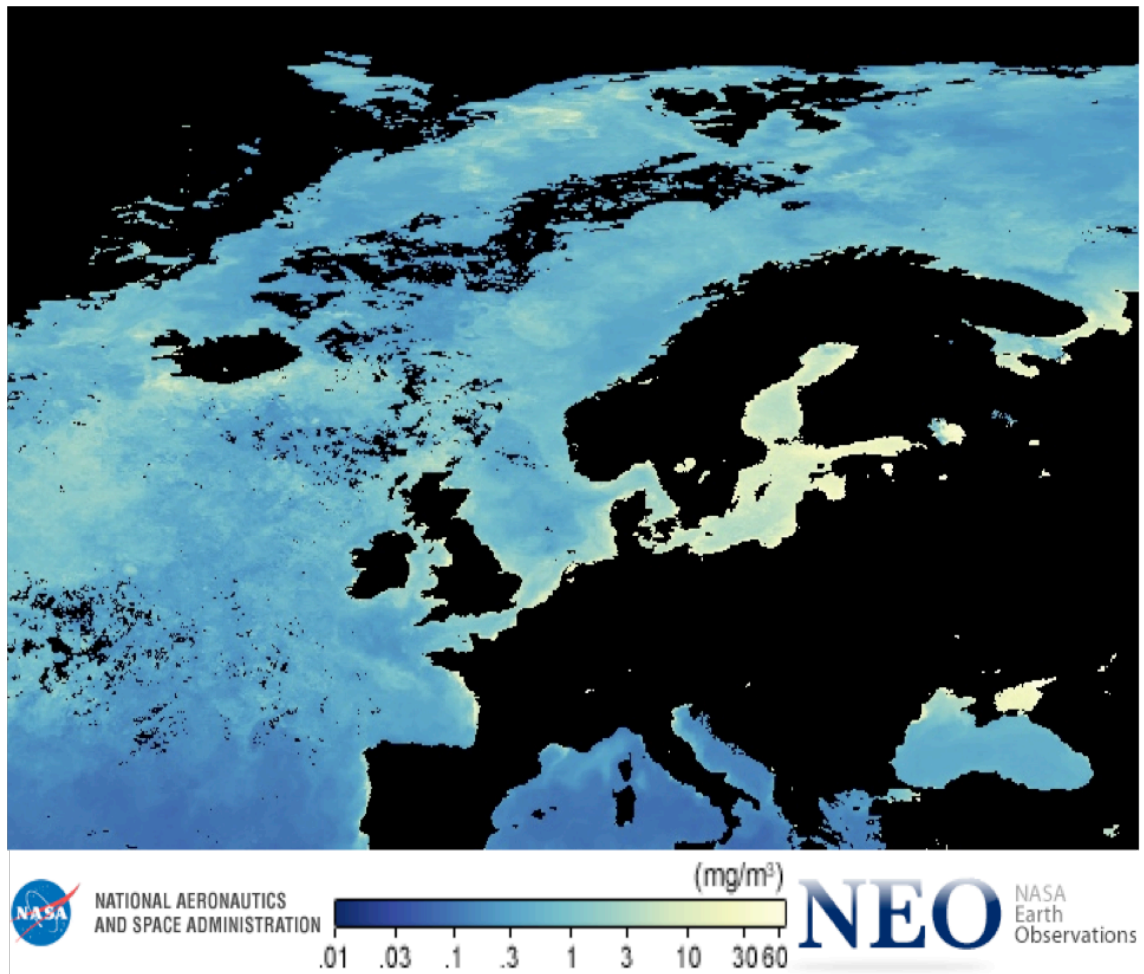


Figure S6. Surface chlorophyll concentrations in the North Atlantic and Arctic ocean for the sampling period (July 2007). Reproduced from <http://neo.sci.gsfc.nasa.gov>.

Additional References

Cortes, D.R.; Basu, I.; Sweet, C.W.; Brice, K.A.; Hoff, R.M.; Hites, R.A. Temporal trends in gas-phase concentrations of chlorinated pesticides measured at the shores of the great lakes. *Environ. Sci. and Technol.* **1998**, *32*(13), 1920-7. DOI 10.1021/es970955q

Draxler, R.R.; Rolph, G.D. HYSPLIT (HYbrid Single-Particle Lagrangian Integrated Trajectory) Model access via NOAA ARL READY Website (<http://ready.arl.noaa.gov/HYSPLIT.php>). **2011**, NOAA Air Resources Laboratory, Silver Spring.

Jantunen, L.M.; Bidleman, T.F.; Henry's law constants for hexachlorobenzene, p,p'-DDE and components of technical chlordane and estimates of gas exchange for lake Ontario. *Chemosphere.* **2006**, *62*(10), 1689-96. DOI 10.1016/j.chemosphere.2005.06.035

Sahsuvar, L.; Helm, P.A.; Jantunen, L.M.; Bidleman, T.F. Henry's law constants for α -, β -, and γ -hexachlorocyclohexanes (HCHs) as a function of temperature and revised estimates of gas exchange in Arctic regions. *Atmos. Environ.* **2003**, *37*, 983-992. DOI 10.1016/S1352-2310(02)00936-6

Shen, L.; Wania, F. Compilation, evaluation, and selection of physical-chemical property data for organochlorine pesticides. *J. Chem. Eng. Data.* **2005**, *50*, 740-768. DOI 10.1021/je049693f

Xiao, H.; Li, N.; Wania, F. Compilation, evaluation, and selection of physical-chemical property data for α -, β -, and γ -hexachlorocyclohexane. *J. Chem. Eng. Data.* **2004**, *49*(2), 173-185. DOI 10.1021/je034214i

Appendix C

Supporting Information to Chapter 5

Polychlorinated biphenyls, Hexachlorocyclohexanes and Hexachlorobenzene in seawater and phytoplankton from the Southern Ocean (Weddell, South Scotia, and Bellingshausen Seas)

Appendix C.1: Ancillary data for samples taken during the ICEPOS, ESSASI and ATOS-II cruises.

Table S1. Seawater samples ancillary data...271

Table S2a. Phytoplankton ancillary data for the ICEPOS and ESSASI cruises...272

Table S2b. Phytoplankton ancillary data for the ATOS-II cruise...273

Appendix C.2: Quality Control and Assessment.

Cleaning methodology during the preparation of the sampling devices and during sampling...274

Quality Control and Assessment for Seawater and Phytoplankton Analysis...275

Table S3. Blank average and standard deviation values for each compound...276

Table S4. Recoveries of surrogates PCBs 65 and 200 for each matrix...277

Table S5. Instrumental detection limits...278

Table S6. Calculated limits of detection and quantification...279

Appendix C.3: Concentrations in seawater and phytoplankton.

Table S7. Sample concentrations resume table...280

Table S8a. Seawater concentrations for individual compounds during the ESSASI and ATOS-II cruises...281

Table S8b. Seawater concentrations for individual compounds during the ESSASI and ATOS-II cruises...282

Table S9a. Phytoplankton phase concentrations for individual compounds during the ICEPOS, ESSASI and ATOS-II cruises...283

Table S9b. Phytoplankton concentrations for individual compounds during the ICEPOS, ESSASI and ATOS-II cruises...284

Appendix C.4: Additional Tables and Figures

Table S10. Physico-Chemical properties used in the present study...285

Table S11. Seawater Half-lives for PCBs and HCHs retrieved from the bibliography...286

Appendix C

Table S12. Relationship between Phytoplankton Concentrations against the Biomass (mg L^{-1}) for all the studied compounds...287

Table S13a. BCF_{TD} for phytoplankton from the ESSASI cruise against the temperature corrected Log K_{OW} ...288

Table S13b. BCF_{TD} for phytoplankton from the ESSASI cruise against the temperature corrected Log K_{OW} ...288

Figure S1a. Relationship between the logarithm of the trully dissolved bioconcentration factors (BCF_{TD}) and logarithm of the temperature corrected octanol-water partition constant(K_{OW}) in ESSASI samples...289

Figure S1b. Relationship between the logarithm of the trully dissolved bioconcentration factors (BCF_{TD}) and logarithm of the temperature corrected octanol-water partition constant(K_{OW}) in ATOS II samples..290

Additional References...291

Appendix C.1 :Ancillary data for the samples taken in the ICEPOS, ESSASI and ATOS-II cruises

Table S1. Ancillary data for seawater samples taken during the ESSASI and ATOS-II cruises

Cruise	Sample	Date	Location		Volume L	Radiation W m ⁻²	Pressure atm	Water Temp °C	Salinity pps	Conductivity mΩ cm-1	Fluorescence V
			°S	°E							
ESSASI	DE1	3/01/08	65.05	-56.09	289	280.82	986.51	3.14	33.892	26.97	0.97
	DE2	5/01/08	57.06	-60.81	211	187.64	985.06	1.06	34.076	27.30	0.84
	DE3	6/01/08	54.77	-60.80	249	235.61	989.78	0.56	34.272	27.49	0.82
	DE4	9/01/08	51.88	-60.27	212	149.58	984.86	0.47	34.279	27.50	0.83
	DE5	10/01/08	51.42	-61.45	227	116.23	986.10	-0.35	34.301	27.56	0.78
	DE6	12/01/08	50.91	-61.19	204	269.88	984.74	-0.35	34.342	27.59	0.83
	DE7	13/01/08	50.08	-60.38	291	152.20	986.35	0.42	34.223	27.46	0.83
	DE8	14/01/08	50.75	-60.21	303	270.79	983.12	0.12	34.307	27.54	0.86
	DE9	16/01/08	47.26	-60.17	213	229.65	995.07	-0.25	33.395	26.82	0.83
	DE10	19/01/08	51.11	-61.26	299	187.99	989.93	-0.07	34.307	27.55	0.89
ATOS-II	DA1	29/01/09	55.63	-62.02	175	222.14	984.19	1.22	34.230	27.41	0.09
	DA2	1/02/09	51.95	-63.84	257	88.89	995.68	-0.10	33.871	27.20	1.40
	DA3	8/02/09	58.40	-62.49	237	76.48	986.63	2.18	33.968	27.13	0.50
	DA4	10/02/09	61.24	-63.93	248	139.07	982.04	2.61	33.799	26.96	0.77
	DA5	13/02/09	70.97	-67.44	210	85.06	988.93	0.65	33.227	26.63	1.80
	DA6	15/02/09	74.49	-69.55	272	111.41	981.11	0.91	33.119	26.53	2.44
	DA7	19/02/09	69.82	-67.37	237	61.82	985.77	2.21	33.487	26.74	2.69
	DA8	21/02/09	64.02	-64.86	378	91.56	984.02	1.48	34.039	27.23	1.09
	DA9	26/02/09	55.80	-64.94	223	110.77	987.96	2.53	33.986	27.08	0.54

Appendix C

Table S2a. Ancillary data for the phytoplankton samples taken during the ICEPOS and ESSASI cruises. DCM is the deep chlorophyll maximum depth. *B* is the phytoplankton biomass. *P* is the atmospheric pressure. Some of the ancillary information is not available for the ICEPOS samples.

Cruise	Sample	Date	Time	$^{\circ}\text{S}$	Location $^{\circ}\text{E}$	<i>B</i> mg L^{-1}	Dry Weight <i>g</i>	DCM m	Radiation W m^{-2}	<i>P</i> atm	Water T $^{\circ}\text{C}$	Salinity pps	Conductivity $\text{m}\Omega \text{ cm}^{-1}$	Fluorescence <i>V</i>
ICEPOS	FI1	2/2/05		65.00	-64.20	0.003	0.276							
	FI2	4/2/05		56.10	-64.80	0.015	0.376							
	FI3	6/2/05		55.00	-64.10	0.018	0.229							
ESSASI	FE1	5/1/08	17:47	56.14	-61.07	0.083	0.042	40	603.84	985.02	1.191	34.131	27.334	2.904
	FE2	6/1/08	15:23	54.77	-60.80	0.089	0.090	80	280.85	988.16	0.453	34.223	27.455	1.485
	FE3	7/1/08	13:30	52.55	-60.42	0.095	0.060	50	159.15	986.32	0.052	34.361	27.588	1.363
	FE4	8/1/08	13:00	52.55	-60.42	0.042	0.037	70	159.15	986.32	0.052	34.361	27.588	1.363
	FE5	9/1/08	14:30	51.88	-60.31	0.031	0.034	85	238.72	977.45	-0.104	34.389	27.618	0.002
	FE6	11/1/08	15:30	51.22	-61.55	0.070	0.066	75	500.86	986.13	-0.432	34.33	27.587	0.161
	FE7	12/1/08	13:50	50.90	-61.18	0.035	0.044	100	950.23	979.67	-0.391	34.367	27.615	1.49
	FE8	13/1/08	13:35	50.02	-60.75	0.044	0.044	80	500.86	986.69	-0.23	34.04	27.343	0.059
	FE9	14/1/08	13:30	50.04	-60.12	0.110	0.069	50	411.92	985.95	0.486	34.158	27.400	1.729
	FE10	15/1/08	13:45	50.60	-60.20	0.043	0.040	75	360.43	983.18	0.219	34.293	27.524	2.662

Table S2b Ancillary data for the phytoplankton samples taken during the ATOS-II cruise. DCM is the deep chlorophyll maximum depth. B is the phytoplankton biomass. P is the atmospheric pressure.

Cruise	Sample	Date	Time	Location	B	Dry Weight	DCM	Radiation	P	Water T	Salinity	Conductivity	Fluorescence	
				$^{\circ}\text{S}$	$^{\circ}\text{E}$	mg L^{-1}	g	m	W m^{-2}	atm	$^{\circ}\text{C}$	pps	$\text{m}\Omega \text{cm}^{-1}$	V
	FA1	26/1/09	11:00	64.59	-57.46	1.040	0.785	60						
	FA2	28/1/09	12:00	59.01	-62.65	0.116	0.044	30						
	FA3	29/1/09	13:41	55.71	-62.02	0.117	0.066	45	463.41	987.98	2.125	34.246	27.357	0.054
	FA4	30/1/09	11:00	52.50	-61.68	0.157	0.089	45	238.72	980.04	1.077	34.065	27.289	0.041
	FA5	1/2/09	13:12	51.81	-63.86	0.068	0.060	70	271.49	990.93	0.199	33.403	26.807	0.122
	FA6	2/2/09	10:30	53.88	-63.93	0.161	0.101	40	51.48	993.34	-0.427	33.637	27.026	0.148
	FA7	3/2/09	14:00	55.75	-65.03	1.523	0.670	35	786.4	996.85	0.267	33.665	27.015	2.879
	FA8	4/2/09	15:49	55.85	-64.25	2.067	1.039	40	402.56	992.6	0.208	34.190	27.441	0.867
	FA9	5/2/09	14:00	56.64	-63.47	0.512	0.451	70	847.25	998.51	-0.004	34.330	27.565	2.74
	FA10	6/2/09	12:22	57.21	-62.18	0.118	0.089	60	285.53	1000.17	2.075	34.242	27.359	2.74
	FA11	7/2/09	17:00	58.20	-62.42	0.134	0.101	60	613.2	1006.08	2.193	34.217	27.329	0.242
	FA12	8/2/09	9:30	60.50	-62.74	0.103	0.052	40	0	997.21	2.585	34.046	27.160	0.332
	FA13	9/2/09	11:30	61.27	-63.57	1.939	0.974	40	65.53	982.62	2.007	34.200	27.330	0.417
	FA14	10/2/09	10:30	62.68	-64.58	0.222	0.196	70	131.06	980.22	1.584	33.965	27.174	0.158
	FA15	11/2/09	10:35	62.75	-63.63	0.024	0.021	70	28.08	981.15	2.748	33.727	26.891	0.757
	FA16	12/2/09	12:00	66.91	-65.05	0.055	0.042	60	140.42	981.88	2.849	33.758	26.907	0.545
	FA17	13/2/09	11:45	70.85	-67.41	0.171	0.108	50	290.21	984.29	2.259	33.676	26.891	0.381
	FA18	14/2/09	10:30	75.10	-69.04	0.077	0.039	40	4.67	988.53	1.070	33.281	26.659	3.954
	FA19	15/2/09	15:37	74.51	-69.55	0.220	0.083	30	65.53	991.49	-1.332	32.523	26.156	2.503
	FA20	18/2/09	22:11	67.25	-68.20	0.075	0.038	40	60.84	977.82	0.536	33.099	26.544	0.745
	FA21	19/2/09	15:25	69.81	-67.37	0.491	0.278	45	383.83	990.01	1.878	33.541	26.812	3.382
	FA22	20/2/09	11:50	67.29	-66.03	0.066	0.050	60	46.80	987.79	2.379	33.615	26.832	1.600
	FA23	21/2/09	14:00	64.55	-64.93	0.060	0.030	40	205.96	978.93	2.555	33.834	26.993	2.811
	FA24	22/2/09	14:00	60.49	-63.01	5.041	1.394	20	201.27	981.88	2.407	33.828	27.000	2.024
	FA25	23/2/09	10:00	57.63	-63.04	0.396	0.149	30	14.03	989.64	-0.168	34.273	27.528	0.740
	FA26	24/2/09	11:00	54.92	-63.04	0.268	0.202	60	196.59	973.57	-0.309	34.260	27.524	0.635

ATOS-II

Appendix C

Appendix C.2. Information on the Quality Control and Assessment Cleaning procedures during the preparation of the sampling devices and during sampling.

Sampling equipment and materials were cleaned carefully. PUFs were conditioned prior to sampling by a soxhlet extraction during 24 hours with acetone:hexane (3:1), later PUFs were dried under vacuum and wrapped in precombusted (450°C 4h) aluminium foil envelopes. Wrapped PUFs were introduced into two zip-sealed bags before sampling. XAD-2 columns were cleaned by elution with 200mL of methanol followed by 300 mL of DCM and finally followed by 200mL of methanol, once the column was full of methanol was sealed and kept at 4°C until sampling. All the filters used for the phytoplankton (47 mm Ø GF/D, Whatman, GE, UK) and for particulate matter (142 mm Ø GF/F, Whatman, GE, UK) were precombusted before sampling (450°C for 4 hours) and them were enveloped in precombusted aluminium envelopes (450°C for 4 hours), which were kept into a zip-sealed bags until sampling.

Stainless steel sampling devices were rinsed with acetone three times before packing the material, before their use for sampling and between samples. All the glass material was precombusted (450°C for 4 hours) and rinsed with acetone 3x and wrapped in aluminium foil before transport to the ship. Once at the ship, all the devices were cleaned by rinsing with acetone before sampling and between samples. The net for sampling of phytoplankton was cleaned with distilled water, dried and packed in a zip sealed bag until sampling. During sampling the net was cleaned with seawater followed by unsalted water before and after sampling. Phytoplankton samples were transferred from the sampling net to a clean screw-cap glass jar until filtration (never more than 10 minutes after sampling). All the solvents (Acetone, Hexane, Dichloromethane and Methanol) used during the cleaning and extraction procedures of samples were Gas Chromatography quality branded (Merck, KGaA).

Quality Control and Assessment for the analysis of Seawater and Phytoplankton samples

Recoveries were assessed adding 10 ng of PCBs 65 and 200 prior to extraction (Supporting table S4). Quantification was done adding 5 ng of PCBs 30 and 142 as internal standard prior to injection and subtracting the blank signal prior to quantification. HCHs, HCB and PCBs analyses for seawater and phytoplankton samples were carried out using a GC-uECD (Agilent Technologies) with a HP-5MS capillary column (60 m x 0.25 mm i.d. x 0.25 µm) internally coated with Poly-di-methyl-syloxane (Agilent Technologies). Splitless injection mode was selected as injection procedure. Oven temperature was programmed from 90°C (holding time 2 min) to 190°C at 15°C/min (holding time 1 min) to 203°C at 3°C/min (holding time 5 min), then to 290°C at 3°C/min (holding time 1 min), and finally to 310°C at 5°C min⁻¹ keeping the final temperature for 10 min.

Three field blanks and three laboratory blanks were collected for each matrix, average and standard deviation of blanks are given on table S3. Field blanks (adsorbents or filters) were placed in the sampling devices for 30 minutes to measure the cross contamination from the sampling devices and then followed the same process as the field samples. All the concentrations were corrected using the recovery values of PCB 65 and 200 (Summary table S4). Instrumental detection limits (IDLs) are provided in Table S5. Limits of detection (LOD) and quantification (LOQ) were calculated using field and laboratory blanks following equations 1 and 2 from the mean and standard deviation (LOD and LOQ values are given in Table S6).

$$LOD = \bar{x} + 3sd \quad [C.1]$$

$$LOQ = \bar{x} + 10sd \quad [C.2]$$

Appendix C

Table S3. Average and standard deviation of blank values (ng on column) for each compound.

Compound ng on column	Dissolved		Phyto	
	average	sd	average	sd
α-HCH	0.003	0.0002	0.025	0.001
β-HCH	0.005	0.0003	0.011	<0.001
δ-HCH	0.003	0.0002	0.020	0.001
γ-HCH	0.002	0.0001	0.013	0.001
HCB	0.006	0.0006	0.034	0.004
PCB18	0.008	0.0001	0.034	0.002
PCB17	0.005	0.0003	0.029	0.002
PCB31	0.004	0.0003	0.036	0.003
PCB28	0.003	0.0000	0.018	0.001
PCB33	0.006	0.0003	0.045	0.003
PCB52	0.002	0.0001	0.017	0.001
PCB49	0.006	0.0001	0.038	<0.0001
PCB99/101	0.003	0.0002	0.139	0.011
PCB110	0.004	0.0000	0.025	0.002
PCB82	0.005	0.0002	0.028	0.001
PCB151	0.001	0.0000	0.073	0.002
PCB149	0.003	0.0002	0.009	<0.001
PCB118	0.003	0.0001	0.054	0.001
PCB153	0.001	<0.0001	0.029	0.002
PCB132/105	0.004	<0.0001	0.010	<0.001
PCB138	0.007	0.0003	0.019	0.001
PCB158	0.003	0.0002	0.009	<0.0001
PCB187	0.005	0.0004	0.009	<0.001
PCB183	0.006	0.0004	0.033	0.002
PCB128	0.004	0.0003	0.028	0.002
PCB177	0.003	<0.0001	0.021	0.001
PCB171/156	0.004	<0.0001	0.014	<0.001
PCB180	0.002	0.0001	0.001	<0.001

Table S4. Recoveries of surrogates PCBs 65 and 200 for phytoplankton and dissolved phase samples. Recoveries are given for the three sampling cruises separately.

% Recovery	PCB65			PCB200		
	Average	Min	Max	Average	Min	Max
ICEPOS cruise						
Phytoplankton	46	29	72	58	43	91
ESSASI cruise						
Dissolved	69.3	60.2	90	69.4	56.5	83.8
Phytoplankton	69.2	42.1	88.6	69.2	42.1	101.6
ATOS-2 cruise						
Dissolved	77.2	65.5	85.6	70.2	55.3	81.9
Phytoplankton	72.3	51.2	97.7	71.2	51.4	97.7

Appendix C

Table S5. Instrumental detection limits as concentrations (estimated using a volume of 250 L for dissolved phase and 0.5 g of biomass for phytoplankton)

Compounds	µg L⁻¹	ng g⁻¹
HCHs and HCB	0.0016	0.0079
PCB17	0.0080	0.0401
PCB18	0.0016	0.0079
PCB28	0.0016	0.0079
PCB31	0.0012	0.0060
PCB33	0.0016	0.0079
PCB49	0.0016	0.0080
PCB52	0.0016	0.0080
PCB82	0.0004	0.0020
PCB99/101	0.0032	0.0159
PCB132/105	0.0004	0.0020
PCB110	0.0016	0.0079
PCB118	0.0016	0.0080
PCB128	0.0016	0.0080
PCB138	0.0016	0.0080
PCB149	0.0016	0.0080
PCB151	0.0016	0.0080
PCB153	0.0016	0.0079
PCB171/156	0.0016	0.0079
PCB158	0.0004	0.0020
PCB177	0.0016	0.0079
PCB180	0.0016	0.0079
PCB183	0.0016	0.0079

Table S6. Calculated Limits of detection (LOD) and quantification (LOQ) from the field blanks.

Compound ng on column	Dissolved		Phytoplankton	
	LOD	LOQ	LOD	LOQ
α-HCH	0.004	0.005	0.028	0.033
β-HCH	0.006	0.007	0.012	0.015
δ-HCH	0.004	0.006	0.023	0.029
γ-HCH	0.002	0.003	0.016	0.023
HCB	0.008	0.012	0.045	0.070
PCB18	0.008	0.009	0.040	0.055
PCB17	0.006	0.008	0.034	0.047
PCB31	0.005	0.007	0.045	0.066
PCB28	0.003	0.003	0.021	0.030
PCB33	0.007	0.009	0.055	0.077
PCB52	0.002	0.003	0.020	0.027
PCB49	0.006	0.007	0.040	0.043
PCB99/101	0.003	0.004	0.172	0.249
PCB110	0.004	0.004	0.030	0.041
PCB82	0.006	0.008	0.032	0.040
PCB151	0.001	0.001	0.080	0.095
PCB149	0.004	0.006	0.010	0.012
PCB118	0.003	0.004	0.056	0.062
PCB153	0.001	0.001	0.036	0.053
PCB132/105	0.004	0.004	0.010	0.011
PCB138	0.008	0.010	0.022	0.028
PCB158	0.004	0.005	0.010	0.012
PCB187	0.006	0.008	0.010	0.011
PCB183	0.007	0.010	0.040	0.054
PCB128	0.005	0.007	0.033	0.046
PCB177	0.003	0.003	0.023	0.027
PCB171/156	0.004	0.004	0.015	0.019
PCB180	0.002	0.003	0.001	0.001

Appendix C

Appendix C.3. Concentrations in the dissolved and phytoplankton phases.

Table S7. Summary of concentrations (median, minimum and maximum) in the dissolved (pg L⁻¹) and phytoplankton (ng g⁻¹_{dw}) phases. ΣPCBs is the sum of the 26 PCB congeners detected of the 41 congeners analyzed. Σ_{ICES}PCBs is the sum of the 7 ICES congeners.

Cruise	Area	n	α-HCH ^a	β-HCH ^a	δ-HCH ^a	γ-HCH ^a	ΣHCHs ^a	HCB ^a	ΣPCBs	Σ _{ICES} PCBs	%ICES
Phytoplankton (ng g ⁻¹)	ATOS-II	Median	0.069	0.413	0.140	0.636	1.988	0.416	11.108	3.414	31%
		Min	0.006	0.045	0.007	0.084	0.121	0.015	0.512	0.145	28%
	Weddell	Max	0.840	0.801	0.711	4.892	5.687	7.098	33.499	14.126	42%
		Median	0.180	0.168	0.084	0.710	1.247	0.657	6.939	1.646	24%
	ICEPOS-ATOS-II	Min	0.008	0.022	0.008	0.146	0.163	0.016	0.361	0.098	27%
		Max	0.608	0.854	0.140	4.276	4.460	3.513	58.725	18.162	31%
	ICEPOS-ATOS-II	Median	0.102	0.343	0.035	0.494	0.939	2.384	10.087	3.643	36%
		Min	0.008	0.206	0.008	0.051	0.094	0.021	0.475	0.096	20%
	Bellinghausen	Max	0.439	0.355	0.209	0.573	1.348	10.599	24.319	7.788	32%
		Median	0.331	0.278	0.382	0.412	1.424	1.849	2.560	0.863	34%
	ESSASI	Min	0.198	0.143	0.106	0.211	0.670	0.360	1.456	0.567	39%
		Max	0.565	0.410	0.712	2.369	3.327	16.000	3.770	1.760	47%
Dissolved (pg L ⁻¹)	ESSASI-ATOS-II	Median	0.953	0.929	1.048	0.787	3.716	0.453	3.727	1.404	38%
		Min	0.918	0.890	0.510	0.380	2.768	0.221	2.690	0.608	23%
	Drake-Weddell transect	Max	0.987	0.968	1.585	1.193	4.665	0.684	4.764	2.200	46%
		Median	0.264	2.885	2.148	1.062	6.360	0.976	1.391	0.611	44%
	ATOS-II	Min	0.212	0.092	0.516	0.443	1.264	0.391	1.268	0.512	40%
		Max	0.316	5.678	3.780	1.682	11.456	1.562	1.513	0.709	47%
	ATOS-II	Median	0.197	3.132	0.734	0.360	1.468	0.446	1.213	0.719	59%
		Min	0.092	0.282	0.285	0.326	1.279	0.229	1.182	0.660	56%
	Bransfield	Max	0.278	5.982	5.762	0.797	12.348	0.565	1.519	0.751	49%
		Median	0.158	0.261	0.413	0.824	1.315	0.313	2.167	1.240	57%
	ATOS-II	Min	0.141	0.261	0.333	0.539	1.207	0.191	1.791	0.893	50%
		Max	0.295	0.261	0.526	1.264	2.233	0.337	3.153	1.863	59%
Bellinghausen	Median	0.226	0.286	0.246	0.809	1.448	0.400	1.389	0.789	57%	
	Min	0.126	0.047	0.149	0.617	1.237	0.281	0.738	0.355	48%	
ESSASI	Max	0.371	0.913	0.408	1.205	2.180	0.579	1.863	0.920	49%	

a: HCHs and HCB were analyzed in ESSASI and ATOS-II sampling campaigns but not in the ICEPOS campaign.

Table S8a. Dissolved phase concentrations (pg L^{-1}) for individual compounds for each one of the samples from the ESSASI and ATOS-II cruises.

Cruise	pgL ⁻¹	α -HCH	B-HCH	δ -HCH	γ -HCH	Σ HCHs	HCB	PCB1 8	PCB1 7	PCB3 1	PCB2 8	PCB3 3	PCB5 2	PCB4 9	PCB99/10 1	PCB11 0	PCB8 2
ESSASI	DE1	0.987	0.890	0.510	0.380	2.768	0.684	0.307	0.113	0.095	0.107	0.069	0.127	0.294	0.437	0.100	0.318
	DE2	0.280		0.252	0.710	1.242	0.503	0.051	0.036	0.045	0.049		0.031	0.099	0.189	0.048	0.122
	DE3	0.329	0.913	0.321	0.617	2.180	0.375	0.107	0.084	0.044	0.044	0.023	0.153	0.049	0.372	0.022	0.015
	DE4	0.188		0.408	1.035	1.630	0.400	0.039	0.107	0.063	0.028		0.119	0.099	0.473	0.050	0.061
	DE5	0.210	0.419	0.250	0.809	1.688	0.359	0.092	0.072	0.058	0.051		0.045	0.083	0.377	0.027	0.017
	DE6	0.226	0.047	0.170	0.838	1.281	0.308	0.073	0.063	0.037		0.020	0.075	0.025	0.239	0.030	0.011
	DE7	0.126	0.286	0.149	0.676	1.237	0.281	0.037	0.051	0.024		0.018	0.037	0.021	0.216	0.019	0.029
	DE8	0.245	0.237	0.155	0.736	1.374	0.448	0.117	0.069	0.051	0.027		0.075	0.056	0.252	0.032	0.000
	DE9	0.371			1.205	1.575	0.579	0.116	0.170	0.085	0.054	0.015	0.182	0.060	0.405	0.048	0.056
DE1 0	0.201		0.243	1.004	1.448	0.479	0.072	0.080	0.041	0.022	0.001	0.234	0.055	0.364	0.037	0.041	
ATOS-II	DA1	0.918	0.968	1.585	1.193	4.665	0.221	0.154	0.256	0.418	0.185	0.498	0.165	0.262	0.142	0.036	0.120
	DA2	0.212	0.092	0.516	0.443	1.264	0.391	0.052	0.101	0.077	0.045	0.045	0.018	0.024	0.399	0.029	
	DA3	0.092	0.282	0.734	0.360	1.468	0.229	0.050	0.037	0.075	0.041	0.063	0.071	0.047	0.481	0.037	0.081
	DA4	0.278	5.982	5.762	0.326	12.348	0.446	0.033	0.332	0.068	0.034	0.045	0.028	0.031	0.360	0.024	0.075
	DA5	0.141		0.526	0.539	1.207	0.191	0.036	0.053	0.054	0.031	0.044	0.006	0.040	0.639	0.035	0.119
	DA6	0.295	0.261	0.413	1.264	2.233	0.313	0.031	0.030	0.061	0.044	0.048	0.074	0.011	0.463	0.307	0.072
	DA7	0.158		0.333	0.824	1.315	0.337	0.035	0.021	0.111	0.070	0.211	0.078	0.070	1.133	0.036	0.092
	DA8	0.197		0.285	0.797	1.279	0.565	0.062	0.090	0.065	0.057	0.037	0.033	0.032	0.422	0.016	0.013
	DA9	0.316	5.678	3.780	1.682	11.456	1.562	0.098	0.370	0.057	0.082	0.030	0.017	0.070	0.068	0.037	0.027

Table S8b. Dissolved phase concentrations (pg L^{-1}) for individual compounds for each one of the samples from the ESSASI and ATOS-II cruises (continuation of Table S8a). ΣPCBs is the sum of the 26 PCB congeners detected of the 41 congeners analyzed. $\Sigma_{\text{ICES}}\text{PCBs}$ is the sum of the 7 ICES congeners.

Cruise	pg L^{-1}	PCB151	PCB149	PCB118	PCB153	PCB132/105	PCB138	PCB158	PCB187	PCB183	PCB128	PCB177	PCB171/156	PCB180	PCBs	$\Sigma_{\text{ICES}}\text{PCBs}$
ESSASI	DE1	0.248	0.639	0.643	0.457	0.079	0.342	0.059	0.108	0.031	0.009	0.032	0.064	0.086	4.764	2.200
	DE2	0.078	0.307	0.218	0.184	0.043	0.178	0.027	0.069	0.008	0.005	0.003	0.045	0.028	1.863	0.877
	DE3	0.014	0.124	0.084	0.073	0.024	0.052	0.010	0.051	0.004	0.005	0.003	0.033	0.010	1.397	0.789
	DE4	0.013	0.221	0.146	0.070	0.044	0.080	0.013	0.047	0.005	0.003	0.012	0.034	0.004	1.718	0.920
	DE5	0.027	0.138	0.085	0.051	0.021	0.035	0.007	0.050	0.008	0.006	0.003	0.026	0.008	1.293	0.651
	DE6	0.014	0.083	0.050	0.050	0.015	0.035	0.009	0.082	0.004	0.008	0.001	0.033	0.013	0.970	0.462
	DE7	0.015	0.051	0.038	0.031	0.018	0.027	0.006	0.038	0.001	0.026	0.001	0.029	0.005	0.738	0.355
	DE8	0.010	0.056	0.042	0.043	0.008	0.014	0.004	0.040	0.007	0.004	0.003	0.020	0.002	0.932	0.455
	DE9	0.012	0.176	0.141	0.057	0.042	0.051	0.010	0.054	0.004	0.004	0.002	0.023	0.004	1.762	0.893
	DE10	0.024	0.127	0.107	0.040	0.019	0.039	0.004	0.053	0.004	0.005	0.002	0.025	0.005	1.389	0.810
ATOS-II	DA1	0.292		0.017	0.068		0.028		0.045					0.003	2.690	0.608
	DA2	0.042	0.060	0.099	0.066	0.048	0.067	0.004	0.044		0.003		0.030	0.015	1.268	0.709
	DA3	0.041	0.011	0.021	0.071		0.067	0.007	0.004				0.009	0.000	1.213	0.751
	DA4	0.054	0.090	0.096	0.061	0.041	0.067	0.003	0.037				0.027	0.015	1.519	0.660
	DA5	0.092	0.178	0.191	0.132	0.099	0.140	0.014	0.075	0.016	0.007	0.017	0.050	0.101	2.167	1.240
	DA6	0.038	0.126	0.109	0.078	0.058	0.092	0.008	0.052	0.003	0.010	0.004	0.038	0.033	1.791	0.893
	DA7	0.196	0.261	0.132	0.213	0.014	0.111	0.011	0.137	0.040		0.012	0.043	0.128	3.153	1.863
	DA8	0.006	0.082	0.085	0.068	0.003	0.044	0.004	0.032	0.002			0.020	0.010	1.182	0.719
	DA9	0.060	0.142	0.113	0.134	0.001	0.061	0.002	0.071	0.006			0.032	0.037	1.513	0.512

Table S9a. Phytoplankton phase concentrations ($\text{ng g}^{-1}_{\text{dw}}$) for individual compounds for each one of the samples of the ICEPOS, ESSASI and ATOS-II cruises.

Cruise	ng g^{-1}	α -HCH	β -HCH	δ -HCH	γ -HCH	Σ HCHs	HCB	PCB18	PCB17	PCB31	PCB28	PCB33	PCB52	PCB49	PCB99/101	PCB110	PCB82
ICEPOS	FI1							1.823	0.786	0.634	1.392		2.863	0.670	5.483	0.801	0.431
	FI2								0.295				0.540	0.128	1.641	1.080	0.162
	FI3												0.175				
ESSASI	FE1	0.565	0.524	0.524	2.219	3.308	2.098	0.303	0.044	0.194	0.044	0.391	0.069	0.025	0.456	0.081	0.081
	FE2	0.263	0.402	0.402	2.369	3.327	16.000	0.212	0.157	0.075	0.075	0.030	0.048	0.025	0.224	0.024	0.053
	FE3	0.439	0.143	0.712	0.250	1.544	1.600	0.229	0.209	0.058	0.081	0.057	0.420	0.038	0.462	0.031	0.123
	FE4	0.384	0.512	0.896	0.896	1.793	2.689	0.282	0.090	0.064	0.038	0.647	0.051	0.198	0.378	0.045	0.077
	FE5	0.382	0.162	0.410	1.224	1.473	1.473	0.431	0.351	0.138	0.059	0.067	0.095	0.041	0.447	0.056	0.264
	FE6	0.198	0.124	0.347	0.347	0.670	3.199	0.107	0.074	0.045	0.040	0.176	0.020	0.206	0.206	0.027	0.045
	FE7	0.335	0.454	0.355	1.374	0.669	1.374	0.268	0.201	0.043	0.053	0.031	0.060	0.067	0.234	0.036	0.076
	FE8	0.226	0.362	0.211	0.799	7.532	0.169	0.169	0.039	0.060	0.068	0.014	0.080	0.026	0.339	0.026	0.066
	FE9	0.328	0.278	0.459	1.474	0.360	1.474	0.187	0.167	0.067	0.450	0.523	0.855	0.192	0.192	0.021	0.051
	FE10	0.248	0.288	0.106	0.414	1.056	1.171	0.289	0.205	0.053	0.047	0.124	0.263	0.041	0.263	0.040	0.141
ATOS-II	FA1	0.023	0.007	0.007	0.154	0.183	0.170	0.084	0.035	0.060	0.060	0.128	0.019	0.026	0.015	0.008	0.005
	FA2	0.101	0.259	0.259	4.386	4.746	0.388	0.173	1.266	0.072	0.086	0.532	0.518	0.058	0.906	0.173	0.173
	FA3	0.085	0.711	0.711	4.892	5.687	2.251	0.127	3.588	0.330	0.212	1.303	0.482	0.118	1.109	0.220	0.008
	FA4	0.053	0.156	0.084	0.084	0.293	0.365	0.160	0.038	0.030	0.103	0.110	0.342	0.091	0.981	0.091	0.114
	FA5	0.840	0.473	1.099	1.099	3.213	7.098	1.084	1.191	3.564	3.084	1.122	0.634	2.336	1.549	0.420	0.580
	FA6	0.059	0.148	0.059	0.981	1.247	0.657	0.266	0.731	0.384	0.369	0.531	0.465	0.089	1.417	0.184	0.125
	FA7	0.608	0.034	0.012	0.174	0.829	0.046	1.815	0.079	0.193	0.159	4.224	0.809	0.043	0.039	0.012	0.012
	FA8	0.006	0.009	0.009	0.106	0.121	0.015	0.448	0.014	0.029	0.021	1.661	0.022	0.069	0.048	0.008	0.004
	FA9	0.053	0.123	0.123	0.173	0.762	2.406	0.829	0.332	1.623	0.219	3.344	0.127	0.035	0.325	0.049	0.049
	FA10	0.241	0.045	0.098	3.570	3.955	0.444	2.855	1.507	0.392	0.309	0.746	1.265	0.143	0.384	0.188	0.188
	FA11	0.092	0.854	0.069	1.062	2.078	0.958	0.104	0.439	0.115	0.254	0.312	0.231	0.035	0.416	0.081	0.081
	FA12	0.418	0.140	0.140	0.710	1.494	3.513	2.978	7.416	3.932	0.011	5.100	7.747	2.890	5.956	1.275	3.027
	FA13	0.008	0.008	0.146	0.146	0.163	0.016	0.022	0.032	0.011	0.019	0.065	0.029	0.020	0.019	0.006	0.002
	FA14	0.127	0.188	0.098	1.494	1.906	2.392	0.233	0.384	0.739	0.457	0.412	0.425	0.371	0.572	0.131	0.171
	FA15	0.184	0.139	0.127	4.276	4.460	0.220	0.679	3.138	0.367	0.844	0.294	0.275	0.349	0.349	0.312	0.312
	FA16	0.139	0.139	0.139	0.672	0.938	1.599	0.151	0.944	0.162	0.151	0.730	0.243	0.440	0.440	0.127	0.127
FA17	0.180	0.355	0.131	0.415	1.080	2.384	0.551	0.551	0.944	0.982	0.311	1.244	0.698	0.873	0.166	0.267	
FA18	0.102	0.009	0.009	0.573	0.684	10.599	0.471	0.499	0.379	0.231	0.342	0.277	0.314	0.314	0.166	0.166	
FA19	0.439	0.206	0.209	0.494	1.348	6.950	0.856	0.450	1.438	1.581	0.472	0.274	0.626	1.274	0.274	0.428	
FA20	0.062	0.343	0.008	0.526	0.939	1.725	0.325	0.147	0.077	1.222	0.325	0.209	0.005	0.317	0.116	0.116	
FA21	0.008	0.035	0.035	0.051	0.094	0.021	0.074	0.074	0.012	0.138	0.066	0.066	0.005	0.005	0.021	0.199	
FA22	0.056	0.087	0.087	0.414	0.557	0.040	0.223	1.098	0.072	0.207	0.167	0.111	0.159	0.159	0.127	0.084	
FA23	0.111	0.008	0.008	0.593	0.712	0.087	0.261	0.704	0.142	0.174	0.206	0.166	0.340	0.340	0.127	0.127	
FA24	0.277	0.022	0.152	0.199	0.650	0.342	0.229	0.008	0.008	0.025	0.819	0.044	0.049	0.049	0.011	0.084	
FA25	1.299	0.067	0.050	2.214	3.630	0.074	0.489	0.179	0.081	0.052	0.670	0.145	0.007	0.119	0.029	0.029	
FA26	0.038	0.007	0.007	0.608	0.653	0.129	0.334	0.036	0.009	0.066	0.863	0.140	0.018	0.018	0.034	0.118	

Appendix C

Table S9b. Phytoplankton phase concentrations (ng g⁻¹_{dwt}) for individual compounds for each one of the samples of the ICEPOS, ESSASI and ATOS-II cruises (Continuation of Table S9a). Σ PcBs is the sum of the 26 PCB congeners detected of the 41 congeners analyzed. Σ _{ICES}PcBs is the sum of the 7 ICES congeners.

Cruise	PCB151	PCB149	PCB118	PCB153	PCB132/105	PCB138	PCB158	PCB187	PCB183	PCB128	PCB177	PCB171/156	PCB180	PCBs	Σ _{ICES} PCB	
ICEPOS	FE1	0.475	0.986	1.355	0.786	0.623	0.199	0.236	0.007	3.374			0.602	24.319	7.788	
	FE2	0.144	0.354	0.362	0.261	0.245	0.088	0.072		1.213			0.162	6.868	1.449	
	FE3		1.541		1.471		1.934			0.441		2.139		7.700	1.646	
ESSASI	FE1		0.117	0.141	0.278	0.340	0.357	0.089	0.100	0.148	0.058	0.165	0.313	3.770	1.659	
	FE2	0.006	0.087	0.060	0.195	0.179	0.253	0.003	0.048	0.139	0.023	0.057	0.118	2.178	0.927	
	FE3	0.030	0.086	0.089	0.147	0.227	0.409	0.066	0.248	0.019	0.022	0.018	0.101	3.193	1.710	
	FE4	0.074	0.070	0.045	0.102	0.215	0.114	0.042	0.244	0.048	0.051	0.038	0.062	2.749	0.727	
	FE5	0.010	0.106	0.129	0.134	0.222	0.117	0.017	0.243	0.354	0.051	0.012	0.036	3.508	1.043	
	FE6	0.010	0.119	0.047	0.171	0.103	0.103	0.042	0.243	0.354	0.051	0.012	0.036	3.508	1.043	
	FE7	0.011	0.117	0.091	0.114	0.202	0.114	0.019	0.411	0.046	0.030	0.024	0.036	1.456	0.690	
	FE8	0.014	0.096	0.095	0.080	0.158	0.116	0.006	0.043	0.010	0.010	0.004	0.025	2.158	0.567	
	FE9	0.051	0.051	0.056	0.090	0.126	0.101	0.034	0.676	0.074	0.074	0.074	0.016	1.554	0.799	
	FE10	0.011	0.060	0.080	0.092	0.139	0.159	0.047	0.369	0.020	0.043	0.019	0.028	3.737	1.760	
ATOS-II	FA1	0.015	0.017	0.017	0.005	0.014	0.018	0.026	0.003	0.003	0.001	0.009	0.025	0.512	0.158	
	FA2	0.230	1.337	0.187	1.998	2.609	3.190	1.461	0.179	0.760	0.313	0.805	2.027	18.879	8.912	
	FA3	0.745	2.615	0.144	3.378	3.186	3.214	2.913	1.141	1.096	1.981	1.981	5.588	33.499	14.126	
	FA4		0.308	0.152	0.071	1.001	0.071	0.482		0.054	0.054	0.051	0.101	4.262	1.731	
	FA5	0.214	0.656	0.878	1.156	1.797	1.729	0.233	1.418	0.359	0.243	3.400	2.807	30.715	11.836	
	FA6	0.089	0.258	0.155	0.354	0.598	0.393	0.189	0.189	0.016	0.094	0.094	0.205	6.911	3.358	
	FA7	0.023	0.085	0.006	0.026	0.019	0.017		0.007	0.007	0.029	0.100	0.027	6.993	0.353	
	FA8	0.004	0.027	0.022	0.010	0.008	0.013	0.006		0.007	0.012	0.049	0.008	0.010	2.492	0.145
	FA9	0.053	0.095	0.060	0.017	0.194	0.066	0.125	0.003	0.007	0.066	0.066	0.100	7.675	0.914	
	FA10	0.090	0.211	0.399	0.490	0.819	1.561	0.291	1.423	0.138	0.490	0.015	0.138	6.889	14.541	
	FA11				0.083	0.566	0.012		1.510	0.138	0.490	0.015	0.138	6.889	14.541	
	FA12	0.506	0.876	0.905	1.812	2.363	1.462	0.006	3.874	5.286	0.491	0.190	0.360	58.725	18.162	
	FA13		0.004	0.010	0.007	0.030	0.007	0.026	0.026	0.004	0.004	0.003	0.037	0.008	0.361	
	FA14	0.029	0.441	0.392	0.157	0.577	0.345	0.056	0.056	0.303	0.075	0.187	0.172	6.939	2.658	
	FA15		0.018	0.037	0.215	0.984	0.107	0.089	2.057	0.303	0.075	0.187	0.172	6.939	2.658	
	FA16		0.035	0.695	0.241	0.880	0.107	0.089	2.057	0.303	0.075	0.187	0.172	6.939	2.658	
	FA17	0.131	0.431	0.327	0.552	2.139	0.784	0.107	4.353	1.406	0.031	0.121	0.054	10.213	2.131	
	FA18			0.028	0.056	0.383	0.056	0.107	4.353	1.406	0.031	0.121	0.054	10.213	2.131	
	FA19	0.077	0.560	0.648	0.836	1.960	1.192	0.019	1.980	0.274	0.302	0.037	0.206	5.491	1.009	
	FA20			0.023	0.114	0.163	0.147	2.440	2.440	0.274	0.302	0.037	0.206	5.491	1.009	
	FA21			0.008	0.004	0.037	0.011	5.082	5.082	0.274	0.302	0.037	0.206	5.491	1.009	
	FA22			0.008	0.008	0.049	0.049	0.087	0.087	0.011	0.011	0.011	0.011	0.001	0.475	
	FA23		0.016	0.008	0.025	0.369	0.017	3.382	3.382	0.011	0.011	0.011	0.011	0.001	0.475	
	FA24	0.007	0.010	0.020	0.018	0.031	0.021	0.013	0.098	0.027	0.015	0.015	0.005	0.008	1.690	
	FA25			0.031	0.031	0.135	0.255	0.050	1.535	0.029	0.211	0.149	0.141	0.305	4.611	
	FA26	0.061	0.022	0.054	0.227	0.268	0.869	0.263	3.284	0.167	0.386	0.184	0.514	0.775	8.962	

Appendix C.4. Additional tables and figures

Table S10. Physico-Chemical properties of PCBs, HCH and HCB used in the present study. K_{ow} is the octanol-water partition coefficient. MW is the molecular weight.

Compound	Log K_{ow} (298 K)	Reference	MW (g mol⁻¹)	# Cl
α-HCH	3.94		290.83	6
β-HCH	3.92	Xiao et al. 2004	290.83	6
γ-HCH	3.83		290.83	6
HCB	5.64	Shen & Wania. 2005	284.782	6
δ-HCH	4.14		290.83	6
PCB18	5.6		257.543	3
PCB17	5.76		257.543	3
PCB33	5.87		257.543	3
PCB49	6.38	Hansch et al. 1995	291.988	4
PCB151	6.85		360.878	6
PCB128	7.32		360.878	6
PCB132/105	7.04		360.878	6
PCB171/156	7.57		360.878	6
PCB31	5.78		257.543	3
PCB28	5.66		257.543	3
PCB52	5.91		291.988	4
PCB118	6.69	Li et al. 2003	326.433	5
PCB153	6.87		360.878	5
PCB138	7.22		360.878	6
PCB180	8.51		395.323	7
PCB149	6.47		368.99	5
PCB187	7.05	Makino 1998	395.323	7
PCB177	6.92		395.323	7
PCB82	6.73		326.433	5
PCB158	7.69	Ran et al. 2002	360.878	6
PCB183	8.27		395.323	7
PCB99/101	6.98	Hardy 2002	326.433	5
PCB110	6.2	Sangster 1993	326.433	5

Appendix C

Table S11. Seawater Half-lives (or e-folding times) for PCBs and HCHs as estimated in previous studies.

Compound	Half-Live (d)	Reference
α-HCH	145	Wöhrnschimmel et al., 2012 ^a
β-HCH	437.5	
PCB18	1000	Sedlak & Andren 1991
PCB17	1000	
PCB31	1000	
PCB33	1000	
PCB49	1000	
PCB110	1000	
PCB28	60	
PCB52	1250	Sinkkonen and Passivirta, 2000
PCB99 /101	2500	
PCB118	2500	
PCB153	5000	
PCB138	5000	
PCB180	7500	
PCBs averaged	2293	

a: Based on organic matter mediation process

Table S12. Relationship between concentrations in phytoplankton versus biomass. Compound specific values of the slope (m) obtained by fitting equation [4] ($\log C_p = -m \log B + a$) to the measured concentrations. C_p is the concentration in phytoplankton. B is the water column average phytoplankton biomass (mg L^{-1}). P-values of the least square linear regression are given. n.s. means no significant regression ($p > 0.05$).

Compound	m	p
α-HCH	0.304	n.s.
β-HCH	0.896	0.025
δ-HCH	0.398	n.s.
γ-HCH	0.583	0.0011
HCB	0.703	0.0154
PCB18	0.220	n.s.
PCB17	0.994	0.0001
PCB31	0.665	0.0153
PCB28	0.671	0.0003
PCB33	0.090	n.s.
PCB52	0.575	0.0017
PCB49	0.694	0.0215
PCB99 /101	0.833	0.0002
PCB110	0.897	0.0001
PCB82	1.028	0.0206
PCB151	1.020	0.0001
PCB149	0.543	n.s.
PCB118	0.608	0.0158
PCB153	0.861	0.0039
PCB132 /105	0.986	0.0001
PCB138	0.695	0.017
PCB158	0.493	n.s.
PCB187	1.158	0.0001
PCB183	1.116	0.0049
PCB128	1.320	0.0006
PCB177	0.596	0.016
PCB171/156	0.879	0.001
PCB180	0.906	0.0053

Appendix C

Table S13a. Biocentration factors (BCF) for phytoplankton, as described by equation [4.2] of the main manuscript, for samples from the ESSASI cruise against the temperature corrected Log K_{OW} . m: slope, b: independent term and N: number of compounds in sample.

Sample	m	b	$R^2(\%)$	p-value	N
FE1	0.7	2.4	53	<0.0005	21
FE2	0.52	3.31	20	<0.05	24
FE2	0.52	3.72	20	<0.05	23
FE3	0.49	4.01	32	<0.005	23
FE4	0.62	3.23	40	<0.005	19
FE5	0.74	2.5	57	<0.0001	23
FE6	0.71	2.29	42	<0.005	17
FE7	0.71	2.44	59	<0.0001	20
FE7	0.68	2.74	72	<0.0001	20
FE8	0.46	4.11	31	<0.005	22
FE8	0.42	4.48	32	<0.005	21
FE8	0.41	4.68	27	<0.005	21
FE9	0.47	4.51	30	<0.05	17
FE9	0.62	3.39	32	<0.05	16
FE10	0.71	2.64	61	<0.0001	21

Table S13b. Biocentration factors (BCF) for phytoplankton, as described by equation [4.2] of the main manuscript, for samples from the ATOS-2 cruise against the temperature corrected Log K_{OW} . m: slope, b: independent term and N: number of compounds in sample. n.s. means that the regression is not significant ($p\text{-value} > 0.05$).

Sample	m	b	$R^2(\%)$	p-value	N
FA1	0.13	4.615	n.s	n.s	15
FA2	1.2	-1.53	52	<0.005	15
FA3	0.87	0.84	23	<0.05	16
FA4	0.96	-0.32	50	<0.005	15
FA5	0.49	3.8	n.s	n.s.	20
FA5	0.66	3.04	48	<0.0005	20
FA6	0.5	3.45	44	<0.005	18
FA7	5.7	0.07	n.s	n.s	18
FA8	3.54	0.34	n.s	n.s	19
FA9	0.24	5.02	n.s	n.s.	20
FA10	0.62	2.87	35	<0.005	20
FA11	0.41	3.9	21	<0.05	16
FA12	0.25	6.09	n.s	n.s	18
FA12	0.2	6.46	n.s	n.s	17
FA13	0.41	2.82	n.s	n.s	17
FA14	0.26	5.19	n.s	n.s	18
FA14	0.51	3.4	35	<0.005	20
FA15	0.53	3.29	19	<0.05	18
FA16	0.62	2.54	32	<0.05	14
FA16	0.51	3.33	19	<0.05	16
FA17	0.28	5.18	n.s	n.s	21
FA18	0.06	7.38	n.s	n.s	18
FA19	0.39	4.55	21	<0.05	23
FA19	0.65	2.73	42	<0.001	23
FA20	0.19	5.38	n.s	n.s	16
FA21	0.14	4.65	n.s	n.s	14
FA21	0.01	5.49	n.s	n.s	14
FA22	0.28	8.1	n.s	n.s	13
FA23	0.21	4.99	n.s	n.s	16
FA23	0.3	4.48	n.s	n.s	14
FA24	0.38	3.55	n.s	n.s	19
FA25	0.86	0.61	47	<0.005	16
FA26	1.21	-1.7	61	<0.0001	20
FA26	1.12	-1.43	59	<0.0001	20

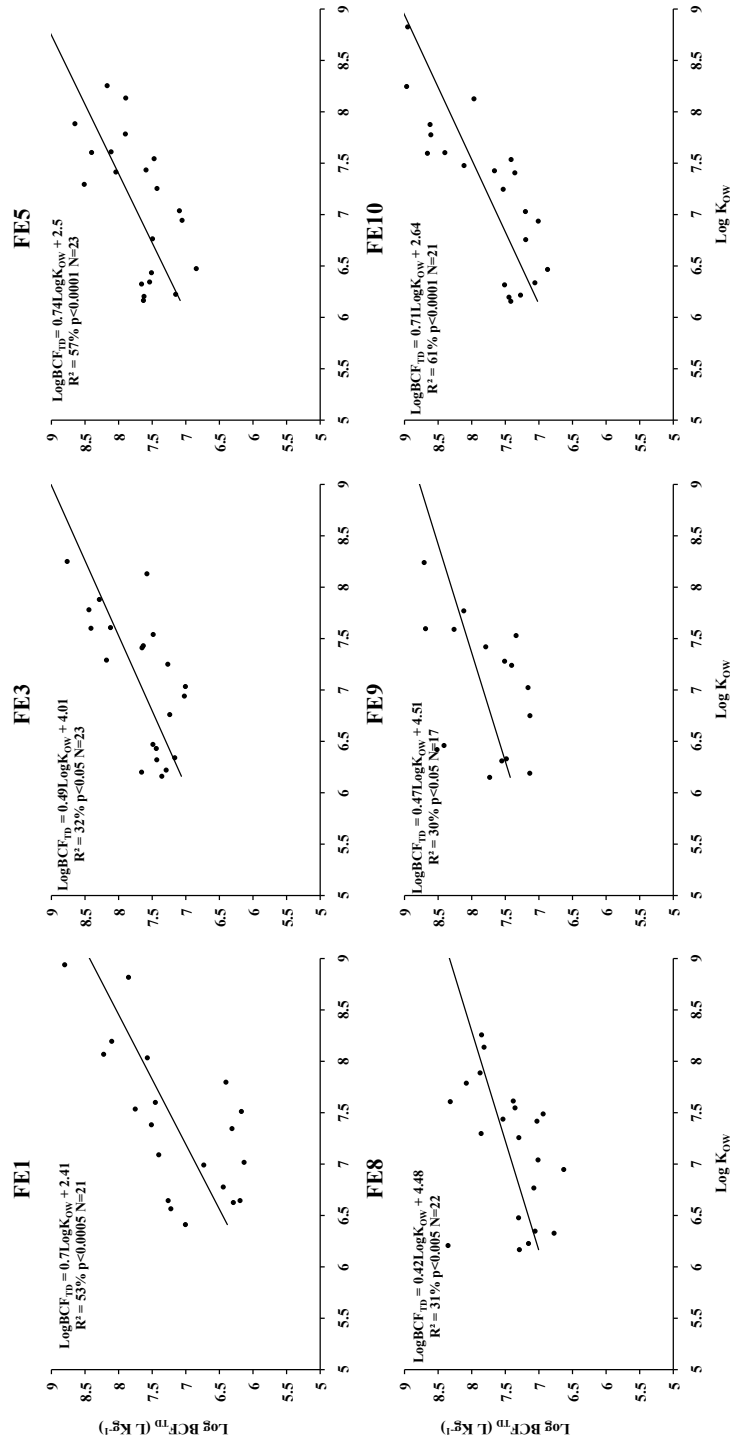


Figure S1a. Bioconcentration factors obtained by using the truly dissolved concentration (BCF_{TD}), as described in equation [2], versus the temperature-corrected octanol-water partition coefficient (K_{OW}) for some characteristic samples from the ESSASI cruise.

Appendix C

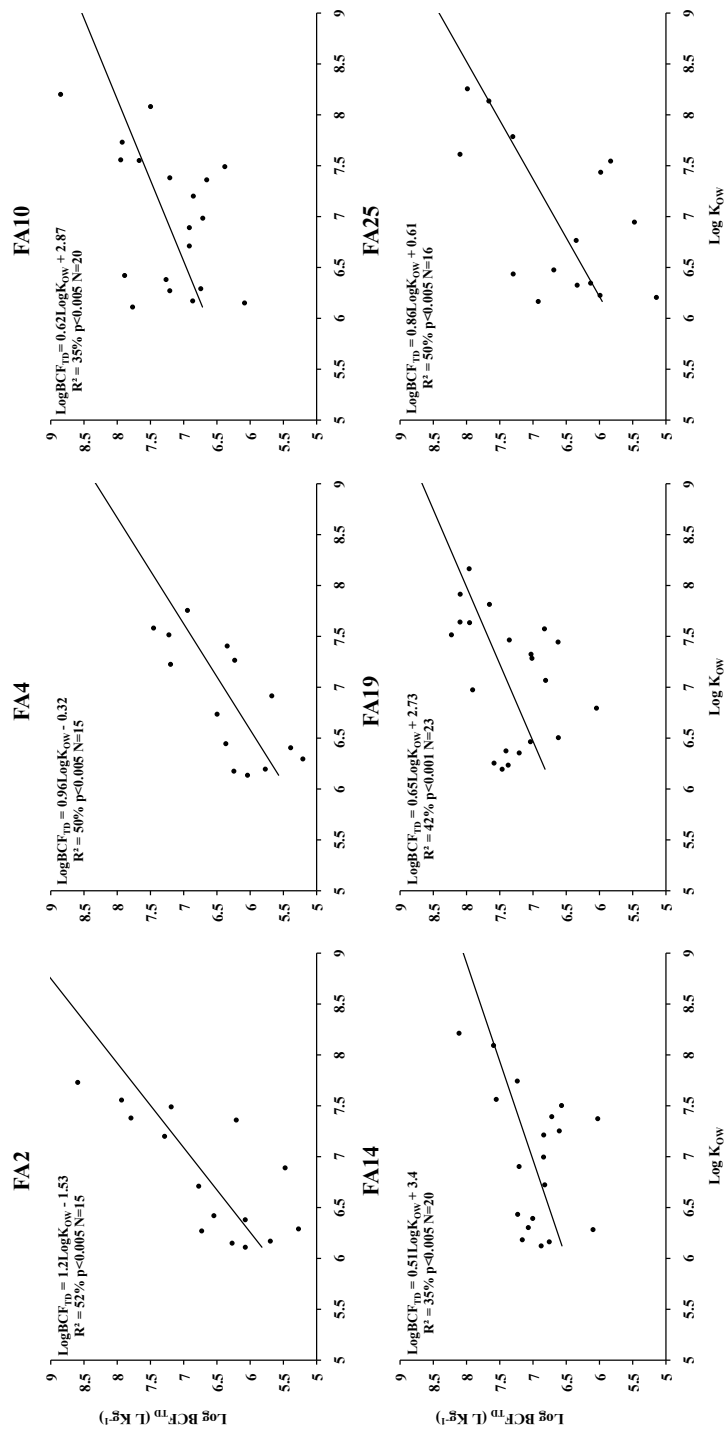


Figure S1b Bioconcentration factors obtained by using the truly dissolved concentration (BCF_{TD}), as described in equation [2], versus the temperature-corrected octanol-water partition coefficient (K_{OW}) for some characteristic samples from the ESSASI cruise.

Additional References

Hardy, M.L. A comparison of the properties of the major commercial PBDPO/PBDE product to those of major PBB and PCB products. *Chemosphere*. **2002**46, 717–728.

Li, N.; Wania, F.; Lei, Y.D.; Daly, G.L. A comprehensive and critical compilation, evaluation, and selection of physical- chemical property data for selected polychlorinated biphenyls. *J. Phys. Chem. Ref. Data* **2003** 32, 1545–1590.

Makino, M. Prediction of *n*-octanol/water partition coefficients of polychlorinated biphenyls by use of computer calculated molecular properties. *Chemosphere*. **1998** 37, 13–26.

Ran, Y.; He, Y.; Hang, G.; Johnson, J.L.H.; Yalkowsky, S.H. (2002) Estimation of aqueous solubility of organic compounds by using the general solubility equation. *Chemosphere*. **2002** 48, 487–509.

Sangster, J. LOGKOW, A Databank of Evaluated Octanol-Water Partition Coefficients. First ed., Montreal, Quebec, Canada. **1993**

Sedlak, D.L.; Andren, A.W. Aqueous-phase oxidation of polychlorinated biphenyls by hydroxyl radicals. *Environ. Sci. Technol.* **1991** 25, 1419–1427

Shen, L.; Wania, F. Compilation, evaluation, and selection of physical-chemical property data for organochlorine pesticides. *J. Chem. Eng. Data*. **2005**, 50(3), 742-768.

Sinkkonen, S.; Passivirta, J. Degradation half-life times of PCDDs, PCDFs and PCBs for environmental fate modeling. *Chemosphere*. **2000** 40, 943–949.

Wöhrnschimmel, H.; Tay, P.; Von Waldow, H.; Hung, H.; Li, Y.-F.; MacLeod, M.; Hungerbuehler, K. Comparative assessment of the global fate of alpha- and beta-hexachlorocyclohexane before and after phase-out. *Environ. Sci. Technol.*, **2012** 46 (4), 2047–2054

Xiao, H.; Li N.; Wania, F. Compilation, Evaluation, and Selection of PhysicalChemical Property Data for α -, β -, and γ -Hexachlorocyclohexane. *J. Chem. Eng. Data*. **2005** 49: 173-185.

Appendix D

Supporting information to Chapter 6: Atmospheric Occurrence and Deposition of Hexachlorobenzene and Hexachlorocyclohexanes in the Southern Ocean and Antarctic Peninsula

Appendix D.1

Table S1 Ancillary data for atmospheric samples taken during ESSASI and ATOS II cruises...295

Figure S1. Courses of the ESSASI and ATOS II sampling campaigns...296

Figure S2. Sampling sites at Livingston Island (Southern Shetlands, Antarctica)...297

Appendix D.2

Figure S3. Atmospheric aerosol-phase concentrations during the ATOS II cruise...298

Figure S4a Air mass backtrajectories for the ESSASI cruise samples calculated using the HYSPLIT model from NOAA...299

Figure S4b Air mass backtrajectories for the ESSASI cruise samples calculated using the HYSPLIT model from NOAA...300

Figure S5a Air-mass backtrajectories for the ATOS II cruise calculated using the HYSPLIT model from NOAA...301

Figure S5b Air-mass backtrajectories for the ATOS II cruise calculated using the HYSPLIT model from NOAA...302

Figure S5c Air-mass backtrajectories for the ATOS II cruise calculated using the HYSPLIT model from NOAA...303

Appendix D.3

Text 1. Henry's Law Constant (HLC) correction for temperature and salinity...304

Text2. Degradation Flux estimations...305

Table S2. α -HCH, γ -HCH and HCB physico-chemical properties used for the fugacity ratio calculations and the fluxes estimated in the present work...306

Table S3. Truly dissolved seawater concentrations used for the estimations of fugacity ratios and air-water diffusive fluxes...306

Table S4. Gas and aerosol phase concentrations (pg m^{-3}) over the Southern Ocean in 2008 and 2009...307

Table S5. Gas phase concentrations for HCB and γ -HCH (pg m^{-3}) at Livingston Island...308

Appendix D

Table S6. Estimated air-water fugacity ratios (f_A/f_W) for the ESSASI and ATOS cruises...309

Table S7 Air-Sea diffusive exchange fluxes ($\text{ng m}^{-2}\text{d}^{-1}$) for each gas-phase sampling event during the ESSASI and ATOS cruises)...309

Table S8 Dry deposition fluxes ($\text{ng m}^{-2}\text{d}^{-1}$) estimated for each one of the four aerosol-phase samples where HCB and HCH could be quantified...309

Table S9. Estimations of the total degradation flux...310

Additional References...311

Appendix D.1

Table S1: Ancillary data for the atmospheric samples taken during the ESSASI and ATOS II cruises. Long: longitude, Lat: latitude, Vol: total volume sampled, TA: air temperature (25 m height) and TS: sea surface temperature during sampling. Only aerosol phase samples where HCH and HCB concentrations above limits of quantification are shown.

Matrix	Cruise	CODE	Long	Lat	Date	Vol m ³	wind speed m s ⁻¹	wind direction °	TA °C	TS °C
Gas phase	ESSASI	GE1	-54.06	-60.53	4/2/08	975.00	7.63	203.29	1.29	0.02
		GE2	-51.41	-61.45	11/2/08	745.00	5.25	252.18	0.58	-0.36
		GE3	-51.31	-61.30	14/1/08	1024.00	6.69	204.90	0.26	-0.25
		GE4	-50.65	-60.19	16/1/08	862.00	7.94	249.20	0.92	0.32
		GE5	-47.04	-60.20	18/1/08	1556.00	6.20	155.56	0.12	-0.49
		GE6	-52.38	-61.67	20/1/08	865.00	9.97	307.63	1.04	-0.04
	ATOS II	GA1	-57.87	-62.43	29/1/09	1006.00	8.25	245.03	1.19	0.92
		GA2	-51.78	-63.84	1/2/09	890.00	6.36	144.73	-1.44	-0.04
		GA3	-55.85	-64.20	4/2/09	1414.00	7.60	207.31	1.47	1.34
		GA4	-71.36	-67.62	8/2/09	1691.00	6.56	101.84	2.19	2.40
		GA5	-71.40	-67.64	13/2/09	1145.00	4.36	138.76	-2.01	0.23
		GA6	-74.41	-69.54	15/2/09	1414.00	8.73	104.41	1.38	0.73
		GA7	-57.38	-63.05	19/2/09	1940.00	7.90	118.78	-1.50	-0.23
		GA8	-63.62	-64.83	21/2/09	1990.00	4.70	204.49	1.60	1.47
		GA9	-55.81	-64.53	24/2/09	1500.00	5.00	172.54	-2.79	-0.36
Aerosol	ATOS II	A1	-51.51	-62.76	4/2/09	2724.00	7.49	196.06	0.07	0.49
		A2	-58.40	-62.20	6/2/09	1899.00	7.08	247.26	2.81	2.25
		A3	-72.34	-67.98	12/2/09	1043.00	7.05	134.64	0.54	1.04
		A4	-66.38	-65.50	19/2/09	1114.00	8.84	130.22	1.10	2.20

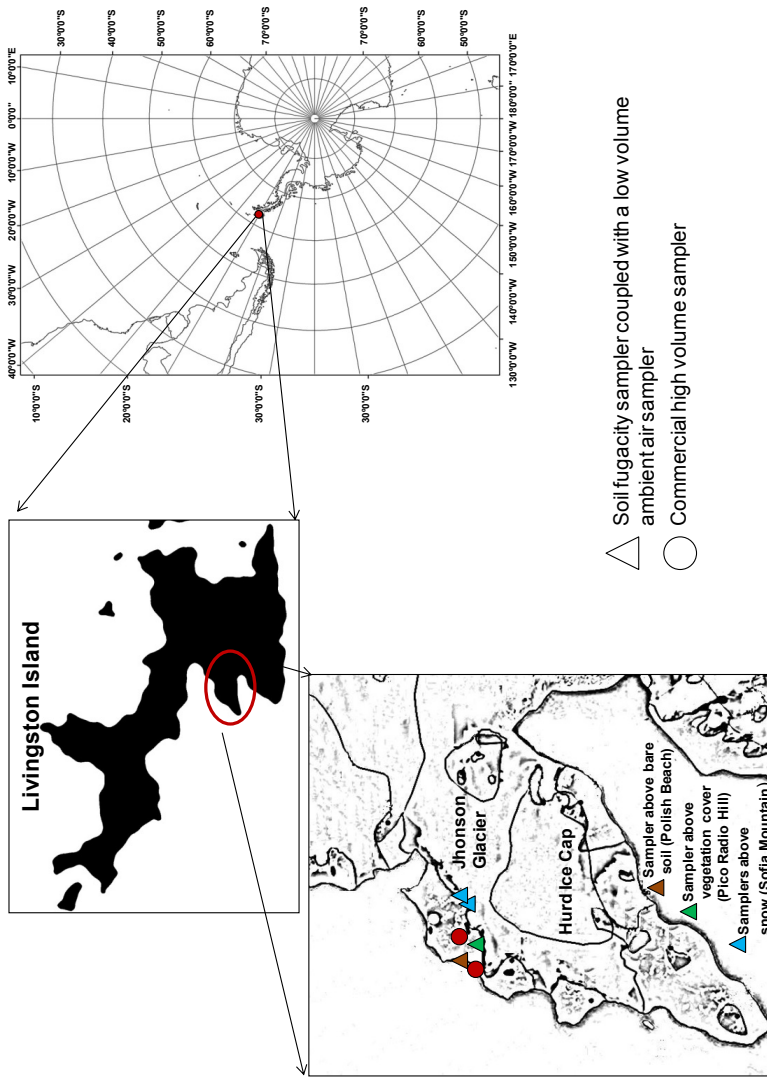


Figure S2: Sampling sites at Livingston Island (Southern Shetlands, Antarctica) for the campaign carried out in austral summer 2009.

Appendix D

APPENDIX D.2

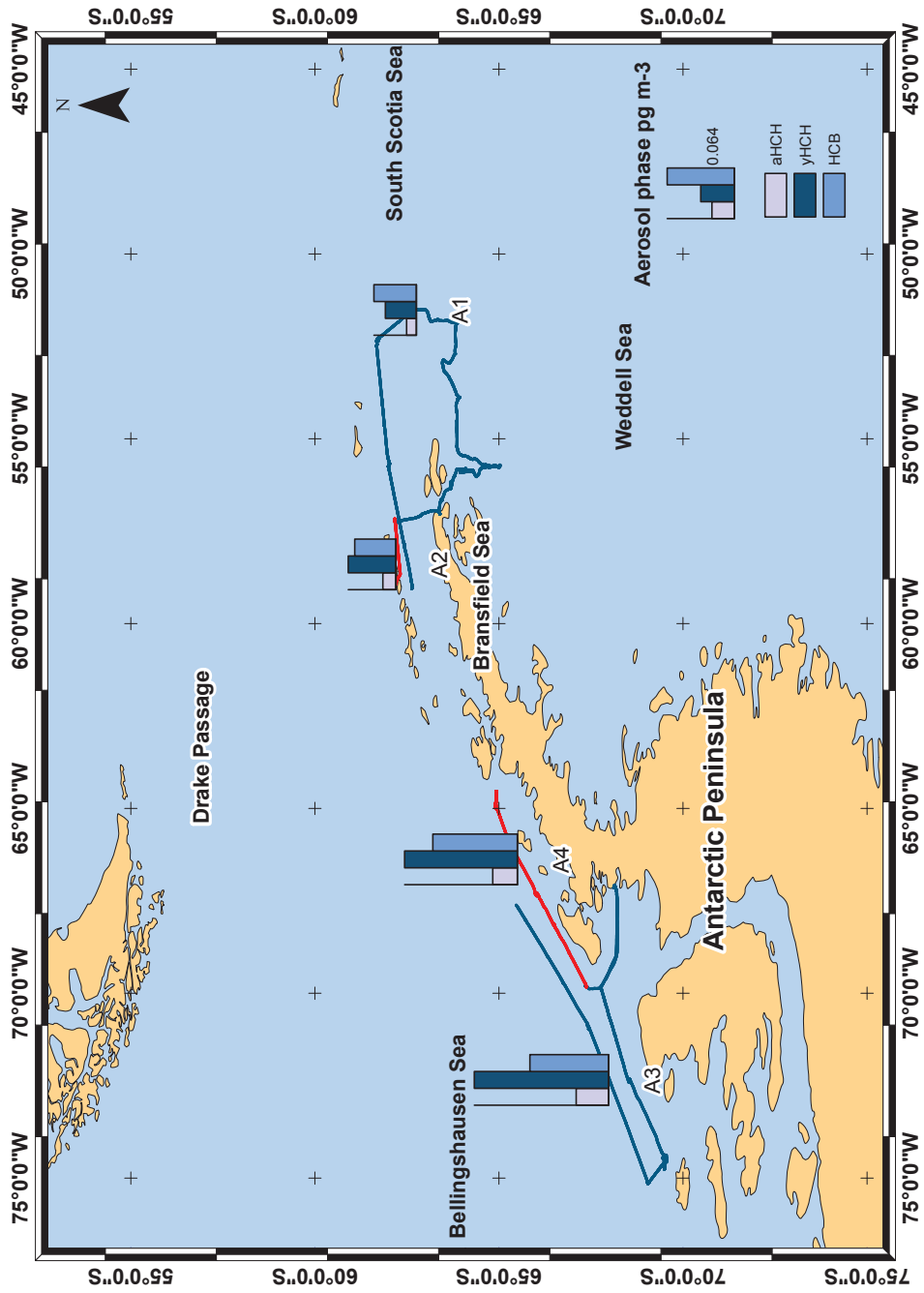
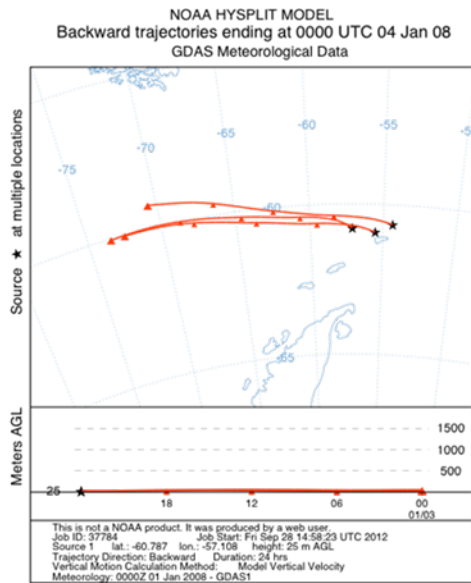
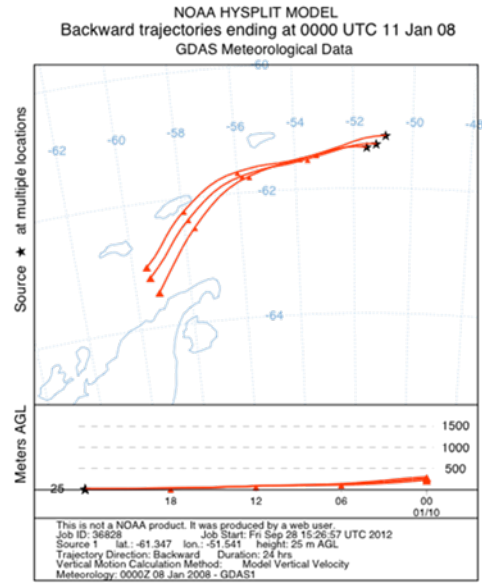


Figure S3. Atmospheric aerosol-phase concentrations (pg m^{-3}) during the ATOS II cruise.

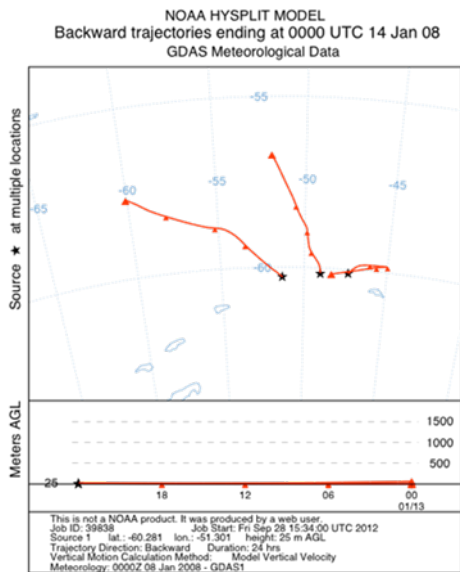
GE1



GE2



GE3



GE4

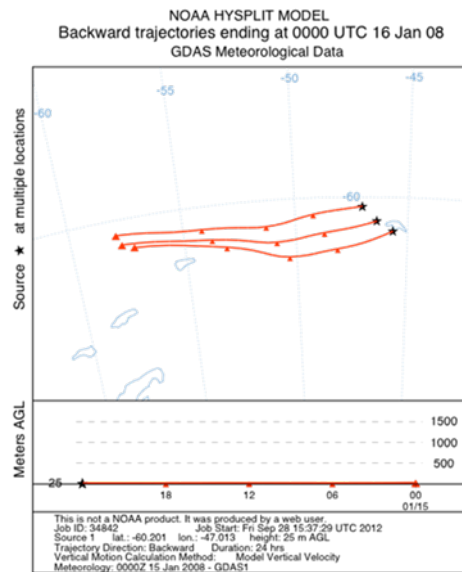


Figure S4a. Air mass backtrajectories for the ESSASI cruise samples calculated using the HYSPLIT model from NOAA (Draxler and Rolph, 2011).

Appendix D

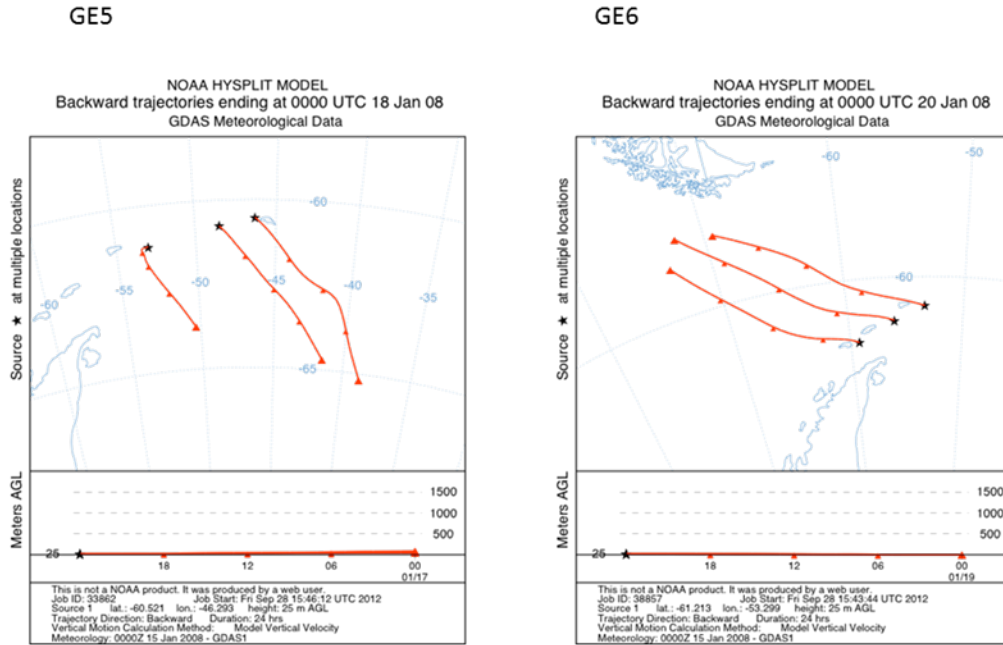
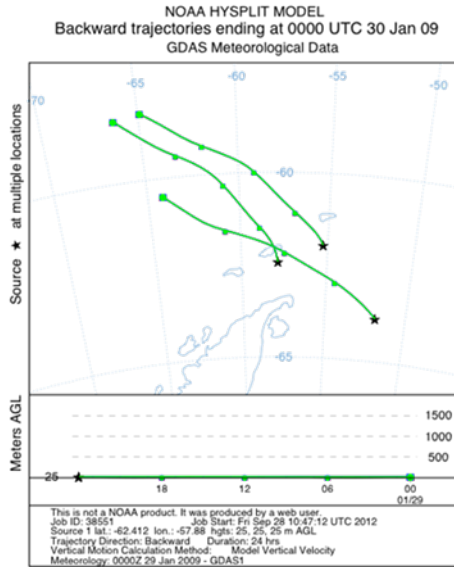
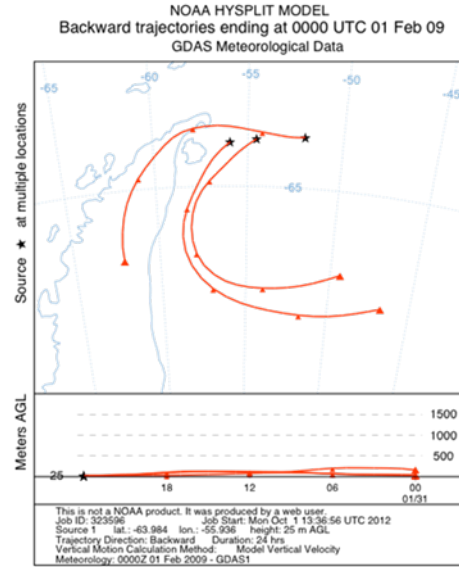


Figure S4b. Air-mass backtrajectories for the ESSASI cruise calculated using the HYSPLIT model from NOAA (Draxler and Rolph, 2011).

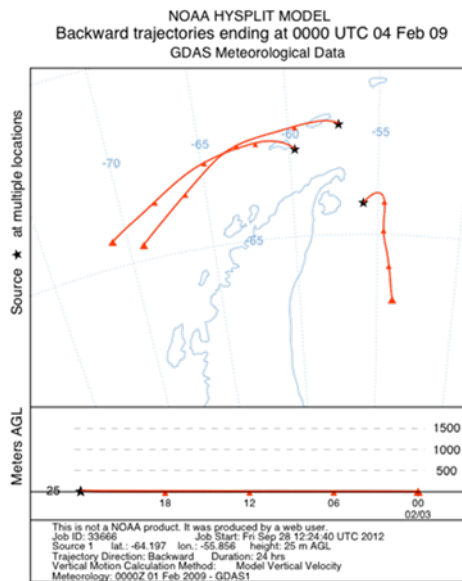
GA1



GA2



GA3



GA4

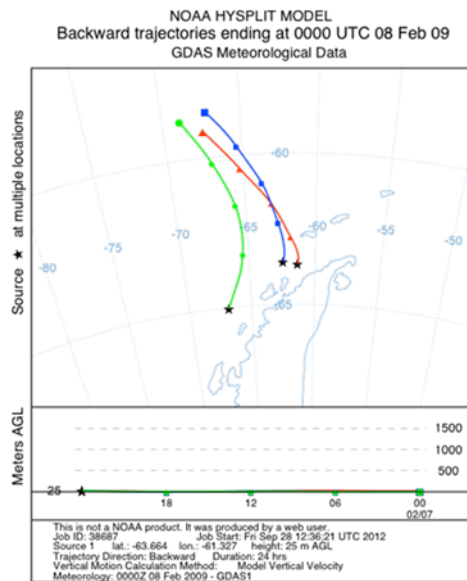
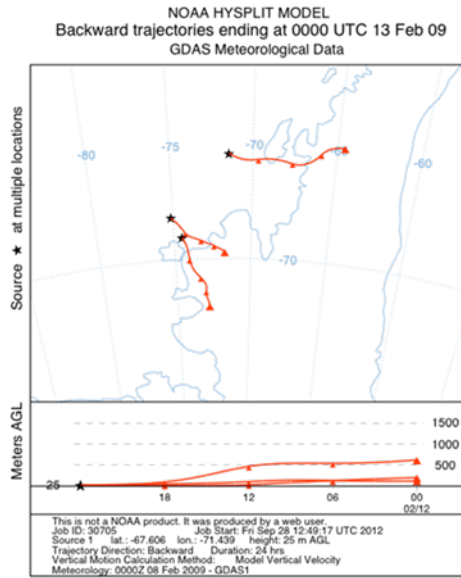


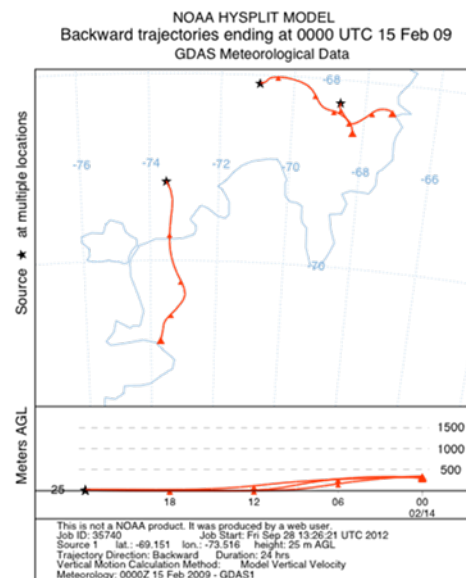
Figure S5a. Air-mass backtrajectories for the ATOS II cruise calculated using the HYSPLIT model from NOAA (Draxler and Rolph, 2011).

Appendix D

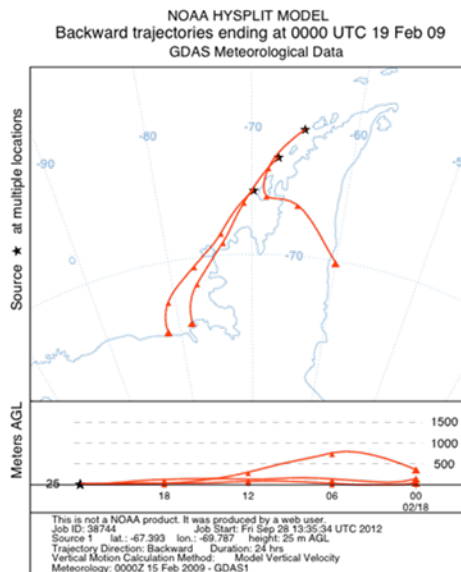
GA5



GA6



GA7



GA8

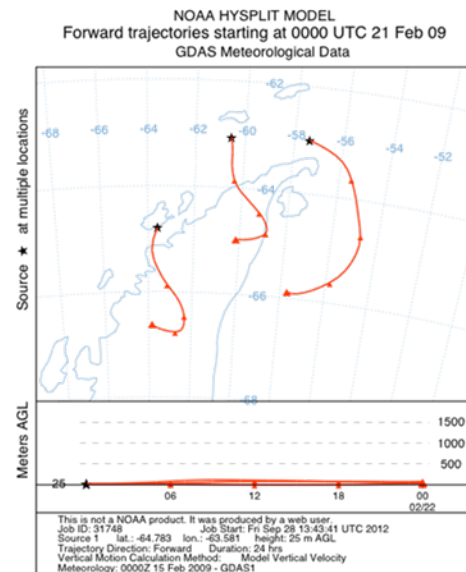


Figure S5b. Air-mass backtrajectories for the ATOS II calculated using the HYSPLIT model from NOAA (Draxler and Rolph, 2011).

GA9

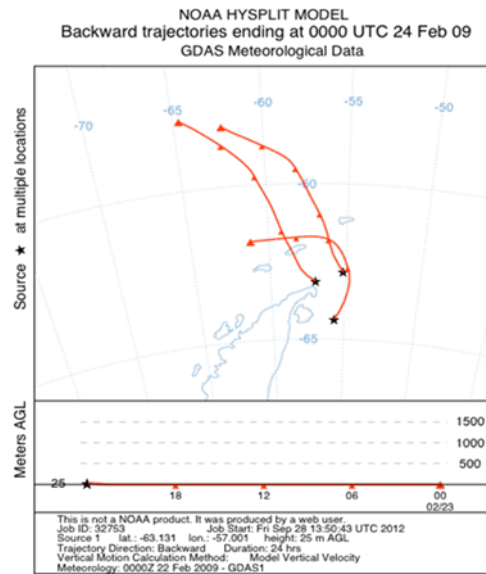


Figure S5c. Air-mass backtrajectories for the ATOS II cruise calculated using the HYSPLIT model from NOAA (Draxler and Rolph, 2011).

Appendix D

APPENDIX D.3

Text 1. Henry's Law Constant (HLC) correction for temperature and salinity

HLC used in the estimations of air-to-water fugacity ratios and diffusive exchange fluxes must be corrected by temperature due to the low temperatures in the Southern Ocean. We followed the approach described in Schwarzenbach et al., 1993 (Equations D.1 and D.2). For the T correction we used the surface water temperature (Achman et al., 1993 and Bruhn et al., 2003).

$$\frac{H_{T_0}}{H_{T_{298.15}}} = e^{\left[\frac{-\Delta U_{AW}}{R} \left(\frac{1}{T_0} - \frac{1}{298.15} \right) \right]} \quad [\text{D.1}]$$

$$H_{T_0S} = 1.3H_{T_0} \quad [\text{D.2}]$$

Where H_{T_0} , $H_{298.15}$ and H_{T_0S} are the temperature corrected HLC, the HLC at 298K and HLC corrected by temperature and salinity, $-\Delta U_{AW}$ is heat of phase change (kJ mol^{-1}), and R is the ideal gas constant ($\text{KJ mol}^{-1} \text{K}^{-1}$). The dimensionless HLC (H') was calculated following:

$$H' = \frac{H_{T_0S}}{RT} \quad [\text{D.3}]$$

Text 2. Degradation Flux estimations

Degradation Fluxes were calculated from the microbial and hydrolysis degradation rates proposed for α and γ in Arctic waters (Harner et al., 1999 and 2000). Microbial degradation rates were scaled by the bacterial abundance at surface following the approach previously reported for the Arctic (Galbán-Malagón et al., 2013b). The relative bacterial abundance at surface and at 1000 m depth was taken from the assessment of bacterial abundance for the global oceans (Aristegui et al., 2009).

$$k_{mh} = \frac{k_{m1000} B_{mh}}{B_{m1000}} \quad [\text{D.4}]$$

Where k_{mh} is the microbial degradation constant in a 25 m depth water-column, and k_{m1000} is the microbial degradation constant in a 1000 depth water-column, B_{mh} is the bacterial biomass in the upper water-column and B_{m1000} is the bacterial biomass in a 1000 m depth water column. The degradation flux was estimated following equation D.5 for α -HCH and equation S6 for γ -HCH.

$$F_{Deg_{\alpha}} = (k_{mh\alpha+} 0.5C_{Dis} + k_{mh\alpha-} 0.5C_{Dis} + k_{h\alpha})h \quad [D.5]$$

$$F_{Deg_{\gamma}} = (k_{mh\gamma} C_{Dis} + k_{h\gamma} C_{Dis})h \quad [D.6]$$

Where $F_{Deg_{\alpha}}$ and $F_{Deg_{\gamma}}$ are the total degradation fluxes ($\text{ng m}^{-2} \text{d}^{-1}$) for α -HCH and γ -HCH; $k_{mh\alpha+}$, $k_{mh\alpha-}$ and $k_{mh\gamma}$ are the corrected microbial degradation rate constants for the α -HCH racemic mixture (+/-) and γ -HCH; $k_{h\alpha}$ and $k_{h\gamma}$ are the hydrolysis rate constants for α -HCH and γ -HCH, $0.5C_{Dis}$ is the dissolved concentration reported for ESSASI and ATOS II cruise in ng m^{-3} (See table S3 on Appendix D.3) corrected by the enantiomeric fraction (Jantunen et al., 2004) and h is the 50 m average depth of the surface mixed layer as determined during the cruise based on CTD measurements. Results are shown in Table S7 on Appendix D.3.

Appendix D

Table S2. α -HCH, γ -HCH and HCB physico-chemical properties used for the fugacity ratio calculations and the fluxes estimated in the present work. Mw: molecular weight (g mol^{-1}), Mv is the molar volume, $-\Delta U_{AW}$ is the heat of phase change (kJ mol^{-1}) and HLC is the Henry's law constant ($\text{Pa m}^3 \text{mol}^{-1}$).

Compound	Mw	Mv	$-\Delta U_{AW}$	Ref	HLC	Ref
α-HCH	290.83	243.6	59.3	Sahsuvar et	0.360	Sahsuvar et al.,
γ-HCH	290.83	243.6	65	al., 2003	0.165	2003
	284.78			Cortés et al.		Jantunen and
HCB	2	221.4	35	1998	5	Bidleman 2006

Table S3 Truly dissolved seawater concentrations used for the estimations of fugacity ratios and air-water diffusive fluxes. Details on methods and discussion of these concentrations have been reported elsewhere (Galbán-Malagón et al., 2013).

Cruise	CODE	α-HCH	γ-HCH	HCB	Surface Temp (°C)
ESSASI	DE1	0.986	0.380	0.645	3.136
	DE2	0.280	0.709	0.472	1.054
	DE3	0.329	0.616	0.352	0.520
	DE4	0.188	1.034	0.375	0.404
	DE5	0.209	0.808	0.335	-0.350
	DE6	0.226	0.837	0.288	-0.355
	DE7	0.126	0.675	0.263	0.418
	DE8	0.245	0.735	0.420	0.119
	DE9	0.370	1.203	0.542	-0.259
	DE10	0.201	1.003	0.448	-0.073
ATOS II	DA1	0.917	1.192	0.208	1.221
	DA2	0.212	0.442	0.366	-0.092
	DA3	0.092	0.360	0.215	2.201
	DA4	0.278	0.326	0.420	2.628
	DA5	0.141	0.539	0.179	0.650
	DA6	0.294	1.262	0.294	0.873
	DA7	0.158	0.823	0.318	2.206
	DA8	0.197	0.796	0.531	1.482
	DA9	0.316	1.680	1.471	2.523

Table S4. Gas and aerosol phase concentrations (pg m^{-3}) over the Southern Ocean in 2008 and 2009.

Matrix	Area	Sample	α-HCH	γ-HCH	HCB
Gas Phase	South Scotia Sea	GE1	0.87	3.89	9.33
		GE2	5.84	5.11	13.54
		GE3	0.06	3.93	2.18
		GE4	0.18	5.84	3.28
		GE5	1.20	7.10	5.01
		GE6	2.09	1.47	15.82
	Weddell	GA1	0.31	0.54	2.35
		GA2	0.14	1.87	30.13
		GA9	0.05	0.11	25.98
	Bransfield	GA8	0.04	0.20	3.31
		GA4	0.23	0.25	34.24
		GA3	0.46	3.00	12.62
	Bellinghausen	GA6	0.22	0.19	51.82
		GA7	0.16	0.07	27.31
		GA5	0.10	0.16	49.71
Aerosol Phase	Weddell	A1	0.009	0.029	0.040
	Bransfield	A2	0.012	0.045	0.039
	Bellinghausen	A3	0.031	0.127	0.075
		A4	0.023	0.107	0.080

Appendix D

Table S5. Gas phase concentrations for HCB and γ -HCH (pg m^{-3}) in ambient air as measured at 1.5 m height and in the gas phase equilibrated with soil and snow as measured with the soil fugacity sampler.

Area		γ -HCH				HCB			
		Mean	SD	Min	Max	Mean	SD	Min	Max
Ambient Air (1.5 m)	Polish Bluff	0.94	0	loq	0.94	11.97	2.67	8.41	13.02
	Radio Peak	2.27	0.68	loq	2.73	10.3	4.81	4.19	15.73
	Sofia Mountain	0.79	0.77	loq	2.29	11.79	1.82	9.74	13.94
Gas phase equilibrated with soil and snow	Polish Bluff	2.7	1.27	1.43	4.34	16.82	2.91	13.13	19.69
	Radio Peak	2.03	2.08	0.13	4.79	208	105	142	362
	Sofia Mountain	1.91	1.04	1.17	3.76	124	38	81	186

Table S6. Estimated air-water fugacity ratios (f_A/f_W) for the ESSASI and ATOS cruises.

Cruise	Area	Code	α -HCH	γ -HCH	HCB
ESSASI	South Scotia Sea	GE1	0.0014	0.0020	0.2785
		GE2	0.0008	0.0006	0.4022
		GE3	0.0695	0.0008	2.4224
		GE4	0.0176	0.0007	0.8869
		GE5	0.0048	0.0004	1.3990
		GE6	0.0169	0.0005	1.3413
ATOS II	Weddell	GA1	0.0291	0.0393	0.1093
		GA2	0.0614	0.0216	0.1011
		GA9	0.0464	0.0071	2.0297
	Bransfield	GA3	0.0248	0.0084	0.1469
		GA4	0.1214	0.0205	2.1552
		GA8	0.0307	0.0647	0.2627
		GA5	0.1527	0.0603	0.6546
	Bellingshausen	GA6	0.0091	0.0029	0.2912
		GA7	0.0356	0.0010	0.2022

Table S7 Air-Sea diffusive exchange fluxes ($\text{ng m}^{-2}\text{d}^{-1}$) for each gas-phase sampling event during the ESSASI and ATOS cruises. Code refers to the gas-phase sample code as in Tables S1 and S4.

Cruise	Area	Code	α -HCH	γ -HCH	HCB
ESSASI	South Scotia Sea	GE1	-0.1866	-0.3449	0.4436
		GE2	-0.0618	-0.8868	-0.9949
		GE3	-0.2582	-1.7276	-0.3943
		GE4	-0.1495	-0.1650	-2.2788
		GE5	-0.0532	-0.0835	-2.2919
		GE6	-0.0797	-0.1246	-5.4825
ATOS II	Weddell	GA1	-0.2001	-0.3678	0.1930
		GA2	-0.0720	-1.0336	-1.3839
		GA9	-0.0184	-0.0478	-0.3921
	Bransfield	GA3	-0.2882	-1.9202	-0.6599
		GA4	-0.1281	-0.1421	-1.8912
		GA8	-0.0151	-0.0873	0.1123
		GA5	-0.0394	-0.0637	-1.3117
	Bellingshausen	GA6	-0.1538	-0.1372	-5.0109
		GA7	-0.1003	-0.0401	-1.8843

Table S8 Dry deposition fluxes ($\text{ng m}^{-2}\text{d}^{-1}$) estimated for each one of the four aerosol-phase samples where HCB and HCH could be quantified. Codes refer to aerosol phase samples as shown in Table S1 and S4.

Dry Deposition Flux $\text{ng m}^{-2}\text{d}^{-1}$	α -HCH	γ -HCH	HCB
A1	0.003	0.008	0.011
A2	0.004	0.013	0.011
A3	0.007	0.030	0.023
A4	0.009	0.036	0.021

Appendix D

Table S9. Estimations of the total degradation flux (microbial plus hydrolysis following Equations S5 and S6) using the dissolved phase concentrations reported for surface waters during ESSASI and ATOS II cruises (Galbán Malagón et al., 2013). See table S3 on Appendix D.3. Codes refer to each one of the gas-phase samples, for which the corresponding degradation flux in water was estimated.

Cruise	Area	Code	α-HCH	γ-HCH
ESSASI	South Scotia Sea	<i>GE1</i>	-0.016	-0.081
		<i>GE2</i>	-0.006	-0.106
		<i>GE3</i>	-0.007	-0.025
		<i>GE4</i>	-0.008	
		<i>GE5</i>	-0.006	
		<i>GE6</i>	-0.006	
ATOS II	Weddell	<i>GA1</i>	-0.03	-0.208
		<i>GA2</i>	-0.008	-0.102
		<i>GA9</i>	-0.014	-0.315
	Bransfield	<i>GA3</i>	-0.01	-0.054
		<i>GA4</i>	-0.01	-0.049
		<i>GA8</i>	-0.01	-0.113
	Bellingshausen	<i>GA5</i>	-0.013	-0.101
		<i>GA6</i>	-0.011	-0.125
		<i>GA7</i>	-0.008	-0.209

Additional references

Achman, D. R., Hornbuckle, K. C., Eisenreich, S. J. 1993. Volatilization of polychlorinated biphenyls from green-bay, lake michigian. *Environ. Sci. Technol.* 27(1), 75-87.

Aristegui, J., Gasol, J.M., Duarte, C.M., Herndl, G.J. 2009 Microbial oceanography of the dark ocean's pelagic realm. *Limnol Oceanogr.* 54(5):1501-29.

Bruhn, R., Lakaschus, S., & McLachlan, M. S. 2003. Air/sea gas exchange of PCBs in the southern baltic sea. *Atmos. Environ.* 37(24), 3445-3454.

Galbán-Malagón, C. J., Del Vento, S., Berrojalbiz, N., Ojeda, M.J., & Dachs, J. 2013. Polychlorinated Biphenyls, Hexachlorocyclohexanes and Hexachlorobenzene in Seawater and Phytoplankton from the Southern Ocean (Weddell, South Scotia, and Bellingshausen Seas). *Environ. Sci Technol.* DOI: 10.1021/es400030q

Cortes, D.R., Basu, I., Sweet, C.W., Brice, K.A., Hoff, R.M., Hites, R.A. 1998. Temporal trends in gas-phase concentrations of chlorinated pesticides measured at the shores of the great lakes. *Environ. Sci Technol.* 32(13):1920-7

Harner, T., Kylin, H., Bidleman, T.F., Strachan, W.M.J. 1999. Removal of and α -hexachlorocyclohexane and enantiomers of γ -hexachlorocyclohexane in the eastern Arctic Ocean. *Environ. Sci Technol.* 33(8):1157-64.

Harner, T., Jantunen, L. M. M., Bidleman, T. F., Barrie, L. A., Kylin, H., Strachan, W. M. J., et al. 2000. Microbial degradation is a key elimination pathway of hexachlorocyclohexanes from the arctic ocean. *Geophys. Res. Lett.*, 27(8), 1155-1158.

Jantunen, L.M., Bidleman, T.F. 2006. Henry's law constants for hexachlorobenzene, p,p'-DDE and components of technical chlordane and estimates of gas exchange for lake Ontario. *Chemosphere.* 62(10):1689-96.

Sahsuar, L., Helm, P.A., Jantunen, L.M., Bidleman, T.F. 2003 Henry's law constants for α -, β -, and γ -hexachlorocyclohexanes (HCHs) as a function of temperature and revised estimates of gas exchange in Arctic regions. *Atmos. Environ.* 37, 983-992.

Schwarzenbach, R.P., Gschwend, P.M., Imboden, D.M. 1993. Environmental organic chemistry. John Wiley & Sons. Chichester.

Appendix E

Supporting Information to Chapter 7

Factors affecting the atmospheric occurrence and deposition of polychlorinated biphenyls in the Southern Ocean

Appendix E.1

Table S1. Ancillary data for samples taken during the ICEPOS, ESSASI and ATOS II cruises and at Livingston Island...315

Figure S1. Trajectories of of the ICEPOS, ESSASI and ATOS II sampling campaigns...317

Figure S2. Map of sea ice extent during the ICEPOS, ESSASI and ATOS II sampling campaigns...318

Appendix E.2

Table S2. Recovery rates for surrogates PCBs 65 and 200...319

Tables S3. Instrumental detection limits (IDLs), limits of detection (LODs) and limits of quantification (LOQs)...320

Figure S3. Characteristic air mass back-trajectories for samples taken during the ICEPOS, ESSASI and ATOS II cruises during austral summer...321

Appendix E.3

Table S4. Gas phase concentrations of PCBs for samples taken during the ICEPOS cruise in 2005. ...322

Table S5. Gas phase concentrations of PCBs for samples taken during the ESSASI in 2008 ...323

Table S6. Gas phase concentrations of PCBs for samples taken during the ATOS II cruise and landbase sampling at Polish Bluff in Livingston Island during 2009 ...324

Table S7. Gas phase concentrations of PCBs for samples taken during the ATOS II landbase sampling at Livingston Island during 2009 austral summer...325

Table S8. Aerosol phase concentrations of PCBs for samples taken during the ATOS II cruise and concurrent sampling at Radio Peak and Polish Beach in Livingston Island during 2009...326

Table S9. Summary of gas phase concentrations for the ICEPOS (2005), ESSASI (2008) and ATOS II (2009) cruises and at Livingston Island ...327

Figure S4. Comparison of gas and aerosol phase concentrations for the different campaigns. ...328

Figure S5. Comparison of the gas phase concentrations for samples of the three characteristic air mass back trajectories ...329

Appendix E

Appendix E.4

- Table S10. Physico-chemical properties for the studied compounds...330**
- Table S11. Truly dissolved seawater concentrations used for the estimations of fugacity ratios and air-water diffusive fluxes...331**
- Table S12. Estimated air-water fugacity ratios (f_w/f_A) for the ESSASI and ATOS cruises...332**
- Table S13. Net air-Sea diffusive exchange fluxes for each gas-phase sampling event during the ESSASI and ATOS cruises...333**
- Table S14. Dry deposition fluxes estimated for each one of the aerosol-phase samples...334**
- Figure S6. Estimated fugacity ratios ($\text{Log } f_w/f_A$) against the logarithm of temperature corrected octanol-water partition constant ($\text{Log } K_{OWT}$) for samples taken during ATOS II Cruise...335**
- Figure S7. Estimated fugacity ratios ($\text{Log } f_w/f_A$) against the logarithm of temperature corrected octanol-water partition constant ($\text{Log } K_{OWT}$) for samples taken during ESSASI Cruise...336**

Appendix E.5

- Table S15. Measured gas-particle partition coefficient ($\text{Log } K_p$) for each gas phase sampling event during the ATOS II cruise and concurrent sampling at Livingston Island...337**
- Table S16. Predicted gas-particle partition coefficient ($\text{Log } K_p$) estimated from the $\text{Log } K_{OA}$ corrected by temperature for each gas phase sampling event at Livingston Island...338**
- Table S17. Model predicted gas-particle partition coefficient ($\text{Log } K_p$) estimated from the $\text{Log } K_{OA}$ corrected by temperature for for each gas phase sampling event during the ATOS II cruise in the Southern Ocean...339**
- Figure S18. Measured versus predicted gas-particle partition constant ($\text{Log } K_p$) for samples taken at Polish Beach in Livingston Island and over the Southern Ocean during ATOS II cruise in 2009...340**
- Figure S19. Measured versus predicted gas-particle partition constant ($\text{Log } K_p$) for samples taken at Radio Peak in Livingston Island in 2009 ...341**
- Additional References...342**

Appendix E.1

Table S1. Ancillary data for samples taken during the ICEPOS, ESSASI and ATOS II surveys around the Antarctic Peninsula and South Scotia Sea, and for samples taken at Polish Beach (Livingston Island). Long: longitude, Lat: latitude, Vol: total volume sampled, TA: air temperature (20 m height) during sampling.

Matrix	Cruise	CODE	LONG	LAT	DATE	Vol m ³	wind speed m s ⁻¹	wind direction °	TA °C
Gas	ICEPOS	GI1	-68.40	-64.50	02/02/05	469	6.57	-	
		GI2	-70.01	-66.57	03/02/05	362	6.66	-	
		GI3	-70.40	-67.00	04/02/05	422	6.65	-	
		GI4	-67.10	-65.69	06/02/05	590	10.64	-	
		GI5	-60.44	-63.80	09/02/05	432	9.19	-	
		GI6	-56.23	-64.46	10/02/05	909	12.47	-	
		GI7	-56.31	-64.71	12/02/05	872	17.34	-	
		GI8	-58.93	-62.20	13/02/05	814	13.78	-	
		GI9	-60.68	-62.97	16/02/05	541	11.63	-	
		GI10	-60.44	-62.97	20/02/05	928	11.33	-	
		GI11	-60.00	-62.97	21/02/05	676	11.32	-	
Gas	ESSASI	GE1	-54.06	-60.53	04/02/08	975	7.63	203.29	1.29
		GE2	-51.41	-61.45	11/02/08	745	5.25	252.18	0.58
		GE3	-51.31	-61.30	14/01/08	1024	6.69	204.90	0.26
		GE4	-50.65	-60.19	16/01/08	862	7.94	249.20	0.92
		GE5	-47.04	-60.20	18/01/08	1556	6.20	155.56	0.12
		GE6	-52.38	-61.67	20/01/08	865	9.97	307.63	1.04
Gas	ATOS II	GA1	-57.87	-62.43	29/01/09	1006	8.25	245.03	1.19
		GA2	-51.78	-63.84	01/02/09	890	6.36	144.73	-1.44
		GA3	-55.85	-64.20	04/02/09	1414	7.60	207.31	1.47
		GA4	-71.36	-67.62	08/02/09	1691	6.56	101.84	2.19
		GA5	-71.40	-67.64	13/02/09	1145	4.36	138.76	-2.01
		GA6	-74.41	-69.54	15/02/09	1414	8.73	104.41	1.38
		GA7	-57.38	-63.05	19/02/09	1940	7.90	118.78	-1.50
		GA8	-63.62	-64.83	21/02/09	1990	4.70	204.49	1.60
		GA9	-55.81	-64.53	24/02/09	1500	5.00	172.54	-2.79
Gas	ATOS II LANDBASE	GLI1	-60.39	-62.66	11/02/09	816			4.4
		GLI2	-60.39	-62.66	12/02/09	833			3.1
		GLI3	-60.39	-62.66	13/02/09	897			3
Aerosol	ATOS II CRUISE	A1	-51.51	-62.76	04/02/09	2724	7.49	196.06	0.07
		A2	-58.40	-62.20	06/02/09	1899	7.08	247.26	2.81
		A3	-72.34	-67.98	12/02/09	1043	7.05	134.64	0.54
		A4	-66.38	-65.50	19/02/09	1114	8.84	130.22	1.10
	ATOS II LANDBASE	AB1	-60.4	-62.67	22/01/09	1129			3.3
		AB2	-60.4	-62.67	23/01/09	1651			1.9
		AB3	-60.4	-62.67	27/01/09	2608			2.9
		AB4	-60.4	-62.67	30/01/09	2612			3.6
		AB5	-60.4	-62.67	02/02/09	2786			2.4
		AB6	-60.4	-62.67	05/02/09	2426			0.4
		AB7	-60.4	-62.67	09/02/09	2815			2.6
		AB8	-60.4	-62.67	12/02/09	2515			3

Appendix E

AB9¹	-60.39	-62.66	24/01/09	2204	3.4
AB10¹	-60.39	-62.66	13/02/09	2596	4

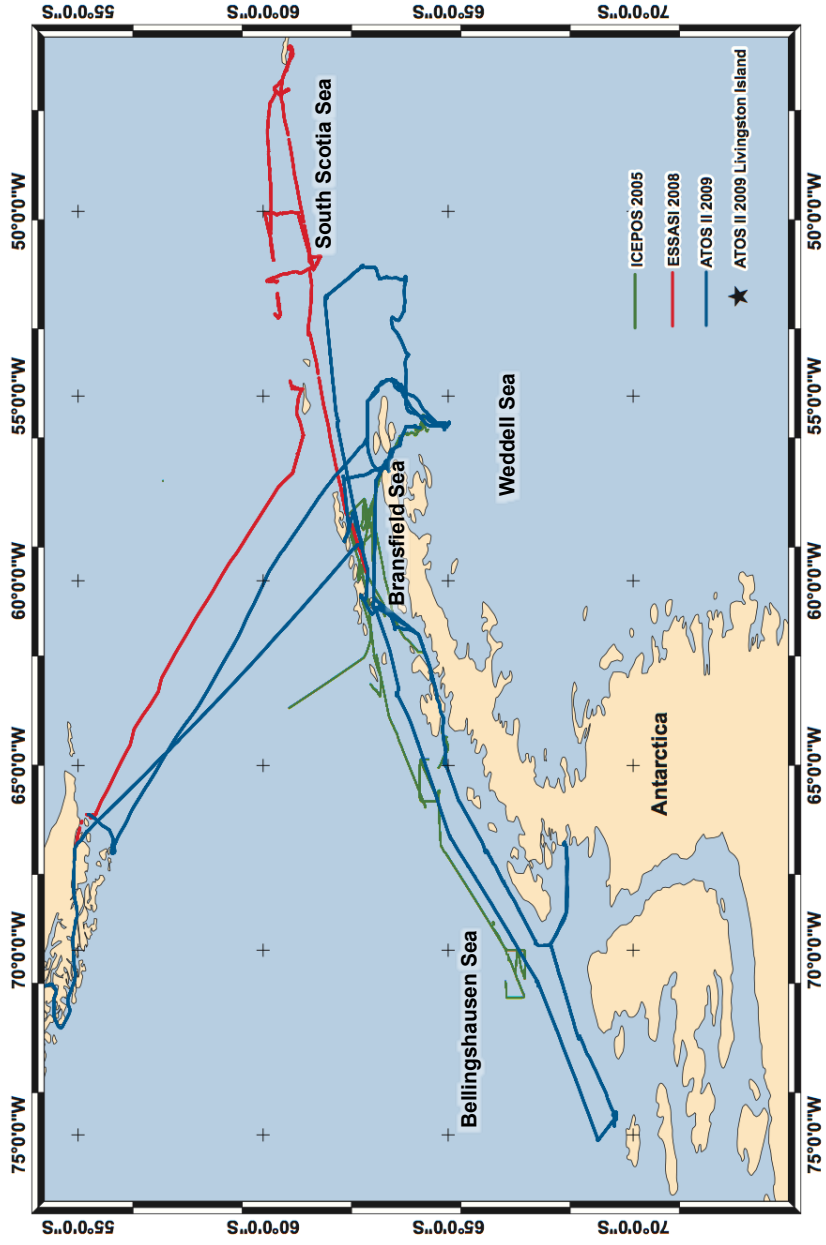


Figure S1. Map of cruises' trajectory during summer 2005 (ICEPOS), 2008 (ESSASI) and 2009 (ATOS II) around the Antarctic Peninsula and South Scotia Sea

Appendix E

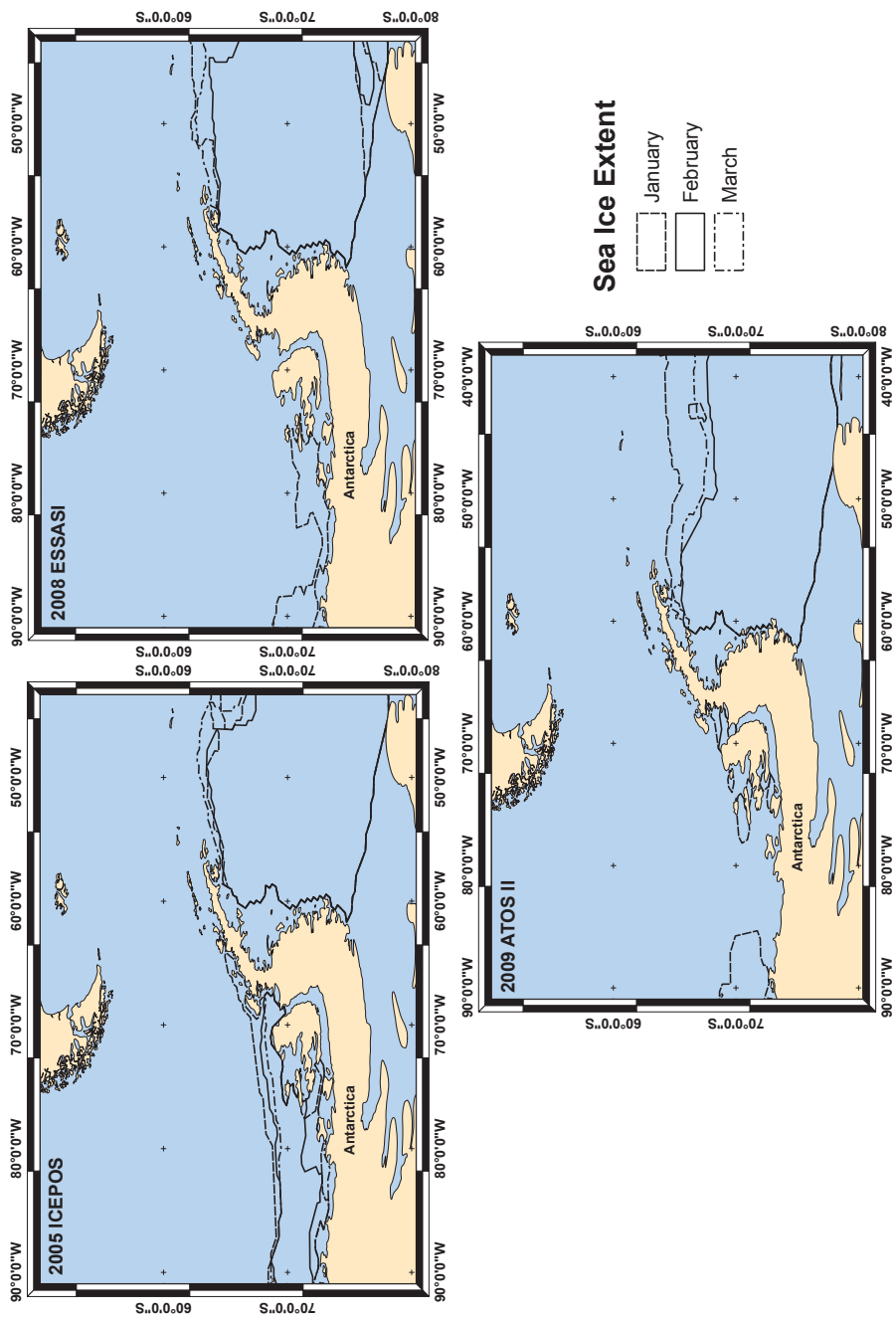


Figure S2. Map of sea ice extent during sampling in ICEPOS, ESSASI and ATOS II cruises taken during austral summer around the Antarctic Peninsula and South Scotia Sea. Data were retrieved from the NSIDC online dataset (www.nsidc.org)

Appendix E.2

Table S2. Recovery percentages for surrogates PCBs 65 and 200.

		% Recovery					
		PCB65			PCB200		
		Mean	Min	Max	Mean	Min	Max
ATOS II	Gas	70.6	66.9	76.2	76.8	67.1	84.8
	Aerosol	70.6	61.8	77.7	78.4	69.2	85.1
ESSASI	Gas	67.2	53.3	77.9	71.0	57.2	87.3
ICEPOS	Gas	59.0	51.0	75.0	59.0	51.0	81.0

Appendix E

Table S3. Instrumental detection limits (IDLs), limits of detection (LODs) and limits of quantification (LOQs). x: blank averaged ,SD: blank standard deviation.

pg on column	IDLs	x	SD	LODs	LOQs
PCB18	0.004	0.015	0.024	0.089	0.260
PCB17	0.02	0.021	0.090	0.291	0.921
PCB31	0.003	0.032	0.043	0.162	0.465
PCB28	0.004	0.131	0.090	0.401	1.031
PCB33	0.004	0.037	0.088	0.302	0.920
PCB52	0.004	0.021	0.056	0.190	0.584
PCB49	0.004	0.012	0.031	0.106	0.326
PCB99/101	0.008	0.153	0.200	0.753	2.153
PCB110	0.004	0.018	0.141	0.440	1.425
PCB151	0.004	0.005	0.283	0.855	2.838
PCB149	0.004	0.128	0.178	0.663	1.910
PCB118	0.004	0.038	0.078	0.273	0.821
PCB153	0.004	0.025	0.229	0.713	2.317
PCB132/105	0.001	0.006	0.036	0.114	0.365
PCB138	0.004	0.028	0.151	0.481	1.537
PCB158	0.001	0.009	0.013	0.049	0.141
PCB187	0.004	0.003	0.160	0.482	1.601
PCB183	0.004	0.011	0.015	0.054	0.157
PCB128	0.004	0.000	0.002	0.006	0.019
PCB177	0.004	0.001	0.005	0.017	0.056
PCB171/156	0.004	0.008	0.026	0.085	0.267
PCB180	0.004	0.006	0.073	0.224	0.734

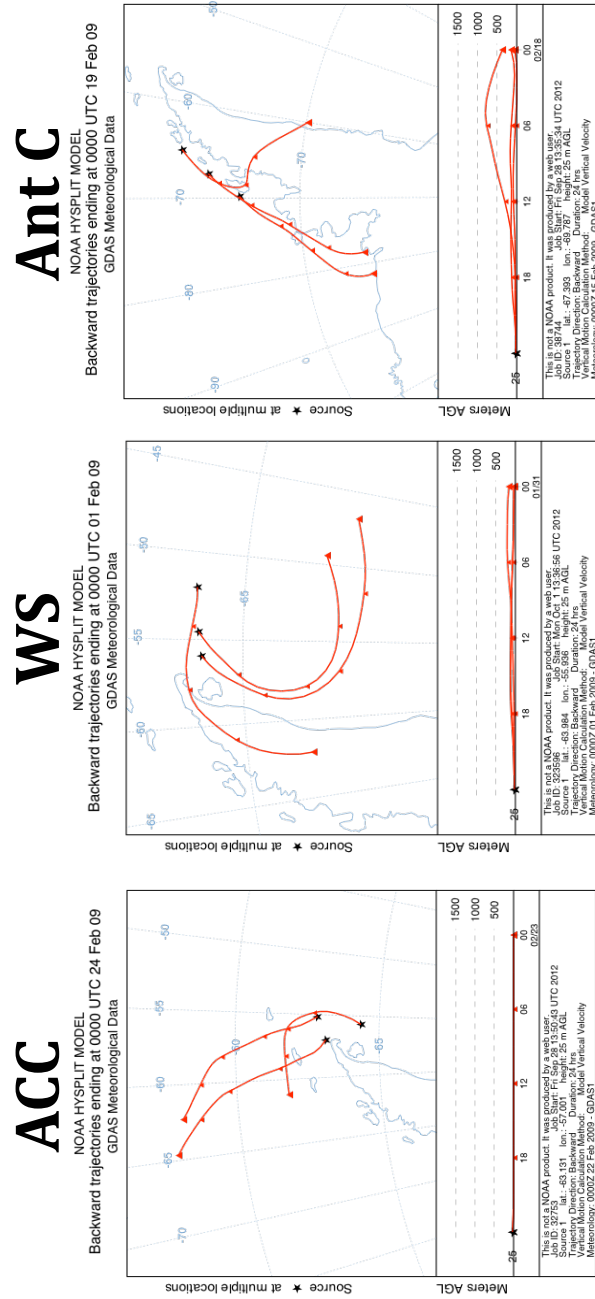


Figure S3. Characteristic atmospheric backtrajectories for samples taken during ICEPOS, ESSASI and ATOS II Antarctic cruises. ACC: Antarctic circumpolar current, WS: Weddell sea, Ant C: Antarctic Continent

Appendix E

Appendix E.3

Table S4. Gas phase concentrations of PCBs (pg m^{-3}) for samples taken during the ICEPOS cruise in 2005.

	ICEPOS 2005										
	G11	G12	G13	G14	G15	G16	G17	G18	G19	G10	G11
PCB18			0.43	2.36	0.62	0.39	1.97	0.13	0.70	0.80	1.64
PCB17											
PCB31	0.41	1.15	0.48	0.91	0.40	0.20	1.75	0.19	0.73	0.93	1.32
PCB28	1.41	1.07	2.62	2.02	0.88	0.53	2.59	0.60	1.56	2.71	1.82
PCB33	0.62	3.17	1.08	1.08		0.40	3.39		0.85	2.53	1.46
PCB52	3.86		4.84	5.01	3.73	1.53		2.38	5.10	5.35	
PCB49	1.42	3.90	1.60	1.49	1.25	0.58	2.68	0.57	1.83	2.11	2.18
PCB99/101											
PCB110											
PCB151	0.90	3.02	0.90	0.70	0.42	0.36	0.85	0.47	0.41	0.75	0.47
PCB149	1.97		1.73	1.46	1.09	0.80	1.87	0.96	1.00	1.58	1.01
PCB118	0.68	1.97	0.51	0.62	0.57	0.25	1.39	0.38	0.51	0.79	0.58
PCB153	1.02	2.38	2.80	1.06	0.71	0.49	2.28	0.69	0.93	1.08	0.56
PCB132/105	0.24	1.34	1.76	0.96	0.56	0.26	1.73	0.37	0.48	0.54	0.41
PCB138	0.88	1.91	2.59	0.94	0.59	0.42	1.92	0.65	1.01	1.10	0.56
PCB158	0.08				0.09	0.04	0.13			0.11	0.07
PCB187		0.56	0.73	0.34	0.16	0.12	0.50	0.18	0.23	0.29	0.14
PCB183						0.03	0.23			0.12	0.05
PCB128	1.08		2.26	1.01	0.94	0.54	1.43		1.04	1.20	0.79
PCB177						0.04	0.23		0.06	0.10	0.01
PCB171/156							0.19				
PCB180			0.51	0.35	0.18	0.13	0.52	0.20	0.30	0.34	0.17
$\Sigma_{25}\text{PCBs}$	14.56	20.47	24.83	20.29	12.17	7.12	25.65	7.78	16.73	22.43	13.23
$\Sigma_{\text{ICES}}\text{PCBs}$	7.84	7.33	13.87	10.00	6.65	3.35	8.70	4.90	9.42	11.37	3.69

Table S5. Gas phase concentrations of PCBs (pg m^{-3}) for samples taken during the ESSASI cruise in 2008.

	ESSASI 2008					
	GE1	GE2	GE3	GE4	GE5	GE6
PCB18	5.90	0.38	0.06	0.05	2.72	4.75
PCB17		2.48	0.12	0.13	7.78	2.53
PCB31	7.19	0.32	0.10	0.12	17.34	2.55
PCB28	3.89	5.11	0.39	0.58	12.96	2.93
PCB33	9.38	3.40	0.14	0.25	1.96	4.91
PCB52	6.10	0.56	0.09	0.09	1.77	4.56
PCB49	2.62	0.44	0.24	0.05	1.43	
PCB99/10 1	7.56	7.90	9.95	2.02	9.10	
PCB110	1.23	1.40	0.17	0.18	0.66	0.73
PCB151	1.25	1.10	0.24	0.26	2.86	1.57
PCB149	6.02	3.05	0.75	0.77	7.19	5.33
PCB118	2.27	4.07	0.59	0.26	1.80	0.89
PCB153	2.87	2.68	0.22	0.48	1.75	11.21
PCB132/1 05	5.52	0.86	0.26	0.13	2.15	1.59
PCB138	4.39	2.75	0.17	0.37	1.94	2.17
PCB158	0.83	0.86		0.07	0.75	0.63
PCB187	1.31	4.29	0.21	0.14	0.96	0.62
PCB183	1.14	2.76		0.04	0.90	0.60
PCB128	0.82	0.66	0.01		0.41	0.85
PCB177	0.92	0.92		0.03	0.53	0.98
PCB171/1 56	1.28	1.02	0.05	0.08	0.59	0.39
PCB180		1.90	0.03	0.12	0.75	1.41
$\Sigma_{25}\text{PCBs}$	72.48	48.90	13.77	6.18	78.29	51.18
$\Sigma_{10ES}\text{PCBs}$	27.08	24.97	11.44	3.91	30.05	23.16

Appendix E

Table S6. Gas phase concentrations of PCBs (pg m^{-3}) for samples taken during the ATOS II cruise and concurrent sampling at Polish Beach in Livingston Island during 2009.

	ATOS II Cruise									ATOS II Polish Beach		
	GA1	GA2	GA3	GA4	GA5	GA6	GA7	GA8	GA9	GLI1	GLI2	GLI3
PCB18	0.67	0.73	2.55	1.24	0.37	1.21	1.07	0.28	0.26	0.27		0.07
PCB17	0.94	0.50	1.48	0.62	0.24	0.72	0.50	0.45	0.24	0.24	0.97	0.52
PCB31	1.18	0.59	1.46	0.88	1.17	1.03	0.74	0.60	0.29	0.35	0.15	0.12
PCB28	1.05	1.97	5.10	2.00	1.18	1.50	3.14	1.58	0.89	0.16	0.21	0.20
PCB33		0.89	1.17	0.89	0.36	1.22	0.76	0.29	0.15	0.08	0.14	
PCB52	1.29	0.78	2.92	0.29		0.10	1.15	0.36	0.23	0.43	1.30	0.60
PCB49	0.80	0.45	1.59	0.53	0.06	0.89	0.34		0.36	0.07		
PCB99/101	2.99	1.56	5.43	2.07	2.42	4.90	2.16	1.03	0.66	0.03		
PCB110	0.32		0.91	0.34	0.30	0.63		0.18	0.14	0.02	0.07	
PCB151	1.99	0.39	1.27	0.45	0.21	0.61	0.28	0.25	0.79	0.01	0.04	0.04
PCB149	2.57	1.09	3.58	0.40	0.69	1.70	0.80	1.03	0.44	0.10	0.03	0.04
PCB118	0.43	0.14	1.19	0.33	0.38	1.00	0.33	0.15	0.17	0.02	0.02	0.02
PCB153	1.55	0.71	2.57	0.91	0.55	0.71	0.75	0.87	0.45	0.12	0.07	0.08
PCB132/105	0.68	0.25	0.95	0.33	0.04	0.40	0.39	0.37	0.04			
PCB138	1.22	0.53	2.01	0.74	0.21	0.72	0.70	0.41	0.23	0.05	0.01	0.02
PCB158	0.10	0.03	0.63	0.06	0.04	0.09	0.06	0.07	0.06		0.00	
PCB187	0.64	0.32	1.20	0.43	0.20	0.33	0.35	0.43	0.39	0.10	0.07	0.08
PCB183	0.23	0.09	0.51	0.15	0.06	0.11	0.14	0.11	0.09	0.00	0.01	0.01
PCB128	0.09	0.02	0.16	0.04		0.07	0.07	0.01				
PCB177	0.22	0.07	0.50	0.14	0.01	0.10	0.12	0.15	0.02			
PCB171/156	0.21	0.11		0.09	0.06	0.14	0.12	0.06	0.04			
PCB180	0.39	0.13	0.89	0.26	0.18	0.23	0.27	0.32	0.17	0.04	0.01	0.02
Σ_{25}PCBs	19.56	11.34	38.09	13.18	8.73	18.38	14.22	8.99	6.07	2.09	3.11	1.80

Table S7. Gas phase concentrations of PCBs (pg m^{-3}) for samples taken during the landbase sampling at Pico Radio Hill (Livingston Island) during 2009. Data taken from Cabrerizo et al., 2013.

	220109	230109	240109	250109	260109	270109	280109	290109	300109	310109	10209	20209	30209	40209	50209
	GLI4	GLI5	GLI6	GLI7	GLI8	GLI9	GLI10	GLI11	GLI12	GLI13	GLI14	GLI15	GLI16	GLI17	GLI18
PCB18	0.463	0.29	0.178	0.163	0.62	0.503	0.822	0.3	0.725	0.22	0.356	0.268	0.484	0.223	0.276
PCB17	0.557	0.71	0.695	0.46	0.311	0.217	0.302	0.254	0.39	0.384	0.343	0.663	0.442	0.309	0.376
PCB31	0.873	0.522	0.402	0.535	0.73	0.347	1.079	0.371	0.999	0.288	0.298	0.343	0.351	0.202	0.276
PCB28	0.576	0.29	0.216	0.238	0.633	0.315	0.781	0.281	0.6	0.133	0.186	0.224	0.259	0.144	0.247
PCB33	0.127					0.11	0.693	0.364			0.083				
PCB52		1.775		1.325	0.863	0.672	1.977	0.494	2.133	1.29	1.296	0.88	0.505	0.534	0.691
PCB49	0.423	0.113			0.257	0.116	0.327		0.455				0.055		
PCB99/101	0.063	0.016		0.013	0.021	0.02			0.022	0.037			0.026		0.037
PCB110		0.038	0.031	0.025	0.077	0.061	0.446	0.026	0.26	0.05	0.045	0.06	0.045	0.008	0.063
PCB151	2.399	2.194	2.117	1.722	0.92	0.827	0.615	0.538	0.659	0.828	0.562	0.514	0.414	0.318	0.386
PCB149	1.206	1.004	0.541	0.716	1.612	1.164	1.837	0.824	1.191	0.478	0.549	0.424	0.861	0.522	0.561
PCB118	0.082	0.048	0.02	0.048	0.124	0.108	0.405	0.064	0.339	0.022	0.034	0.02	0.058	0.035	0.036
PCB153	1.359	1.38	1.119	1.175	1.27	1.139	1.211	0.819	1.107	0.854	0.729	0.718	0.783	0.565	0.628
PCB132/105		0.015			0.107	0.011	0.516		0.042				0.084		
PCB138	0.281	0.227	0.126	0.174	0.609	0.454	0.881	0.34	0.581	0.144	0.212	0.159	0.359	0.231	0.262
PCB158	0.024	0.019	0.014	0.014	0.036	0.03	0.079	0.03	0.048	0.012	0.019	0.008	0.024	0.026	0.019
PCB187	0.462	0.481	0.373	0.436	0.478	0.455	0.428	0.316	0.412	0.351	0.305	0.302	0.362	0.245	0.34
PCB183	0.164	0.171	0.121	0.152	0.158	0.155	0.14	0.108	0.144	0.11	0.096	0.085	0.089	0.066	0.088
PCB128	0.003				0.004		0.069								
PCB177	0.004	0.008		0.011	0.064	0.045	0.117	0.034	0.058		0.02	0.01	0.022	0.005	0.029
PCB171/156							0.025	0.046							
PCB180	0.187	0.196	0.153	0.185	0.215	0.2	0.188	0.13	0.221	0.144	0.143	0.108	0.142	0.108	0.129
Σ 25PCBs	9.253	9.497	6.106	7.392	9.109	6.949	12.938	5.339	10.386	5.345	5.276	4.786	5.365	3.541	4.444

Table S8. Aerosol phase concentrations of PCBs (pg m^{-3}) for samples taken during the ATOS II cruise and concurrent sampling at Radio Peak and Polish Beach in Livingston Island during 2009.

	ATOS II Cruise										ATOS II Landbase																	
	Pico Radio Hill										Polish Beach																	
	A1	A2	A3	A4	AB1	AB2	AB3	AB4	AB5	AB6	AB7	AB8	AB9	AB10	A1	A2	A3	A4	AB1	AB2	AB3	AB4	AB5	AB6	AB7	AB8	AB9	AB10
PCB18	0.048	0.135	0.214	0.048																								
PCB17	0.005		0.060																									
PCB31	0.008	0.002		0.004	0.005	0.004	0.002	0.002																				
PCB28	0.019		0.013	0.022	0.044	0.011	0.035	0.015	0.036	0.031	0.008	0.008	0.002	0.004														
PCB33					0.001	0.001	<0.001	0.001	0.001	0.001																		
PCB52	0.014							0.005	0.007																			
PCB49	0.005							0.001																				
PCB99/101	0.057	0.014	0.023	0.070	0.010	0.009	0.008																					
PCB110	0.033	0.021		0.031	0.002	0.001	0.003	<0.001	0.002	0.000	0.001	0.001	0.001	0.002														
PCB151	0.014				0.004	0.002	0.002																					
PCB149	0.034				0.041	0.001	0.003	0.001	0.001	0.001	0.001	0.002	0.001															
PCB118					0.002	0.001		<0.001	0.001	<0.001																		
PCB153	0.062		0.003	0.015	0.090	0.024	0.025	0.011	0.027	0.030	0.011	0.008	0.004	0.003														
PCB132/105	0.020	0.001		0.015	0.043	0.028		0.016	0.006	0.009																		
PCB158	0.049				0.033	0.004	0.003	0.002	0.001	0.002	0.002																	
PCB138	0.004				0.011	0.017	0.003	0.008	0.001	0.002	<0.001	0.002	<0.001	0.001														
PCB187	0.093				0.070	0.032	0.019	0.018	0.019	0.020	0.018	0.016	0.014	0.017														
PCB183	0.004				0.005	0.002	0.001	0.001	0.001	<0.001	0.002	0.001																
PCB128	0.007						0.002																					
PCB177	0.009				0.001	0.001	0.001	<0.001	0.001	<0.001																		
PCB171/156	0.019	0.007	0.009	0.019																								
PCB180	0.105		0.039	0.049	0.022	0.003	0.002	0.002	0.004	0.005	0.010	0.003	0.001	0.003														
Σ_{25} PCBs	0.607	0.181	0.362	0.273	0.384	0.141	0.108	0.084	0.107	0.114	0.072	0.059	0.076	0.039														

Table S9. Summary of gas phase concentrations of PCBs (pg m^{-3}) for samples taken during the ICEPOS (2005), ESSASI (2008) and ATOS II (2009) cruise and sampling at Livingston Island.

pg m^{-3}	ICEPOS						ESSASI			ATOS II Cruise			ATOS II Livingston Island		
	Weddell		Bransfield		Bellingshausen		South Scotia Sea			Weddell		Bransfield	Bellingshausen		Polish Beach
	Mean (Range)	n=3	Mean (Range)	n=3	Mean (Range)	n=6	Mean (Range)	n=6	Mean (Range)	n=6	Mean (Range)	n=3	Mean (Range)	n=3	Mean (Range)
PCB18	0.83 (0.13-1.97)		1.04 (0.70-1.64)		1.96 (0.43-4.44)		2.31 (0.05-5.90)		0.55 (0.26-0.73)		1.36 (0.28-2.55)		0.88 (0.37-1.21)		0.27 (0.27-0.27)
PCB17							2.61 (0.12-7.78)		0.56 (0.24-0.94)		0.85 (0.45-1.48)		0.49 (0.24-0.72)		0.48 (0.24-0.97)
PCB31	0.72 (0.19-1.75)		0.99 (0.73-1.32)		1.10 (0.40-3.27)		4.60 (0.10-17.34)		0.69 (0.29-1.18)		0.98 (0.60-1.46)		0.98 (0.74-1.17)		0.28 (0.15-0.35)
PCB28	1.24 (0.53-2.59)		2.03 (1.56-2.71)		2.36 (0.88-6.18)		4.31 (0.39-12.96)		1.31 (0.89-1.97)		2.89 (1.58-5.10)		1.94 (1.18-3.14)		0.18 (0.16-0.21)
PCB33	1.90 (0.40-3.39)		1.61 (0.84-2.53)		2.42 (0.62-6.15)		3.34 (0.14-9.38)		0.52 (0.15-0.89)		0.78 (0.29-1.17)		0.78 (0.36-1.21)		0.1 (0.08-0.14)
PCB52	4.72 (1.53-10.26)		6.99 (5.10-10.51)		5.83 (3.73-11.71)		2.19 (0.09-6.10)		0.77 (0.23-1.29)		1.19 (0.29-2.92)		0.62 (0.10-1.15)		0.72 (0.43-1.3)
PCB49	1.28 (0.57-2.68)		2.04 (1.83-2.18)		3.13 (1.25-9.11)		0.96 (0.05-2.62)		0.54 (0.36-0.80)		1.06 (0.53-1.59)		0.43 (0.06-0.89)		0.07 (0.07-0.07)
PCB99/101							7.30 (2.01-9.95)		1.74 (0.66-2.99)		2.85 (1.03-5.43)		3.16 (2.16-4.90)		0.03 (0.03-0.03)
PCB110							0.73 (0.17-1.40)		0.23 (0.14-0.32)		0.48 (0.18-0.91)		0.47 (0.30-0.63)		0.03 (0.01-0.07)
PCB151	0.56 (0.36-0.85)		0.54 (0.41-0.75)		1.39 (0.42-3.02)		1.21 (0.24-2.86)		1.06 (0.39-1.99)		0.65 (0.25-1.27)		0.36 (0.21-0.61)		0.02 (0.01-0.04)
PCB149	1.21 (0.80-1.87)		1.19 (1.00-1.58)		2.75 (1.09-5.65)		3.85 (0.74-7.19)		1.37 (0.43-2.57)		1.67 (0.40-3.58)		1.06 (0.69-1.70)		0.08 (0.03-0.1)
PCB118	0.67 (0.25-1.39)		0.63 (0.51-0.79)		1.18 (0.51-2.73)		1.65 (0.26-4.07)		0.25 (0.14-0.43)		0.55 (0.15-1.19)		0.57 (0.33-1.00)		0.02 (0.02-0.02)
PCB153	1.15 (0.49-2.28)		0.86 (0.56-1.08)		1.69 (0.71-2.80)		3.20 (0.22-11.21)		0.90 (0.45-1.54)		1.45 (0.87-2.57)		0.67 (0.54-0.75)		0.1 (0.07-0.12)
PCB132/105	0.78 (0.26-1.72)		0.48 (0.41-0.54)		1.06 (0.24-1.76)		1.75 (0.13-5.52)		0.32 (0.04-0.68)		0.55 (0.33-0.95)		0.27 (0.04-0.40)		
PCB138	1.00 (0.42-1.92)		0.89 (0.56-1.10)		1.53 (0.59-2.59)		1.96 (0.17-4.39)		0.66 (0.23-1.22)		1.05 (0.41-2.01)		0.54 (0.21-0.72)		0.04 (0.01-0.05)
PCB158	0.09 (0.04-0.13)		0.09 (0.07-0.11)		0.09 (0.08-0.09)		0.63 (0.07-0.86)		0.07 (0.03-0.10)		0.25 (0.06-0.63)		0.07 (0.04-0.09)		
PCB187	0.27 (0.12-0.50)		0.22 (0.14-0.29)		0.43 (0.16-0.73)		1.26 (0.14-4.29)		0.45 (0.32-0.64)		0.69 (0.43-1.20)		0.29 (0.20-0.35)		0.09 (0.07-0.1)
PCB183	0.13 (0.03-0.23)		0.08 (0.05-0.12)				1.09 (0.04-2.76)		0.14 (0.09-0.23)		0.26 (0.11-0.51)		0.10 (0.06-0.14)		0 (0-0.01)
PCB128	0.99 (0.54-1.43)		1.01 (0.79-1.20)		1.32 (0.94-2.26)		0.55 (0.01-0.85)		0.05 (0.02-0.09)		0.07 (0.00-0.16)		0.07 (0.07-0.07)		
PCB177	0.14 (0.04-0.23)		0.06 (0.01-0.10)				0.67 (0.03-0.98)		0.11 (0.02-0.22)		0.26 (0.14-0.50)		0.07 (0.01-0.12)		
PCB171/156	0.19 (0.19-0.19)						0.57 (0.04-1.28)		0.12 (0.04-0.21)		0.07 (0.06-0.09)		0.11 (0.06-0.14)		
PCB180	0.28 (0.13-0.52)		0.27 (0.17-0.34)		0.35 (0.18-0.51)		0.84 (0.03-1.90)		0.23 (0.13-0.39)		0.49 (0.26-0.89)		0.23 (0.18-0.27)		0.03 (0.01-0.04)
Σ_{28} PCBs	16.93 (7.12-35.91)		20.97 (16.73-23.74)		25.82 (12.17-45.24)		45.84 (6.21-78.99)		12.11 (5.22-19.15)		20.94 (9.38-39.89)		14.72 (9.25-20.28)		2.43 (2.09-3.11)

Appendix E

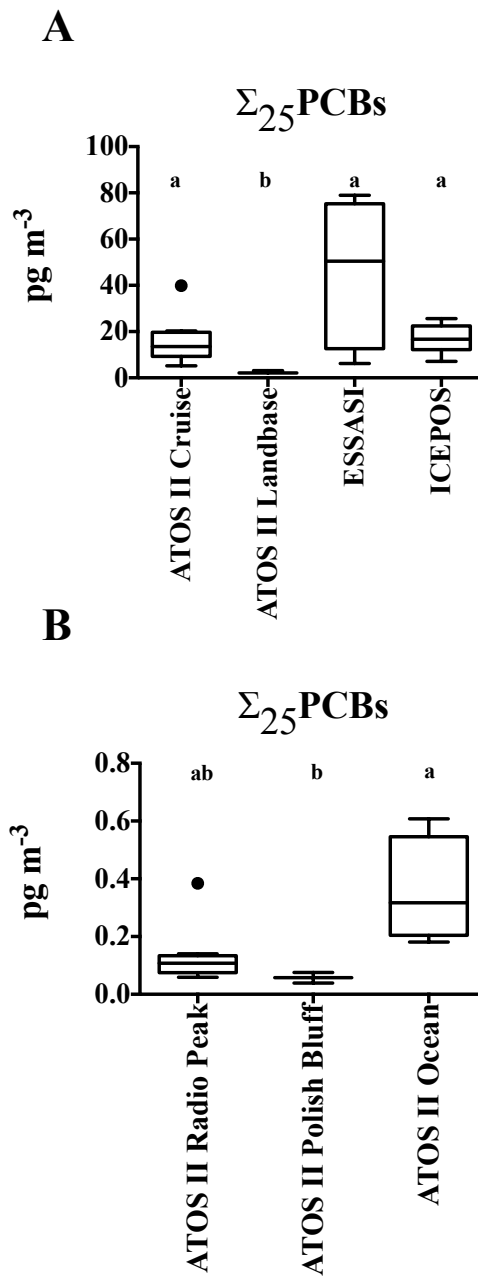


Figure S4. A) BOX-PLOT graph comparing the gas phase atmospheric concentrations from the different sampling campaigns showing that mean levels of samples taken at Polish Beach (a) were different (Kruskall-Wallis $p < 0.05$) and significant lower (post hoc Dunn's test $p < 0.001$) than the rest of the surveys (b) for $\Sigma_{25}\text{PCBs}$. B) BOX-PLOT graph representing the obtained aerosol phase atmospheric concentrations, comparing the different sampling locations and showing that the median levels of samples taken at Polish Beach during values were different (Kruskall-Wallis $p < 0.05$) and significant lower (post hoc Dunn's test $p < 0.001$) than samples from Radio Peak and over the Ocean (b) for $\Sigma_{25}\text{PCBs}$.

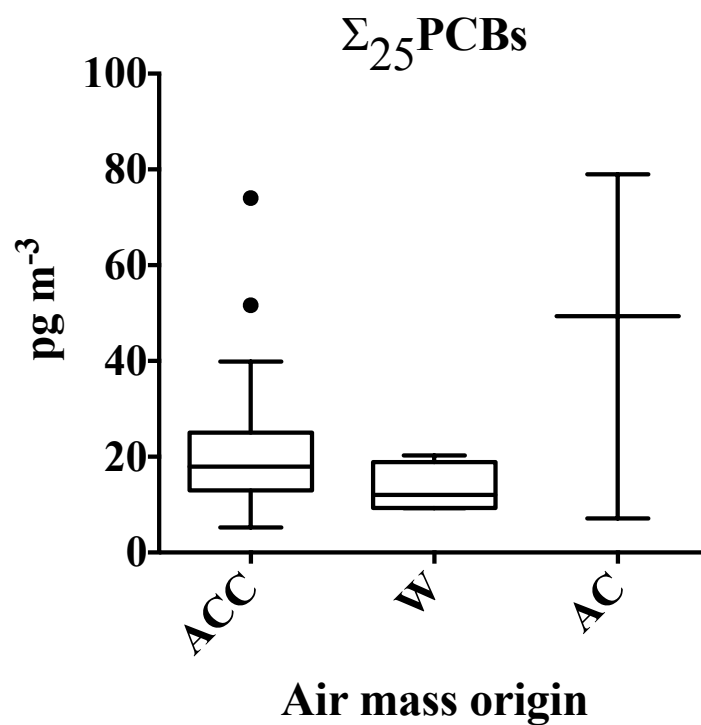


Figure S5. BOX-PLOT graph representing the obtained gas phase concentrations for the three characteristic origins of air masses identified. Obtained results show that samples influenced by the Antarctic Circumpolar water Current (ACC), Weddell Sea (WS) and Antarctic Continent (AC) were not different among them for $\Sigma_{25}\text{PCBs}$.

Appendix E.4

Table S10. physico-chemical properties used for the fugacity ratios, fluxes and gas-particle coefficient estimated in the present work.
 H: Henry's law constant ($\text{Pa m}^3 \text{mol}^{-1}$), $\text{Log } K_{\text{OW}}$: octanol-water partition coefficient, $\text{Log } K_{\text{OA}}$: octanol-air partition coefficient, and
 Mw: molecular weight (g mol^{-1}), ΔH is the heat of phase change (kJ mol^{-1}).

Compound	H ($\text{Pa m}^3 \text{mol}^{-1}$)	Log K_{OW} (at 298 K)	Ref	Log K_{OA} (at 298 K)	Ref	Mw	ΔH (kJ mol^{-1})	Ref
PCB18	25.3	5.6	Hansch et al., 1995	7.48	Chen et al., 2002	257.54	35	
PCB17	32.1	5.76		7.11		257.54	39	
PCB31	30.7	5.78	Li et al., 2003	7.94	Li et al., 2003	257.54	41	
PCB28	30.2	5.66		7.85		257.54	33	
PCB33	29.2	5.87	Hansch et al., 1995	8.03	Chen et al., 2002	257.54	42	
PCB52	25.12	5.91	Li et al., 2003	8.22	Li et al., 2003	291.99	31	
PCB49	39.9	6.38	Hansch et al., 1995	8.57	Harner & Bidleman, 1996	291.99	25	
PCB99/101	51.8	6.97	Hardy, 2002	9.07		326.43	16	
PCB110	42	6.2	Sangster, 1993	9.19		326.43	38	
PCB151	73.5	6.85	Hansch et al., 1995	9.68	Chen et al., 2002	360.88	37	
PCB149	68.4	6.47	Makino, 1998	9.78		368.99	46	Bamford et al., 2002
PCB118	14.45	6.69		9.83		326.43	50	
PCB153	19.95	6.87	Li et al., 2003	9.74	Harner & Bidleman, 1996	360.88	66	
PCB132/105	59.4	7.04	Hansch et al., 1995	10.02		360.88	61	
PCB138	30.2	7.22	Li et al., 2003	9.81		360.88	87	
PCB158	49.9	7.69	Ran et al., 2002	10.28		360.88	80	
PCB187	65.9	7.04	Makino, 1998	10.54		395.32	96	
PCB183	61.5	8.27	Ran et al., 2002	10.83	Chen et al., 2002	395.32	100	
PCB128	32.7	7.32	Hansch et al., 1995	9.93		360.88	118	
PCB177	50.6	6.92	Makino, 1998	10.63		395.32	112	
PCB171/156	37	7.57	Hansch et al., 1995	10.25	Harner & Bidleman, 1996	360.88	101	
PCB180	37.3	8.51	Li et al., 2003	10.52		395.32	144	

Table S11. Truly dissolved water concentration of PCBs (pg L⁻¹) corrected using an average dissolved organic carbon (DOC) concentration for Antarctic region (60 μmol L⁻¹). Data taken from Galbán-Malagón et al., 2013

pg L ⁻¹	ESSASI										ATOS II								
	DE1	DE2	DE3	DE4	DE5	DE6	DE7	DE8	DE9	DE10	DA1	DA2	DA3	DA4	DA5	DA6	DA7	DA8	DA9
PCB18	0.291	0.049	0.101	0.037	0.086	0.068	0.035	0.11	0.109	0.068	0.146	0.049	0.048	0.031	0.034	0.029	0.033	0.059	0.093
PCB17	0.105	0.034	0.077	0.098	0.066	0.058	0.047	0.063	0.156	0.074	0.236	0.093	0.034	0.307	0.048	0.028	0.019	0.083	0.342
PCB31	0.087	0.041	0.04	0.057	0.053	0.034	0.022	0.046	0.078	0.038	0.384	0.071	0.069	0.063	0.049	0.056	0.102	0.06	0.052
PCB28	0.101	0.046	0.042	0.026	0.048			0.025	0.05	0.021	0.173	0.042	0.038	0.032	0.029	0.041	0.065	0.054	0.077
PCB33	0.062		0.021			0.018	0.016		0.014		0.449	0.041	0.057	0.041	0.039	0.043	0.191	0.034	0.027
PCB52	0.115	0.027	0.136	0.106	0.04	0.067	0.033	0.067	0.161	0.207	0.147	0.016	0.063	0.025	0.006	0.066	0.07	0.03	0.015
PCB49	0.221	0.073	0.036	0.072	0.06	0.018	0.015	0.041	0.044	0.04	0.193	0.017	0.035	0.023	0.029	0.008	0.052	0.024	0.052
PCB99/101	0.189	0.078	0.151	0.192	0.150	0.095	0.088	0.101	0.161	0.145	0.059	0.16	0.203	0.154	0.26	0.189	0.479	0.175	0.029
PCB110	0.082	0.039	0.018	0.04	0.022	0.024	0.016	0.026	0.038	0.03	0.029	0.023	0.03	0.02	0.028	0.247	0.03	0.013	0.03
PCB151	0.125	0.038	0.007	0.006	0.013	0.007	0.007	0.005	0.006	0.012	0.142	0.02	0.021	0.027	0.044	0.018	0.098	0.003	0.03
PCB149	0.454	0.212	0.085	0.152	0.094	0.056	0.035	0.038	0.12	0.086		0.041	0.008	0.064	0.123	0.087	0.183	0.057	0.1
PCB118	0.384	0.125	0.048	0.083	0.048	0.028	0.022	0.024	0.079	0.06	0.01	0.056	0.012	0.057	0.11	0.062	0.077	0.049	0.067
PCB153	0.226	0.087	0.034	0.033	0.023	0.023	0.015	0.02	0.026	0.019	0.032	0.030	0.035	0.030	0.062	0.037	0.103	0.033	0.066
PCB132/105	0.032	0.016	0.009	0.017	0.008	0.006	0.007	0.003	0.015	0.007		0.018		0.016	0.037	0.022	0.005		
PCB138	0.104	0.051	0.015	0.022	0.01	0.01	0.008	0.004	0.014	0.011	0.008	0.019	0.02	0.02	0.04	0.026	0.033	0.013	0.018
PCB158	0.008	0.003	0.001	0.002	0.001	0.001	0.001	0.001	0.001	0.001		0.001	0.001	0.001	0.002	0.001	0.001	0.001	
PCB187	0.043	0.026	0.019	0.017	0.018	0.03	0.014	0.015	0.02	0.019	0.017	0.016	0.002	0.014	0.028	0.02	0.053	0.012	0.028
PCB183	0.001	0.001	0.001	0.001	0.001	0.001		0.001							0.001	0.001	0.001		0.001
PCB128	0.002	0.001	0.001	0.001	0.001	0.002	0.006	0.001	0.001						0.002	0.002			
PCB177	0.015	0.002			0.005			0.002							0.007	0.002	0.006		
PCB171/156	0.01	0.007	0.005	0.005	0.004	0.005	0.004	0.003	0.003	0.004		0.004	0.002	0.004	0.007	0.006	0.007	0.003	0.005
PCB180	0.002	0.001	0.001	0.001	0.001	0.001	0.001		0.001	0.001	0.001	0.001	0.001	0.001	0.002	0.001	0.003	0.001	0.001

Table S12. Estimated air-water fugacity ratios calculated for samples from the ESSASI and ATOS II cruise. Code refers to the gas phase sample code as in Table S1

	ESSASI										ATOS II									
	GE1	GE2	GE3	GE4	GE5	GE6	GAI	GA2	GA3	GA4	GA5	GA6	GA7	GA8	GA9					
PCB18	0.113	0.776	4.326	2.787	0.162	0.030	0.607	0.262	0.110	0.112	0.364	0.113	0.188	0.710	1.323					
PCB17		0.102	2.007	1.559	0.036	0.083	0.800	0.804	0.218	1.439	2.630	0.217	0.489	0.543	4.434					
PCB31	0.035	0.465	1.194	0.741	0.010	0.034	0.793	0.464	0.246	0.275	0.204	0.294	0.481	0.592	0.842					
PCB28	0.092		0.110		0.010		0.549	0.109	0.064	0.083	0.157	0.142	0.107	0.212	0.416					
PCB33			0.272	0.233				0.160	0.193	0.177	0.446	0.278	0.606	1.560						
PCB52	0.076	0.420	2.398	1.731	0.174	0.034	0.305	0.095		0.273		1.785	0.219	0.703	0.499					
PCB49	0.418	0.685	0.895	2.895	0.258		1.241	0.350	0.319	0.472	3.153		1.106		1.063					
PCB99/101	0.317	0.225	0.153	0.721	0.184		0.602		0.938											
PCB110	0.254	0.091	0.689	0.542	0.232	0.130			0.318	0.448	2.030			0.770	1.045					
PCB151	0.566	0.076	0.291	0.306	0.018	0.050	0.463		0.306	0.921		0.967	2.224	2.475	0.258					
PCB149	0.352	0.129	0.354	0.336	0.038	0.048	0.112	0.266	0.087	1.816	1.027	0.666	1.251	0.961	1.511					
PCB118	0.130	0.010	0.051	0.114	0.017	0.033	0.099	0.524	0.045	0.366	0.291	0.155	0.289	0.634	0.540					
PCB153	0.052	0.007	0.077	0.032	0.012	0.001	0.021	0.042	0.025	0.057	0.089	0.097	0.112	0.096	0.138					
PCB132/105	0.015	0.024	0.079	0.202	0.005	0.016	0.090	0.251		0.324	2.563	0.212								
PCB138	0.012	0.002	0.028	0.016	0.001	0.003	0.008	0.024	0.013	0.034	0.115	0.036	0.030	0.051						
PCB158	0.010	0.001		0.015	0.001	0.002	0.006	0.020	0.010	0.027	0.038	0.027	0.029	0.027						
PCB187	0.033	0.005	0.076	0.115	0.017	0.026	0.027	0.054	0.007	0.066	0.133	0.122	0.138	0.112	0.079					
PCB183	0.001	0.000								0.003		0.006								
PCB128	0.001	0.001	0.204							0.011										
PCB177	0.005	0.001								0.027		0.024								
PCB171/156	0.004	0.002	0.046							0.044	0.060	0.030	0.029	0.054						
PCB180							<0.001			0.001	0.001	0.001	0.001	0.001	0.001					

Table S13. Estimated net air-water diffusive fluxes for the ESSASI and ATOS II cruises. Code refers to the gas phase sample code as in Table S1

Compound	ESSASI (2008)										ATOS II (2009)						
	South Scotia					Weddell					Bransfield			Bellingshausen			
	GE1	GE2	GE3	GE4	GE5	GE6	GA1	GA2	GA9	GA3	GA4	GA8	GA5	GA6	GA7		
PCB18	-0.01	-0.06	-0.42	-0.23	-0.02	-0.04	-0.08	-0.10	0.01	-0.54	-0.20	-0.01	-0.02	-0.31	-0.22		
PCB17	-0.13	-0.03	-0.20	-0.04	0.01	0.02	-0.06	-0.02	0.08	-0.26	0.00	-0.02	0.03	-0.16	-0.07		
PCB31	-0.22	-0.06	-0.25	-0.17	-0.18	-0.37	-0.08	-0.06	-0.01	-0.28	-0.12	-0.03	-0.09	-0.22	-0.11		
PCB28	-0.14	-0.19	-0.79	-0.39	-0.15	-0.33	-0.12	-0.26	-0.05	-0.95	-0.28	-0.11	-0.08	-0.31	-0.59		
PCB33		-0.12	-0.23	-0.23				-0.14	0.00	-0.24	-0.14	0.01	-0.02	-0.27	-0.11		
PCB52	-0.18	-0.06	-0.43	0.11			-0.22	-0.11	-0.01	-0.56	-0.02	-0.01		0.03	-0.19		
PCB49	0.03	-0.01	-0.13	-0.02	0.02	0.05	0.02	-0.03	0.00	-0.17	-0.03		0.01	-0.10	-0.01		
PCB99/101	-0.06	0.00	-0.21	0.02	-0.01	-0.03	-0.11	0.05	0.03	-0.19	0.07	0.13	0.02	0.00	0.19		
PCB110	-0.01		-0.10	-0.03	-0.02	-0.04	-0.03		0.00	-0.13	-0.02	0.00	0.02	-0.01			
PCB151	-0.14	-0.02	-0.10	-0.04	-0.01	-0.02	-0.14	-0.01	-0.03	-0.11	-0.01	0.01	0.00	0.00	0.02		
PCB149	-0.09	-0.06	-0.37	0.04	-0.01	-0.03	-0.39	-0.09	0.01	-0.49	0.01	-0.01	0.00	-0.13	0.00		
PCB118	-0.06	-0.02	-0.37	-0.10	-0.09	-0.17	-0.17	-0.02	-0.02	-0.43	-0.08	-0.01	-0.05	-0.40	-0.10		
PCB153	-0.58	-0.19	-0.93	-0.40	-0.18	-0.31	-0.70	-0.23	-0.09	-1.05	-0.29	-0.18	-0.10	-0.31	-0.29		
PCB132/105	-0.13	-0.03	-0.18	-0.07	0.00	-0.01	-0.16	-0.03		-0.21	-0.04	-0.03	0.00	-0.09	-0.08		
PCB138	-0.52	-0.16	-0.79	-0.35	-0.07	-0.12	-0.60	-0.20	-0.06	-0.89	-0.26	-0.10	-0.04	-0.36	-0.31		
PCB158	-0.03	-0.01	-0.19	-0.02	-0.01	-0.02	-0.04	-0.01	-0.01	-0.22	-0.02	-0.01	-0.01	-0.03	-0.02		
PCB187	-0.23	-0.08	-0.40	-0.17	-0.06	-0.10	-0.27	-0.10	-0.08	-0.45	-0.12	-0.08	-0.03	-0.13	-0.12		
PCB183	-0.09	-0.02	-0.18						-0.02				-0.05	-0.02	-0.01		
PCB128	-0.05	-0.01	-0.07							-0.02			-0.04	-0.04	-0.04		
PCB177	-0.10	-0.02	-0.21							-0.06	-0.04		0.00	-0.05	-0.06		
PCB171/156	-0.09	-0.03		-0.04	-0.02	-0.04	-0.11	-0.04	-0.01				-0.03	-0.07	-0.06		
PCB180	-0.21	-0.04	-0.45	-0.15	-0.08	-0.13	-0.23	-0.06	-0.06	-0.50	-0.13	-0.11	-0.06	-0.14	-0.15		
Σ_{22} PCBs	-3.05	-1.21	-7.01	-2.26	-0.89	-1.68	-3.48	-1.47	-0.32	-7.67	-1.83	-0.63	-0.45	-3.15	-2.39		
Σ_{105} PCBs	-1.75	-0.66	-3.96	-1.25	-0.59	-1.08	-2.14	-0.84	-0.26	-4.58	-0.99	-0.39	-0.31	-1.49	-1.46		

Appendix E

Table S14. Estimated dry deposition fluxes ($\text{ng m}^{-2} \text{d}^{-1}$). Code refers to the gas phase sample code as in Table S1

ng m ⁻² d ⁻¹	ATOS II cruise										Radio Peak										Polish Bluff						
	A1	A2	A3	A4	AB1	AB2	AB3	AB4	AB5	AB6	AB7	AB8	AB9	AB10	AB1	AB2	AB3	AB4	AB5	AB6	AB7	AB8	AB9	AB10	AB9	AB10	
PCB18	0.014	0.039	0.061	0.014																						0.010	
PCB17	0.001		0.017																							0.002	
PCB31	0.002	0.001		0.001	0.002	0.001	<0.001	0.001							0.001	<0.001	0.001									0.001	0.001
PCB28	0.005		0.004	0.006	0.013	0.003	0.010	0.004	0.010	0.009	0.002	0.002	0.001	<0.001	0.002	0.002	0.002	0.002	0.010	0.009	0.002	0.002	0.001	0.001	0.001	<0.001	
PCB33					<0.001	<0.001	<0.001	<0.001																		0.001	<0.001
PCB52	0.004																									0.002	
PCB49	0.001																									0.002	
PCB99/101	0.016	0.004	0.007	0.020	0.003	0.003	0.002																			0.002	<0.001
PCB110	0.009	0.006		0.009	0.001	<0.001	0.001	<0.001	0.001	0.003	0.002	0.002	0.001	<0.001	<0.001	<0.001	<0.001	<0.001	0.001	<0.001	<0.001	<0.001	<0.001	<0.001	<0.001	<0.001	
PCB151	0.004				0.001	0.001	<0.001																			0.001	0.001
PCB149	0.010				0.012	<0.001	0.001	<0.001	<0.001	<0.001	<0.001	<0.001	<0.001	<0.001	0.001	0.000	0.000	0.000	<0.001	<0.001	<0.001	0.000	0.000	0.000	0.000	0.000	
PCB118					0.001	<0.001	0.001	<0.001	<0.001	<0.001	<0.001	<0.001	<0.001	<0.001	<0.001	<0.001	<0.001	<0.001	<0.001	<0.001	<0.001	<0.001	<0.001	<0.001	<0.001	<0.001	
PCB153	0.018			0.001	0.004	0.026	0.007	0.007	0.007	0.008	0.009	0.003	0.002	0.001	0.003	0.002	0.002	0.002	0.008	0.009	0.003	0.002	0.001	0.001	0.001	0.001	
PCB132/105	0.006	<0.001		0.004	0.012	0.008																				0.001	0.001
PCB158	0.014				0.009	0.001	0.001	0.001	0.001	<0.001	0.001	0.001	0.001	<0.001	0.001	0.001	0.001	0.001	<0.001	0.001	0.001	0.001	<0.001	<0.001	<0.001	<0.001	
PCB138	0.001				0.003	0.005	0.001	0.002	<0.001	<0.001	<0.001	<0.001	<0.001	<0.001	<0.001	<0.001	<0.001	<0.001	<0.001	<0.001	<0.001	<0.001	<0.001	<0.001	<0.001	<0.001	
PCB187	0.027				0.020	0.009	0.005	0.005	0.005	0.006	0.005	0.004	0.004	0.004	0.005	0.004	0.004	0.004	0.005	0.006	0.005	0.004	0.004	0.004	0.004	0.005	
PCB183	0.001				0.002	0.001	<0.001	<0.001	<0.001	<0.001	<0.001	<0.001	<0.001	<0.001	<0.001	<0.001	<0.001	<0.001	<0.001	<0.001	<0.001	<0.001	<0.001	<0.001	<0.001	<0.001	
PCB128	0.002																									<0.001	<0.001
PCB177	0.002				<0.001	<0.001	<0.001	<0.001	<0.001	<0.001	<0.001	<0.001	<0.001	<0.001	<0.001	<0.001	<0.001	<0.001	<0.001	<0.001	<0.001	<0.001	<0.001	<0.001	<0.001	<0.001	
PCB171/156	0.005	0.002	0.003	0.005																						<0.001	<0.001
PCB180	0.030		0.011	0.014	0.006	0.001	<0.001	0.001	0.001	0.001	0.001	0.001	0.001	0.001	0.001	0.001	0.001	0.001	0.001	0.001	0.001	0.001	0.001	0.001	0.001	0.001	
Σ25PCBs	0.173	0.052	0.103	0.078	0.110	0.040	0.031	0.024	0.030	0.033	0.021	0.017	0.022	0.011	0.022	0.023	0.023	0.023	0.030	0.033	0.021	0.017	0.022	0.022	0.022	0.011	
ΣICESPCBs	0.074	0.004	0.022	0.044	0.057	0.015	0.021	0.010	0.022	0.023	0.011	0.007	0.004	0.002	0.004	0.004	0.004	0.004	0.022	0.023	0.011	0.007	0.004	0.004	0.004	0.002	

ATOS II Cruise

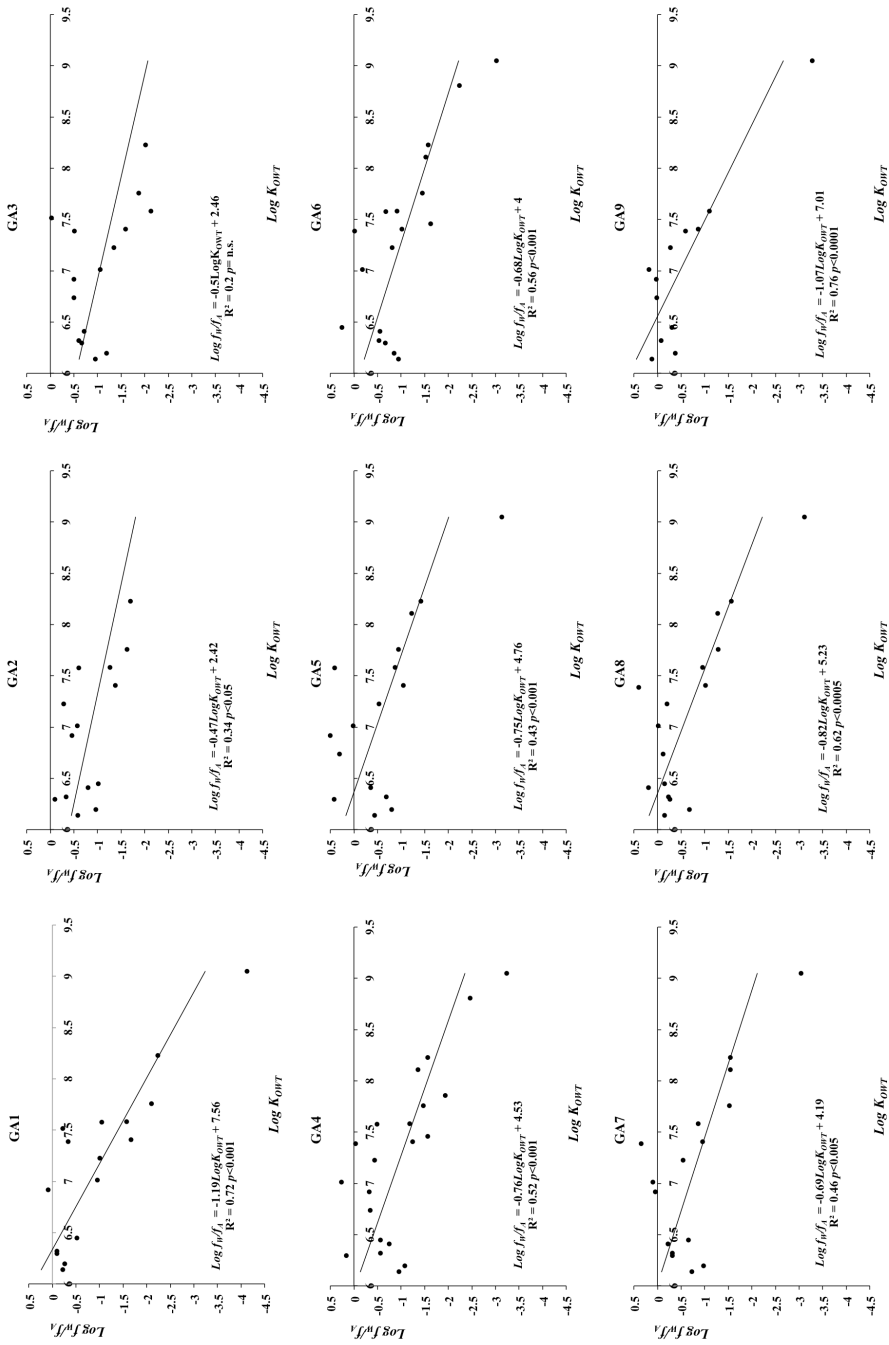


Figure S6: Air-water fugacity ratios ($\text{Log } f_w/f_A$) against the logarithm of temperature corrected octanol-water partition constant ($\text{Log } K_{OW}$) for samples taken during the ATOS II Cruise. Code refers to the gas phase sample code as in Table S1

ESSASI Cruise

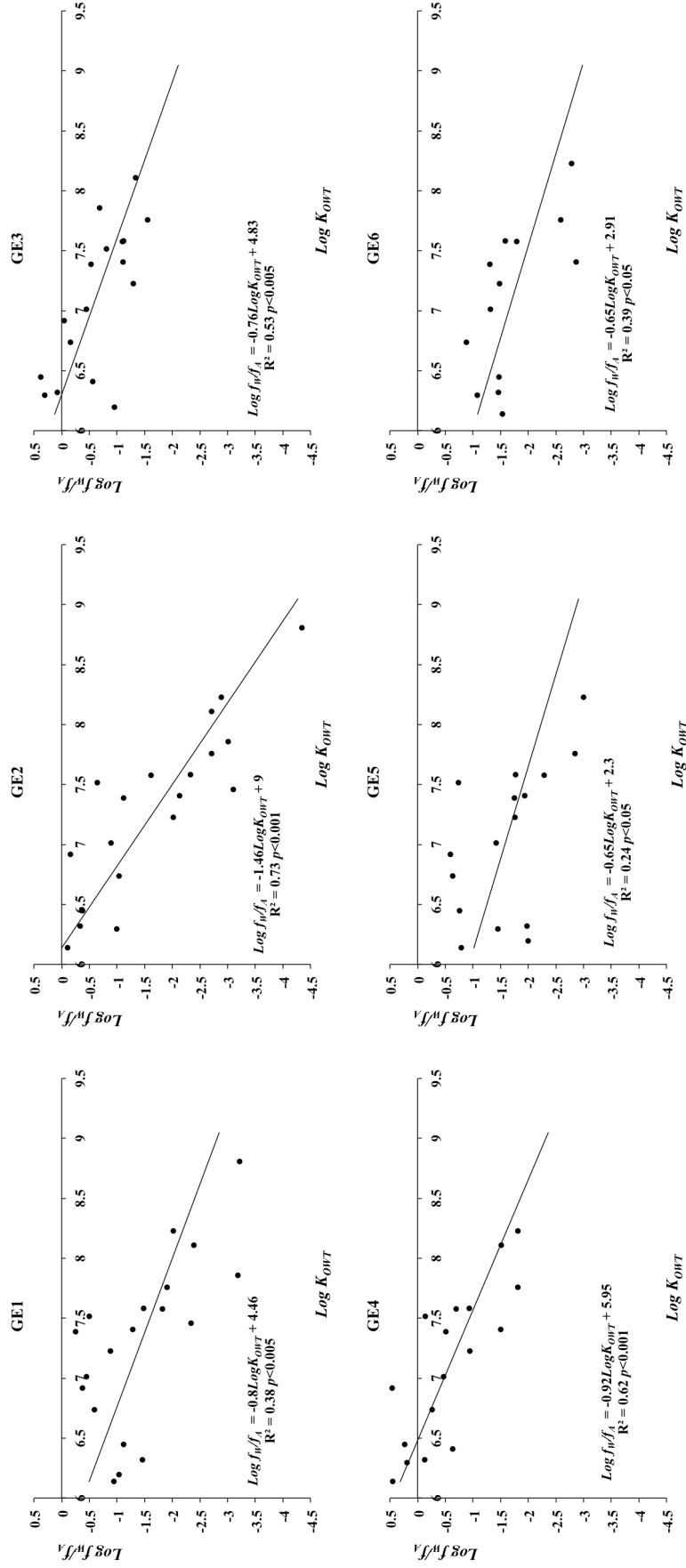


Figure S7: Air-water fugacity ratios ($\text{Log } f_w/f_A$) against the logarithm of temperature corrected octanol-water partition constant ($\text{Log } K_{OW}(T)$) for samples taken during the ESSASI Cruise. Code refers to the gas phase sample code as in Table S1

Appendix E.5

Table S15. Measured $\log K_P$ for samples taken at Livingston Island. Code refers to the gas phase sample code as in Table S1 and TS7.

$\log K_P$ field derived	GLI4	GLI5	GLI6	GLI7	GLI8	GLI9	GLI10	GLI11	GLI12	GLI13	GLI14	GLI15	GLI16	GLI17	GLI18	GLI1	GLI2	GLI3	
	AB1	AB2	AB2	AB3	AB3	AB3	AB4	AB4	AB4	AB5	AB5	AB5	AB6	AB6	AB6	Beach	AB9	Beach	
PCB18																			
PCB17																			
PCB31	-4.613	-4.555	-4.442	-4.941	-5.076	-4.753	-5.070	-4.606	-5.036							-4.543	-4.544	-4.181	
PCB28	-3.512	-3.823	-3.695	-3.227	-3.652	-3.349	-4.116	-3.673	-4.002	-2.962	-3.108	-3.189	-3.315	-3.060	-3.295	-3.716	-3.717	-3.827	
PCB33	-4.554					-4.856	-5.179	-4.899											
PCB52							-4.965	-4.363	-4.998	-4.675	-4.677	-4.509							
PCB49							-5.028		-5.172										
PCB99/101	-3.209	-2.644		-2.627	-2.835	-2.814									-2.936				
PCB110	-4.195	-4.107	-3.367	-3.367	-3.856	-3.754	-5.464	-4.230	-5.230	-3.843	-3.797	-3.922	-4.436	-3.686	-4.582	-3.716	-3.722	-4.391	
PCB151	-5.132	-5.480	-5.464	-5.448	-5.176	-5.130									-5.068	-3.461	-3.449	-3.983	
PCB149	-3.869	-5.316	-5.048	-4.824	-5.177	-5.035	-5.778	-5.430	-5.590	-5.221	-5.281	-5.169	-5.417	-5.199	-5.231				
PCB118	-4.063	-4.297	-3.917				-5.422	-4.621	-5.345	-3.583	-3.772	-3.542	-4.546	-4.327	-4.339				
PCB153	-3.575	-4.165	-4.073	-4.065	-4.099	-4.051	-4.421	-4.251	-4.382	-3.899	-3.831	-3.824	-3.813	-3.672	-3.717	-3.426	-3.428	-3.207	
PCB132/105	-2.120						-3.915		-2.825										
PCB138	-3.331	-4.194	-3.938	-4.101	-4.645	-4.517	-5.061	-4.647	-4.880	-4.399	-4.567	-4.442	-4.639	-4.447	-4.502	-3.779	-3.777	-3.148	
PCB158	-2.752	-2.447	-2.315	-3.057	-3.467	-3.388	-3.412	-2.991	-3.195	-3.621	-3.821	-3.445	-3.464	-3.499	-3.363			-3.325	
PCB187	-3.218	-3.574	-3.463	-3.764	-3.803	-3.782	-3.774	-3.643	-3.758	-3.672	-3.611	-3.607	-3.651	-3.482	-3.624	-3.158	-3.157	-2.959	
PCB183	-3.887	-4.247	-4.096	-4.695	-4.712	-4.704	-4.660	-4.547	-4.672	-4.583	-4.524	-4.471	-4.732	-4.602	-4.727	-2.426	-2.449	-3.148	
PCB128																			
PCB177	-3.053	-3.218		-3.555	-4.319	-4.166	-4.883	-4.346	-4.578										
PCB171/156																			
PCB180	-3.325	-4.209	-4.101	-4.479	-4.545	-4.513	-4.311	-4.151	-4.381	-3.922	-3.919	-3.797	-3.856	-3.737	-3.814	-3.021	-3.024	-2.400	

Table S16. Predicted $Log K_P$ estimated from the $Log K_{O1}$ corrected for temperature for samples taken in at Livingston Island. Code refers to the gas phase sample code as in Table S1.

$Log K_P$ Modelled	AB1	AB2	AB2	AB3	AB3	AB3	AB4	AB4	AB4	AB5	AB5	AB5	AB6	AB6	AB6	AB9 Beach	AB9 Beach	AB9 Beach
PCB18	-5.593	-5.575	-5.568	-5.596	-5.629	-5.625	-5.629	-5.596	-5.623	-5.562	-5.564	-5.509	-5.516	-5.440	-5.503	-5.742	-5.672	-5.666
PCB17	-5.963	-5.945	-5.938	-5.966	-5.999	-5.995	-5.999	-5.966	-5.993	-5.932	-5.934	-5.879	-5.886	-5.810	-5.873	-6.112	-6.042	-6.036
PCB31	-5.133	-5.115	-5.108	-5.136	-5.169	-5.165	-5.169	-5.136	-5.163	-5.102	-5.104	-5.049	-5.056	-4.980	-5.043	-5.282	-5.212	-5.206
PCB28	-5.223	-5.205	-5.198	-5.226	-5.259	-5.255	-5.259	-5.226	-5.253	-5.192	-5.194	-5.139	-5.146	-5.070	-5.133	-5.372	-5.302	-5.296
PCB33	-5.043	-5.025	-5.018	-5.046	-5.079	-5.075	-5.079	-5.046	-5.073	-5.012	-5.014	-4.959	-4.966	-4.890	-4.953	-5.192	-5.122	-5.116
PCB52	-4.762	-4.742	-4.735	-4.765	-4.801	-4.797	-4.801	-4.765	-4.795	-4.728	-4.731	-4.671	-4.679	-4.597	-4.665	-4.920	-4.844	-4.839
PCB49	-4.412	-4.392	-4.385	-4.415	-4.451	-4.447	-4.451	-4.415	-4.445	-4.378	-4.381	-4.321	-4.329	-4.247	-4.315	-4.570	-4.494	-4.489
PCB99/101	-3.887	-3.867	-3.859	-3.890	-3.927	-3.923	-3.927	-3.890	-3.921	-3.853	-3.855	-3.794	-3.802	-3.718	-3.788	-4.048	-3.971	-3.965
PCB110	-3.766	-3.746	-3.738	-3.769	-3.807	-3.802	-3.806	-3.769	-3.800	-3.732	-3.734	-3.673	-3.681	-3.598	-3.667	-3.927	-3.850	-3.844
PCB151	-3.264	-3.244	-3.236	-3.268	-3.305	-3.301	-3.305	-3.268	-3.299	-3.230	-3.232	-3.171	-3.179	-3.094	-3.165	-3.427	-3.349	-3.343
PCB149	-3.176	-3.156	-3.148	-3.179	-3.217	-3.212	-3.216	-3.179	-3.210	-3.142	-3.144	-3.083	-3.091	-3.008	-3.077	-3.337	-3.260	-3.254
PCB118	-3.128	-3.108	-3.100	-3.131	-3.168	-3.163	-3.168	-3.131	-3.162	-3.094	-3.096	-3.035	-3.043	-2.959	-3.029	-3.289	-3.212	-3.206
PCB153	-3.221	-3.201	-3.193	-3.224	-3.262	-3.257	-3.261	-3.224	-3.255	-3.187	-3.189	-3.128	-3.136	-3.053	-3.122	-3.382	-3.305	-3.299
PCB132/105	-2.926	-2.906	-2.898	-2.930	-2.967	-2.963	-2.967	-2.930	-2.961	-2.892	-2.894	-2.833	-2.841	-2.756	-2.827	-3.089	-3.011	-3.005
PCB138	-3.132	-3.112	-3.104	-3.135	-3.173	-3.168	-3.172	-3.135	-3.166	-3.097	-3.100	-3.038	-3.046	-2.962	-3.032	-3.294	-3.216	-3.210
PCB158	-2.664	-2.644	-2.636	-2.668	-2.705	-2.701	-2.705	-2.668	-2.699	-2.630	-2.632	-2.571	-2.579	-2.494	-2.565	-2.827	-2.749	-2.743
PCB187	-2.332	-2.311	-2.303	-2.337	-2.376	-2.371	-2.376	-2.337	-2.369	-2.296	-2.299	-2.234	-2.242	-2.153	-2.227	-2.502	-2.420	-2.414
PCB183	-2.042	-2.021	-2.013	-2.047	-2.086	-2.081	-2.086	-2.047	-2.079	-2.006	-2.009	-1.944	-1.952	-1.863	-1.937	-2.212	-2.130	-2.124
PCB128	-3.014	-2.994	-2.986	-3.018	-3.055	-3.051	-3.055	-3.018	-3.049	-2.980	-2.982	-2.921	-2.929	-2.844	-2.915	-3.177	-3.099	-3.093
PCB177	-2.242	-2.221	-2.213	-2.247	-2.286	-2.281	-2.286	-2.247	-2.279	-2.206	-2.209	-2.144	-2.152	-2.063	-2.137	-2.412	-2.330	-2.324
PCB171/156	-2.691	-2.671	-2.663	-2.695	-2.732	-2.727	-2.732	-2.695	-2.726	-2.657	-2.659	-2.598	-2.606	-2.521	-2.592	-2.854	-2.776	-2.770
PCB180	-2.354	-2.333	-2.324	-2.358	-2.398	-2.393	-2.397	-2.358	-2.391	-2.318	-2.321	-2.256	-2.264	-2.175	-2.249	-2.524	-2.442	-2.436

Table S17. Measured Log K_p and predicted Log K_p estimated using the Log K_{OA} corrected temperature for samples taken during the ATOS II cruise. Code refers to the gas phase sample code as in Table S1.

Measured Log K_p	GA3 A1	GA4 A2	GA5 A3	GA6 A3	GA8 A4	Predicted Log K_p	A1	A2	A3a and b	A4
PCB18	-3.143	-2.826	-3.597	-4.112	-3.351	PCB18	-5.514	-5.664	-5.540	-5.571
PCB17	-3.922					PCB17	-5.884	-6.034	-5.910	-5.941
PCB31	-3.694	-4.494	-5.139	-5.081	-4.719	PCB31	-5.054	-5.204	-5.080	-5.111
PCB28	-3.857		-4.442	-4.547	-4.442	PCB28	-5.144	-5.294	-5.170	-5.201
PCB33						PCB33	-4.964	-5.114	-4.990	-5.021
PCB52	-3.739					PCB52	-4.673	-4.836	-4.702	-4.735
PCB49	-3.953					PCB49	-4.323	-4.486	-4.352	-4.385
PCB99 /101	-3.395	-4.023	-4.249	-4.556	-3.754	PCB99 /101	-3.796	-3.961	-3.825	-3.859
PCB110	-2.866	-3.082	-3.707	-4.024	-3.360	PCB110	-3.675	-3.841	-3.704	-3.738
PCB151	-3.171					PCB151	-3.705	-3.871	-3.734	-3.768
PCB149	-2.989					PCB149	-3.172	-3.339	-3.201	-3.236
PCB118						PCB118	-3.085	-3.251	-3.114	-3.148
PCB153	-2.701		-4.114	-4.537	-3.590	PCB153	-3.037	-3.202	-3.066	-3.100
PCB132 /105	-3.525	-4.651	-4.274	-4.388		PCB132 /105	-3.130	-3.296	-3.159	-3.193
PCB158	-2.709					PCB158	-2.834	-3.001	-2.863	-2.898
PCB138	-4.087					PCB138	-3.040	-3.207	-3.069	-3.103
PCB187	-2.246					PCB187	-2.572	-2.739	-2.601	-2.636
PCB183	-3.864					PCB183	-2.233	-2.410	-2.264	-2.300
PCB128	-3.270					PCB128	-1.943	-2.120	-1.974	-2.010
PCB177	-2.678					PCB177	-2.922	-3.089	-2.951	-2.986
PCB171/156	-2.843	-3.135	-2.186	-3.437	-3.494	PCB171/156	-2.143	-2.320	-2.174	-2.210
PCB180			-2.812	-3.162	-2.706	PCB180	-2.599	-2.766	-2.628	-2.663

Appendix E

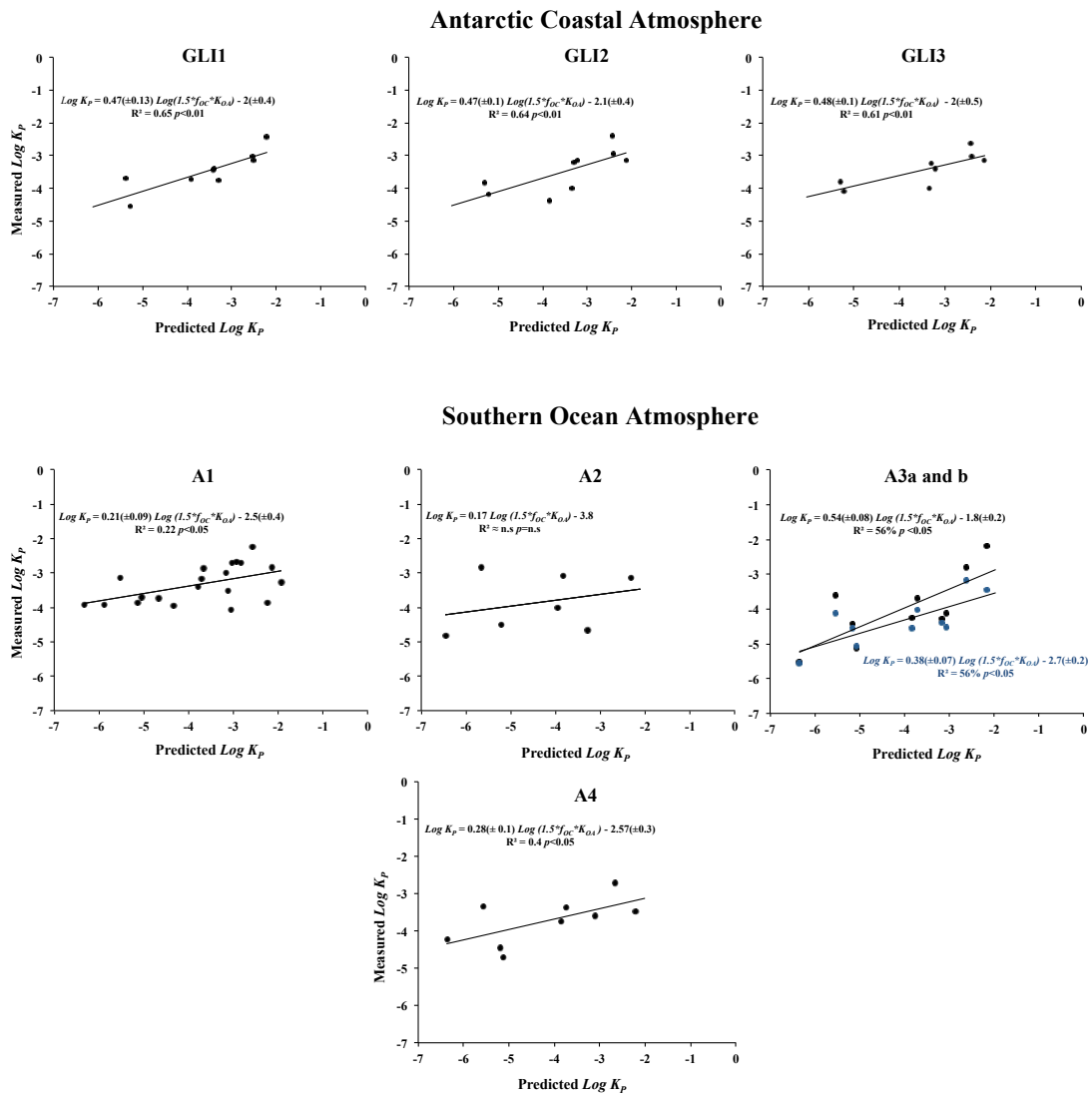


Figure S18. Measured versus predicted gas-particle partition constant ($\text{Log } K_p$) from gas and aerosol phase samples from the Antarctic coastal atmosphere (Livingston Island) and from Southern Ocean atmosphere taken during 2009. Code refers to the gas phase sample code as in Table S1.

Antarctic Atmosphere

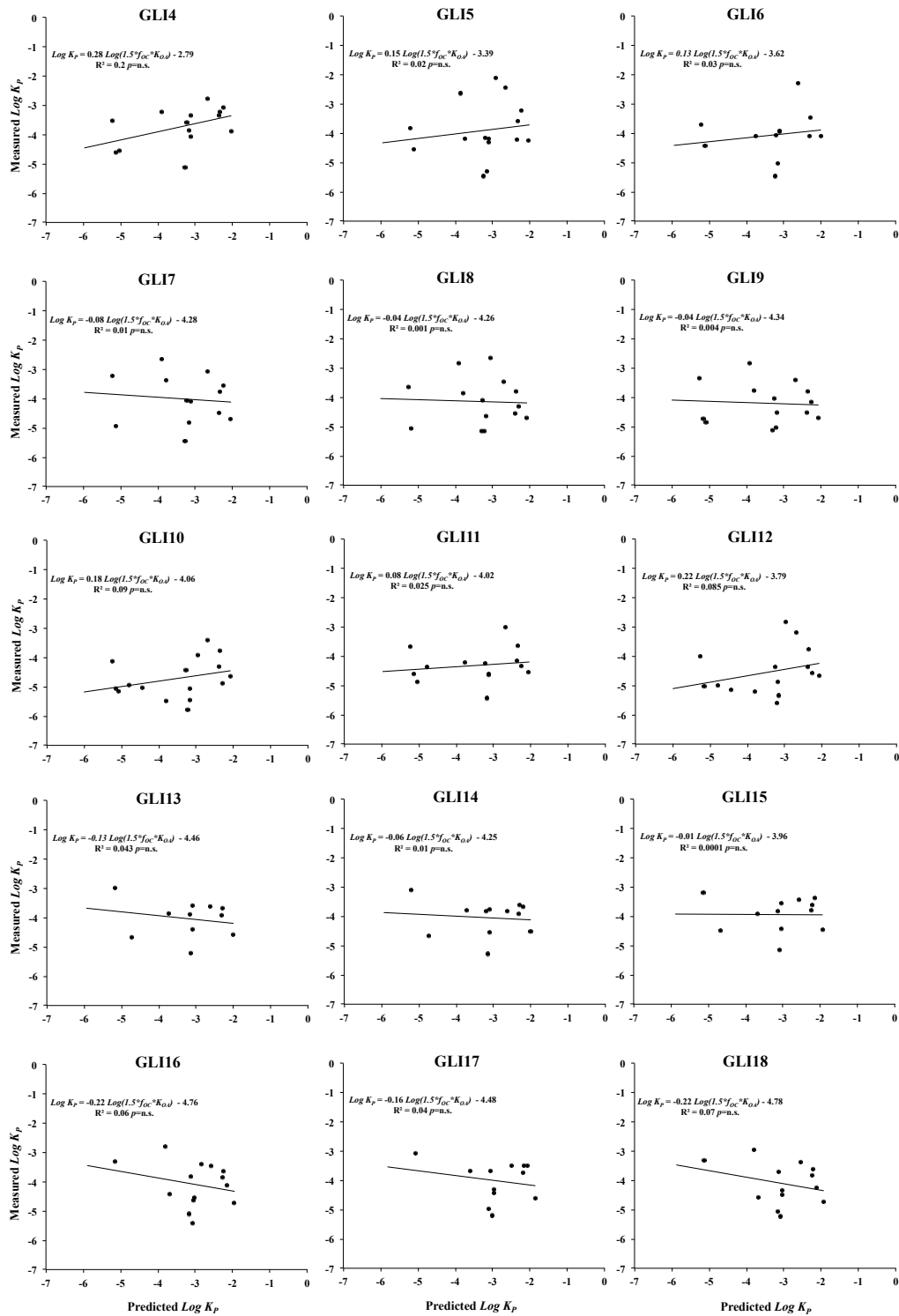


Figure S19. Measured versus predicted gas-particle partition constant ($\text{Log } K_p$) for gas and aerosol phase samples taken at Radio Peak in Livingston Island in 2009 austral summer (Cabrerizo et al., 2013) and aerosols samples reported in the present work. Code refers to the gas phase sample code as in Table S1 and TS7.

Appendix E

Additional References

Bamford, H. A., Poster, D. L., & Baker, J. E. (2000). Henry's law constants of polychlorinated biphenyl congeners and their variation with temperature. *Journal of Chemical and Engineering Data*, 45(6), 1069-1074

Hansch, C.; Leo, A.; Hoekman, D. Exploring QSAR, Hydrophobic, Electronic, and Steric Constants. ACS Professional Reference Book, Am. Chem. Soc., Washington, DC. 1995

Hardy, M.L. A comparison of the properties of the major commercial PBDPO/PBDE product to those of major PBB and PCB products. *Chemosphere*. 2002 46, 717–728.

Li, N.; Wania, F.; Lei, Y.D.; Daly, G.L. A comprehensive and critical compilation, evaluation, and selection of physical- chemical property data for selected polychlorinated biphenyls. *J. Phys. Chem. Ref. Data* 2003 32, 1545–1590.

Makino, M. Prediction of n-octanol/water partition coefficients of polychlorinated biphenyls by use of computer calculated molecular properties. *Chemosphere*. 1998 37, 13–26.

Ran, Y.; He, Y.; Hang, G.; Johnson, J.L.H.; Yalkowsky, S.H. (2002) Estimation of aqueous solubility of organic compounds by using the general solubility equation. *Chemosphere*. 2002 48, 487–509.

Sangster, J. LogK_{OW}, A Databank of Evaluated Octanol-Water Partition Coefficients. First ed., Montreal, Quebec, Canada. 1993.

Chen, J., Xue, X., Schramm, K.-W., Quan, X., Yang, F., Kettrup, A. (2002) Quantitative structure-property relationships for octanol-air partition coefficients of polychlorinated biphenyls. *Chemosphere* 48, 535–544.

Li, N., Wania, F., Lei, Y.D., Daly, G.L. (2003) A comprehensive and critical compilation, evaluation, and selection of physical-chemical property data for selected polychlorinated biphenyls. *J. Phys. Chem. Ref. Data* 32, 1545–1590.

Harner, T., Bidleman, T. F. (1996) Measurements of octanol-air partition coefficients for polychlorinated biphenyls. *J. Chem. Eng. Data* 41, 895–899.

Appendix F

List of Acronyms

-ΔU_{AW} : Heat of phase change from liquid to gas.	C_{WTD} : POPs truly dissolved seawater concentration
a : Surface area	DDT : dichlorodiphenyltrichloroethane
ACC : Antarctic Circumpolar Current	DOC : Dissolved organic carbon
AEPSs : Arctic Environmental Protection Strategies	DOM : Dissolved organic matter
AMAP : Arctic Monitoring and Assessment Program	EC : European Commission
AntC : Antarctic Continent Airmass Origin	ECHA : European Chemicals Agency
AO :Arctic Ocean	EPPR : Emergency Prevention, Preparedness and Response
BCF : Bioconcentration factor	$F_{Biogenic}$: Sinking flux of Biogenic matter
B_{Phyto} : Phytoplankton biomass in the whole mixes layer depth	F_{DD} : Dry deposition flux
C_{Aero} : POPs concentration in the atmospheric aerosol	F_{DegH} : Hydrolytic degradation flux
CAFF : Conservation of Arctic Flora and Fauna	F_{DegM} : Microbial degradation flux
C_G : POPs concentration in the gas phase	F_{DegP} : Photolytic degradation flux
ChlA : Chlorophyll a	f_{EC} : Fraction of elemental carbon
CLRAT : Convention on Long-range Transboundary air pollution	f_{OC} : Fraction of organic carbon
C_{Oct} : POPs concentration associated to octanol	F_{OC} : Organic carbon flux
C_{OH} : OH atmospheric concentration	f_{OM} : Fraction of organic mater
C_p : POPs concentration associated to water particulate matter	F_{OM} : Organic matter flux
C_{Phyto} : POPs associated to phytoplankton	F_{Sink} : Exportation flux from surface to deep waters of POPs associated to organic particles (phytoplankton, bacteria,...)
C_{POM} : concentration of the POPs in the particulate organic phase	F_{Subd} : Flux of POPs transported to deep waters by subduction process
$C_{R/S}$: Concentration of contaminants in the rain or snow	F_{WD} : Wet deposition flux
C_w : POPs concentration in the dissolved seawater	GC : Greenland Current
	h : height of the atmospheric boundary layer or water column mixer layer depth
	HCB : Hexachlorobenzene
	HCHs : Hexachlorocyclohexanes
	HLC : Henry’s Law Constant
	IFSC : Intergovernmental Forum on Chemical Safety

Appendix E

IPCC: Intergovernmental panel for climate change

k_{AW} : Mass transfer coefficient between the air and water

K_{AW} : Air-water partition coefficient

k_D : First order POPs depuration rate

k_{DegH} : Hydrolytic degradation rate

k_{DegM} : Microbial degradation rate

k_{DegP} : Photolytic degradation rate

K_{DOC} : Water-dissolved organic carbon partition coefficient.

k_G : First order growth rate

K_{OA} : Octanol-water partition coefficient

k_{OH} : OH degradation rate

K_{OW} : Octanol-water partition constant.

K_p : Gas-Particle partition constant

K_{SA} : Air-soot carbon partition coefficient

k_{Sink} : Mass transfer coefficient between the surface and deep waters of POPs associated to organic particles.

k_U : First order POPs uptake rate

k_{WP} : mass transfer coefficient between phytoplankton and water

LRAT: Long Range Atmospheric Transport

MLD: Mixed Layer depth

MW_{OCT} : Octanol molecular weight

MW_{OM} : Organic matter molecular weight

OC: Organic Carbon

p_0 : Precipitation rate

PAME: Protection of the Arctic Marine Environment

PCBs: Polychlorinated biphenyls

POC: Particulate organic carbon

POM: Particulate organic matter

POP: Persistent organic pollutant

P_v : Vapour pressure

R: Ideal gas constant

R/V: Research Vessel

REACH: registration, evaluation, authorisation and restriction of chemical substances normative

r_{Subd} : rate of deep-water formation

R_t : Atmospheric residence time

SCAR: Scientific Committee on Antarctic Research

SDU: Sustainable Development and Utilization

S_O : Polarity

S_W : Solubility

T: Environmental temperature

T_W : Surface water temperature

TSP: Total suspended particules

UNECE: United Nations Economic Commission for Europe

UNEP: United Nations Environmental Programme

v_D : Aerosol deposition velocity

W: Weddell Origin Airmass

W_{GW} : Gas washout

WHO: World Health Organization

W_p : Rain/Snow contaminant scavenging ratio

W_{PW} : Particle washout

θ : Fraction of atmospheric POPs bound to aerosol

ρ_{OC}

